



UNIVERSITAT<sup>DE</sup>  
BARCELONA

## Intrinsic tracers for the analysis of habitat use by large marine vertebrates

Alessandra Cani



Aquesta tesi doctoral està subjecta a la llicència **Reconeixement- NoComercial – SenseObraDerivada 4.0. Espanya de Creative Commons.**

Esta tesis doctoral está sujeta a la licencia **Reconocimiento - NoComercial – SinObraDerivada 4.0. España de Creative Commons.**

This doctoral thesis is licensed under the **Creative Commons Attribution-NonCommercial-NoDerivs 4.0. Spain License.**



UNIVERSITAT DE  
BARCELONA

# **Intrinsic tracers for the analysis of habitat use by large marine vertebrates**

PhD programme in Marine Sciences  
Faculty of Biology

PhD candidate:

A handwritten signature in black ink, appearing to read "Alessandra Cani".

Alessandra Cani

Supervisor and tutor:  
Dr. Lluís Cardona Pascual

Supervisor:  
Dr. Massimiliano Drago



The editorial design, cover illustration and figures within this thesis were made by Alessandra Cani.

This thesis was financially supported by Universitat de Barcelona through the PREDOCS-UB grant.



DOCTORAL THESIS

**Intrinsic tracers for the analysis of habitat use by large  
marine vertebrates**

*Trazadores intrínsecos para el análisis del uso de hábitat  
de grandes vertebrados marinos*

*Traçadors intrínsecs per a l'anàlisi de l'ús d'hàbitat de  
grans vertebrats marins*

Alessandra Cani



UNIVERSITAT DE  
BARCELONA





*"It seems to me that the natural world is the greatest source of excitement; the greatest source of visual beauty; the greatest source of intellectual interest. It is the greatest source of so much in life that makes life worth living."*

David Attenborough

*"The sea, once it casts its spell, holds one in its net of wonder forever."*

Jacques Cousteau





## Acknowledgments

En este apartado me gustaría agradecer a todas aquellas personas que, directa o indirectamente, me ayudaron a navegar este camino hacia la Tesis Doctoral. Primero que nada, a mi mamá y a mi papá, por apoyarme en cada locura ocuriente y guiarme cuando hacía falta, estoy aquí en gran parte gracias a ustedes. Mi hermanito Willi, mi primer amigo y apoyo incondicional para lo que sea. Mis nonnas y nonnos, por construir esta hermosa familia que hoy me rodea y apoya sin importar las distancias, ¡los quiero mucho a todos! También quiero agradecer a mis hermanos de la vida, Ale y Dan, por el apoyo incondicional en estos +17 años de amistad, y es que ¡ni la distancia puede con nosotros!

A mi familia de Barcelona, empezando por mis señoras favoritas Vero, Su y Mariona, las que me dieron la bienvenida a esta ciudad y se alegraron casi más que yo cuando me dieron la beca del doctorado. Mis "Amiguis de Miquel", ese grupito en el que ninguno se llama Miquel pero todos somos amigos unidos por la UB, sin ustedes estos 4 años no hubieran sido tan divertidos e interesantes. Especial mención para Jazel, mi compañero fiel del doctorado, Odei, Leia y Diego, mis guías desde el primer día, Marc y Beñat, compañeros de viaje incansables, y Mae, que con tan solo meses compartiendo despacho ya siento que nos conocemos desde hace años.

Asimismo, quiero agradecer profundamente a todos los miembros del Grup de Recerca de Grans Vertebrats Marins, por acogerme y enseñarme tantas cosas entre cafés, charlas, conferencias, viajes y seminarios. Gracias Alex por ayudarme a navegar el mar de las becas doctorales, por darme la bienvenida al grupo y por todos los cuentos llenos de sabiduría y experiencias; a Xon y a Manel por las charlas y momentos compartidos, y por siempre estar dispuestos a brindar apoyo con lo que puedan; y por supuesto a mis supervisores, Max, gracias por introducirme al mundo de los isótopos estables, en el lab y en R, y por el apoyo en cada paso del doctorado; y Luis, por la confianza, el apoyo y el infinito conocimiento sobre bichos marinos, por introducirme al mundo de las tortugas marinas y ayudarme a definir mi camino como bióloga marina.

También quisiera agradecer a Antoni Calafat, coordinador del doctorado, por señalarme el camino hacia el grupo de GVM y por su guía desde el inicio hasta el final del doctorado.

Gracias a todos, ha sido un camino fascinante que repetiría sin dudarlo. Me llevo 4 años intensos de conocimientos, amistades y experiencias inolvidables.

¡A ver qué depara la siguiente fase! Seguro que será igual o más interesante ☺







## Abstract of the thesis

The use of the stable isotopes of different chemical elements as intrinsic biogeochemical tracers offers a unique opportunity to infer information about the foraging and spatial ecology of large marine vertebrates from small tissue samples of alive or dead individuals. Historically, the most commonly used tracers to study the trophic ecology of marine species have been the stable isotope ratios of carbon ( $\delta^{13}\text{C}$ ) and nitrogen ( $\delta^{15}\text{N}$ ), since they allow to identify the contribution of different primary producers with distinct isotopic signatures to the diet of a consumer and to estimate the trophic position of species and individuals within an ecosystem. More recently, the use of these isotopic tracers to analyse the habitat use of marine animals has led to the inclusion of other chemical elements to explore new dimensions of the isotopic niche. Such is the case of the sulphur stable isotope ratio ( $\delta^{34}\text{S}$ ) to differentiate between inshore/benthic habits from offshore/pelagic habits, and the oxygen stable isotope ratio ( $\delta^{18}\text{O}$ ) to study migration patterns across areas with distinct salinity. Nevertheless, the advantages of using additional isotopic tracers to improve the definition of the isotopic niche will depend on the ecosystem and species involved and, particularly, on the existence and scale of environmental isotopic gradients that affect the stable isotope ratios in primary producers and along the respective food webs. Therefore, this thesis aims to assess the suitability of the  $\delta^{34}\text{S}$  and  $\delta^{18}\text{O}$  ratio as habitat tracers for two different aspects, (1) to evaluate the isotopic niche partitioning among species of the same community and (2) to identify individual movement patterns among isotopically distinct foraging grounds. To do this, the  $\delta^{13}\text{C}$ ,  $\delta^{15}\text{N}$ ,  $\delta^{34}\text{S}$  and/or  $\delta^{18}\text{O}$  ratios were analysed in two types of consumer tissues, bone of marine mammals and sea turtles and epidermis of sea turtles, inhabiting ecosystems with marked environmental isotopic gradients such as the Río de la Plata estuary, the Mauritanian coast and the North Atlantic Ocean-Mediterranean Sea system. On one hand, the addition of the  $\delta^{18}\text{O}$  and  $\delta^{34}\text{S}$  ratios to the  $\delta^{13}\text{C}$  and  $\delta^{15}\text{N}$  ratios allowed to better characterize the isotopic niche partitioning among marine consumers in an ecosystem with important inputs of freshwater and terrestrial particulate organic matter, since the spatial scale of the environmental isotopic gradients covered the area used by the species. However, this did not occur everywhere and hence, the inclusion of more tracers does not necessarily translate into an improvement of the characterization of the isotopic niche partitioning among species. On the other hand, the use of at least three of these intrinsic tracers allowed to identify individual specialization in habitat within populations, as well as to trace individual movements among isotopically distinct areas. Furthermore, accounting for as many physical and chemical processes as possible, both environmental and metabolic, is critical when using stable isotopes to assess the habitat use and trophic ecology of large marine vertebrates, as the isotopic ratios of the consumers can be jointly affected by many processes. Finally, results should be validated with other complementary research techniques, such as direct observations, satellite telemetry and genetic analysis.

**Keywords:** habitat use, isotopic niche, marine megafauna, multi-element approach, stable isotope analysis.



## Resumen de la tesis

El uso de isótopos estables de diferentes elementos químicos como trazadores biogeoquímicos intrínsecos ofrece una oportunidad única para inferir información sobre la ecología trófica y espacial de grandes vertebrados marinos a partir de pequeñas muestras de tejido de individuos vivos o muertos. Históricamente, los trazadores más utilizados para estudiar la ecología trófica de las especies marinas han sido las proporciones de isótopos estables de carbono ( $\delta^{13}\text{C}$ ) y nitrógeno ( $\delta^{15}\text{N}$ ), ya que permiten identificar la contribución de diferentes productores primarios con distintas señales isotópicas a la dieta de un consumidor y estimar la posición trófica de especies e individuos dentro de un ecosistema. Más recientemente, el uso de estos trazadores isotópicos para analizar el uso del hábitat de los animales marinos ha llevado a la inclusión de otros elementos químicos para explorar nuevas dimensiones del nicho isotópico. Tal es el caso de los isótopos estables de azufre ( $\delta^{34}\text{S}$ ) para diferenciar entre hábitos costeros/bentónicos de aquellos oceánicos/pelágicos, y los de oxígeno ( $\delta^{18}\text{O}$ ) para estudiar patrones de migración a través de áreas con distinta salinidad. Sin embargo, las ventajas de usar trazadores isotópicos adicionales para mejorar la definición del nicho isotópico dependerán del ecosistema y especies involucradas y, particularmente, de la existencia y escala de gradientes isotópicos ambientales que afecten las relaciones de isótopos estables en productores primarios y a lo largo de las respectivas redes tróficas. Por lo tanto, esta tesis tiene como objetivo evaluar la idoneidad de los valores de  $\delta^{34}\text{S}$  y  $\delta^{18}\text{O}$  como trazadores de hábitat en dos aspectos diferentes, (1) para evaluar la partición del nicho isotópico entre especies de la misma comunidad y (2) para identificar patrones de movimiento individuales entre áreas de alimentación isotópicamente distintas. Para ello, se analizaron los valores de  $\delta^{13}\text{C}$ ,  $\delta^{15}\text{N}$ ,  $\delta^{34}\text{S}$  y/o  $\delta^{18}\text{O}$  en dos tipos de tejidos de consumidores, hueso de mamíferos marinos y tortugas marinas y epidermis de tortugas marinas, que habitan ecosistemas con gradientes isotópicos ambientales marcados como el estuario del Río de la Plata, la costa de Mauritania y el sistema Atlántico Norte-Mar Mediterráneo. Por un lado, la inclusión de los valores de  $\delta^{18}\text{O}$  y  $\delta^{34}\text{S}$  a los de  $\delta^{13}\text{C}$  y  $\delta^{15}\text{N}$  permitió mejorar la caracterización de la partición del nicho isotópico entre consumidores marinos en un ecosistema con importantes aportes de agua dulce y materia orgánica particulada terrestre, ya que la escala espacial de los gradientes isotópicos ambientales cubría el área utilizada por las especies. Sin embargo, esto no ocurrió en todas partes y, por lo tanto, la inclusión de más trazadores no necesariamente se traduce en una mejora en la caracterización del nicho isotópico entre especies. Por otra parte, el uso de al menos tres de estos trazadores intrínsecos permitió identificar la especialización individual dentro de las poblaciones, así como rastrear los movimientos individuales entre áreas isotópicamente distintas. Además, tener en cuenta tantos procesos físicos y químicos como sea posible, tanto ambientales como metabólicos, es fundamental cuando se utilizan isótopos estables para evaluar el uso del hábitat y la ecología trófica de los grandes vertebrados marinos, ya que las proporciones isotópicas de los consumidores pueden verse afectadas conjuntamente por diversos procesos. Finalmente, los resultados deberían validarse con otras técnicas de investigación complementarias, como observaciones directas, telemetría satelital y análisis genéticos.

Palabras clave: análisis de isótopos estables, enfoque multi-elemento, nicho isotópico, megafauna marina, uso de hábitat.



## Resum de la tesi

L'ús d'isòtops estables de diferents elements químics com traçadors biogeoquímics intrínsecs ofereix una oportunitat única per inferir informació sobre l'ecologia espacial i d'alimentació de grans vertebrats marins a partir de mostres de teixit d'individus vius o morts. Històricament, els traçadors més utilitzats per estudiar l'ecologia tròfica de les espècies marines han estat les proporcions d'isòtops estables de carboni ( $\delta^{13}\text{C}$ ) i nitrogen ( $\delta^{15}\text{N}$ ), ja que permeten identificar la contribució de diferents productors primaris amb diferents senyals isotòpics a la dieta d'un consumidor i estimar la posició tròfica d'espècies i d'individus dins d'un ecosistema. Més recentment, l'ús d'aquests traçadors isotòpics per analitzar l'ús de l'hàbitat dels animals marins ha portat a la inclusió d'altres elements químics per explorar noves dimensions del nínxol isotòpic. Aquest és el cas dels isòtops estables de sofre ( $\delta^{34}\text{S}$ ) per diferenciar entre hàbits costaners/bentònics d'hàbits oceànics/pelàgics i els d'oxigen ( $\delta^{18}\text{O}$ ) per estudiar patrons de migració a través d'àrees de diferent salinitat. No obstant això, els avantatges d'usar traçadors isotòpics addicionals per millorar la definició del nínxol isotòpic dependran de l'ecosistema i les espècies involucrades, particularment de l'existència i l'escala de gradients isotòpics ambientals que afectin les relacions d'isòtops estables en productors primaris i al llarg de les respectives xarxes tròfiques. Per tant, aquesta tesi té com a objectiu avaluar la idoneïtat dels valors de  $\delta^{34}\text{S}$  i  $\delta^{18}\text{O}$  com a traçadors d'hàbitat en dos aspectes diferents, (1) per avaluar la partició del nínxol isotòpic entre espècies de la mateixa comunitat i (2) per identificar patrons de moviment individuals entre àrees d'alimentació isotòpicament diferents. Per això, es van analitzar els valors de  $\delta^{13}\text{C}$ ,  $\delta^{15}\text{N}$ ,  $\delta^{34}\text{S}$  i/o  $\delta^{18}\text{O}$  en dos tipus de teixits animals, os de mamífers marins i tortugues marines i epidermis de tortugues marines, que habiten ecosistemes amb gradients isotòpics ambientals com l'estuari de Riu de la Plata, la costa de Mauritània i el sistema Atlàntic Nord-Mar Mediterrani. D'una banda, la inclusió dels valors de  $\delta^{18}\text{O}$  i  $\delta^{34}\text{S}$  als de  $\delta^{13}\text{C}$  i  $\delta^{15}\text{N}$  va permetre millorar la caracterització de la partició del nínxol isotòpic entre consumidors marins en un mateix ecosistema amb importants aportacions d'aigua dolça i matèria orgànica particulada terrestre, ja que l'escala espacial dels gradients isotòpics ambientals cobria l'àrea utilitzada per les espècies. Tanmateix, això no va passar a tot arreu i, per tant, la inclusió de més traçadors no necessàriament es tradueix en una millora en la caracterització del nínxol isotòpic entre espècies. D'altra banda, l'ús d'almenys tres d'aquests traçadors intrínsecs va permetre identificar l'especialització individual dins de les poblacions i rastrejar els moviments individuals entre àrees isotòpicament diferents. A més, tenir en compte tants processos físics i químics com sigui possible, tant ambientals com metabòlics, és fonamental quan s'utilitzen isòtops estables per avaluar l'ús de l'hàbitat i l'ecologia tròfica dels grans vertebrats marins, ja que les proporcions isotòpiques dels consumidors es poden veure afectades conjuntament per diversos processos. Finalment, els resultats s'haurien de validar amb altres tècniques de recerca complementàries, com a observacions directes, telemetria satel·lital i anàlisis genètiques.

Paraules clau: anàlisi d'isòtops estables, enfocament multi-element, nínxol isotòpic, megafauna marina, ús de l'hàbitat.





# Index

---

Abstract of the thesis.....	I
Resumen de la tesis.....	II
Resum de la tesi.....	III
Index.....	V
List of Figures.....	VIII
List of Tables.....	IX
<b>1. General Introduction.....</b>	<b>3</b>
Stable isotope analysis.....	4
Carbon stable isotope ratio ( $\delta^{13}\text{C}$ ) .....	5
Nitrogen stable isotope ratio ( $\delta^{15}\text{N}$ ) .....	9
Sulphur stable isotope ratio ( $\delta^{34}\text{S}$ ) .....	11
Oxygen stable isotope ratio ( $\delta^{18}\text{O}$ ) .....	14
Characterization of the isotopic niche.....	16
Tissue turnover and diet-to-tissue discrimination.....	18
<b>Objectives of the thesis.....</b>	<b>21</b>
Structure of the thesis.....	21
<b>2. Methodological overview.....</b>	<b>25</b>
Study areas and species involved.....	25
Río de La Plata estuary.....	27
Mauritania.....	28
North Atlantic Ocean and Mediterranean Sea.....	29
Tissues.....	31
Stable isotope analysis.....	31
Isotopic niche partitioning.....	34
<b>3. Results.....</b>	<b>35</b>

<b>Article 1.</b> Niche partitioning among marine mammals inhabiting a large estuary as revealed by stable isotopes of C, N, S and O.....	37
Abstract.....	39
Introduction.....	40
Methods.....	42
Results.....	47
Discussion.....	53
References.....	59
 <b>Article 2.</b> Fine-tuning the isotopic niche of a marine mammal community through a multi-element approach and variable spatial scales.....	67
Abstract.....	69
Introduction.....	70
Methods.....	72
Results.....	79
Discussion.....	87
References.....	95
 <b>Article 3.</b> The journey of loggerhead turtles from the Northwest Atlantic to the Mediterranean Sea as recorded by the stable isotope ratios of O, C and N of their bones.....	103
Abstract.....	105
Introduction.....	106
Methods.....	108
Results.....	116
Discussion.....	123
References.....	130
 <b>Article 4.</b> Identifying the foraging grounds of the new loggerhead turtle nesters in the western Mediterranean.....	137
Abstract.....	139
Introduction.....	140
Methods.....	142
Results.....	148
Discussion.....	155
References.....	158
 <b>Summary of Results</b> .....	167
Community level characterization of the isotopic niche.....	169
Species level characterization of the isotopic niche.....	170

<b>4. General discussion</b> .....	175
Resource partitioning and habitat use.....	176
Characterization of the isotopic niche in a marine mammal community.....	179
Individual characterization of the isotopic niche in sea turtles.....	182
<b>Conclusions</b> .....	189
General references.....	193
<b>Annex</b> .....	205
Article 1 (original).....	207
Supplementary material from Article 1.....	224
Article 2 (original).....	227
Supplementary material from Article 2.....	242
Article 3 (original).....	245
Supplementary material from Article 3.....	259
Article 4 (original).....	267
Supplementary material from Article 4.....	284



## List of Figures

---

<b>Figure 1.1.</b> Carbon diffusion and $\delta^{13}\text{C}$ fractionation.....	9
<b>Figure 1.2.</b> Nitrogen cycle and $\delta^{15}\text{N}$ trophic enrichment.....	11
<b>Figure 1.3.</b> Sulphur molecules distribution and $\delta^{34}\text{S}$ fractionation .....	13
<b>Figure 1.4.</b> Water cycle and $\delta^{18}\text{O}$ distribution and fractionation .....	16
<b>Figure 2.1.</b> Study areas.....	26
<b>Article 1:</b>	
<b>Figure 3.1.</b> Study area and sampling locations of Río de la Plata.....	43
<b>Figure 3.2.</b> Boxplots of the isotopic values of marine mammals from Río de la Plata.....	50
<b>Figure 3.3.</b> Standard ellipses of marine mammals from Río de la Plata.....	51
<b>Figure 3.4.</b> Estimated habitat preferences of marine mammals from Río de la Plata .....	52
<b>Article 2:</b>	
<b>Figure 3.5.</b> Study area and upwelling zones off Mauritania.....	74
<b>Figure 3.6.</b> Scatterplot of the $\delta^{34}\text{S}$ values of marine mammals from Mauritania .....	80
<b>Figure 3.7.</b> Boxplots of the isotopic values of marine mammals from Mauritania .....	82
<b>Figure 3.8.</b> Standard ellipses of marine mammals from Mauritania.....	83
<b>Figure 3.9.</b> Sighting and stranding reports of marine mammals off Mauritania.....	87
<b>Article 3:</b>	
<b>Figure 3.10.</b> Currents and sea surface $\delta^{18}\text{O}$ values of the North Atlantic Ocean and Mediterranean Sea.....	109
<b>Figure 3.11.</b> Method for loggerhead turtle's bone sampling and aging.....	112
<b>Figure 3.12.</b> Correlation and GAM of individual isotopic values and age.....	120
<b>Figure 3.13.</b> Differences between incremental layers of each loggerhead turtle.....	121
<b>Figure 3.14.</b> Standard ellipses and correlation with age for loggerhead turtles.....	122
<b>Article 4:</b>	
<b>Figure 3.15.</b> Sampled nests and tagging location of female loggerhead turtles.....	143
<b>Figure 3.16.</b> Stable isotope ratios of stranded and nesting loggerhead turtles.....	148
<b>Figure 3.17.</b> Standard ellipses of stranded and nesting loggerhead turtles.....	151
<b>Figure 3.18.</b> Tracks of the satellite-tracked female loggerhead turtles.....	153
<b>Figure 3.19.</b> Estimates of Kernel habitat use.....	154
<b>Figure 3.20.</b> Movement segmentation analysis for each satellite-tracked turtle .....	154

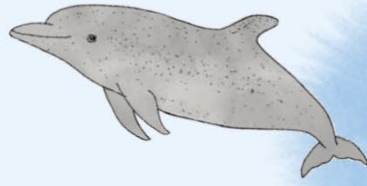


## List of Tables

---

<b>Table 1.1.</b> Types of photosynthetic pathways .....	6
<b>Table 1.2.</b> Methods for stable isotope analysis per group and tissue.....	34
<b>Article 1:</b>	
<b>Table 3.1.</b> Study area and sampling locations of Río de la Plata.....	48
<b>Article 2:</b>	
<b>Table 3.2.</b> Overlap area (%) among marine mammals from Mauritania.....	84
<b>Article 3:</b>	
<b>Table 3.3.</b> $\delta^{18}\text{O}$ values and estimated age of the sampled bone layers.....	119
<b>Article 4:</b>	
<b>Table 3.4.</b> Details of satellite-tracked female loggerhead turtles.....	146
<b>Table 3.5.</b> Stable isotope ratios of loggerhead turtle hatchlings from Spanish Mediterranean beaches.....	150
<b>Table 3.6.</b> Overlap between standard ellipses of loggerhead turtles.....	150





# **Chapter 1: General Introduction**

---







## 1. General Introduction

Large marine vertebrates spend most of their time underwater and perform long-distance migrations between their feeding and breeding or calving grounds, which can be hundreds to thousands of kilometres apart (Hays and Scott, 2013; Modest et al., 2021). Consequently, the use of traditional methods to study their habitat use, such as ship-based observations for marine mammals and flipper-tagging for sea turtles, is often challenging due to the inherent constraints of working in the marine environment, including a difficult access, low encounter rates and high economic costs (Newsome et al., 2010; Ramos and González-Solís, 2012).

New technologies like satellite telemetry have allowed to remotely monitor the movements of marine animals with a high precision, thus generating new knowledge about habitat use of numerous marine species worldwide (Hussey et al., 2015). However, despite the undeniable advantages offered by these techniques, there are several limitations to consider. Animal-borne telemetry devices can potentially affect the behaviour of individuals and compromise the data collected if is not properly chosen and handled (Newsome et al., 2010; Kingsbury and Robinson, 2016). They also come with a high economic cost that limits the sample size, along with the difficulties to find and retain individuals; plus, data collection depends mostly on the survival of the animal and the correct functioning of the device (Kingsbury and Robinson, 2016). In addition, they often provide biased information towards species and life stages that are easier to find, capture and handle, leaving information gaps on other species and components of the population (Newsome et al., 2010; Balmer et al., 2014). For instance, satellite tracked sea turtles have provided new knowledge about migration patterns, population dynamics and the connection between rookeries and foraging grounds (e.g., Eckert et al., 2008; Abalo-Morla et al., 2023), but the primary focus of most of these studies is on adult females nesting in accessible beaches, providing limited information on juveniles and males (Hays and Hawkes, 2018; Fuentes et al., 2023).

Overall, the difficult access to living specimens restrains the *in-situ* study of large marine vertebrates, whereas other techniques such as the analysis of intrinsic biogeochemical tracers can offer a viable and minimally invasive alternative to obtain information on elusive species, using only a small tissue sample from either dead or alive individuals (Rubenstein and Hobson, 2004). In this context, the stable isotope ratios of



several chemical elements have become one of the most widely used intrinsic tracers to make inferences about the trophic and spatial ecology of species and individuals and even to complement the information obtained with other research techniques (Newsome et al., 2010; West et al., 2010; Haywood et al., 2019).

### 1.1. Stable isotope analysis

Many chemical elements exist in more than one stable form, which differ from each other in their atomic mass due to a distinct number of neutrons in the nucleus. Since the number of protons and electrons remains the same, this only affects their physical properties in chemical reactions, leading to variations in the ratio of heavy to light isotopes between a source and the respective product. This difference is known as isotopic fractionation (Wassenaar, 2019; Ben-David and Flaherty, 2012).

There are two main types of fractionation processes; the equilibrium fractionation happens in fully or partially reversible reactions, whereas the kinetic fractionation occurs in unidirectional or irreversible reactions and is usually much larger than the former (Michener and Lajtha, 2007; Ben-David and Flaherty, 2012). In any case, the isotopic ratios of a chemical element in an organic molecule can be measured using a thermal ionization mass spectrometer, which transforms the organic compound into inorganic gaseous molecules that are separated based on mass, obtaining abundance estimates for each mass as a ratio count expressed in delta ( $\delta$ ) notation. This value is then compared to that of an internationally recognized standard to make all values comparable (Michener and Lajtha, 2007; Ben-David and Flaherty, 2012). Consequently, the product of a fractionation process can be “enriched” (show higher  $\delta$  values) or “depleted” (show lower  $\delta$  values) in the heavy isotope with respect to the source (Michener and Lajtha, 2007).

The use of stable isotope ratios as tracers in ecology is based on the fact that stable isotope ratios in consumers are determined by those in their diet, modified according to the fractionation of the metabolic chemical reactions and the routing of chemical elements across metabolic pathways (Pecquerie et al., 2010). In this context, the trophic discrimination factor (TDF), also known as diet-to-tissue discrimination factor (DTDF), represents the difference between the stable isotope ratio of the diet and that of the consumer’s tissues (McCutchan Jr. et al., 2003; Vander Zanden et al., 2015).



The stable isotope ratios of carbon ( $^{13}\text{C}/^{12}\text{C}$ ; hereon as  $\delta^{13}\text{C}$ ) and nitrogen ( $^{15}\text{N}/^{14}\text{N}$ ; hereon as  $\delta^{15}\text{N}$ ) have been commonly used for diet reconstruction over the past few decades (Newsome et al., 2010; Layman et al., 2012). The sulphur stable isotope ratio ( $^{34}\text{S}/^{32}\text{S}$ ; hereon as  $\delta^{34}\text{S}$ ) is mostly used in combination with  $\delta^{13}\text{C}$  and  $\delta^{15}\text{N}$  as a habitat tracer, whereas the oxygen stable isotope ratio ( $^{18}\text{O}/^{16}\text{O}$ ; hereon as  $\delta^{18}\text{O}$ ) is often used for paleoclimate reconstruction but is less common as a habitat tracer for large marine vertebrates (Newsome et al., 2010).

As mentioned above, the stable isotope ratios in consumers are determined by those in the diet plus the discrimination resulting from several metabolic and environmental processes, which depend on factors such as the available sources of each chemical element to primary producers, the physiological processes used by the organisms to assimilate these sources, the position of the consumer in the food web and the type of tissue used in the analysis (Ben-David and Flaherty, 2012).

The following subsections present the basis of the stable isotopes of each chemical element used in this thesis and the factors that generate the respective environmental gradients, which are necessary for their use as habitat tracers.

### **1.1.1. Carbon stable isotope ratio ( $\delta^{13}\text{C}$ )**

The  $\delta^{13}\text{C}$  ratio of a consumer results mostly from its diet, which in turn reflects the primary source of carbon at the base of the food web since different groups of primary producers differ in their discrimination against the  $\text{CO}_2$  molecules carrying the  $^{13}\text{C}$  isotope during photosynthesis (Peterson and Howarth, 1987; Michener and Lajtha, 2007). Terrestrial primary producers with a  $\text{C}_3$  metabolism (i.e., those relying on  $\text{CO}_2$  diffusion into photosynthetic cells and the Calvin cycle with the ribulose bisphosphate carboxylase, or RuBisCO, as the carbon fixing enzyme) show a high discrimination against  $\text{CO}_2$  molecules carrying the  $^{13}\text{C}$  and hence, are characterized by  $\delta^{13}\text{C}$  values lower than  $-24\text{‰}$  (Table 1). On the other hand, those relying on a  $\text{C}_4$  metabolism (i.e., those using the Hatch-Slack pathway with the phosphoenolpyruvate carboxylase, or PEPC, as the carbon fixing enzyme) have  $\delta^{13}\text{C}$  values ranging from  $-14$  to  $-10\text{‰}$  (Table 1), since PEPC has a lower discrimination between carbon molecules than RuBisCO (Falkowski and Raven, 2007; Ben-David and Flaherty, 2012). Likewise, primary producers using the crassulacean acid metabolism (CAM), an adaptation that combines PEPC and RuBisCO



as carbon fixing enzymes to improve photosynthetic performance in water-limiting environments (Cushman and Borland, 2002), also show a lower discrimination against the CO<sub>2</sub> molecules carrying the heavier C isotope and hence have higher  $\delta^{13}\text{C}$  ratios than C<sub>3</sub> plants (Table 1; Falkowski and Raven, 2007; Ben-David and Flaherty, 2012). In general, C<sub>3</sub> plants prevail in most terrestrial ecosystems, with C<sub>4</sub> plants dominating vegetation only in some tropical grasslands and CAM plants in some xeric ecosystems (Falkowski and Raven, 2007).

**Table 1.1.** Comparison between the different types of photosynthetic pathways found in terrestrial and aquatic primary producers (Falkowski and Raven, 2007)

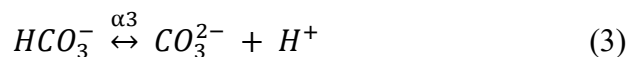
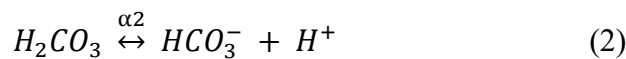
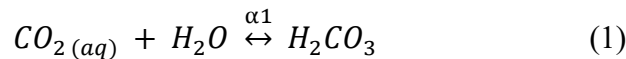
Type of metabolism	C <sub>3</sub>	C <sub>4</sub>	CAM
Photosynthetic pathways	Calvin Cycle	Hatch-Slack Pathway	Both
Carbon-fixing enzyme	RuBisCO (ribulose-1,5-bisphosphate carboxylase/oxygenase)	PEPC (phosphoenolpyruvate carboxylase)	Both
Fractionation factor ( $\alpha$ )	High discrimination against $^{13}\text{C}$	Less discrimination against $^{13}\text{C}$	Depending on the metabolic path activated
Type of carbon used in photosynthesis	<u>Terrestrial</u> : atmospheric CO <sub>2</sub> <u>Marine</u> : dissolved inorganic carbon (mostly HCO <sub>3</sub> <sup>-</sup> )		
$\delta^{13}\text{C}$ values	<u>Terrestrial</u> : - 33 to - 24 ‰ <u>Marine</u> : - 24 to - 18 ‰	- 14 to - 10 ‰	- 25 to - 10 ‰

In the marine environment, just like on land, most primary producers rely on the C<sub>3</sub> metabolism, including the vast majority of marine macroalgae, diatoms, dinoflagellates and coccolithophores, as well as some seagrasses (Raven et al., 2002; Reinfelder, 2011). On the other hand, a C<sub>4</sub>-like metabolism has been reported in a few diatom and macroalgae species and in several seagrasses (Reinfelder, 2011; Larkum et al., 2017; Liu et al., 2020), whereas some cyanobacteria and algae, along with other species inhabiting intertidal zones, can change to a C<sub>4</sub> or CAM-like metabolism under high stress conditions, which likely affects the  $\delta^{13}\text{C}$  values of their tissues (Reinfelder et al., 2000; Raven and Beardall, 2003; Falkowski and Raven, 2007). However, marine primary producers are often more enriched in  $^{13}\text{C}$  compared to terrestrial primary producers using the same photosynthetic pathway, because their primary source of



inorganic carbon is naturally more enriched in  $^{13}\text{C}$  than the atmospheric  $\text{CO}_2$  (Zeebe and Wolf-Gladrow, 2001).

Atmospheric  $\text{CO}_2$  is the main carbon source available for terrestrial primary producers, while marine primary producers have access to a pool of dissolved inorganic carbon (DIC) in different chemical forms, depending on the temperature and pH of the water where they grow (Zeebe and Wolf-Gladrow, 2001; Emerson and Hedges, 2008). Initially, the diffusion of gaseous  $\text{CO}_2$  from the atmosphere to the water forming aqueous  $\text{CO}_2$  involves only a small isotopic fractionation, but the products of the subsequent hydration reactions (equations 1-3), namely carbonic acid ( $\text{H}_2\text{CO}_3$ ), bicarbonate ( $\text{HCO}_3^-$ ) and carbonate ( $\text{CO}_3^{2-}$ ), get gradually enriched in  $^{13}\text{C}$  due to the “equilibrium isotope effects”. This is because the stronger and more stable chemical bonds of the molecules carrying the heavier  $^{13}\text{C}$  isotope are more likely to be incorporated into the products of each reaction (Figure 1.1; Zeebe, 2014). In general, most marine primary producers rely on  $\text{HCO}_3^-$  as the main C source and use different carbon-concentrating mechanisms to convert it into  $\text{CO}_2$  to decrease photorespiration and increase photosynthetic efficiency (Figure 1.1; Reinfelder, 2011). As  $\text{HCO}_3^-$  is naturally enriched in  $^{13}\text{C}$  compared to atmospheric  $\text{CO}_2$ , the  $\delta^{13}\text{C}$  ratio of marine primary producers tends to be higher than that of their equivalents on land (Table 1; Figure 1.1; Emerson and Hedges, 2008).



Nevertheless, the use of the different forms of dissolved C in the marine environment will depend on the availability of aqueous  $\text{CO}_2$  relative to the rates of primary production. The slow diffusion of aqueous  $\text{CO}_2$  and its rapid hydration with the water molecules (Zeebe, 2014) make it a limiting factor for photosynthesis; thus, its accessibility for biological processes becomes highly dependent on physical factors such as the water turbulence, the thickness of the boundary layer and the surface area-to-volume ratio of primary producers (Finlay et al., 1999; Falkowski and Raven, 2007). For instance, sheltered regions allow the formation of thick boundary layers that limit the  $\text{CO}_2$  diffusion, making it less accessible for primary producers and especially for those with a



low surface-to-volume ratio. On the contrary, high water turbulence constantly removes the boundary layer and enhances CO<sub>2</sub> supply, facilitating its diffusion towards primary producers and especially for those with a high surface-to-volume ratio (Finlay et al., 1999; Schlichting and Gersten, 2016). As a result, phytoplankton is typically depleted in <sup>13</sup>C compared to macroalgae, which in turn are depleted in <sup>13</sup>C compared to C3 seagrasses (Raven et al., 2002; Reinfelder, 2011; Larkum et al., 2017; Liu et al., 2020). Similarly, low light availability reduces the CO<sub>2</sub> demand due to lower photosynthetic activity and hence, macroalgae growing in colder mesophotic habitats are often characterized by δ<sup>13</sup>C values in the range of terrestrial C3 plants (Raven and Beardall, 2003).

From the above follows that the δ<sup>13</sup>C values of consumers are typically higher in more productive coastal regions compared to oceanic regions, whereas deep waters with low primary production are associated with low δ<sup>13</sup>C values, as the abundance and contribution of <sup>13</sup>C-enriched primary producers to the total C pool fuelling the food web declines (Figure 1.1; Rubenstein and Hobson, 2004; Newsome et al., 2010). Furthermore, it is possible to identify the influence of upwelling-derived phytoplankton in a consumer's diet, because the high photosynthetic activity derived from these blooms rapidly depletes the aqueous CO<sub>2</sub>, forcing the use of other <sup>13</sup>C-enriched forms of DIC as a C source and producing a local increase of δ<sup>13</sup>C values (Newsome et al., 2010; Carrier et al., 2015).

Finally, some confounding factors in the interpretation of a consumer's δ<sup>13</sup>C values include the diet-to-tissue discrimination along the food web and the alteration of the inshore-offshore δ<sup>13</sup>C gradient, either by the input of large amounts of terrestrial detritus bringing <sup>13</sup>C-depleted organic matter into coastal areas, or by the preferential uptake of molecules carrying the <sup>12</sup>C isotope during photosynthesis which can increase the concentration of molecules with the <sup>13</sup>C isotope in the surrounding surface waters, especially during coastal blooms (Rubenstein and Hobson 2004; Michener and Lajtha 2007; Newsome et al., 2010). Therefore, knowing the available C sources and the primary producers that make up the ecosystem will reduce the uncertainty associated with the use of δ<sup>13</sup>C values to make inferences on the trophic ecology and habitat use of consumers.

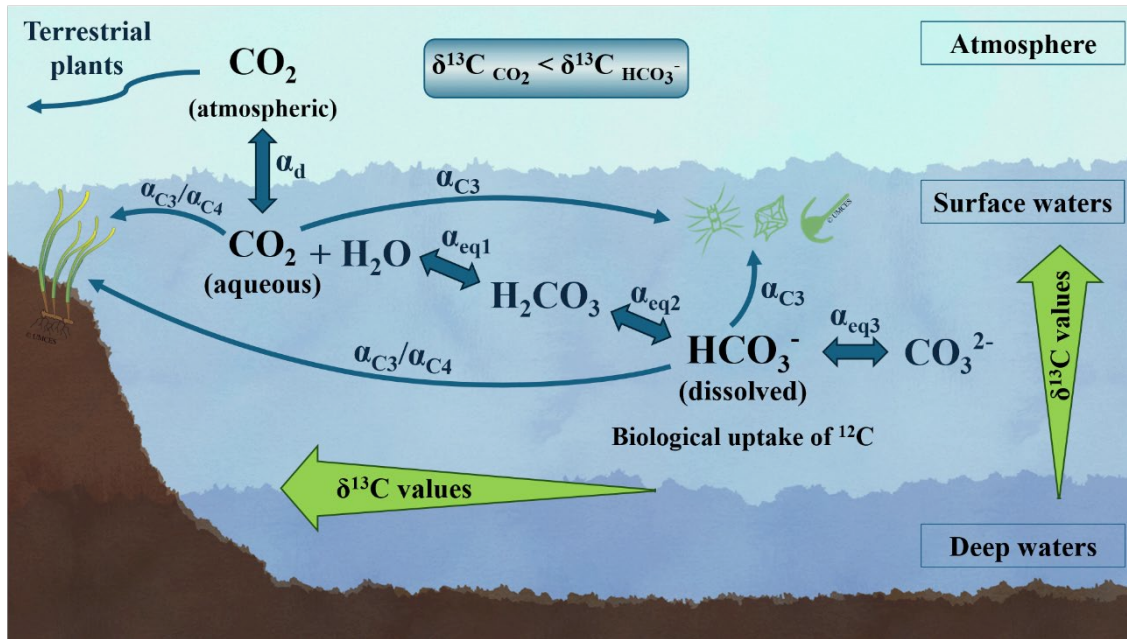


**Figure 1.1.** General features of the carbon diffusion between atmosphere and water, showing some of the fractionation factors ( $\alpha$ ) involved in the carbon fixation process by primary producers, where  $\alpha_d$  corresponds to the fractionation resulting from the  $\text{CO}_2$  diffusion between air and water,  $\alpha_{\text{eq1}}/\alpha_{\text{eq2}}/\alpha_{\text{eq3}}$  correspond to the fractionation observed due to the “equilibrium isotope effect”, and  $\alpha_{\text{C3}}/\alpha_{\text{C4}}$  correspond to the fractionation of the respective carbon fixing enzyme (C3 or C4 metabolism). The thick green arrows represent the direction in which the  $\delta^{13}\text{C}$  values tend to increase along the coastal-oceanic gradient (horizontal arrow) and between deep and surface waters (vertical arrow), assuming no significant terrestrial input.

### 1.1.2. Nitrogen stable isotope ratio ( $\delta^{15}\text{N}$ )

Similarly to carbon, the only source of N for consumers comes through the diet and it also presents diet-to-tissue discrimination against the heavy  $^{15}\text{N}$  isotope (Post, 2002). In this case, the largest global nitrogen reservoir is atmospheric nitrogen ( $\text{N}_2$ ), which has  $\delta^{15}\text{N}$  values close to 0.0 ‰ and, since the rate of nitrogen supply limits important biological reactions such as plant growth, available nitrogen is often used without fractionation (Peterson and Fry, 1987). Nevertheless, both terrestrial and marine primary producers rely exclusively on dissolved inorganic nitrogen (DIN) for their biological processes, especially ammonium and nitrate, which are products of the microbial fixation of  $\text{N}_2$  molecules (Newton, 2007).



On one hand, atmospheric  $N_2$  is transformed into ammonia ( $NH_3$ ) or ammonium ( $NH_4^+$ ) by N-fixating organisms called diazotrophs (Newton, 2007; Pierella Karlusich et al., 2021), a process that occurs with little isotope fractionation and hence, the  $\delta^{15}N$  values of the produced  $NH_3/NH_4^+$  are also close to 0.0 ‰ (Figure 1.2; Peterson and Fry, 1987). On the other hand,  $NH_4^+$  is converted into nitrite ( $NO_2^-$ ) and then into nitrate ( $NO_3^-$ ) by ammonia- and nitrite-oxidizing bacteria, respectively, during the nitrification process. Since the lighter  $^{14}N$  isotope is preferentially used in microbial processes, the  $NO_2^-$ ,  $NO_3^-$  and the remaining pool of  $NH_4^+$  become enriched in  $^{15}N$  (Figure 1.2; Peterson and Fry, 1987; Boyer and Howarth, 2013). However, the largest fractionation of bioavailable inorganic N comes from the denitrification process, which is the microbial reduction of  $NO_3^-$  into nitrogen gas ( $N_2$  or  $N_2O$ ), which is released back into the atmosphere. This is because the chemical bonds of the  $NO_3^-$  and  $NO_2^-$  with the lighter  $^{14}N$  isotope are easier to break, leaving behind a  $^{15}N$ -enriched pool of DIN with  $\delta^{15}N$  values that can exceed the +10.0 ‰, depending on the local microbial activity, which is highest in anoxic or  $O_2$ -depleted environments (Figure 1.2; Peterson and Fry, 1987).

Likewise, the  $\delta^{15}N$  ratio also increases consistently along the food web due to a process called “trophic enrichment” (Post, 2002). Higher-level consumers (predators) obtain their nitrogen supply from lower-level consumers (prey), and primary consumers (herbivores) acquire their N from primary producers (Figure 1.2). In each case, biological processes such as protein synthesis and nitrogen excretion show a preferential use of molecules carrying the lighter isotope and leave the  $^{15}N$ -enriched molecules in the consumer’s tissues. Therefore, as the nitrogen moves up the food chain the  $\delta^{15}N$  values typically increase with a mean trophic discrimination factor (TDF) of 3.4 ‰ per trophic position (Post, 2002), although this factor can vary depending on the available sources of DIN, the type of primary producers and the species that make up the food web. Consequently, the input of sewage into coastal environments can increase the  $\delta^{15}N$  values of nearby waters and thus alter the respective values of all organisms feeding in the area (Figure 1.2; McClelland and Valiela, 1998). In addition, differences in the turnover rate between the tissues analysed for prey and predator can also produce an offset on the TDF, which is calculated as a diet-to-tissue  $\delta^{15}N$  discrimination factor (Turner Tomaszewicz et al., 2017a).



In general, the  $\delta^{15}\text{N}$  ratio is a highly useful tool to study the trophic ecology of marine consumers, providing a convenient method to assess the trophic position of species and individuals within an ecosystem (Post, 2002).

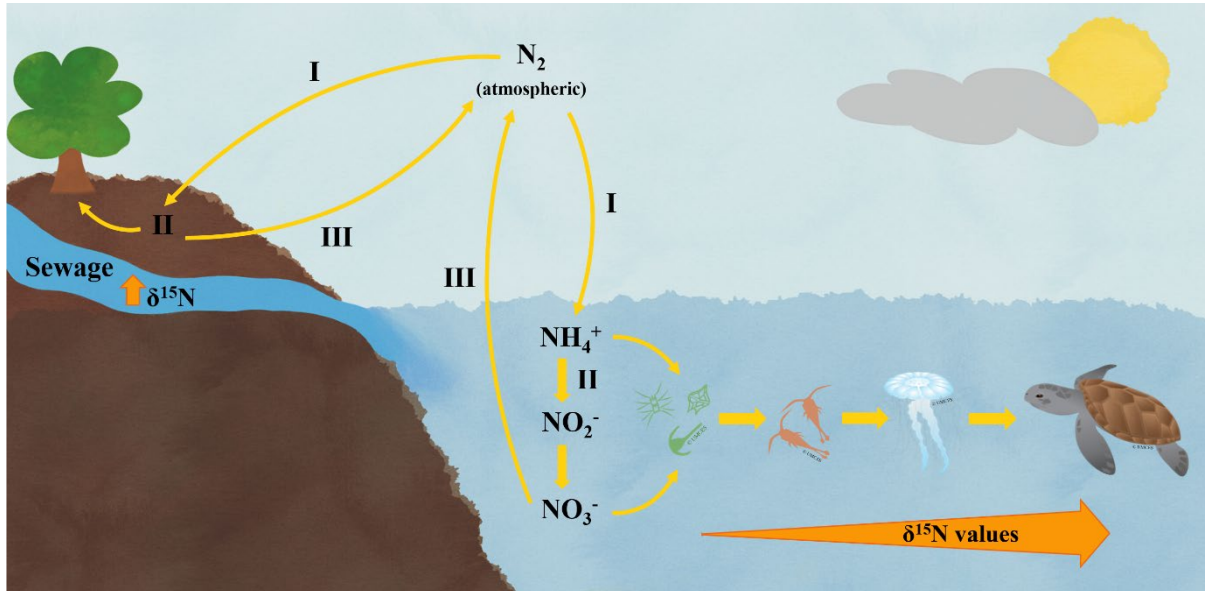


**Figure 1.2.** General reactions within the nitrogen cycle resulting in the formation of biologically available forms of nitrogen: **I. Nitrogen fixation** by diazotrophs, converting atmospheric  $\text{N}_2$  into ammonium ( $\text{NH}_4^+$ ) with little to no isotope fractionation; **II. Nitrification**, a two steps process where  $\text{NH}_4^+$  is oxidized into nitrite ( $\text{NO}_2^-$ ) and then into nitrate ( $\text{NO}_3^-$ ) by ammonia- and nitrite-oxidizing bacteria, resulting in a slight enrichment in  $^{15}\text{N}$  with each reaction; **III. Denitrification**, the reduction of  $\text{NO}_3^-$  into atmospheric  $\text{N}_2$ , resulting in a larger enrichment in  $^{15}\text{N}$ . The products of I and II are used by terrestrial and aquatic primary producers in their biological processes, and the predominance of each reaction and the resulting  $\delta^{15}\text{N}$  values will depend on the oxidative state of the environment and the microbial activity. The thick orange arrow shows the trophic enrichment observed for the  $\delta^{15}\text{N}$  values along a typical pelagic food web, starting with the absorption of bioavailable N, such as  $\text{NH}_4^+$  or  $\text{NO}_3^-$ , by primary producers and increasing towards higher-level consumers, such as sea turtles, due to the preferential use of the lighter isotope in biological processes.

### 1.1.3. Sulphur stable isotope ratio ( $\delta^{34}\text{S}$ )

The  $\delta^{34}\text{S}$  ratio is often used in combination with the  $\delta^{13}\text{C}$  and  $\delta^{15}\text{N}$  ratios as a complementary habitat tracer to separate between marine species with benthic and pelagic



habits (Haywood et al., 2020a; Borrell et al., 2021). This is because of the redox gradient often formed from the more oxidizing conditions in offshore/pelagic regions, mostly due to a continuous vertical mixing of the water column, to the more reducing and hypoxic or anoxic conditions of sediments found in sheltered areas (Peterson et al., 1985; Connolly et al., 2004).

Biologically available S can be either as sulphates ( $\text{SO}_4^{2-}$ ), if formed under aerobic conditions, or as sulphides ( $\text{S}^{2-}$ ), if formed under anaerobic conditions (Peterson and Howarth, 1987; Canfield, 2001). Sulphate in the atmosphere can originate from several natural sources such as sea spray, volcanic emissions and the oxidation of sulphur gases, as well as from anthropogenic inputs through the burning of fossil fuels and other industrial pollutants (Eckardt, 2001; Liu et al., 2021). In terrestrial ecosystems,  $\text{SO}_4^{2-}$  reaches the substrate primarily through atmospheric deposition (i.e., rain, snow, dust and aerosol particles) and with the continuous decomposition of organic matter. These processes promote anaerobic conditions in the soil, where the microbial  $\text{SO}_4^{2-}$  reduction uses preferentially the lighter  $^{32}\text{S}$  molecules producing isotopically light  $\text{S}^{2-}$  that can be assimilated by rooted plants (Figure 1.3; Peterson et al., 1985; Canfield, 2001). Similar conditions prevail in hypoxic or anoxic soft bottoms, particularly in estuaries, tidal marshes and other sheltered habitats with fine sediments (Figure 1.3; Peterson et al., 1985). On the other hand, seawater  $\text{SO}_4^{2-}$  originates mainly from the weathering of sulphate-bearing minerals and terrestrial rocks, volcanic emissions and the oxidation of S compounds in the water. Other sources of S into the ocean are the river inputs from land and deep-sea hydrothermal vents, both bringing reduced  $\text{S}^{2-}$  that produce a local decrease in  $\delta^{34}\text{S}$  values which, as they get mixed in the water column, will eventually become part of the marine  $\text{SO}_4^{2-}$  pool when oxidized (Peterson et al., 1985; Eckardt, 2001). Despite these local changes in  $\delta^{34}\text{S}$  values, dissolved  $\text{SO}_4^{2-}$  is one of the most abundant ions in seawater and its long residence time allows for the ocean to act as a large and well-mixed reservoir, integrating the various S sources into consistent isotopic values close to +20.0 ‰ over large periods of time (Peterson and Howarth, 1987; Connolly et al., 2004). Therefore, consumers in marine pelagic food webs relying on phytoplankton and unrooted macrophytes, such as macroalgae, will consistently show higher  $\delta^{34}\text{S}$  values in comparison to those from benthic and coastal communities, especially those supported by rooted macrophytes such as seagrasses and mangroves (Figure 1.3; Peterson, 1999; Connolly et al., 2004).



As in the previous cases, the acquisition of S by consumers also comes from the diet, but the diet-to-tissue discrimination factor of this chemical element is poorly known. The initial use of terrestrial and freshwater food sources to estimate the  $\delta^{34}\text{S}$  fractionation factor led to the wrong conclusion that it was small in comparison to environmental differences (Peterson and Howarth, 1987; McCutchan Jr. et al., 2003), but recent research suggests that it is largely dependent on the  $\delta^{34}\text{S}$  values of the diet (Raoult et al., 2024). For instance, trophic fractionation seems to be much higher in consumers relying on marine food sources with  $\delta^{34}\text{S}$  values close to +20 ‰, than those using terrestrial food sources with  $\delta^{34}\text{S}$  values close to +8 ‰ (Florin et al., 2010; Raoult et al., 2024).

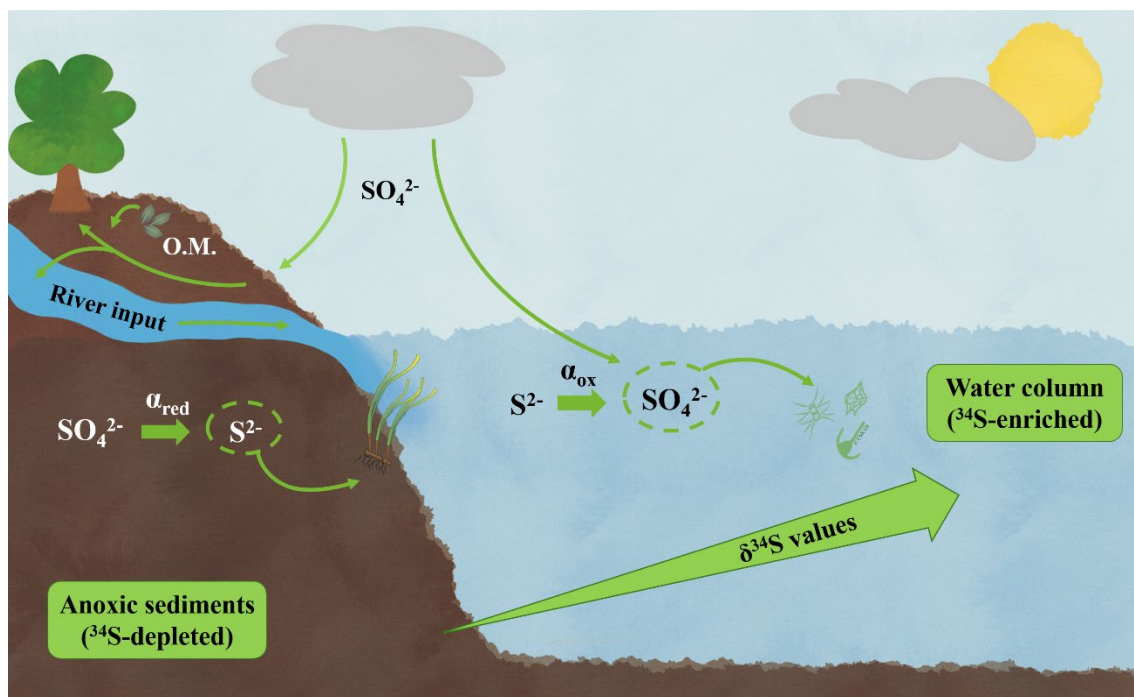


**Figure 1.3.** General distribution of the most abundant sulphur molecules (thin arrows) and of the  $\delta^{34}\text{S}$  values (thick green arrow) according to the oxidative state and the biological processes taking place in each habitat. The constant accumulation of organic matter (O.M.) in terrestrial soils and marine sediments, combined with microbial decomposition creates hypoxic and anoxic conditions where  $\text{SO}_4^{2-}$  is rapidly reduced to  $\text{S}^{2-}$ , which involves a large fractionation ( $\alpha_{\text{red}}$ ) due to the preferential use of the lighter  $^{32}\text{S}$  isotope by microbes. This results in  $\text{S}^{2-}$  with low  $\delta^{34}\text{S}$  values that are assimilated by rooted plants. On the contrary, the well-mixed water column of the open ocean allows for the  $^{34}\text{S}$ -enriched  $\text{SO}_4^{2-}$  to be the most common S source for pelagic primary producers, unrooted macrophytes and those attached to rocks.



## Oxygen stable isotope ratio ( $\delta^{18}\text{O}$ )

In a global spatial scale, the  $\delta^{18}\text{O}$  values of the different water sources depend on the hydrological cycle (Figure 1.4; Gat, 1996). Phase changes (i.e., vapor to liquid to ice and vice versa) have an estimated fractionation of about  $\pm 5\text{‰}$  due to different diffusion rates between molecules carrying the lighter and heavier O isotopes. Thus, the preferential evaporation of the lighter molecules causes precipitation of rain and snow to be  $^{18}\text{O}$ -depleted, whereas the remaining water pool gets enriched in  $^{18}\text{O}$ , especially in warmer regions with higher surface evaporation rates (Gat, 1996). On the other hand, photosynthesis produces  $\text{O}_2$  with similar  $\delta^{18}\text{O}$  values to that of the water used in the reaction (Luz and Barkan, 2011 and references therein) and respiration removes preferentially the lighter  $^{16}\text{O}$  molecules from the atmosphere, leaving the heavier  $^{18}\text{O}$  molecules behind. As a result, atmospheric  $\text{O}_2$  is naturally enriched by a factor of about +20.0 ‰ compared to seawater  $\text{O}_2$ , which is known as the “Dole effect” (Kiddon et al., 1993; Luz and Barkan, 2011). This large-scale variations in the  $\delta^{18}\text{O}$  composition of water sources are useful to track individual migrations, but the use of this intrinsic tracer to make dietary inferences along a food web requires a closer look into regional hydrological processes as well as relevant metabolic pathways used by the involved organisms (Vander Zanden et al., 2016).

Water used by terrestrial primary producers comes from local precipitation and typically shows low  $\delta^{18}\text{O}$  values, which are incorporated into plant tissues through photosynthesis with little fractionation (Gat, 1996). River water also comes primarily from precipitation and hence, in estuarine regions, river runoff brings water with low  $\delta^{18}\text{O}$  values as well as terrestrial plant detritus with a similar isotopic signal into coastal areas (Figure 1.4; Gat, 1996). On the other hand, ocean waters are relatively enriched in  $^{18}\text{O}$  due to the preferential evaporation of the lighter molecules, especially in surface waters (Hoefs, 2018). As in the previous case, this isotopic signal is incorporated into marine primary producers through photosynthesis with little fractionation and then transferred into marine consumers through their prey. Thus, in a typical estuary, the  $\delta^{18}\text{O}$  values will gradually increase from the river mouth towards the open ocean, creating a horizontal gradient that allows to differentiate between consumers feeding in different parts of the ecosystem (Gat, 1996; Vander Zanden et al., 2016). Furthermore, in coastal and oceanic regions without any significant river input, regional variations in the  $\delta^{18}\text{O}$  values of



surface waters can be caused by temperature changes, since warmer regions have a higher evaporation rate which can increase the  $\delta^{18}\text{O}$  values locally and along the respective food web (Gat, 1996; Hoefs, 2018). In some cases, the resulting  $\delta^{18}\text{O}$  gradient can be related to local variations in salinity, since they are controlled by the same processes (e.g., higher evaporation rates in surface waters, freshwater inputs). Hence, in the upper water layers where most marine vertebrates feed, a positive and linear relationship between the  $\delta^{18}\text{O}$  values and the salinity has been described in several water masses across different oceans (LeGrande and Smith, 2006; Conroy et al., 2014; Belem et al., 2019) and occasionally, this relationship seems to hold at great depths (Belem et al., 2019). This has provided the basis for numerous studies on the migration ecology and habitat use of several marine species (e.g., Trueman et al., 2012; Matthews et al., 2016; Drago et al., 2020).

The trophic fractionation of the  $\delta^{18}\text{O}$  values is small compared to environmental gradients, but it can still play an important role when studying the trophic ecology of individuals (Gat, 1996). In both terrestrial and marine ecosystems, the main source of O in a consumer's tissues, and hence the main determinant of their  $\delta^{18}\text{O}$  values, is the ingested water ( $\text{H}_2\text{O}$ ), either through the diet or by direct drinking (Vander Zanden et al., 2016). For air-breathing organisms, the isotopic enrichment caused by the inhaled  $\text{O}_2$  used in respiration can vary with temperature and  $\text{O}_2$  concentration, but it is relatively low despite atmospheric  $\text{O}_2$  being naturally enriched in  $^{18}\text{O}$  (Kiddon et al., 1993). On the other hand, the solubility of  $\text{O}_2$  in water, and thus its concentration, decreases as temperature increases, resulting in a lower discrimination between  $^{16}\text{O}$  and  $^{18}\text{O}$  molecules in biological processes at higher temperatures (Tobias et al., 2007; Hoefs, 2018). Furthermore, the resulting  $\delta^{18}\text{O}$  values of the tissues of ectothermic consumers can be more affected by changes in environmental temperature than those of endothermic consumers, which may produce tissues with more consistent  $\delta^{18}\text{O}$  values independently of the environmental temperature (Kiddon et al., 1993).

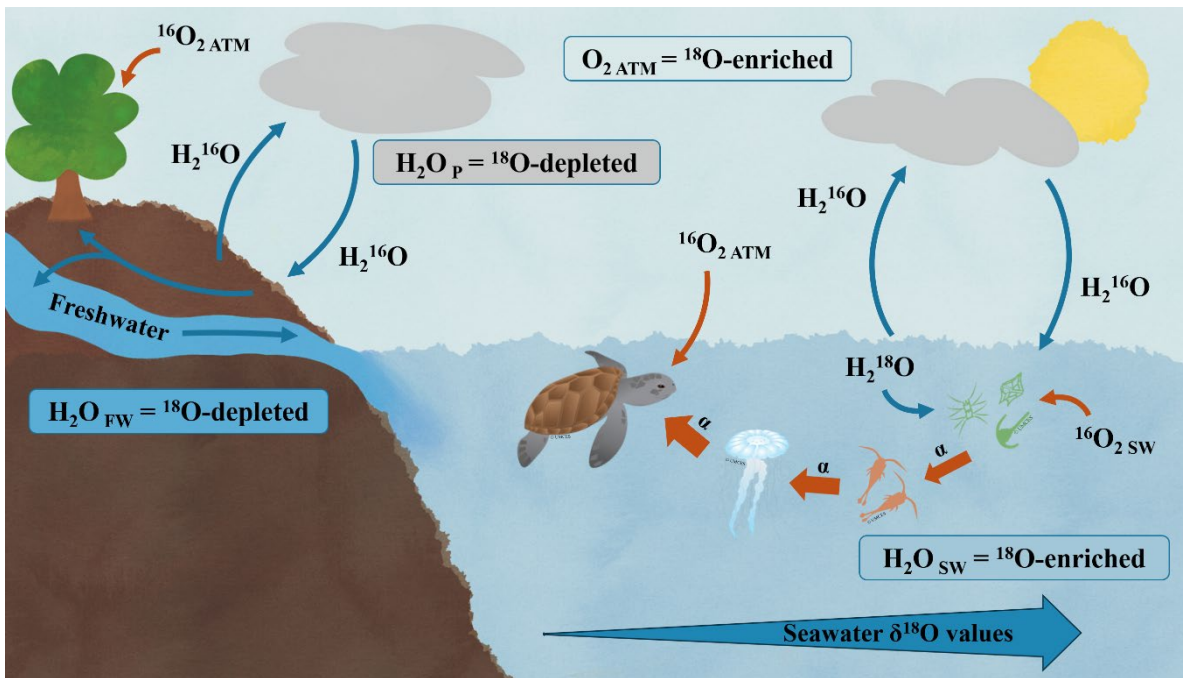


**Figure 1.4.** General distribution of the oxygen stable isotopes ( $^{16}\text{O}/^{18}\text{O}$ ) through the main biological and physical processes of a typical ecosystem. Thin blue arrows indicate the phase changes of water within the hydrological cycle, where downward arrows indicate precipitation and upward arrows indicate evaporation. The preferential use of  $^{16}\text{O}_2$  molecules in respiration (thin orange arrows) causes atmospheric  $\text{O}_2$  ( $\text{O}_2_{\text{ATM}}$ ) to be enriched in  $^{18}\text{O}$  (Dole effect), whereas the preferential evaporation of  $\text{H}_2^{16}\text{O}$  molecules causes precipitation ( $\text{H}_2\text{O}_\text{P}$ ) and hence, freshwater sources ( $\text{H}_2\text{O}_{\text{FW}}$ ), to be depleted in  $^{18}\text{O}$  and produces an enrichment of  $\text{H}_2^{18}\text{O}$  molecules in the remaining surface seawaters ( $\text{H}_2\text{O}_{\text{SW}}$ ). This results in the typical increase of the  $\delta^{18}\text{O}$  values towards oceanic waters in estuarine systems (thick blue arrow). Finally, thick orange arrows demonstrate the transference of  $\delta^{18}\text{O}$  values through the food web, where the discrimination against the heavier molecules ( $\alpha$ ) in biological and metabolic processes in each trophic position results in a slight enrichment of  $^{18}\text{O}$  in top predators.

## 1.2. Characterization of the isotopic niche

One of the most common tools to compare the stable isotope ratio between species or individuals, especially when combining different chemical elements, is through the analysis of the isotopic niche, which is defined as the area in the  $\delta$ -space where the isotopic values concentrate (Newsome et al., 2006; Jackson et al., 2011). This area can be characterized with the calculation of the isotopic niche width, using a Bayesian approach



to create standard ellipses in defined isotopic spaces (isospaces) and the use of multivariate ellipse-based metrics that allow to make robust comparisons among data sets with different sample sizes (Jackson et al., 2011). Here, two species are considered to have different isotopic niches if they do not overlap in at least one of the analysed isospaces (Newsome et al., 2010; Jackson et al., 2011; Syväranta et al., 2013). Nowadays, this method is widely accepted and easy to use (e.g., using the SIBER package in R statistical software; Jackson et al., 2011); however, as explained in the previous sections, the interpretation of the isotopic values of a consumer can be complex. Consequently, the use of a multi-element approach in isotopic ecology has progressively increased to improve the resolution of the isotopic niche by considering various aspects of the ecosystems (e.g., Rossman et al., 2016; Borrell et al., 2021; García-Vernet et al., 2021). Nevertheless, as we will show throughout this thesis, resolution will only improve if there are steep environmental gradients at the appropriate spatial scales.

The presence of intra- and inter-specific variability in isotopic niches among consumers depends not only on the preferred type of diet and habitat used by the species, but also on the degree of isotopic variation among food sources within an ecosystem and among foraging grounds (Matthews and Mazumder, 2004; Newsome et al., 2006). The lack of isotopic differentiation among primary producers can lead to a larger overlap between species and hence, to an underestimation of the variability in resource use, whereas the presence of unique isotopic signals can be a strong indicative of individual or species-specific specialization (Matthews and Mazumder, 2004). Therefore, for a correct characterization of the isotopic niche it is highly important to know the available food sources and their isotopic composition, as well as any temporal and spatial variation on the composition of the diet of consumers and their respective prey items (Matthews and Mazumder, 2004; Newsome et al., 2006).

In addition, there are many factors that can affect the isotopic ratio of an animal's tissue. Physiological processes such as the metabolic pathways used to assimilate nutrients from the diet can be affected by environmental factors such as temperature, salinity and presence of pollutants, which in turn can affect the general health status of an individual and the quality of the food ingested and the routing of nutrients. This can influence both the observed isotopic ratio of a tissue and the trophic enrichment along the food web (Jones et al., 2009; Browning et al., 2014).



### 1.3. Tissue turnover and diet-to-tissue discrimination

The use of stable isotope ratios to study the trophic ecology and habitat use of consumers also requires an understanding of the transference of chemical elements and their respective isotopic signatures along the food webs (Newsome et al., 2010). There are two main factors affecting the relationship between the isotopic compositions of a consumer with that of its prey. The first one relates to the time period integrated by the analysed tissue, which is given by the half-life or turnover rate of a chemical element in a consumer's tissue (Hobson and Clark, 1992; Newsome et al., 2006). The second one is the isotopic diet-to-tissue discrimination factor or trophic fractionation that takes place when an element is integrated into the consumer's tissue through the diet (McCutchan Jr. et al., 2003; Vander Zanden et al., 2015).

The turnover rate of a tissue varies with the taxa and depends on factors such as the physiology of the species (e.g., endothermic or ectothermic) and the metabolic rate of the tissue (Hobson, 1999). In general, metabolically active tissues with a fast turnover rate can reflect the diet of the last days or weeks of an individual (e.g., blood, liver, muscle), whereas those with a slower turnover rate can cover several months (e.g., skin) or even years (e.g., bone, teeth). On the other hand, metabolically inert tissues (e.g., keratinous tissues such as carapace and hair) can also provide several years of data depending on the growth rate and the natural wear of the exposed parts (Tieszen et al., 1983; Rubenstein and Hobson, 2004; Vander Zanden et al., 2015). Furthermore, unfavourable conditions such as extreme temperatures, low quality food or prolonged fasting can also affect the isotopic composition of consumers, especially in ectotherms and tissues with a fast turnover rate (Kidson et al., 1993; Jones et al., 2009).

Similarly, the isotopic trophic fractionation between consumer and prey also depends on the turnover rate of the analysed tissue, as well as the pathways used to metabolize the nutrients carrying each chemical element, which can be considerably different among consumers, tissues and food web systems (McCutchan Jr. et al., 2003; Vander Zanden et al., 2015). For instance, the mean diet-to-tissue enrichment for the  $\delta^{13}\text{C}$  ratio in fin whales ranged from +1.28 ‰ in epidermis to +3.11 ‰ in bone protein (Borrell et al., 2012) and in seals from +0.7 ‰ in red blood cells to +1.9 ‰ in hair (Pinzone et al., 2017). Likewise, the mean  $\delta^{15}\text{N}$  diet-to-tissue enrichment in fin whales ranged from +2.03 ‰ in bone protein to +4.27 ‰ in brain tissue (Borrell et al., 2012), in seals from +3.3 ‰



in red blood cells to +4.3 ‰ in muscle (Pinzone et al., 2017), and from +4.1 ‰ in epidermis to +5.1 ‰ in bone in green turtles (Turner Tomaszewicz et al., 2017b). Furthermore, the rate of isotopic incorporation can also be affected by the individual's age, size and growth rate (Reich et al., 2008; Vander Zanden et al., 2012). As an example, the  $\delta^{13}\text{C}$  enrichment in epidermis of rapidly growing loggerhead turtle hatchlings was larger than in juveniles of the same species kept under identical conditions (+2.62 ‰ and +1.11 ‰, respectively) (Reich et al., 2008). Similar findings were reported between juvenile and adult green turtles (1.87 ‰ and 1.62 ‰, respectively), although in this case, the difference was smaller (Vander Zanden et al., 2012). On the other hand,  $\delta^{15}\text{N}$  enrichment in epidermis of the same loggerhead turtle hatchlings was similar to that of juveniles (+1.65 ‰ and +1.60 ‰, respectively) (Reich et al., 2008), whereas adult green turtles showed a slightly higher enrichment than juveniles (+4.04 ‰ and +3.77 ‰, respectively) (Vander Zanden et al., 2012).

In the case of the  $\delta^{34}\text{S}$  ratio, the enrichment factor of consumers depends mostly on the  $\delta^{34}\text{S}$  values of the diet and less on the type of tissue, with highly  $^{34}\text{S}$ -enriched systems such as the marine showing considerably larger trophic enrichment factors than those relying on  $^{34}\text{S}$ -depleted sources of sulphur (Florin et al., 2010; Raoult et al., 2024). For instance, mean diet-to-tissue enrichment for  $\delta^{34}\text{S}$  in seals was similar in muscle (+0.9 ‰), hair (+1.0 ‰) and red blood cells (+1.1 ‰) (Pinzone et al., 2017). On the contrary, mean  $\delta^{34}\text{S}$  enrichment between salmon (prey) with a mean  $\delta^{34}\text{S}$  value of 19.5 ‰ and bears (consumers) was -3.7 ‰, whereas that between terrestrial grain diets (based on corn, wheat or lentils) with  $\delta^{34}\text{S}$  values under 4.0 ‰ and rats (consumers) was between -0.4 and +1.2 ‰ (Florin et al., 2010). In addition, species with a high-protein diet tend to have a larger enrichment than those with a low-protein diet (McCutchan Jr. et al., 2003). Finally, diet-to-tissue enrichment for the  $\delta^{18}\text{O}$  ratio have been less studied but they are assumed to be low compared to environmental changes, mostly varying with the temperature, the  $\text{O}_2$  concentration, the  $\delta^{18}\text{O}$  values of the food and water ingested by the consumers and the proportion of each water source contributing to tissue formation (Gat, 1996; Vander Zanden et al., 2016).

In this thesis, two metabolically active tissues with different turnover rates were used in two distinct animal groups: bone of marine mammals and sea turtles, and skin (epidermis) of sea turtles. Remodelling in vertebrate's bone varies according to its type,



origin, shape and size, but it also differs among taxa. On one hand, irregular and flat bones such as those from the mandible and skull have a lower volume-to-surface ratio than longer bones and, at least for mammals, they appear to have a slower remodelling rate and thus provide a longer-term dietary signal through the stable isotope analysis (Fahy et al., 2017; de Buffr enil and Quilhac, 2021). Bone samples from marine mammals are often taken in specific parts of the skull (e.g., the pterygoid or the maxilla for odontocetes, the nasal cavity or auditory bulla for pinnipeds) to minimize the damage either for subsequent studies or because they belong to museum collections. Hence, these samples include different parts of the bone tissue and tend to reflect a mean of several years of dietary and habitat use information of each analysed individual (Hobson et al., 2010; Fahy et al., 2017), which was the case for subchapters 3.1 and 3.2.

On the other hand, long tubular bones from limbs, such as the humerus, have two well-differentiated types of tissue with distinct turnover rates. The medullary (spongy) bone at the centre has a higher remodelling rate and hence, a faster turnover rate than the cortical bone, a more compact tissue that surrounds the medullar cavity and is usually formed by parallel layers representing annual growth marks of an individual (de Buffr enil and Quilhac, 2021). Furthermore, the cortical bone can have different deposition methods in different vertebrate groups. In endotherms, such as marine mammals, the cortical bone grows by endosteal deposition of osseous tissue, with the most recent layers deposited in the innermost part of the cortical cavity, whereas in ectotherms, such as sea turtles, this tissue grows by periosteal deposition, meaning that the new layers are deposited at the outermost part of the cortical cavity (Zug et al., 1986; de Buffr enil and Quilhac, 2021). Bone samples from sea turtles can often come from dead stranded or incidentally caught individuals where it is possible to extract the whole humerus and use more specific methods to obtain the samples. However, significant differences in stable isotope ratios have been found between medullar and cortical bone (Brady et al., 2008) and the proportion of these two tissues in a sample can alter the isotopic results (Fahy et al., 2017). Hence, when possible, it is best to only use the cortical bone for stable isotope analysis, as was done in subchapter 3.3. Finally, epidermal tissue in sea turtles has a faster turnover rate compared to bone and can integrate dietary and habitat use information for an individual over several months (Reich et al., 2008), which was the case in subchapter 3.4.



## 1.4. Objectives of the thesis

The main objective of this doctoral thesis is to assess the suitability of  $\delta^{34}\text{S}$  and  $\delta^{18}\text{O}$  as habitat tracers to better understand the habitat use by large marine vertebrates, in combination with the more commonly used isotopic markers  $\delta^{13}\text{C}$  and  $\delta^{15}\text{N}$ . To do so, I have studied a diversity of marine megafauna species from different regions to achieve two main subobjectives:

- I. To improve the resolution of isotopic niche partitioning among marine mammal species of the same community through the stable isotope analysis of bone tissue (subchapters 3.1 and 3.2).
- II. To identify with higher precision the movement patterns and foraging grounds of individual loggerhead turtles across isotopically distinct regions through the stable isotope analysis of different tissues (subchapters 3.3 and 3.4).

## 1.5. Structure of the thesis

The results of this thesis are organized in four subchapters. The first two subchapters (3.1 and 3.2) focus on understanding the isotopic niche partitioning among marine mammal species of two estuarine communities. In **subchapter 3.1**, the distribution of seven marine mammal species from Río de La Plata estuary in Uruguay is described using the  $\delta^{13}\text{C}$ ,  $\delta^{15}\text{N}$ ,  $\delta^{34}\text{S}$  and  $\delta^{18}\text{O}$  values in the bone of stranded individuals and the environmental isotopic gradients formed in the area, where there is a large and constant input of freshwater and terrestrial detritus into the sea (positive estuary). In **subchapter 3.2**, the same was done for seven marine mammal species found along the Mauritanian coast, an area with high temperatures and evaporation rates nearshore that create the opposite salinity gradient (negative estuary) and with constant upwelling events influencing the distribution of nutrients available for primary producers. The results of these research were published in the following scientific articles:



**Cani, A.**, Cardona, L., Valdivia, M., González, E.M. and Drago, M. 2023. Niche partitioning among marine mammals inhabiting a large estuary as revealed by stable isotopes of C, N, S, and O. *Estuaries and Coasts*, 46(4), pp.1083-1097. <https://doi.org/10.1007/s12237-023-01193-y> (3.1)

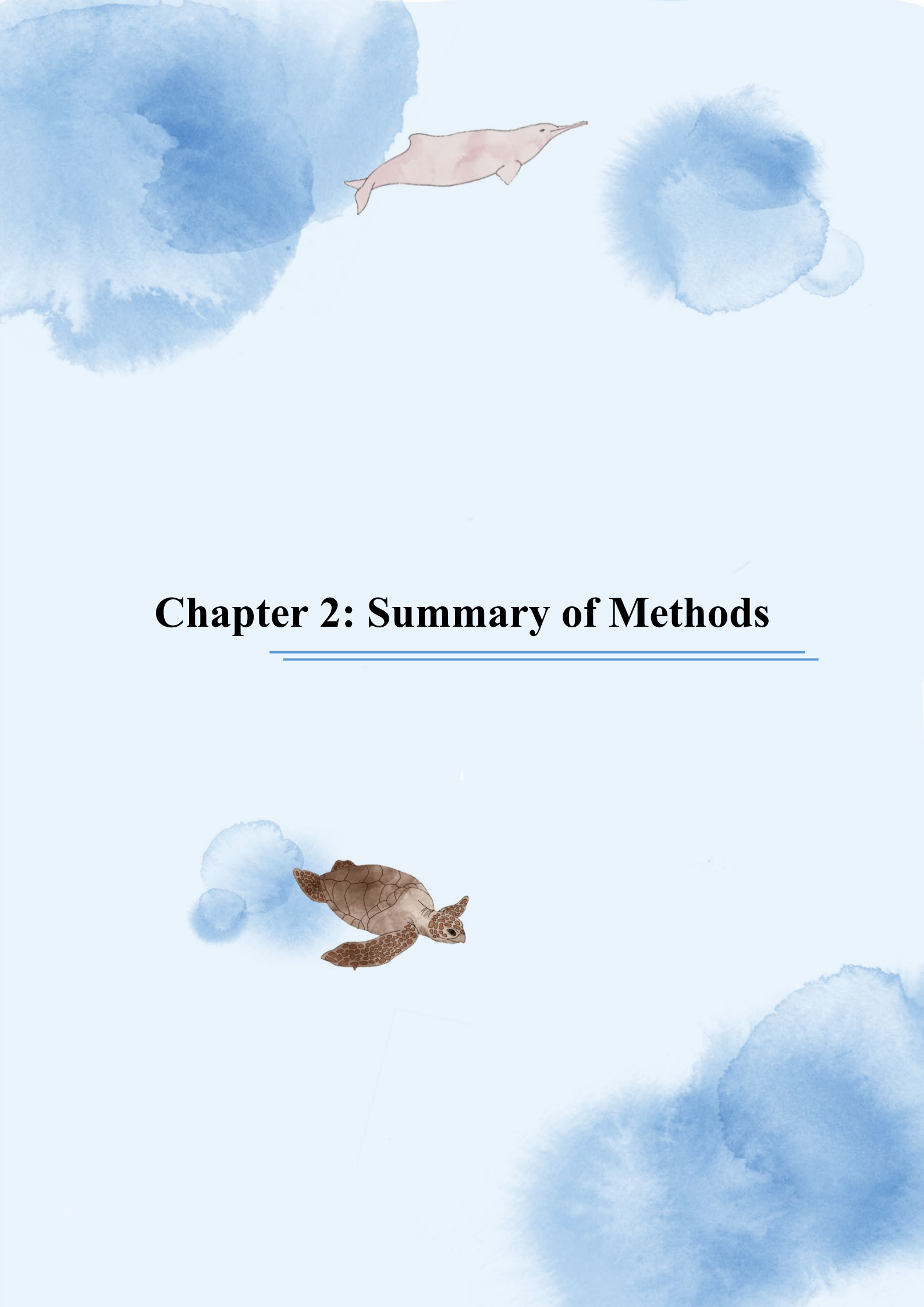
**Cani, A.**, Cardona, L., Aguilar, Á., Borrell, A. and Drago, M. 2024. Fine-tuning the isotopic niche of a marine mammal community through a multi-element approach and variable spatial scales. *Estuarine, Coastal and Shelf Science*, 298, p.108641. <https://doi.org/10.1016/j.ecss.2024.108641> (3.2)

Finally, the last two subchapters (3.3 and 3.4) focus on understanding the movement patterns, habitat use and trophic ecology of individual loggerhead turtles inside the Mediterranean Sea. In **subchapter 3.3**, the  $\delta^{13}\text{C}$ ,  $\delta^{15}\text{N}$  and  $\delta^{18}\text{O}$  values in the bone of juvenile loggerhead turtles born at the nesting beaches of the Northwest Atlantic Ocean and found dead stranded in the western Mediterranean Sea were combined with skeletochronology to determine their movement patterns across isotopically distinct water masses. In **subchapter 3.4**, the  $\delta^{13}\text{C}$ ,  $\delta^{15}\text{N}$  and  $\delta^{34}\text{S}$  values in the epidermis of female loggerhead turtles that had recently nested in Spanish Mediterranean beaches were combined with satellite telemetry to identify their foraging grounds. The results of these research were published in the following scientific articles:

**Cani, A.**, Besén, C., Carreras, C., Pascual, M. and Cardona, L. 2025. The journey of loggerhead turtles from the Northwest Atlantic to the Mediterranean Sea as recorded by the stable isotope ratios of O, C and N of their bones. *Marine Environmental Research*, 203, p.106851. <https://doi.org/10.1016/j.marenvres.2024.106851> (3.3)

Cardona, L., Abalo-Morla, S., **Cani, A.**, Feliu-Tena, B., Izaguirre, N., Tomás, J. and Belda, E.J. 2024. Identifying the foraging grounds of the new loggerhead turtle nesters in the western Mediterranean. *Aquatic Conservation: Marine and Freshwater Ecosystems*, 34(1), p.e4059. <https://doi.org/10.1002/aqc.4059> (3.4)

Furthermore, a summary of the methodologies used in the different subchapters and a synthesis of the results obtained throughout the thesis are presented. Finally, a general discussion and the general conclusions of the research are provided. The thesis concludes with the references cited in the General Introduction and Discussion sections.



## **Chapter 2: Summary of Methods**

---





---

## **2. Methodological overview**

### **2.1. Study areas and species involved**

For this thesis, species inhabiting ecosystems with marked environmental isotopic gradients were chosen. On one hand, a positive and a negative estuary from Uruguay and Mauritania, respectively, were selected for subchapters 3.1 and 3.2 due to the strong and permanent isotopic gradients formed by the physical and chemical conditions of each area. On the other hand, subchapter 3.3 involves the North Atlantic Ocean and the Mediterranean Sea and subchapter 3.4 focuses mostly on the western Mediterranean basin, where weaker but well-defined isotopic gradients are also present (Figure 2.1). The isotopic environmental gradients in each area are detailed below.

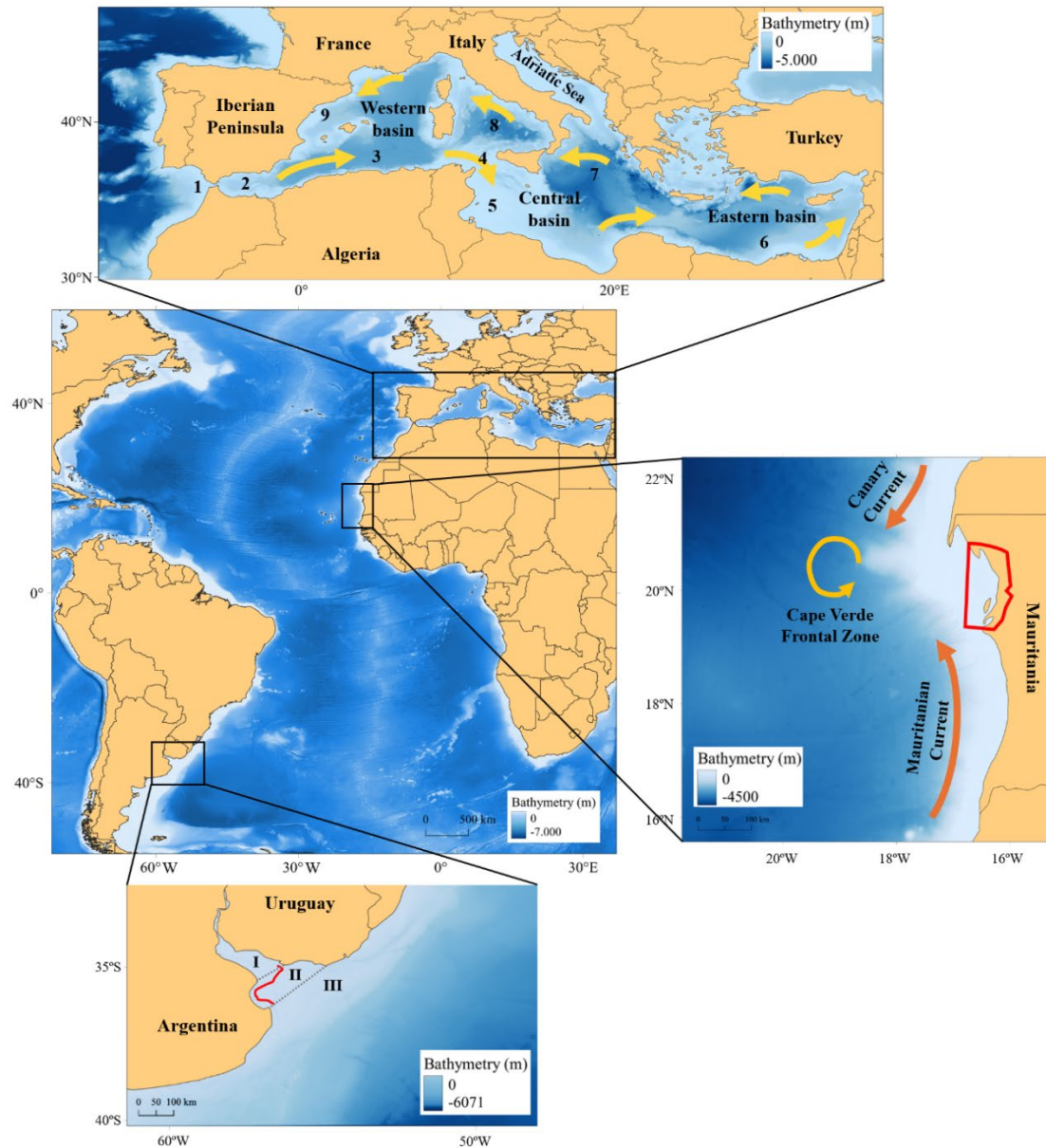


**Figure 2.1.** Central panel: **Atlantic Ocean** and the location of the study areas (black squares). Top panel: **Mediterranean Sea**, showing the general path of surface currents and subregions as 1) Strait of Gibraltar, 2) Alboran Sea, 3) Algerian basin, 4) Channel of Sicily, 5) Tunisian Plateau, 6) Levantine Sea, 7) Ionian Sea, 8) Tyrrhenian Sea, 9) Balearic Sea. Right panel: **Mauritanian coast**, showing the Parc National du Banc d'Arguin (red polygon), the two main surface currents (orange arrows) and their zone of confluence (yellow arrow). Bottom panel: **Río de La Plata estuary**, showing the modal position of the maximum turbidity front (red line) and the division of the three zones as I. Inner estuary, II. Estuary/mixohaline, III. Marine. Background colours represent the respective bathymetry of each area (Gridded Bathymetry Data available at the General Bathymetric Chart of the Ocean 2024: <https://download.gebco.net/>).



### 2.1.1. Río de La Plata estuary

The Río de la Plata estuary represents the greatest fresh-water inflow to the southwestern Atlantic Ocean (Figure 2.1), influencing water circulation at a regional scale. In addition, the nearby confluence of two main currents (the Malvinas and Brazil currents), the abundant terrestrial run-off and the relatively shallow waters produce a unique hydrographic system (Guerrero et al., 1997; Miloslavich et al., 2011). This area is defined as a “positive estuary” because freshwater input exceeds local evaporation, which creates a strong horizontal salinity gradient that increases towards oceanic waters (Pritchard, 1952; Guerrero et al., 1997). In addition, the estuary is characterized by an almost constant vertical stratification and the formation of a salinity wedge in between the saltier marine waters, which move upstream along the bottom and bring marine (high)  $\delta^{34}\text{S}$  and  $\delta^{18}\text{O}$  values into the estuary, and the freshwater layer from the river discharge, which moves top and brings terrestrial (low)  $\delta^{34}\text{S}$  and  $\delta^{18}\text{O}$  values towards the ocean (Peterson and Howarth, 1987; Acha et al., 2008; Botto et al., 2011). Furthermore, a well-developed turbidity front at the tip of the salinity wedge (Figure 2.1, bottom panel) marks the area with the highest accumulation of terrestrial particulate organic matter (POM), which limits primary productivity due to low light availability (Framiñan and Brown, 1996; Acha et al., 2008; Botto et al., 2011). As a result, food webs at the inner estuary are mostly detritus-based whereas phytoplankton concentration notably increases from the estuary mouth and towards the open ocean (Acha et al., 2008).

There are at least three sources of organic matter that support the food webs of the estuary, each with a specific isotopic composition (Framiñan and Brown, 1996; Acha et al., 2008; Botto et al., 2011). At the innermost part, there is a high influence of terrestrial and freshwater marsh detritus characterized by low  $\delta^{13}\text{C}$  and  $\delta^{34}\text{S}$  values. Immediately offshore the turbidity front and within the estuarine zone, there is a higher influence of salt marsh detritus from nearby coastal areas, characterized by high  $\delta^{13}\text{C}$  and low  $\delta^{34}\text{S}$  values, whereas the phytoplankton concentration, characterized by low  $\delta^{13}\text{C}$  and high  $\delta^{34}\text{S}$  values, increases as the light becomes more available, becoming the dominant primary producer at the marine zone (Carreto et al., 2003 and 2008; Acha et al., 2008; Botto et al., 2011). Lastly, the high  $\delta^{15}\text{N}$  values of the POM inside the estuary suggest a strong influence of sewage in the area, affecting the typical increase with trophic position described for this tracer (McClelland and Valiela, 1998; Botto et al., 2011). This



distribution of resources allows for the isotopic distinction of consumers using the different regions of the Río de la Plata estuary (Botto et al., 2011; Drago et al., 2021).

Finally, the following seven species of marine mammals inhabiting the Río de la Plata estuary and nearby waters were selected to analyse their isotopic niche partitioning: two otariids, the South American sea lion *Otaria flavescens* and the South American fur seal *Arctocephalus australis*; and five odontocetes, the pontoporiid franciscana dolphin *Pontoporia blainvillei*, the phocoenid Burmeister's porpoise *Phocoena spinipinnis*, and the delphinids Fraser's dolphin *Lagenodelphis hosei*, false killer whale *Pseudorca crassidens* and bottlenose dolphin *Tursiops truncatus*. More detailed information on this study area and the considered species can be found in subchapter 3.1.

### 2.1.2. Mauritania

The Islamic Republic of Mauritania is located at the Northwestern coast of Africa (Figure 2.1), an area with almost constant upwelling events due to the presence of persistent and strong southward winds which, combined with the Coriolis effect, constantly transport surface waters offshore allowing subsurface waters to be upwelled alongshore (Sevrin-Reyssac, 1993; Cropper et al., 2014). Furthermore, the Mauritanian coast can be defined as a “negative estuary” because the high environmental temperatures and shallow shelf, especially inside the Parc National du Banc d'Arguin (PNBA; Figure 2.1, right panel), result in high evaporation rates and create regions of particularly high salinity values nearshore that gradually decrease towards oceanic waters (Pritchard, 1952; Sevrin-Reyssac, 1993).

Mauritanian waters represent a transition between tropical and subtropical waters with constantly enhanced coastal primary production, hence supporting a large biodiversity of tropical, subtropical and boreal species (Robineau and Vely, 1998; Cropper et al., 2014; Pelegrí et al., 2017). From the north, the salty, cold and nutrient-rich Canary Current, characterized by high  $\delta^{18}\text{O}$  values, flows southward along the northern coast of Mauritania in the “Permanent Annual Upwelling Zone” (Cropper et al., 2014). These waters reach the northern parts of the PNBA where the shallow seas, pronounce tidal changes and high temperatures result in particularly high  $\delta^{18}\text{O}$  values and create anoxic sediments characterized by low  $\delta^{34}\text{S}$  values, which likely affects rooted benthic primary producers such as seagrasses and mangroves (Wolff and Smith, 1990; Araujo



and Campredon, 2016; Pottier et al., 2021). From the south, the less salty, warmer, and nutrient-poorer Mauritanian Current, characterized by low  $\delta^{18}\text{O}$  values, flows northward along the Mauritanian coast (Mittelstaedt, 1991; Fischer et al., 2016) where the seasonal trade winds produce a series of upwelling events, more frequently during winter, in the “Mauritania-Senegalese Upwelling Zone” (Cropper et al., 2014). In addition, the offshore convergence of these two currents creates the Cape Verde Frontal Zone, a boundary defined by the location of the 36 isohaline at the 150 m depth (Zenk et al., 1991) and where both water masses can get upwelled and laterally mixed, adding more complexity and dynamism to the area (Meunier et al., 2012).

Different habitats can be found along the Mauritanian coast. Rocky cliffs with scattered and tide-dependent sandy beaches with seagrass patches can be found to the north, whereas the southern coast is mostly covered by sandy beaches with scattered sublittoral seagrass patches. Furthermore, the inner parts of the PNBA are composed of tidal mudflats with no vegetation in the northern region and seagrass patches and mangroves in the southern regions (Lebigre, 1991; Pottier et al., 2021; Pinela et al., 2010). In this case, the  $\delta^{15}\text{N}$  values appear to be a good indicator of trophic position while the isotopic differentiation between local primary producers allows the distinction between food webs and habitats used by consumers, since benthic rooted primary producers are characterized by high  $\delta^{13}\text{C}$  values and oceanic phytoplankton by low  $\delta^{13}\text{C}$  values, whereas the upwelling-derived phytoplankton presents values in-between these two (Cardona et al., 2009; Pinela et al., 2010; Carlier et al., 2015).

Lastly, the following seven species of marine mammals inhabiting Mauritanian waters were selected to analyse their isotopic niche partitioning: Atlantic humpback dolphin *Sousa teuszii*, bottlenose dolphin *Tursiops truncatus*, harbour porpoise *Phocena phocena*, long-finned pilot whale *Globicephala melas*, Atlantic spotted dolphin *Stenella frontalis*, common short-beak dolphin *Delphinus delphis*, and Mediterranean monk seal *Monachus monachus*. More detailed information on this study area and the considered species can be found in subchapter 3.2.

### 2.1.3. North Atlantic Ocean and Mediterranean Sea

The Gulf Stream is one of the main currents of the North Atlantic Ocean, showing a significant influence over water circulation and climate for the northern hemisphere



(Palter, 2015). It originates at the Gulf of Mexico, flows northward along the coast of Florida and separates from the continental slope at around 35° N, moving eastward towards the Azores and splitting into the North Atlantic Current, which continues towards northern Europe, and the Azores Current, which then turns into the Canary Current and flows southward along the western coast of South Africa to then return to the Northwest Atlantic as the North Equatorial Current (Fofonoff, 1981; Schmitz and McCartney, 1993). Nevertheless, part of the Azores Current extends to the Strait of Gibraltar, where it enters the Mediterranean Sea as the Algerian Current and flows counter-clockwise throughout the entire basin, getting gradually transformed into a denser water mass that will eventually sink and outflow back into the Northeast Atlantic as a deep water current (Figure 2.1; Fofonoff, 1981; Schmitz and McCartney, 1993; Millot and Taupier-Letage, 2005).

The Mediterranean Sea is a semi-enclosed system divided into three main basins: western, central and eastern. The western basin receives a steady inflow of fresher Atlantic surface waters, characterized by relatively low  $\delta^{18}\text{O}$  values, from the Strait of Gibraltar in the southwest, which then reaches the Alboran Sea and the Algerian Basin (Millot and Taupier-Letage, 2005). Part of these waters remain within the western basin to form the western Mediterranean gyre, moving northward through the Tyrrhenian Sea and reaching the Balearic Sea from the north before returning to the Alboran Sea. Meanwhile, another part continues alongslope towards the central basin, going through the Strait of Sicily and eventually reaching the eastern Mediterranean gyre (Figure 2.1, top panel; Millot and Taupier-Letage, 2005). As the water circulates, the higher evaporation rates in the eastern Mediterranean lead to a parallel increase of salinity and  $\delta^{18}\text{O}$  values, reaching the highest values at the Levantine Sea (Millot and Taupier-Letage, 2005; LeGrande and Smith, 2006). On the other hand, the western Mediterranean presents a high primary production in both oceanic (pelagic) and coastal (neritic) areas, whereas the central and eastern regions, except for the Adriatic Sea, are highly oligotrophic and only show relatively high primary production in certain coastal regions (Bosc et al., 2004). Therefore, food webs relying on pelagic primary producers with low  $\delta^{13}\text{C}$  and  $\delta^{15}\text{N}$  values are more likely to be found in the western basin, while neritic food webs showing higher  $\delta^{13}\text{C}$  and  $\delta^{15}\text{N}$  values are probably common in the central and eastern basins, thus allowing the isotopic differentiation between consumers with different trophic habits (Cardona et al., 2009; DiMatteo et al., 2022).



Lastly, juvenile loggerhead turtles *Caretta caretta* of Northwestern Atlantic origin were selected to analyse changes in habitat use and trophic ecology throughout their time at the Mediterranean Sea, whereas adult females of the same species that had recently nested along the Mediterranean coast of Spain were used to identify their foraging grounds. More detailed information on these area and considered individuals can be found in subchapters 3.3 and 3.4.

## 2.2. Tissues

Throughout this thesis, two different tissues (bone and skin) were analysed using three different sampling methods. All tissues were cleaned with distilled water and dried in a stove at 60 °C prior to treatment and analysis. For subchapters 3.1 and 3.2, a small fragment of the skull was sampled from dead stranded marine mammals and grounded into a fine powder using a mortar and pestle. Bone tissue was also used in subchapter 3.3 but, in this case, different incremental layers of the cortical bone of loggerhead turtles' humeri were sampled separately for each individual using a hand drill with a fine diamond tip. Finally, for subchapter 3.4, skin samples of loggerhead turtles were taken either from dead stranded individuals, dead hatchlings found inside the nests, or directly from the nesting females on the beach.

Bone tissue has a relatively slow turnover rate in tetrapods, thus the isotopic values obtained from these samples integrate several years of information on the habitat use of the considered individuals (Hobson et al., 2010; Schoeninger 2010; Fahy et al., 2017). On the other hand, epidermal tissue has a faster turnover rate, integrating dietary information over several months prior to sampling (Reich et al., 2008). More details on each sampling method are given in the respective subchapters.

## 2.3. Stable isotope analysis

Each sample was cleaned and dried following the standard procedures for stable isotope analysis considering the species, tissue and chemical element analysed, as explained below and throughout chapter 3. Stable isotope abundances are expressed in delta ( $\delta$ ) notation, with the relative variations of stable isotope ratios expressed in per mil (‰) deviations from predefined international standards, and they are calculated as:



$$\delta^jX = \left[ \frac{(^jX / ^iX)_{\text{sample}}}{(^jX / ^iX)_{\text{standard}}} \right] - 1 \quad (4)$$

where  $^jX$  is the heavier isotope and  $^iX$  is the lighter isotope in the analytical sample and international measurement standard, respectively (Bond and Hobson, 2012).

This thesis uses the stable isotope ratios of C, N, S and O to make inferences about the habitat use and trophic ecology of the considered species. In each case, a combination of three or four of these chemical elements were used, and the recognized international standards used for comparison were the Vienna Peedee Belemnite (VPDB) for the  $\delta^{13}\text{C}$ , the atmospheric nitrogen (AIR) for the  $\delta^{15}\text{N}$ , the Vienna Cañon Diablo Meteorite Troilite (VCDT) for the  $\delta^{34}\text{S}$ , and the Vienna Standard Mean Ocean Water (VSMOW) for the  $\delta^{18}\text{O}$ , although other materials of known stable isotope ratio were used as internal laboratory standards, which is a common practice since the stocks of some of the official materials are either depleted or highly expensive (Ben-David and Flaherty, 2012; Bond and Hobson, 2012).

### 2.3.1. Carbon stable isotope analysis

Animal tissues contain two main types of macromolecules, proteins and lipids that can differ largely in their  $\delta^{13}\text{C}$  values. This is because lipids are naturally depleted in  $^{13}\text{C}$ , which may add undesirable variability for the  $\delta^{13}\text{C}$  values in lipid-rich tissues (DeNiro and Epstein, 1978). Furthermore, carbonate occur in the bone tissue as a component of biological apatite (bioapatite), but also as inorganic carbon of environmental origin that might have precipitated during tissue formation (Yokoyama et al., 2005). In addition, mineral compounds such as bioapatite in bone contain information about the whole diet, making it more susceptible to have a higher  $\delta^{13}\text{C}$  variability, whereas the collagen (protein fraction) mostly represents the  $\delta^{13}\text{C}$  values from dietary proteins, thus allowing to track the diet with a greater precision especially for consumers with a protein-rich diet such as cetaceans and pinnipeds (Newsome et al., 2010). For these reasons, bone powder samples from marine mammals were treated with 0.5 N hydrochloric acid (HCl) for 24h to dissolve the inorganic matrix and remove all the inorganic C (Lorrain et al., 2003; Newsome et al., 2006) and with a chloroform-methanol 2:1 solution for lipid extraction, which was changed every 24h until it was transparent (Table 2; Bligh and Dyer, 1959; Bas et al., 2019). Such pre-processing was not necessary for cortical bone and skin of sea



turtles due to the low carbonate and lipid content of both tissues (Table 2; Turner Tomaszewicz et al., 2015; Bergamo et al., 2016).

### **2.3.2. Nitrogen stable isotope analysis**

Contrary to carbon, the  $\delta^{15}\text{N}$  values in a consumers' tissue come exclusively from the proteins in the diet, thus eliminating the need to remove other molecules from the tissue samples. The  $\delta^{15}\text{N}$  analysis is often performed together with the  $\delta^{13}\text{C}$  using the same tissue sample, which was the case for sea turtles' bone and skin. However, acid treatment and lipid extraction can significantly affect the  $\delta^{15}\text{N}$  values in marine mammal's bone tissue; therefore, separate subsamples of powdered bone were used in these cases for the  $\delta^{15}\text{N}$  analysis, without any chemical pre-treatment (Table 2; Schlacher and Connolly, 2014; Bas et al., 2019).

### **2.3.3. Sulphur stable isotope analysis**

Similarly to nitrogen, a consumer's  $\delta^{34}\text{S}$  values come strictly from the dietary amino acids, more specifically methionine and cysteine (Francioso et al., 2020). Hence, there is no need for any treatment of the tissue samples previous to the  $\delta^{34}\text{S}$  analysis (Table 2; Nehlich, 2015).

### **2.3.4. Oxygen stable isotope ratio analysis**

The  $\delta^{18}\text{O}$  values in consumers come from a combination of dietary and metabolic water (Kirsanow and Tuross, 2011; Vander Zanden et al., 2016) and the analysis is best carried out in the inorganic matrix of calcified structures such as bone, since they show a more stable  $\delta^{18}\text{O}$  signature than soft tissues (Koch et al., 1997; Mooney, 2004). Therefore, all bone samples from marine mammals and sea turtles were treated, previous to the  $\delta^{18}\text{O}$  analysis of bone carbonate, with 30% hydrogen peroxide ( $\text{H}_2\text{O}_2$ ) for 48h to remove the organic compounds and with 1 M calcium acetate–acetic acid buffer for 24h to remove the diagenetic carbonate (Table 2; Koch et al., 1997).

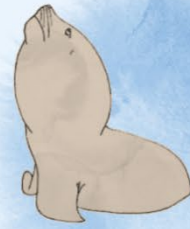
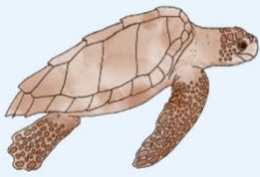


**Table 1.2.** Summary of the methods for stable isotope analysis for each group and tissue selected for this thesis. In sea turtle's bone (\*) and skin (x) the  $\delta^{13}\text{C}$  and  $\delta^{15}\text{N}$  were analysed simultaneously with the same sample.

Isotopic ratio	Group	Tissue	Pre-treatment	Sample	
				Type	Weight
$\delta^{13}\text{C}$	Marine mammals	Bone	I. Inorganic carbon removal: 0.5 N HCl II. Lipid removal: chloroform-methanol (2:1)	Skull	1.0 mg
	Sea Turtles	Bone	None	Humerus	1.0 mg <sup>x</sup>
		Skin	None	Epidermis	0.3 mg <sup>*</sup>
$\delta^{15}\text{N}$	Marine mammals	Bone	None	Skull	1.0 mg
	Sea Turtles	Bone	None	Humerus	1.0 mg <sup>x</sup>
		Skin	None	Epidermis	0.3 mg <sup>*</sup>
$\delta^{34}\text{S}$	Marine mammals	Bone	None	Skull	10 mg
	Sea Turtles	Skin	None	Epidermis	3.0 mg
$\delta^{18}\text{O}$	Marine mammals	Bone	I. Organic matrix removal: 30 % $\text{H}_2\text{O}_2$ II. Diagenetic carbonate removal: 1 M calcium acetate–acetic acid	Skull	1.0 mg
	Sea Turtles	Bone	I. Organic matrix removal: 30 % $\text{H}_2\text{O}_2$ II. Diagenetic carbonate removal: 1 M calcium acetate–acetic acid	Humerus	1.0 mg

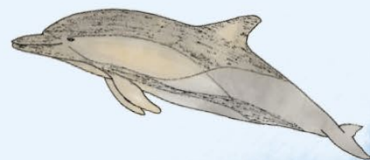
## 2.4. Isotopic niche partitioning

Differences among the isotopic niches of the considered species (subchapters 3.1 and 3.2) or groups (subchapters 3.3 and 3.4) were analysed by estimating the isotopic niche width and niche overlaps through the construction of two-dimensional plots for the different pairs of stable isotope ratios (isospaces) using the package “SIBER” (Stable Isotope Bayesian Ellipses; Jackson et al., 2011) in R Statistical Software (R Core Team, 2021). In this case, two species/groups were considered to have different isotopic niches if they did not overlap in at least one of the analysed isospaces. More details on each statistical analysis are given in the respective subchapters.



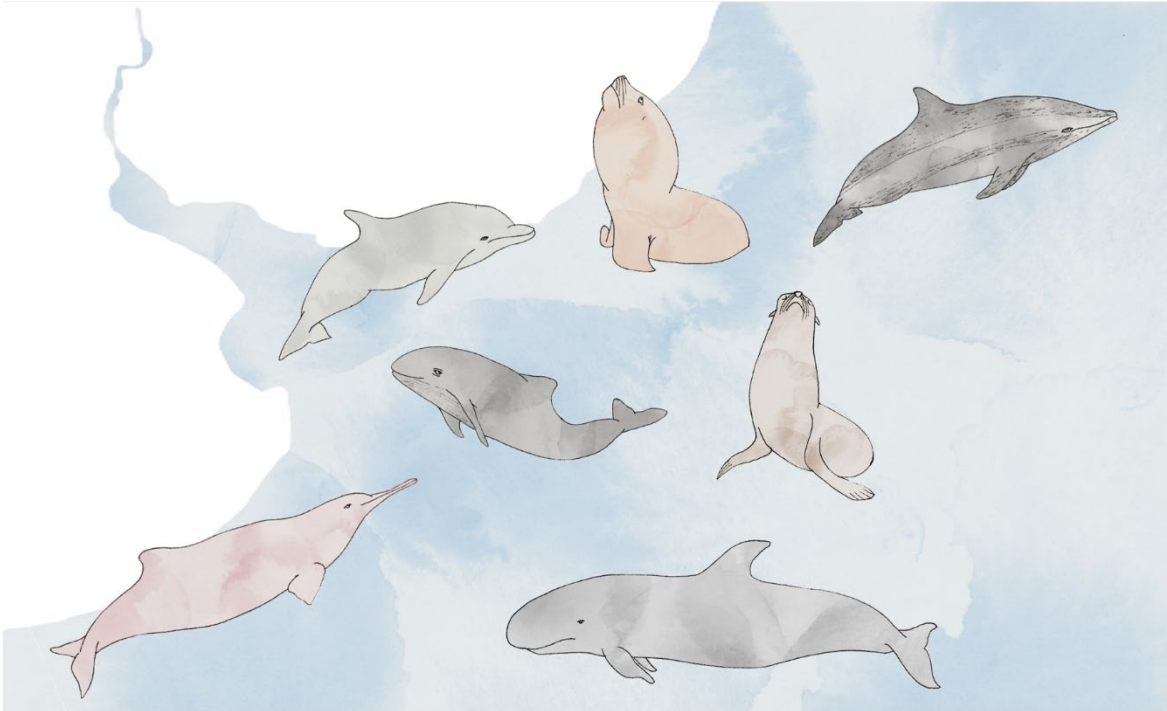
## **Chapter 3: Results**

---





**3.1. Article 1: “Niche partitioning among marine mammals inhabiting a large estuary as revealed by stable isotopes of C, N, S and O”**



**Cani, A., Cardona, L., Valdivia, M., González, E.M. and Drago, M. 2023. Niche Partitioning Among Marine Mammals Inhabiting a Large Estuary as Revealed by Stable Isotopes of C, N, S, and O. *Estuaries and Coasts*, 46(4), pp.1083-1097, <https://doi.org/10.1007/s12237-023-01193-y>**





## Niche partitioning among marine mammals inhabiting a large estuary as revealed by stable isotopes of C, N, S and O.

### ABSTRACT

Detailed knowledge on habitat use by marine mammals is critical to understand their role in the ecosystem. The stable isotope ratios of carbon ( $\delta^{13}\text{C}$ ) and nitrogen ( $\delta^{15}\text{N}$ ) have been widely used to study the trophic ecology of marine mammals, but the stable isotope ratios of other elements such as sulphur ( $\delta^{34}\text{S}$ ) and oxygen ( $\delta^{18}\text{O}$ ) can better inform about habitat use in areas with strong salinity and redox gradients. The Río de la Plata estuary represents the largest freshwater runoff in the south-western Atlantic Ocean and supports a rich community of marine mammals. Here, we analysed  $\delta^{34}\text{S}$  values in bone from seven marine mammal species inhabiting the estuary and the adjacent Atlantic Ocean, in order to complement previous isotopic data ( $\delta^{13}\text{C}$ ,  $\delta^{15}\text{N}$  and  $\delta^{18}\text{O}$ ) and compare their resolution as habitat tracers. As expected,  $\delta^{34}\text{S}$  and  $\delta^{18}\text{O}$  offered relevant insights into the characterization of the habitat used by marine mammals and allowed a better delineation of habitat partitioning between them. Bottlenose dolphins, South American sea lions and South American fur seals seem to be frequent users of the less saline areas of the estuary, whereas Burmeister's porpoises, franciscana dolphins and false killer whales seemed to prefer the saltier marine waters close to the bottom. Fraser's dolphins were the only inhabitants of true offshore waters. Our findings demonstrate how the integration of different stable isotope ratios can help disentangle fine habitat partitioning between marine mammals living in a complex ecosystem such as Río de la Plata.

**Keywords:** stable isotopes, marine mammals, habitat use, resource partitioning, positive estuary.



## INTRODUCTION

Knowledge on the habitat use of the different marine mammal species is key to understand their ecological function in an ecosystem, to evaluate direct and indirect interactions with anthropogenic activities, and to ensure a proper management of the marine biodiversity (Barlow 2018; Roman and Ester 2018). Río de la Plata is one of the largest estuaries in South America. It not only has a relevant role in the regional circulation pattern, but also supports a rich community of marine mammals of disparate origins (Guerrero et al., 1997; Miloslavich et al., 2011). The franciscana dolphin (*Pontoporia blainvillei*) is an endemic species to Río de la Plata and adjoining regions in the southwestern Atlantic Ocean, whereas the South American sea lion (*Otaria flavescens*), the South American fur seal (*Arctocephalus australis*) and the Burmeister's porpoise (*Phocoena spinipinnis*) are widespread in the temperate and cold regions of South America, from southern Brazil to Peru. On the other hand, the Fraser's dolphin (*Lagenodelphis hosei*), the bottlenose dolphin (*Tursiops truncatus*) and the false killer whale (*Pseudorca crassidens*) have circumtropical distributions, although the latter two also occur in temperate regions and the false killer whale may even reach the sub-Antarctic tip of South America (Reeves et al. 2002).

Species such as bottlenose dolphins, South American sea lions and fur seals have been intensively studied and there is no doubt that they make an extended use of the Río de la Plata estuary, although sea lions and fur seals may also forage in adjoining coastal waters (Wells and Scott, 2018; Cárdenas-Alayza, 2018a; Drago et al., 2021). On the contrary, the Fraser's dolphin is a poorly studied species, although the scarce information available suggests an oceanic niche (Dolar, 2018; Drago et al., 2021). Moreover, the habitat preferences of false killer whales, franciscana dolphins and Burmeister's porpoises in the region are not completely understood, because contradictory information has been reported in the literature about their distribution in the estuary, and no good model of habitat partitioning exists to date in the regions where they coexist (Baird, 2018; Cárdenas-Alayza, 2018b; Crespo, 2018; Reyes, 2018; Drago et al., 2020; Drago et al., 2021).

Detailed information on the habitat use of marine mammals is difficult to collect, because direct observations are often challenging and satellite tracking is of limited utility for the study of small cetaceans (Balmer et al., 2014). This is why the stable isotopes of several chemical elements have been used increasingly since the 1970s as intrinsic



markers to study the trophic ecology and habitat use patterns of marine mammals (Newsome et al., 2010; Ramos and González-Solís 2012).

The stable isotopes of carbon (C) and nitrogen (N) are the most widely used elements in studies related to the trophic ecology of marine mammals, but the interest on the stable isotopes of sulphur (S) and oxygen (O) has increased recently (Rubenstein and Hobson 2004; Newsome et al., 2010; Ramos and González-Solís 2012; Drago et al., 2020; Borrell et al., 2021). The C stable isotope ratio ( $^{13}\text{C}/^{12}\text{C}$ ;  $\delta^{13}\text{C}$ ) is informative about the primary source of carbon in a specific food web, mostly due to a different discrimination against the heavier  $^{13}\text{C}$  isotope during photosynthesis between primary producers (Peterson and Howarth 1987; Michener and Lajtha 2007). In general, the highest  $\delta^{13}\text{C}$  values are observed in species with inshore benthic habits, and the lowest in offshore epipelagic consumers (Rubenstein and Hobson 2004; Newsome et al., 2010). On the other hand, the N stable isotope ratio ( $^{15}\text{N}/^{14}\text{N}$ ;  $\delta^{15}\text{N}$ ) increases consistently along the food web due to the trophic enrichment caused by the preferential use and excretion of the light  $^{14}\text{N}$  isotope, providing a convenient and simple method to assess the trophic position of the species (Post 2002).

Although popular as proxies for diet reconstruction, the use of  $\delta^{13}\text{C}$  and  $\delta^{15}\text{N}$  as habitat tracers can be hindered by geographic shifts in diet and the isotopic baseline (Rubenstein and Hobson 2004; Michener and Lajtha 2007; Newsome et al., 2010). For this reason, the use of the S stable isotope ratios ( $^{34}\text{S}/^{32}\text{S}$ ;  $\delta^{34}\text{S}$ ) as a habitat tracer in marine mammals has increased in the last decade, often in combination with  $\delta^{13}\text{C}$  and  $\delta^{15}\text{N}$  (Croisetière et al., 2009; Pinzone et al., 2019; Borrell et al., 2021). Differences in  $\delta^{34}\text{S}$  values are caused by the variability in source of inorganic sulphur available to primary producers, with little to no trophic discrimination (Peterson et al., 1985). In estuarine food webs, both terrestrial plants and aquatic primary producers using anoxic sediments with intense sulphate reduction (i.e., seagrasses and marsh plants) have lower  $\delta^{34}\text{S}$  values than marine phytoplankton and benthic macroalgae using  $^{34}\text{S}$ -enriched sulphates from the water-column (Peterson et al., 1985; Peterson 1999; Croisetière et al., 2009). As fractionation during uptake and assimilation is minimal (Peterson et al., 1985), the  $\delta^{34}\text{S}$  values in animal tissues reflect their food sources and allow to position them along the redox gradient existing from reduced, anoxic sediments found often inshore and in benthic regions, to the more oxidizing conditions found within the water column in offshore and pelagic regions (Peterson et al., 1985; Rubenstein and Hobson 2004; Ramos and González-Solís 2012).



On the contrary, the O stable isotope ratio ( $^{18}\text{O}/^{16}\text{O}$ ;  $\delta^{18}\text{O}$ ) has been rarely used in ecological studies on marine mammals, despite being relatively common in other research areas such as paleontology (Seyboth et al., 2018; Newsome et al., 2010). The  $\delta^{18}\text{O}$  values in the marine environment are positively and linearly correlated with the salinity of the water (Gat 1996; Conroy et al., 2014), and therefore, it can be a useful habitat tracer in areas where an abundant freshwater input creates marked horizontal and vertical salinity gradients (Guerrero et al., 1997; Conroy et al., 2014; Belem et al., 2019). The  $\delta^{18}\text{O}$  values in animal tissues often reflect with great precision those of the body of water where they feed (Yoshida and Miyazaki 1991; Ben-David and Flaherty 2012), allowing to discriminate between species with estuarine, coastal and marine habits (Clementz and Koch 2001; Rubenstein and Hobson 2004; Newsome et al., 2010; Matthews et al., 2016; Drago et al., 2020).

The present study combines previously published values of  $\delta^{13}\text{C}$ ,  $\delta^{15}\text{N}$  (Drago et al., 2021) and  $\delta^{18}\text{O}$  (Drago et al., 2020), with unpublished  $\delta^{34}\text{S}$  values from the bone tissue of seven marine mammal species, in order to provide a fine resolution model of habitat partition between marine mammals in estuarine habitats. In addition, it was aimed to assess the usefulness of the less common  $\delta^{34}\text{S}$  and  $\delta^{18}\text{O}$  values to obtain reliable information of habitat use in these ecosystems.

## METHODS

### *Study area*

The Río de la Plata estuary is located at approximately 35° S and 55° W, in the south-western Atlantic Ocean (Figure 3.1). It is 320 km long (Framiñan and Brown 1996) and has an average discharge of  $2.0 - 2.5 \times 10^4 \text{ m}^3 \text{ s}^{-1}$ , representing the biggest fresh-water inflow and terrestrial run-off to the region (Guerrero et al., 1997; Miloslavich et al., 2011). In addition, the confluence of two major currents off the estuary – the cold, nutrient-rich Falkland/Malvinas current, and the warm, nutrient-poor Brazil current – creates a series of oceanographic structures (i.e. eddies, marine fronts) that increase the biological production in the area (Miloslavich et al., 2011).

Primary production is particularly high at the estuary, considered one of the most productive environments in the world, and it plays a major role in supporting the rich biodiversity found along the Uruguayan coast (Acha et al., 2004; Guerrero et al., 1997; Miloslavich et al., 2011; Ortega and Martinez 2007). This includes several marine



mammal species that feed and breed along its large basin (Bastida et al., 2007; Miloslavich et al., 2011).

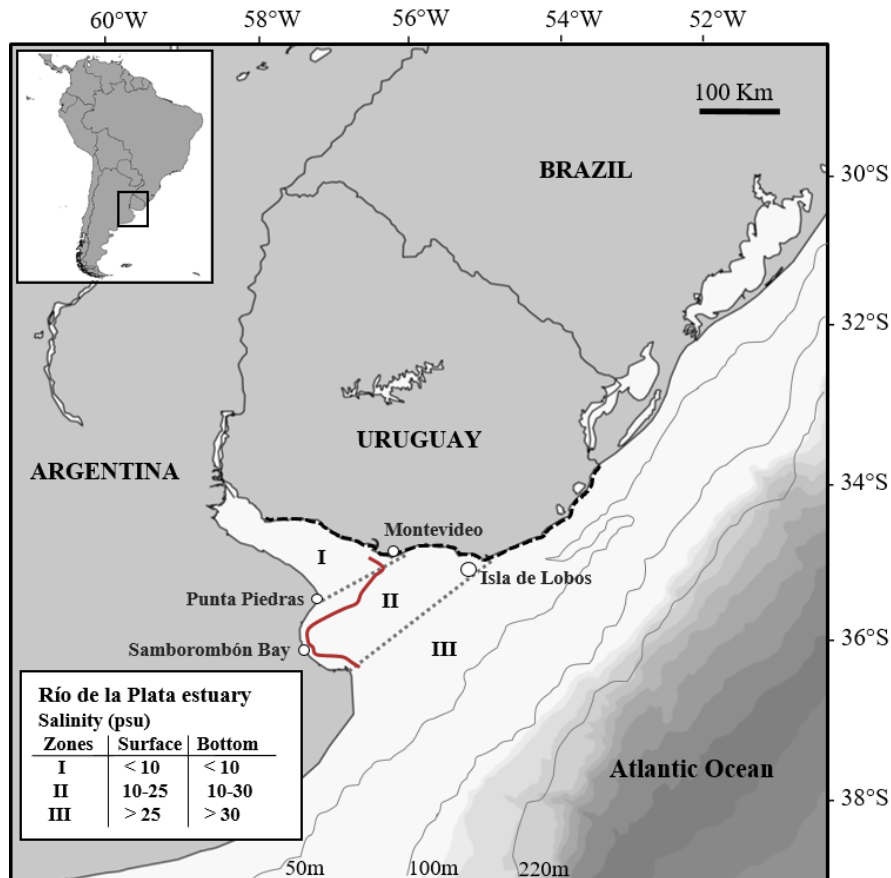


**Figure 3.1.** Study area and sampling locations. The black dashed lines show the sampling area along the Uruguayan coast for the skulls of the seven marine mammal species included in this study; the grey dashed lines delineate the boundaries between the zones with different salinity: (I) the inner estuarine zone, defined by the bottom salinity front; (II) the estuary/mixohaline zone, defined between the surface and bottom salinity fronts; (III) the marine zone. Sea surface salinity and bottom salinity values (Guerrero et al., 1997; Moreira and Simionato 2019) are reported in practical salinity units (psu). The red line represents the modal position of the maximum turbidity zone for the estuary (Acha et al., 2008)

The bathymetry of the relatively shallow waters of the Río de la Plata estuary creates a unique hydrographic system. Since the freshwater input exceeds local evaporation, this area can be defined as a “positive estuary”, with a strong horizontal gradient as salinity increases steadily towards oceanic waters (Pritchard, 1952; Guerrero et al., 1997). In addition, the estuary is characterized by an almost constant vertical stratification, with the saltier marine waters moving upstream along the bottom of the estuary, and the freshwater layer originating from the river discharge remaining atop the



water column, thus creating a salinity wedge in between the two water masses (Guerrero et al., 1997; Acha et al., 2008). A bottom salinity front is defined at the upstream reach of the salt wedge by the topography, and a surface salinity front results from the convergence of estuarine and marine waters combined with the direction and velocity of the winds, among other factors (Figure 3.1; Framiñan and Brown 1996; Guerrero et al., 1997; Acha et al., 2008). Typically, salinity increases with the distance from the inner estuary, varying from 0 psu at the river mouth to 33 psu at the marine zone, and with depth, more evident towards the estuarine zone (Figure 3.1; Framiñan and Brown, 1996; Guerrero et al., 1997; Acha et al., 2008; Moreira and Simionato, 2019).

A well-developed turbidity front, also known as the maximum turbidity zone, is formed by the flocculation of suspended matter at the tip of the salinity wedge, and the resuspension of sediment due to the tidal stirring over the Barra del Indio shoal, between Punta Piedras and Montevideo (Figure 3.1). Furthermore, the food webs within the estuary seem to be supported by at least three sources of organic matter: terrestrial detritus, marsh plant detritus, and phytoplankton (Framiñan and Brown, 1996; Acha et al., 2008; Botto et al., 2011), although their distribution is not equal. At the innermost part of the estuary, around the maximum turbidity zone, there is a high influence of terrestrial and freshwater marsh plant detritus due to light limitations. Immediately offshore these turbidity front and within the estuary/mixohaline zone, the influence of the salt marsh detritus coming from Samborombón Bay (Figure 3.1) increases, as well as the phytoplankton concentration as the light becomes more available. Finally, the marine zone is dominated mostly by phytoplankton (Carreto et al., 2003 and 2008; Acha et al., 2008; Botto et al., 2011). This distribution of resources will determine the distinct isotopic values found along the Río de la Plata estuary (Botto et al., 2011).

### ***Sampling***

A total of 133 bone samples of seven marine mammal species were analyzed, including two otariids, the South American sea lion *Otaria flavescens* (n = 11 ♀, 10 ♂), and the South American fur seal *Arctocephalus australis* (n = 14 ♀, 13 ♂); and five odontocetes, the pontoporiid franciscana dolphin *Pontoporia blainvillei* (n = 11 ♀, 11 ♂), the phocoenid Burmeister's porpoise *Phocoena spinipinnis* (n = 1 ♀, 4 ♂, 5 unknown), and the delphinids Fraser's dolphin *Lagenodelphis hosei* (n = 3 ♀, 2 ♂, 5 unknown), false killer whale *Pseudorca crassidens* (n = 3 ♀, 3 ♂, 4 unknown), and bottlenose dolphin *Tursiops truncatus* (n = 5 ♂, 5 unknown). Bone tissue has a relatively slow turnover rate



and hence, the values reported here integrate information on the habitat use of each individual over several years (Hobson et al., 2010; Schoeninger, 2010; Fahy et al., 2017).

Every specimen included in this study was found dead stranded along the Uruguayan coastline or was incidentally caught by Uruguayan fishermen between 1958 and 2012. All bone samples were collected from skulls in the scientific collection of the Museo Nacional de Historia Natural (MNHN) and the Facultad de Ciencias of the Universidad de la República (UdelaR) at Montevideo (Uruguay), and consisted of a small fragment of crushed bone from the nasal cavity (turbinate bone) for the otariids, and the maxilla for the odontocetes.

It should be noted that, based on their skull characteristics, all bottlenose dolphins included in this study belong to specimens of the subspecies *T. t. gephyreus* (Lahille's bottlenose dolphin), the coastal ecotype (Costa et al., 2016; Wickert et al., 2016). All the skulls from South American sea lions, South American fur seals and franciscana dolphins were considered to belong to adult or physically mature specimens (see Drago et al., 2017 and 2018 for details on age determination). The age and standard length of the individuals of the remaining species were unknown, but the condylobasal length of each skull was measured to ensure that only specimens of similar body size were included and thus avoid any age-related bias (Drago et al., 2018 and 2020). The condylobasal length ranged 55 - 59 cm for bottlenose dolphins, 27 - 29 cm for Burmeister's porpoises, 39 - 44 cm for Fraser's dolphins, 61 - 65 cm for false killer whales (Drago et al., 2020).

### ***Stable isotope analysis***

Bone samples were cleaned with distilled water, oven dried at 60°C for 36 h, and ground into a fine powder using a mortar and pestle. For the  $\delta^{34}\text{S}$ , no pre-treatment was applied to the bone prior to the analysis in order to avoid eliminating amino acids that contain this element. Approximately 10 mg of each bone sample was weighed into a tin capsule, and vanadium pentoxide ( $\text{V}_2\text{O}_5$ ) was added as catalyst to accelerate the combustion and reduce variability (Nehlich and Richards 2009). Samples were loaded and combusted at 1035 °C and analysed with an Elemental Analyzer (Carlo Erba 1108) coupled to a Delta Plus XP mass spectrometer through a ConFlow III interface (both from Thermofisher) at Centres Científics i Tecnològics (CCiT-UB) of the University of Barcelona, Spain. International isotope secondary standards distributed by the International Atomic Energy Agency (IAEA) of known  $^{34}\text{S}/^{32}\text{S}$  ratios, in relation to the Vienna- Canyon Diablo Troilite (VCDT) were used. These consisted in barium sulphate



(NBS-127:  $\delta^{34}\text{S} = +21.2\text{‰}$ , IAEA SO-5:  $\delta^{34}\text{S} = +0.5\text{‰}$  and IAEA SO-6:  $\delta^{34}\text{S} = -34.1\text{‰}$ ) and YCEM ( $\delta^{34}\text{S} = +12.8$ ), and they were employed once every 12 samples. Analytical precision for repeat measurements of the reference material, run in parallel with the bone samples, was 0.1 ‰.

The  $\delta^{18}\text{O}$ ,  $\delta^{13}\text{C}$  and  $\delta^{15}\text{N}$  values from the same samples were compiled from Drago et al., (2020 and 2021).

The Suess effect (Keeling, 1979) correction was applied to all the original values of  $\delta^{13}\text{C}$  to compensate for the increment of atmospheric  $\text{CO}_2$  over time and to allow for comparison of  $\delta^{13}\text{C}$  values of specimens from different periods (see Drago et al., 2021 for details on Suess effect correction factor determination). Furthermore, because  $\delta^{18}\text{O}$  values in animal studies are more commonly presented relative to the Vienna Standard Mean Oceanic Water (V-SMOW) index,  $\delta^{18}\text{O}$  values were converted from PDB to SMOW according to the following equation (Koch et al., 1997):

$$\delta^{18}\text{O}_{(\text{SMOW})} = [\delta^{18}\text{O}_{(\text{PDB})} \times 1.03086] + 30.86 \quad (1)$$

Stable isotope abundances are expressed in delta ( $\delta$ ) notation, with the relative variations of stable isotope ratios expressed in per mil (‰) deviations from predefined international standards, and they were calculated as:

$$\delta^j\text{X} = [(^j\text{X}/^i\text{X})_{\text{sample}}] / [(^j\text{X}/^i\text{X})_{\text{standard}}] - 1 \quad (2)$$

where  $^j\text{X}$  is the heavier isotope ( $^{13}\text{C}$ ,  $^{15}\text{N}$ ,  $^{18}\text{O}$  or  $^{34}\text{S}$ ), and  $^i\text{X}$  is the lighter isotope ( $^{12}\text{C}$ ,  $^{14}\text{N}$ ,  $^{16}\text{O}$  or  $^{32}\text{S}$ ) in the analytical sample and international measurement standard (Bond and Hobson, 2012).

### ***Data analysis.***

Normality was tested by means of the Lilliefors test, and homoscedasticity by means of the Levene test, with only  $\delta^{34}\text{S}$  and  $\delta^{15}\text{N}$  values showing homogeneity of variances. Differences between the stable isotope ratios ( $\delta^{18}\text{O}$ ,  $\delta^{34}\text{S}$ ,  $\delta^{13}\text{C}$  and  $\delta^{15}\text{N}$ ) of males and females of the three species with the largest sample size (franciscana dolphins, South American sea lions and South American fur seals) were assessed through a Permutational Multivariate Analysis of Variance (PERMANOVA; Anderson 2001 and 2014), using the *vegan* package version 2.5-7 with 999 permutations (Oksanen et al., 2020). Since differences were found between sexes for the two otariids (see Results for details), nine groups were considered for further analysis: the five odontocetes species plus females and males of the two otariid species. Boxplots of the original values for each



stable isotope ratio were built to compare the average values and ranges of each species using one-way ANOVA followed by a Scheffe post-hoc test.

In order to identify differences in the isotopic niches of the considered marine mammal groups, the  $\delta^{18}\text{O}$ ,  $\delta^{34}\text{S}$ ,  $\delta^{13}\text{C}$  and  $\delta^{15}\text{N}$  values were combined using a PERMANOVA test followed by a pairwise multilevel comparison with the Bonferroni correction for multiple comparisons (Chen et al., 2017), using the package *pairwiseAdonis* with 999 permutations (Martinez Arbizu, 2020). However, since the pairwise comparison seemed to account more for the similarities than the differences between species (i.e. if two species had similar values in at least two stable isotope ratios, they were sometimes considered ‘similar’), two-dimensional plots were built using the package “SIBER” (Stable Isotope Bayesian Ellipses; Jackson et al., 2011) to estimate the isotopic niche width and overlaps between the marine mammal groups for the different pairs of stable isotope ratios. This was also used to recognize the dimensions in which those ‘similar’ species differed, and to estimate the best isotopic niche discriminator among the analyzed stable isotope ratios. Two complementary approaches were used to estimate the isotopic niche width (Jackson et al., 2011): the standard ellipse areas corrected for small sample size (SEAc) were used to plot the isotopic niche of each species within the isotopic space (isospace) and to calculate the overlap among species, and the Bayesian standard ellipse areas (SEAb) were used to obtain an unbiased estimate of the isotopic niche width with 95% credibility intervals.

All statistical analyses and plots were carried out using R Statistical Software v 4.1.2 (R Core Team, 2021). Statistical results are reported according to Smith (2020).

## RESULTS

Given the small difference between the average values of  $\delta^{34}\text{S}$ ,  $\delta^{18}\text{O}$ ,  $\delta^{15}\text{N}$  and  $\delta^{13}\text{C}$  of female and male franciscana dolphins (0.07 ‰, 0.09 ‰, 0.24 ‰ and 0.23 ‰, respectively; Table 3.1), both sexes were pooled in one group for later analysis. On the contrary, the average  $\delta^{34}\text{S}$  and  $\delta^{15}\text{N}$  values of South American sea lions were higher in males than in females (1.68 ‰ and 1.10 ‰, respectively) and hence, considered biologically different (Table 3.1). Therefore, both sexes were considered independently in further analysis. Similarly, the average values of  $\delta^{34}\text{S}$ ,  $\delta^{18}\text{O}$  and  $\delta^{15}\text{N}$  of male South American fur seals were higher than those of females (1.15 ‰, 0.34 ‰, 0.87 ‰, respectively; Table 3.1) and both sexes were also treated as separate groups in further analysis.



**Table 3.1** Comparisons between stable isotope ratios ( $\delta^{13}\text{C}$ ,  $\delta^{15}\text{N}$ ,  $\delta^{18}\text{O}$  and  $\delta^{34}\text{S}$ ) in females and males of franciscana dolphins, South American sea lions and South American fur seals, using PERMANOVA. First, the four stable isotope ratios were considered together, if differences between males and females were considered biologically relevant, the stable isotope ratios of each element was compared independently for the two sexes

Species	Stable isotope ratios	R <sup>2</sup>	p-value
Franciscana dolphins ( <i>Pontoporia blainvillei</i> ) ♀ vs ♂	All (n = 11 ♀; 11 ♂)	0.011	0.889
	All (n = 11 ♀; 10 ♂)	0.227	0.009
South American sea lions ( <i>Otaria flavescens</i> ) ♀ vs ♂	$\delta^{34}\text{S}$	0.236	0.037
	$\delta^{18}\text{O}$	0.137	0.119
	$\delta^{13}\text{C}$	0.010	0.698
	$\delta^{15}\text{N}$	0.335	0.014
South American fur seals ( <i>Arctocephalus australis</i> ) ♀ vs ♂	All (n = 14 ♀; 13 ♂)	0.203	0.009
	$\delta^{34}\text{S}$	0.189	0.027
	$\delta^{18}\text{O}$	0.142	0.048
	$\delta^{13}\text{C}$	0.128	0.077
	$\delta^{15}\text{N}$	0.296	0.004

The mean values of the nine groups considered here (five odontocetes species plus females and males of the two otariid species) were scattered along a gradient for the four stable isotope ratios analysed (Figure 3.2). In each case, either bottlenose dolphins or sea lions were at one extreme and Fraser's dolphins at the other (Figure 3.2), with differences between the average values at both extremes of 3.78 ‰ for  $\delta^{34}\text{S}$ , 2.32 ‰ for  $\delta^{18}\text{O}$ , 2.71 ‰ for  $\delta^{13}\text{C}$ , and 6.06 ‰ for  $\delta^{15}\text{N}$ . According to the  $\delta^{18}\text{O}$  values, South American sea lions (both females and males), bottlenose dolphins and female South American fur seals presented the lowest mean  $\delta^{18}\text{O}$  values; male South American fur seals, franciscana dolphins and false killer whales had intermediate values, whereas Burmeister's porpoises and Fraser's dolphins showed the highest  $\delta^{18}\text{O}$  (Figure 3.2). Similar placements between species were found for the  $\delta^{13}\text{C}$  values, although in this case, female South American fur seals presented intermediate values (Figure 3.2). Moreover, bottlenose dolphins, Burmeister's porpoises, female sea lions and franciscana dolphins had similarly low mean  $\delta^{34}\text{S}$ , whereas the Fraser's dolphins and male fur seals presented the highest  $\delta^{34}\text{S}$  (Figure



3.2). In addition, the largest differences found between females and males for both otariids were in the  $\delta^{34}\text{S}$  values, with males having considerably higher mean values than the respective females (Figure 3.2). Lastly, the Fraser's dolphins had the lowest  $\delta^{15}\text{N}$  values and appear to be different from the remaining species, whereas Burmeister's porpoises, franciscana dolphins and South American sea lions (females and males) showed the highest  $\delta^{15}\text{N}$  values (Figure 3.2).

The PERMANOVA and pairwise multilevel comparison comprising the four stable isotope ratios and the seven marine mammal species together, indicated differences between most of the considered groups (Supp. Table 1). On one side, female and male sea lions shared similar isotopic niches ( $R^2 = 0.227$ , adjusted p-value = 0.216;  $n = 11$  and  $n = 10$ , respectively), but only males showed similarities with those of false killer whales ( $R^2 = 0.357$ , adjusted p-value = 0.072;  $n = 10$  and  $n = 10$ , respectively) and Burmeister's porpoises ( $R^2 = 0.337$ , adjusted p-value = 0.072). Likewise, female and male fur seals also showed similar isotopic niches ( $R^2 = 0.203$ , adjusted p-value = 0.072;  $n = 14$  and  $n = 13$ , respectively), but only that of females was similar to that of Burmeister's porpoises ( $R^2 = 0.234$ , adjusted p-value = 0.072;  $n = 14$  and  $n = 10$ , respectively). Other groups with similar isotopic niches, according to this analysis, were female and male fur seals and false killer whales ( $R^2 = 0.086$ , adjusted p-value = 1.000; and  $R^2 = 0.128$ , adjusted p-value = 1.000, respectively) and Burmeister's porpoises with bottlenose dolphins ( $R^2 = 0.263$ , adjusted p-value = 0.072;  $n = 10$  and  $n = 10$ , respectively), franciscana dolphins ( $R^2 = 0.095$ , adjusted p-value = 1.000;  $n = 10$  and  $n = 22$ , respectively) and false killer whales ( $R^2 = 0.220$ , adjusted p-value = 0.072;  $n = 10$  and  $n = 10$ , respectively). However, when comparing these results with the differences found initially with the ANOVA and Scheffe test (Figure 3.2), some groups considered here as 'similar' had different mean values for at least one stable isotope ratio. One clear example was between Burmeister's porpoises and bottlenose dolphins, considered similar by the pairwise comparison (Supp. Table 1) despite the differences in  $\delta^{18}\text{O}$  and  $\delta^{13}\text{C}$  (Figure 3.2) that already showed biologically relevant differences in their isotopic niches.

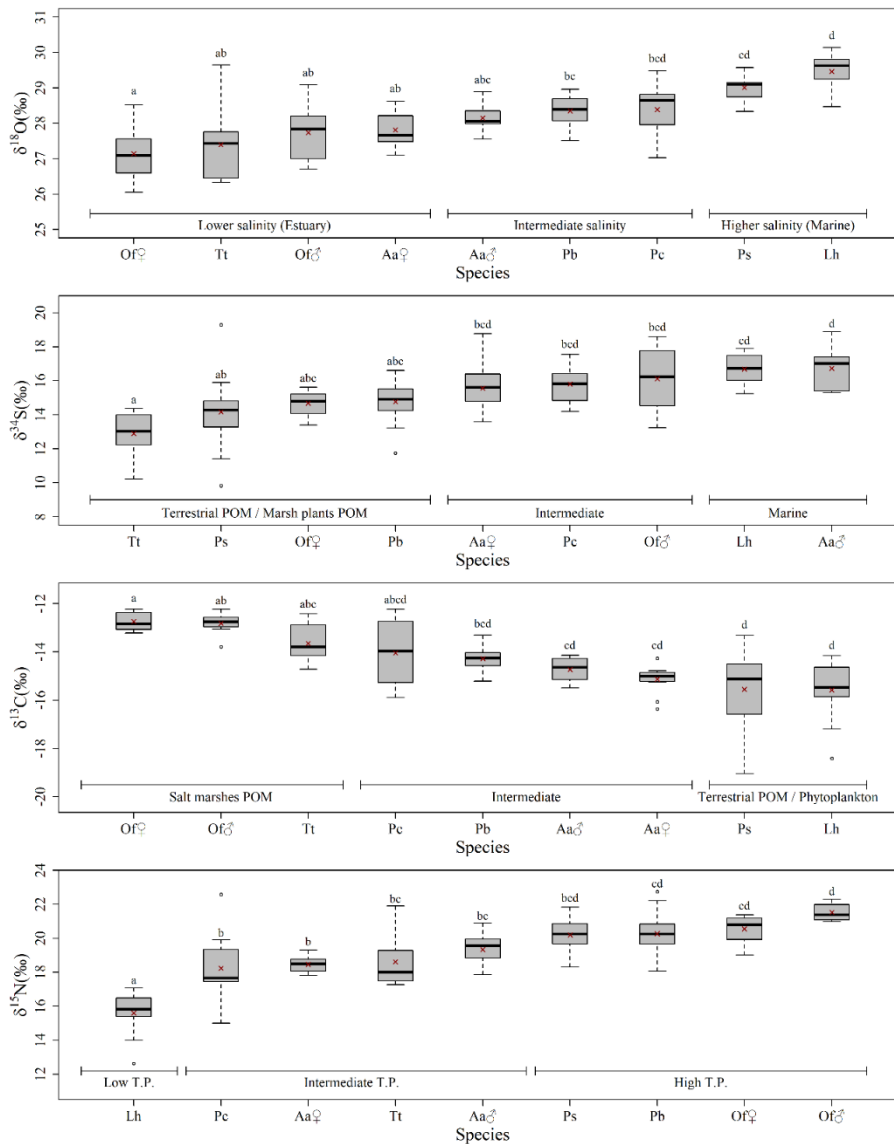


**Figure 3.2.** Boxplots of the isotopic values ( $\delta^{18}\text{O}$ ,  $\delta^{34}\text{S}$ ,  $\delta^{13}\text{C}$  and  $\delta^{15}\text{N}$ ) of the considered marine mammal species from Río de la Plata estuary and adjacent areas, organized by the mean values indicated in each case by a red “x”. Groups with different superscript (lower case letters) are statistically different in their mean values, according to the Scheffe post-hoc test following nested ANOVA. Boxes represent the first and third quartile, lines the median, and whiskers 95% confidence interval. A general description of the habitat and trophic habits suggested by both, the values for each stable isotope ratio and the origin of resources described by Botto et al., (2011) and Peterson and Howarth (1987) is showed underneath the boxes, with POM = Particulate organic matter; and T.P. = Trophic Position. Sample sizes and species/groups: female South American sea lions (Of ♀, n = 11), male South American sea lions (Of ♂, n = 10), female South American fur seals (Aa ♀, n = 14), male South American fur seals (Aa ♂, n = 13), bottlenose dolphins (Tt, n = 10), franciscana dolphins (Pb, n = 22), false killer whales (Pc, n = 10), Burmeister’s porpoises (Ps, n = 10) and Fraser’s dolphins (Lh, n = 10).  $\delta^{13}\text{C}$  values are corrected for Suess effect

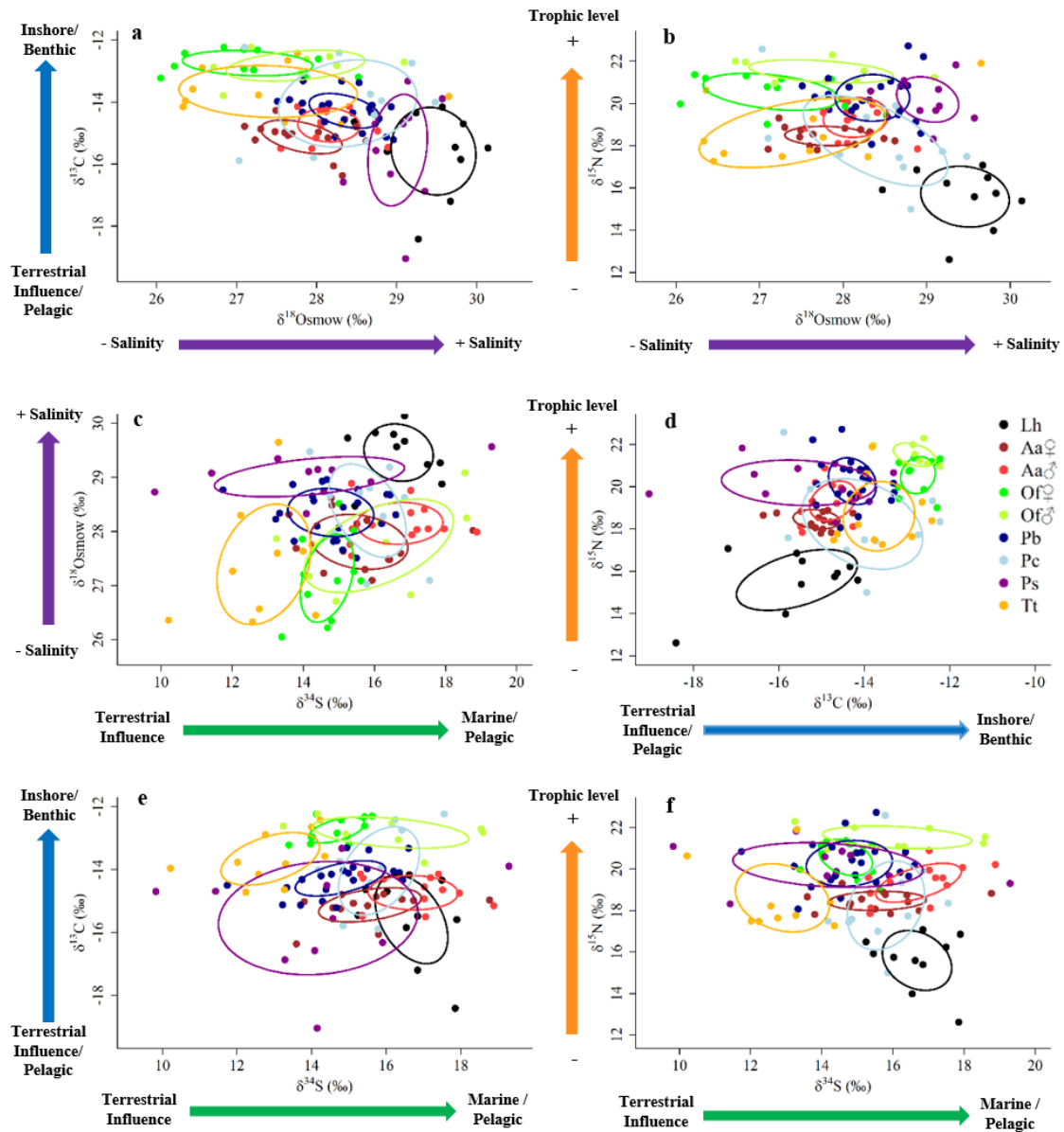


**Figure 3.3.** Standard ellipses of the marine mammal groups from Río de la Plata estuary, corrected for small sample size (SEAc), in the isospace defined by  $\delta^{18}\text{O}$ ,  $\delta^{34}\text{S}$ ,  $\delta^{13}\text{C}$  and  $\delta^{15}\text{N}$ . The colored arrows indicate the general interpretation of the isotopic values for each element as written, where blue corresponds to carbon ( $\delta^{13}\text{C}$ ), purple to oxygen ( $\delta^{18}\text{O}$ ), orange to nitrogen ( $\delta^{15}\text{N}$ ) and green to sulphur ( $\delta^{34}\text{S}$ ) stable isotope ratios. Sample sizes and species/groups: female South American sea lions (Of ♀,  $n = 11$ ), male South American sea lions (Of ♂,  $n = 10$ ), female South American fur seals (Aa ♀,  $n = 14$ ), male South American fur seals (Aa ♂,  $n = 13$ ), bottlenose dolphins (Tt,  $n = 10$ ), franciscana dolphins (Pb,  $n = 22$ ), false killer whales (Pc,  $n = 10$ ), Burmeister's porpoises (Ps,  $n = 10$ ) and Fraser's dolphins (Lh,  $n = 10$ ).  $\delta^{13}\text{C}$  values are corrected for Suess effect. The percentage of overlapped area between each pair of species/groups is available in Supp. Table 2

A better view of these differences between isotopic niches was obtained through the estimation of the area of the standard ellipse of each marine mammal group (Figure 3.3) and the overlapped area between each pair for the different dimensions (Supp. Table 2). Most groups did not overlap in at least one pair of stable isotope ratios and hence were considered to exploit different isotopic niches. However, the following seven pairs showed constant overlap of isotopic niche areas in all the considered dimensions: males and females for both otariids; franciscana dolphins and Burmeister's porpoises; and false killer whales with: Fraser's dolphins, fur seals (females and males) and franciscana dolphins (Figure 3.3; Supp. Table 2).

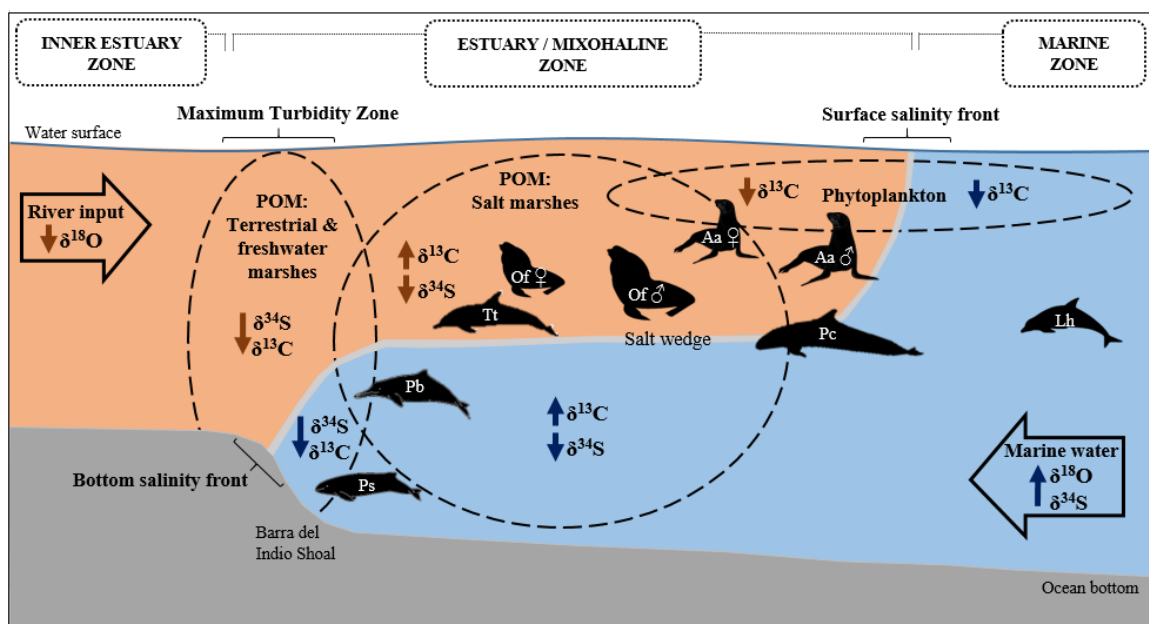


**Figure 3.4.** Graphical representation of the estimated habitat preferences of the considered marine mammal groups from the Río de la Plata estuary, based on the combination of  $\delta^{18}\text{O}$ ,  $\delta^{34}\text{S}$ ,  $\delta^{13}\text{C}$  and  $\delta^{15}\text{N}$  values reported here, the physical and ecological processes of the estuary explained by Acha et al., (2008), and the origin of resources affecting the different zones of the estuary and their respective isotopic values reported by Botto et al., (2011) and Peterson and Howarth (1987). The short arrows show the general tendency of the respective stable isotope ratio in a given zone, where upward arrows indicate high values (enriched) and downward arrows indicate low values (depleted); POM = particulate organic matter. Species/groups: bottlenose dolphins (Tt), female South American sea lions (Of ♀), male South American sea lions (Of ♂), female South American fur seals (Aa ♀), male South American fur seals (Aa ♂), false killer whales (Pc), Burmeister's porpoises (Ps), franciscana dolphins (Pb) and Fraser's dolphins (Lh).



## DISCUSSION

The results reported here revealed fine niche partitioning between the seven species of marine mammals studied, and demonstrated the utility of combining the stable isotope ratios of four elements to characterize the isotopic niche of consumers inhabiting estuaries with strong gradients of salinity and redox potential.

### *Assessing the method*

The addition of  $\delta^{34}\text{S}$  and  $\delta^{18}\text{O}$  to the initial  $\delta^{13}\text{C} - \delta^{15}\text{N}$  isospace described by Drago et al. (2021) provided with unique and useful information about the habitat use of the seven species of marine mammals considered here, allowing a better characterization of their individual isotopic niches (Franco-Trecu et al., 2017).

Each stable isotope ratio ( $\delta^{18}\text{O}$ ,  $\delta^{34}\text{S}$ ,  $\delta^{13}\text{C}$  and  $\delta^{15}\text{N}$ ) characterized a different dimension of the isotopic niche of each group and provided complementary information on their habitat preferences and trophic position. The isotopic niches revealed by combining four stable isotope ratios allowed not only to confirm some of the information reported in the literature, but also to gain new knowledge on the habitat use of some species, as well as to infer differences between apparently similar groups. It is worth noting that species with similar isotopic niches do not necessarily have the same distribution, as isotopic similarity only indicates similar preferences for certain environmental conditions, which could be found in different areas along the estuary (Acha et al., 2008). Furthermore, bone tissue acts as a long-term integrator of the stable isotope ratios due to its relatively slow turnover rate, which makes it useful to obtain information over extended periods of time (Hobson et al., 2010; Schoeninger 2010; Fahy et al., 2017; Skedros et al., 2013; Matsubayashi et al., 2017; Tomaszewicz et al., 2018; Matsubayashi and Tayasu 2019). Accordingly, the values reported here for each individual are averages integrating habitat use over a period of several years, but lack resolution on shorter time scales (weeks to months).

The pairwise multilevel comparison employed after the PERMANOVA has been used in different studies to compare three or more stable isotope ratios between different species of marine mammals (Borrell et al., 2021). It uses random permutations in order to analyze the relationship between the stable isotope ratios and the species, and hence, slightly different results can be expected every time the test is run (Anderson 2001 and 2014). Moreover, based on the results obtained here, this statistical analysis seems to account more for the similarities between groups and not as much for the differences,



which was the main interest of the present study. Hence, to define the isotopic niche of different species in an ecosystem, the Stable Isotope Bayesian Ellipses (Jackson et al., 2011) were considered more appropriate.

### ***Origin of resources according to $\delta^{34}\text{S}$ , $\delta^{18}\text{O}$ , $\delta^{13}\text{C}$ and $\delta^{15}\text{N}$***

The variation in stable isotope ratios within an ecosystem depends mostly on the physical and ecological processes that determine the origin of each chemical element (Peterson and Howarth 1987; Rubenstein and Hobson 2004). In the Río de la Plata estuary, these processes are mainly driven by the constant inflow of a fresh-water surface layer with terrestrial particulate organic matter (POM) over the salty shelf waters that, combined with wind stress and topography, create a series of well-characterized inshore and marine fronts and a strong stratification with marked vertical and horizontal salinity gradients (Figure 3.4; Guerrero et al., 1997; Acha et al., 2004; Botto et al., 2011). Here, the main source of  $\delta^{18}\text{O}$  variation between the marine mammal groups is the salinity of the water where they feed, as demonstrated by the strong positive correlation between these two factors (Conroy et al., 2014; Belem et al., 2019). Indeed, although data for the Río de la Plata estuary are limited, a general increase in  $\delta^{18}\text{O}$  values is observed from inshore ( $\delta^{18}\text{O} = \sim -1 \text{‰ PDB}$ ;  $\sim 29.8 \text{‰ SMOW}$ ) to offshore ( $\delta^{18}\text{O} = \sim +2 \text{‰ PDB}$ ;  $\sim 32.9 \text{‰ SMOW}$ ) marine environments in the nearby Atlantic Ocean (LeGrande and Schmidt 2006; McMahon et al., 2013). Additionally, the almost permanent vertical salinity stratification in the mixohaline zone leads to the formation of a salt wedge and the occurrence of salty marine waters with higher  $\delta^{18}\text{O}$  values just above the bed of the estuary (Figure 3.4; Guerrero et al., 1997).

On the other hand,  $\delta^{13}\text{C}$  and  $\delta^{34}\text{S}$  values are directly affected by the source of the primary producers and plant detritus reaching the estuary (Peterson and Howarth 1987; Connolly et al., 2004). In the Río de la Plata estuary, there are three known sources of organic C: (1) the  $^{13}\text{C}$ -depleted terrestrial and freshwater marsh plants with a C3 metabolism, brought into the estuary by the river; (2) the  $^{13}\text{C}$ -enriched salt marsh plants with a C4 metabolism, found mostly at the southern shore of the estuary along Samborombón Bay (Figure 3.1), mostly *Spartina* spp.; and (3) the marine phytoplankton, also  $^{13}\text{C}$ -depleted (Peterson and Howarth 1987; Botto et al., 2011; Bergamino et al., 2017). The first two sources reach the estuary mostly as detritus and the presence of phytoplankton is light-dependent; as a result, the relevance of each source is spatially variable (Botto et al., 2011).



At the innermost part of the estuary, the maximum turbidity zone (Figure 3.1; Figure 3.4) is characterized by a high concentration of suspended particles originated from terrestrial plants and freshwater marsh plants, since water turbidity does not allow phytoplankton growth (Framiñan and Brown 1996; Acha et al., 2003; Botto et al., 2011). Here, the base of the food web seems to be supported by this allochthonous detritus with low  $\delta^{13}\text{C}$  values (Figure 3.4; Peterson 1999; Botto et al., 2011). Once in the estuary/mixohaline zone, most of the suspended POM seems to originate from the salt marshes with high  $\delta^{13}\text{C}$  values, representing the only known source of  $^{13}\text{C}$ -enriched particles for the consumers in the area (Figure 3.4; Botto et al., 2011). Nonetheless, a considerable increase in phytoplankton concentration has been found inside the estuary following the maximum turbidity zone (Carreto et al., 2008), so it is also possible to find consumers with low  $\delta^{13}\text{C}$  values associated to this zone. In the marine waters, the food web is supported mostly by phytoplankton and hence consumers are characterized by low  $\delta^{13}\text{C}$  values (Figure 3.4; Peterson 1999; Botto et al., 2011). In contrast, the variation in  $\delta^{34}\text{S}$  values depend on the source of inorganic S (Peterson et al., 1985). Terrestrial and marsh plants use  $^{34}\text{S}$ -depleted sulphides originated, respectively, from precipitation and anoxic sediments with high sulphate reduction (Peterson et al., 1985; Peterson 1999). As a result, the consumers associated to the maximum turbidity zone are expected to have low  $\delta^{34}\text{S}$  values, as well as those from the estuary/mixohaline zone (Figure 3.4). On the other hand, planktonic organisms use the  $^{34}\text{S}$ -enriched seawater sulphates product of the sulphide oxidation within the water-column, and are responsible for the high  $\delta^{34}\text{S}$  typical of offshore/pelagic species (Figure 3.4; Peterson and Howarth 1987; Peterson 1999).

#### ***Habitat use according to $\delta^{34}\text{S}$ , $\delta^{18}\text{O}$ , $\delta^{13}\text{C}$ and $\delta^{15}\text{N}$***

From the section above, results that the isotopic niche of each marine mammal species inhabiting the Río de la Plata estuary and adjoining waters, can be used to characterize their habitat use pattern (Figure 3.4).

The differences between females and males for both otariid species (South American sea lions and fur seals) were consistent with their sexual dimorphism and distinct behavior (Cárdenas-Alayza 2018a and 2018b). In both cases, females usually stay closer to the coast and near to their breeding grounds (Rodríguez et al., 2013; González Carman et al., 2016), whereas males often perform long-distance foraging trips further from their rookeries and reach more marine waters with less terrestrial influence (Giardino et al., 2016; de Lima et al., 2022), as evidenced here by the higher  $\delta^{34}\text{S}$  values



found in males (Connolly et al., 2004). Nonetheless, the low  $\delta^{18}\text{O}$  values (Figure 3.2) reported for these four groups indicated a preference for low salinity foraging grounds, suggesting that even though males use more marine habits than females, the estuarine zone above the salt wedge is still an important feeding ground for both sexes in both species. Moreover, the higher  $\delta^{13}\text{C}$  values of sea lions of both sexes compared to fur seals indicated a higher reliance of the former on the food web supported by salt marsh detritus, while the combination of low  $\delta^{13}\text{C}$  and high  $\delta^{34}\text{S}$  values typical of fur seals, particularly males, better fits with a phytoplankton-based food web (Figure 3.4; Saporiti et al., 2016; Drago et al., 2017). This is consistent with the prevalence of pelagic and demersal-pelagic fishes and squids in the diet of fur seals (Naya et al., 2002; Franco-Trecu et al., 2014; de Lima et al., 2022), compared to the prevalence of benthic prey in the diet of sea lions throughout the year, although they increase the consumption of more pelagic prey during the pre-breeding season (Franco-Trecu et al., 2014; Drago et al., 2015). The different trophic positions of the two otariid species is further supported by the higher  $\delta^{15}\text{N}$  values of sea lions (Drago et al., 2021).

Bottlenose dolphins shared similarities with female sea lions on three out of the four stable isotope ratios analyzed (Figure 3.2), suggesting similar preferences of habitat but differences in their trophic positions. The low  $\delta^{18}\text{O}$  and  $\delta^{34}\text{S}$  values indicated the use of low salinity areas with high terrestrial influence, and the high  $\delta^{13}\text{C}$  confirmed an affinity for the mixohaline zone in areas with high influence of salt marsh detritus (Figure 3.4; Connolly et al., 2004; Botto et al., 2011). These results are consistent with the demerso-pelagic diet described for bottlenose dolphins in the Río de la Plata estuary (Botta et al., 2012; Wells and Scott 2018), although some individuals might be using the marine waters at the bottom of the estuary as they presented high  $\delta^{18}\text{O}$  values, similar to those found in marine species (Figure 3.2; Acha et al., 2008; Secchi et al., 2017).

False killer whales had a broad isotopic niche, overlapping with marine species such as the Fraser's dolphins, as well as with species associated with the estuary/mixohaline zone such as fur seals and franciscana dolphins (Figure 3.3, Supp. Table 2). This was likely due to the wide range of values presented by the species for most stable isotope ratios, especially  $\delta^{18}\text{O}$ ,  $\delta^{13}\text{C}$  and  $\delta^{15}\text{N}$ . In Southern Brazil, Botta et al., (2012) also reported intraspecific variation for the false killer whales and divided them into two groups, one similar to the local inshore predators (bottlenose dolphins and killer whales) and another one with lower  $\delta^{13}\text{C}$  and  $\delta^{15}\text{N}$  values that suggested offshore/oceanic habits. Likewise, based on the different  $\delta^{18}\text{O}$  values found for Río de la Plata, there might



be at least two groups of false killer whales with different feeding habits, one using the upper layers of the estuary/mixohaline zone above the salinity wedge, and another group using the waters below the salinity wedge, although a larger sample size is needed to test this hypothesis (Figure 3.4). It is worth noting that bottlenose dolphins and false killer whales have similar isotopic niches within the  $\delta^{13}\text{C} - \delta^{15}\text{N}$  isospace (Bisi et al., 2013, Drago et al., 2021) but differed largely when  $\delta^{34}\text{S}$  and  $\delta^{18}\text{O}$  are considered (Figure 3.3 and Figure 3.4).

On the other hand, the high  $\delta^{18}\text{O}$  values reported for the Burmeister's porpoise combined with relatively low  $\delta^{13}\text{C}$  values, previously led to report offshore habits for this species in Río de la Plata (Drago et al., 2020 and 2021). However, the Burmeister's porpoise is generally described as a coastal species based on sightings and incidental catches (Reyes 2018), and diet often includes inshore prey, either demersal or pelagic (Reyes and Van Waerebeek 1995; Molina-Schiller et al., 2005; Riccialdelli et al., 2010; Reyes 2018). Considering the low mean  $\delta^{34}\text{S}$  values reported here (Figure 3.2), the combination of high  $\delta^{18}\text{O}$  and low  $\delta^{13}\text{C}$  values can be explained by the use of benthic areas close to the bottom salinity front and below the salt wedge in the mixohaline zone (Figure 3.4). Here, there is a high influence of  $^{18}\text{O}$ - and  $^{34}\text{S}$ -enriched marine waters entering the estuary from the bottom, the formation of the maximum turbidity zone with high influence of  $^{13}\text{C}$ - and  $^{34}\text{S}$ -depleted terrestrial POM, and the presence of  $^{13}\text{C}$ -enriched detritus from salt marshes associated with the estuary/mixohaline zone (Peterson and Howarth, 1987; Guerrero et al., 1997; Acha et al., 2008; Botto et al., 2011). Although the preference for areas with high salinity is clear, the merging of all these different isotopic sources in a relatively small area is likely the reason for the wide intraspecific variation of  $\delta^{13}\text{C}$  and  $\delta^{34}\text{S}$  found for the Burmeister's porpoise.

In the case of the franciscana dolphin, both females and males seem to have similar foraging habits (Crespo, 2018), consistent with the similarities found here between their isotopic values. Moreover, the high  $\delta^{18}\text{O}$  combined with relatively high  $\delta^{13}\text{C}$  and low  $\delta^{34}\text{S}$  indicated the use of the mixohaline zone below the salinity wedge, likely with the influence of salt marsh detritus as C and S sources, although some individuals might be using areas with higher influence of terrestrial POM (Figure 3.4; Peterson and Howarth, 1987; Acha et al., 2008; Botto et al., 2011). These descriptions of habitat use also appear to be consistent with the demersal and benthopelagic diet described for the southern populations of this species through stomach content analysis (Franco-Trecu et al., 2017; Tellechea et al., 2017; Botta et al., 2022).



Opposite to the other groups, the isotopic niche of the Fraser's dolphin is consistent with an off-shore, pelagic feeding, most likely supported by a food chain relying on phytoplankton using water-column sulphates (Figure 3.4; Drago et al., 2021). This species is often found in deep waters, from 250m to up to 3500m deep, probably following the distribution of their preys (Dolar 2018), and stomach content analysis of stranded and incidentally caught individuals have confirmed a preference for mesopelagic and deep-water fishes and squids (Dolar et al., 2003; Wang et al., 2011; Dolar 2018). Previous studies have also reported constantly low  $\delta^{13}\text{C}$  values for Fraser's dolphins in different regions (Bisi et al., 2013; Botta et al., 2012; Costa et al., 2020), and their offshore/marine habits are further confirmed here with the high  $\delta^{34}\text{S}$  and  $\delta^{18}\text{O}$  values (Peterson and Howarth 1987; Carreto et al., 2008; Belem et al., 2019).

Finally,  $\delta^{15}\text{N}$  values are used as a proxy of the trophic position through the estimation of a trophic discrimination factor, which vary between 1.57 and 2.7 ‰ for different species of marine mammals (Borrell et al., 2012; Aurióles-Gamboa et al., 2013; Beltran et al., 2016; Giménez et al., 2016). If so, the range reported here, from 12.62 ‰ in one of Fraser's dolphins to 22.73 ‰ in one of franciscana dolphins, would suggest that the assemblage is foraging along more than three trophic levels. This is highly unlikely and certainly an artefact caused by the high input of sewage reaching Río de la Plata estuary from Montevideo and Buenos Aires, and the resulting shift in the  $\delta^{15}\text{N}$  baseline between estuarine and oceanic waters (McClelland and Valiela 1998; Botto et al., 2011; McMahon et al., 2013; Troina et al., 2020; Troina et al., 2021).

### **Conclusions**

Our isotopic data suggest the extended use of the estuarine/mixohaline zone as a foraging ground by several marine mammal species inhabiting the Río de la Plata estuary and adjacent south-western Atlantic waters. On one side, bottlenose dolphins, South American sea lions and fur seals showed a higher affinity to the low salinity layers above the salt wedge, characterized also by distinct C and S sources: POM from salt marshes and phytoplankton (Figure 3.4). A second group of species, including the Burmeister's porpoises, franciscana dolphins and false killer whales, seemed to prefer the saltier marine waters close to the bottom of the estuary. However, the porpoises showed affinity for the maximum turbidity zone with high terrestrial influence, whereas the other two species showed a higher influence from salt marsh detritus (Figure 3.4). Finally, the Fraser's dolphin was the only species that showed an affinity for the marine zone, an area with



high salinity and phytoplankton and water-column sulphates as C and S sources, respectively (Figure 3.4). Considering the disparate distribution ranges of the seven species studied here (Reeves et al., 2002), the pattern of habitat partitioning reported is unlikely to have resulted from coevolution, but emerges probably because of differences in their fundamental niches and the possible role of competition. The actual relevance of competitive exclusion has yet to be assessed, but the restriction of bottlenose dolphins to the less saline areas of the estuary is striking, as the species inhabits mostly coastal waters elsewhere in the south-western Atlantic Ocean (Lodi et al. 2016).

In conclusion, the use of  $\delta^{18}\text{O}$  and  $\delta^{34}\text{S}$  provided additional and important insights into the habitat use of the considered marine mammal species in an estuarine setting, allowing to differentiate between species using different salinity ranges and food webs with different contributions of terrestrial detritus. Both stable isotope ratios worked as complementary habitat tracers, without discarding the useful information on trophic relationships provided by  $\delta^{13}\text{C}$  and  $\delta^{15}\text{N}$ . Furthermore, the combination of at least three habitat tracers allowed a better visualization of the different dimensions that make up the whole ecosystem, thus improving the understanding of habitat partitioning between marine mammal species.

## REFERENCES

- Acha, E.M., Mianzan, H.W., Iribarne, O., Gagliardini, D.A., Lasta, C. and Daleo, P. 2003. The role of the Río de la Plata bottom salinity front in accumulating debris. *Marine Pollution Bulletin*, 46(2), 197-202. doi:10.1016/s0025-326x(02)00356-9.
- Acha, E.M., Mianzan, H.W., Guerrero, R.A., Favero, M. and Bava, J. 2004. Marine fronts at the continental shelves of austral South America: physical and ecological processes. *Journal of Marine systems*, 44(1-2), 83-105.
- Acha, E.M., Mianzan, H., Guerrero, R., Carreto, J., Giberto, D., Montoya, N. and Carignan, M. 2008. An overview of physical and ecological processes in the Río de la Plata Estuary. *Continental shelf research*, 28(13), 1579-1588. doi:10.1016/j.csr.2007.01.031.
- Anderson, M.J. 2001. A new method for non-parametric multivariate analysis of variance. *Austral Ecol.* 26, 32–46.
- Anderson, M.J. 2014. Permutational multivariate analysis of variance (PERMANOVA). *Wiley statsref: statistics reference online*, 1-15. doi:10.1002/9781118445112.stat07841.
- Aurioles-Gamboa, D., Rodríguez-Pérez, M.Y., Sánchez-Velasco, L. and Lavín, M.F. 2013. Habitat, trophic level, and residence of marine mammals in the Gulf of California assessed by stable isotope analysis. *Marine Ecology Progress Series*, 488, 275-290. doi: 10.3354/meps10369.

- Baird, R.W. 2018. False killer whale. In *Encyclopedia of Marine Mammals* (third edition), eds. Würsig, B., Thewissen, J.G.M. and Kovacs, K.M., 347-349. San Diego: Academic Press.
- Balmer, B.C., Wells, R.S., Howle, L.E., Barleycorn, A.A., McLellan, W.A., Ann Pabst, D., Rowles, T.K., Schwacke, L.H., Townsend, F.I., Westgate, A.J. and Zolman, E.S. 2014. Advances in cetacean telemetry: A review of single-pin transmitter attachment techniques on small cetaceans and development of a new satellite-linked transmitter design. *Marine Mammal Science*, 30(2), 656-673.
- Barlow, J. 2018. Management. In *Encyclopedia of Marine Mammals* (third edition), eds. Würsig, B., Thewissen, J.G.M. and Kovacs, K.M., 555-558. San Diego: Academic Press.
- Bastida, R., Rodríguez, D., Secchi, E.R., da Silva, V. 2007. *Mamíferos acuáticos de Sudamérica y Antártida*. Buenos Aires: Vazquez Mazzini Editores.
- Belem, A.L., Caricchio, C., Albuquerque, A.L.S., Venancio, I.M., Zucchi, M., Santos, T.H.R. and Alvarez, Y.G. 2019. Salinity and stable oxygen isotope relationship in the Southwestern Atlantic: constraints to paleoclimate reconstructions. *Anais da Academia Brasileira de Ciências*, 91.
- Beltran, R.S., Peterson, S.H., McHuron, E.A., Reichmuth, C., Hückstädt, L.A. and Costa, D.P. 2016. Seals and sea lions are what they eat, plus what? Determination of trophic discrimination factors for seven pinniped species. *Rapid Communications in Mass Spectrometry*, 30(9), 1115-1122. DOI: 10.1002/rcm.7539.
- Ben-David, M. and Flaherty, E.A. 2012. Stable isotopes in mammalian research: a beginner's guide. *Journal of Mammalogy*, 93(2), 312-328, doi:10.1644/11-MAMM-S-166.1.
- Bergamino, L., Schuerch, M., Tudurí, A., Carretero, S. and García-Rodríguez, F. 2017. Linking patterns of freshwater discharge and sources of organic matter within the Río de la Plata estuary and adjacent marshes. *Marine and Freshwater Research*, 68(9), 1704-1715.
- Bisi, T.L., Dorneles, P.R., Lailson-Brito, J., Lepoint, G., Azevedo, A.D.F., Flach, L., Malm, O. and Das, K. 2013. Trophic relationships and habitat preferences of delphinids from the southeastern Brazilian coast determined by carbon and nitrogen stable isotope composition. *PLoS One*, 8(12), p.e82205.
- Bond, A.L. and Hobson, K.A. 2012. Reporting stable-isotope ratios in ecology: Recommended terminology, guidelines and best practices. *Waterbirds*, 35(2), 324-331.
- Borrell, A., Abad-Oliva, N., Gómez-Campos, E., Giménez, J. and Aguilar, A. 2012. Discrimination of stable isotopes in fin whale tissues and application to diet assessment in cetaceans. *Rapid Communications in Mass Spectrometry*, 26(14), 1596-1602. DOI: 10.1002/rcm.6267.
- Borrell, A., Gazo, M., Aguilar, A., Raga, J.A., Degollada, E., Gozalbes, P. and García-Vernet, R. 2021. Niche partitioning amongst northwestern Mediterranean cetaceans using stable isotopes. *Progress in Oceanography*, 193, p.102559.
- Botta, S., Hohn, A.A., Macko, S.A. and Secchi, E.R. 2012. Isotopic variation in delphinids from the subtropical western South Atlantic. *Journal of the Marine Biological Association of the United Kingdom*, 92(8), 1689-1698.
- Botta, S., Bassoi, M. and Troina, G. C. 2022. Chapter 2 - Overview of franciscana diet. In *The Franciscana Dolphin: On the edge of survival*, eds. Paulo César Simões-Lopes, Marta Jussara Cremer, 15-48, Academic Press, ISBN 9780323909747. <https://doi.org/10.1016/B978-0-323-90974-7.00003-3>.



- Botto, F., Gaitán, E., Mianzan, H., Acha, M., Giberto, D., Schiariti, A., and Iribarne, O. 2011. Origin of resources and trophic pathways in a large SW Atlantic estuary: An evaluation using stable isotopes. *Estuarine, Coastal and Shelf Science*, 92(1), 70-77. doi:10.1016/j.ecss.2010.12.014.
- Cárdenas-Alayza, S. 2018a. South American Sea Lion (*Otaria byronia*). In *Encyclopedia of Marine Mammals* (third edition), eds. Würsig, B., Thewissen, J.G.M. and Kovacs, K.M., 907-910. San Diego: Academic Press.
- Cárdenas-Alayza, S. 2018b. South American Fur Seal (*Arctocephalus australis*). In *Encyclopedia of Marine Mammals* (third edition), eds. Würsig, B., Thewissen, J.G.M. and Kovacs, K.M., 905-907. San Diego: Academic Press.
- Carreto, J.I., Montoya, N.G., Benavides, H.R., Guerrero, R.A., Carignan, M.O. 2003. Characterization of spring phytoplankton communities in the Río de la Plata maritime front using pigment signatures and cell microscopy. *Marine Biology*, 143(5), 1013-1027.
- Carreto, J.I., Montoya, N., Akselman, R., Carignan, M.O., Silva, R.I. and Cucchi Colleoni, D.A. 2008. Algal pigment patterns and phytoplankton assemblages in different water masses of the Río de la Plata maritime front. *Continental Shelf Research*, 28(13), 1589-1606. doi:10.1016/j.csr.2007.02.012.
- Chen, S.Y., Feng, Z. and Yi, X. 2017. A general introduction to adjustment for multiple comparisons. *Journal of thoracic disease*, 9(6), 1725-1729. doi:10.21037/jtd.2017.05.34.
- Clementz, M.T. and Koch, P.L. 2001. Differentiating aquatic mammal habitat and foraging ecology with stable isotopes in tooth enamel. *Oecologia*, 129(3), 461-472.
- Connolly, R.M., Guest, M.A., Melville, A.J. and Oakes, J.M., 2004. Sulfur stable isotopes separate producers in marine food-web analysis. *Oecologia*, 138, pp.161-167. <https://doi.org/10.1007/s00442-003-1415-0>.
- Costa, A. P.B., Rosel, P.E., Daura-Jorge, F.G. and Simoes-Lopes, P.C. 2016. Offshore and coastal common bottlenose dolphins of the western South Atlantic face-to-face: what the skull and the spine can tell us. *Marine Mammal Science*, 32(4), 1433-1457.
- Costa, A.F., Botta, S., Siciliano, S. and Giarrizzo, T. 2020. Resource partitioning among stranded aquatic mammals from Amazon and Northeastern coast of Brazil revealed through Carbon and Nitrogen Stable Isotopes. *Scientific reports*, 10(1), 1-13.
- Conroy, J.L., Cobb, K.M., Lynch-Stieglitz, J. and Polissar, P.J. 2014. Constraints on the salinity–oxygen isotope relationship in the central tropical Pacific Ocean. *Marine Chemistry*, 161, 26-33.
- Crespo, E.A. 2018. Franciscana dolphin *Pontoporia blainvillei*. In *Encyclopedia of Marine Mammals* (third edition), eds. Würsig, B., Thewissen, J.G.M. and Kovacs, K.M., 388-392. San Diego: Academic Press.
- Croisetière, L., Hare, L., Tessier, A. and Cabana, G. 2009. Sulphur stable isotopes can distinguish trophic dependence on sediments and plankton in boreal lakes. *Freshwater Biology*, 54(5), 1006-1015.
- de Lima, R.C., Franco-Trecu, V., Carrasco, T.S., Inchausti, P., Secchi, E.R. and Botta, S. 2022. Segregation of diets by sex and individual in South American fur seals. *Aquatic Ecology*, 56(1), 251-267.
- Dolar, M.L.L., Walker, W.A., Kooyman, G.L. and Perrin, W.F. 2003. Comparative feeding ecology of spinner dolphins (*Stenella longirostris*) and Fraser's dolphins (*Lagenodelphis hosei*) in the Sulu Sea. *Marine Mammal Science*, 19(1), 1-19.



- Dolar, M.L. 2018. Fraser's dolphin *Lagenodelphis hosei*. In *Encyclopedia of Marine Mammals* (third edition), eds. Würsig, B., Thewissen, J.G.M. and Kovacs, K.M., 392-395. San Diego: Academic Press.
- Drago, M., Franco-Trecu, V., Zenteno, L., Szteren, D., Crespo, E.A., Sapriza, F.R., de Oliveira, L., Machado, R., Inchausti, P. and Cardona, L. 2015. Sexual foraging segregation in South American sea lions increases during the pre-breeding period in the Río de la Plata plume. *Marine Ecology Progress Series*, 525, 261-272.
- Drago, M., Cardona, L., Franco-Trecu, V., Crespo, E.A., Vales, D.G., Borella, F., Zenteno, L., Gonzáles, E.M. and Inchausti, P. 2017. Isotopic niche partitioning between two apex predators over time. *Journal of Animal Ecology*, 86(4), 766-780. doi: 10.1111/1365-2656.12666.
- Drago, M., Franco-Trecu, V., Segura, A.M., Valdivia, M., González, E.M., Aguilar, A. and Cardona, L. 2018. Mouth gape determines the response of marine top predators to long-term fishery-induced changes in food web structure. *Scientific Report*. 8(1), 1-12.
- Drago, M., Valdivia, M., Bragg, D., González, E.M., Aguilar, A. and Cardona, L. 2020. Stable oxygen isotopes reveal habitat use by marine mammals in the Río de la Plata estuary and adjoining Atlantic Ocean. *Estuarine, Coastal and Shelf Science*, 238, p.106708.
- Drago, M., Signaroli, M., Valdivia, M., González, E.M., Borrell, A., Aguilar, A. and Cardona, L. 2021. The isotopic niche of Atlantic, biting marine mammals and its relationship to skull morphology and body size. *Scientific Reports*, 11(1), 1-14.
- Fahy, G.E., Deter, C., Pitfield, R., Miszkiewicz, J.J., and Mahoney, P. 2017. Bone deep: variation in stable isotope ratios and histomorphometric measurements of bone remodelling within adult humans. *Journal of Archaeological Science*, 87, 10-16.
- Framiñan, M.B. and Brown, O.B. 1996. Study of the Río de la Plata turbidity front, Part 1: spatial and temporal distribution. *Continental Shelf Research*, 16(10), 1259-1282.
- Franco-Trecu, V., Auriolos-Gamboa, D. and Inchausti, P. 2014. Individual trophic specialization and niche segregation explain the contrasting population trends of two sympatric otariids. *Marine Biology*, 161(3), 609-618.
- Franco-Trecu, V., Drago, M., Costa, P., Dimitriadis, C. and Passadore, C. 2017. Trophic relationships in apex predators in an estuary system: a multiple-method approximation. *Journal of Experimental Marine Biology and Ecology*, 486, 230-236.
- Gat, J.R. 1996. Oxygen and hydrogen isotopes in the hydrologic cycle. *Annual Review of Earth and Planetary Sciences*, 24(1), 225-262.
- Giardino, G.V., Mandiola, M.A., Bastida, J., Denuncio, P.E., Bastida, R.O. and Rodríguez, D.H. 2016. Travel for sex: Long-range breeding dispersal and winter haulout fidelity in southern sea lion males. *Mammalian Biology*, 81(1), 89-95.
- Giménez, J., Ramírez, F., Almunia, J., Forero, M.G. and de Stephanis, R., 2016. From the pool to the sea: Applicable isotope turnover rates and diet to skin discrimination factors for bottlenose dolphins (*Tursiops truncatus*). *Journal of Experimental Marine Biology and Ecology*, 475, 54-61. <http://dx.doi.org/10.1016/j.jembe.2015.11.001>.
- González Carman, V., Mandiola, A., Alemany, D., Dassis, M., Seco Pon, J.P., Prosdociami, L., Ponce de León, A., Mianzan, H., Acha, E.M., Rodríguez, D. and Favero, M. 2016. Distribution of megafaunal species in the Southwestern Atlantic: key ecological areas and opportunities for marine conservation. *ICES Journal of Marine Science*, 73(6), 1579-1588.



- Guerrero, R.A., Acha, E.M., Framin, M.B. and Lasta, C.A., 1997. Physical oceanography of the Río de la Plata Estuary, Argentina. *Continental shelf research*, 17(7), 727-742.
- Hobson, K.A., Barnett-Johnson, R. and Cerling, T. 2010. Chapter 13: Using Isoscapes to Track Animal Migration. In *Isoscapes: Understanding movement, pattern, and process on Earth through isotope mapping*, eds. West, J.B., Bowen, G.J., Dawson, T.E. and Tu, K.P., 273-298. Dordrecht: Springer Science & Business Media.
- Jackson, A.L., Inger, R., Parnell, A.C. and Bearhop, S. 2011. Comparing isotopic niche widths among and within communities: SIBER Stable Isotope Bayesian Ellipses in R. *Journal of Animal Ecology*, 80(3), 595–602.
- Koch, P.L., Tuross, N., Fogel, M.L. 1997. The effects of sample treatment and diagenesis on the isotopic integrity of carbonate in biogenic hydroxyapatite. *Journal of Archaeological Science*, 24(5), 417–429.
- Keeling, C.D. 1979. The Suess effect: <sup>13</sup>Carbon-<sup>14</sup>Carbon interactions. *Environment International*, 2(4-6), 229–300.
- LeGrande, A.N., Schmidt, G.A. 2006. Global gridded data set of the oxygen isotopic composition in seawater. *Geophysical research letters*, 33(12).
- Lodi, L., Domit, C., Laporta, P., Di Tullio, J.C., Martins, C.C.A. and Vermeulen, E. 2016. Report of the Working Group on the Distribution of *Tursiops truncatus* in the Southwest Atlantic Ocean. *Latin American Journal of Aquatic Mammals*, 11(1-2), 29–46.
- Martinez Arbizu, P. 2020. Pairwise Adonis: Pairwise multilevel comparison using adonis. R package version 0.4. <https://github.com/pmartinezarbizu/pairwiseAdonis>. Accessed 13 June 2022.
- Matthews, C.J., Longstaffe, F.J. and Ferguson, S.H. 2016. Dentine oxygen isotopes ( $\delta^{18}\text{O}$ ) as a proxy for odontocete distributions and movements. *Ecology and Evolution*, 6(14), 4643-4653.
- Matsubayashi, J., Saitoh, Y., Osada, Y., Uehara, Y., Habu, J., Sasaki, T., and Tayasu, I. 2017. Incremental analysis of vertebral centra can reconstruct the stable isotope chronology of teleost fishes. *Methods in Ecology and Evolution*, 8(12), 1755–1763.
- Matsubayashi, J. and Tayasu, I. 2019. Collagen turnover and isotopic records in cortical bone. *Journal of Archaeological Science*, 106, 37-44.
- McClelland, J.W. and Valiela, I. 1998. Changes in food web structure under the influence of increased anthropogenic nitrogen inputs to estuaries. *Marine Ecology Progress Series*, 168, 259-271.
- McMahon, K.W., Hamady, L.L., Thorrold, S.R. 2013. A review of ecogeochemistry approaches to estimating movements of marine animals. *Limnology and oceanography*, 58(2), 697–714.
- Michener, R. H. and Lajtha, K. 2007. *Stable isotopes in ecology and environmental science*. Second Edition. Malden: Blackwell publishing.
- Miloslavich, P., Klein, E., Díaz, J.M., Hernández, C.E., Bigatti, G., Campos, L., Artigas, F., Castillo, J., Penchaszadeh, P.E., Neill, P.E., Carranza, A., Retana, M.V., Díaz de Astarloa, J.M., Lewis, M., Yorrio, Y., Piriz, M.L., Rodríguez, D., Yoneshigue-Valentin, Y., Gamboa, L., Martín, A. 2011. Marine biodiversity in the Atlantic and Pacific coasts of South America: knowledge and gaps. *PLoS One*, 6(1), p.e14631.
- Molina-Schiller, D., Rosales, S.A. and De Freitas, T.R.O. 2005. Oceanographic conditions off Coastal South America in relation to the distribution of



- Burmeister's porpoise, *Phocoena spinipinnis*. *Latin American Journal of Aquatic Mammals*, 4(2): 141-156.
- Moreira, D. and Simonato, C.G. 2019. Hidrología y circulación del estuario del Río de la plata. *Meteorologica*, 44(1), 1-30.
- Naya, D.E., Arim, M. and Vargas, R. 2002. Diet of South American fur seals (*Arctocephalus australis*) in Isla de Lobos, Uruguay. *Marine Mammal Science*, 18(3), 734-745.
- Nehlich, O. and Richards, M.P. 2009. Establishing collagen quality criteria for sulphur isotope analysis of archaeological bone collagen. *Archaeological and Anthropological Sciences*, 1(1), 59-75.
- Newsome, S.D., Clementz, M.T. and Koch, P.L. 2010. Using stable isotope biogeochemistry to study marine mammal ecology. *Marine Mammal Science*, 26(3), 509-572.
- Oksanen, J., Blanchet, G.F., Friendly, M., Kindt, R., Legendre, P., McGlenn, D., Minchin, P.R., O'Hara, R.B., Simpson, G.L., Solymos, P., Stevens, M.H.H., Szoecs, E., Wagner, H. 2020. Package 'vegan', version 2.5-7. Community Ecology Package. <http://CRAN.Rproject.org/package=vegan>. Accessed 13 June 2022.
- Ortega, L. and Martínez, A. 2007. Multiannual and seasonal variability of water masses and fronts over the Uruguayan shelf. *Journal of Coastal Research*, 23(3), 618-629.
- Peterson, B.J.; Howarth, R.W. and Garritt, R.H. 1985. Multiple Stable Isotopes Used to Trace the Flow of Organic Matter in Estuarine Food Webs. *Science*, 227(4692), 1361-1363. doi:10.1126/science.227.4692.1361.
- Peterson, B.J. and Howarth, R.W., 1987. Sulfur, carbon, and nitrogen isotopes used to trace organic matter flow in the salt-marsh estuaries of Sapelo Island, Georgia 1. *Limnology and oceanography*, 32(6), 1195-1213.
- Peterson, B.J. 1999. Stable isotopes as tracers of organic matter input and transfer in benthic food webs: a review. *Acta oecologica*, 20(4), 479-487.
- Pinzone, M., Damseaux, F., Michel, L.N. and Das, K. 2019. Stable isotope ratios of carbon, nitrogen and sulphur and mercury concentrations as descriptors of trophic ecology and contamination sources of Mediterranean whales. *Chemosphere*, 237, p.124448.
- Pritchard, D.W., 1952. Estuarine hydrography. In *Advances in geophysics* (Vol. 1, pp. 243-280). Elsevier.
- Post, D.M. 2002. Using stable isotopes to estimate trophic position: models, methods, and assumptions. *Ecology*, 83(3), 703-718.
- R Core Team, 2021. R: A Language and Environment for Statistical Computing. R Foundation for Statistical Computing, Vienna. <https://www.R-project.org>. Accessed 13 June 2022.
- Ramos, R. and González-Solís, J. 2012. Trace me if you can: the use of intrinsic biogeochemical markers in marine top predators. *Frontiers in Ecology and the Environment*, 10(5), 258-266.
- Reeves, R.R., Stewart, B.S, Clapham, P.J., Powell, J.A. 2002. Guide to marine mammals of the world. Knopf, NY. 528 pp.
- Reyes, J.C. and Van Waerebeek, K. 1995. Aspects of the biology of Burmeister's porpoise from Peru. *Rep. Int. Whal. Commn (Special Issue)*, 16, 349-364.
- Reyes, J.C. 2018. Burmeister's porpoise *Phocoena spinipinnis* Burmeister, 1865. In *Encyclopedia of Marine Mammals* (third edition), eds. Würsig, B., Thewissen, J.G.M. and Kovacs, K.M., 146-148. San Diego: Academic Press.

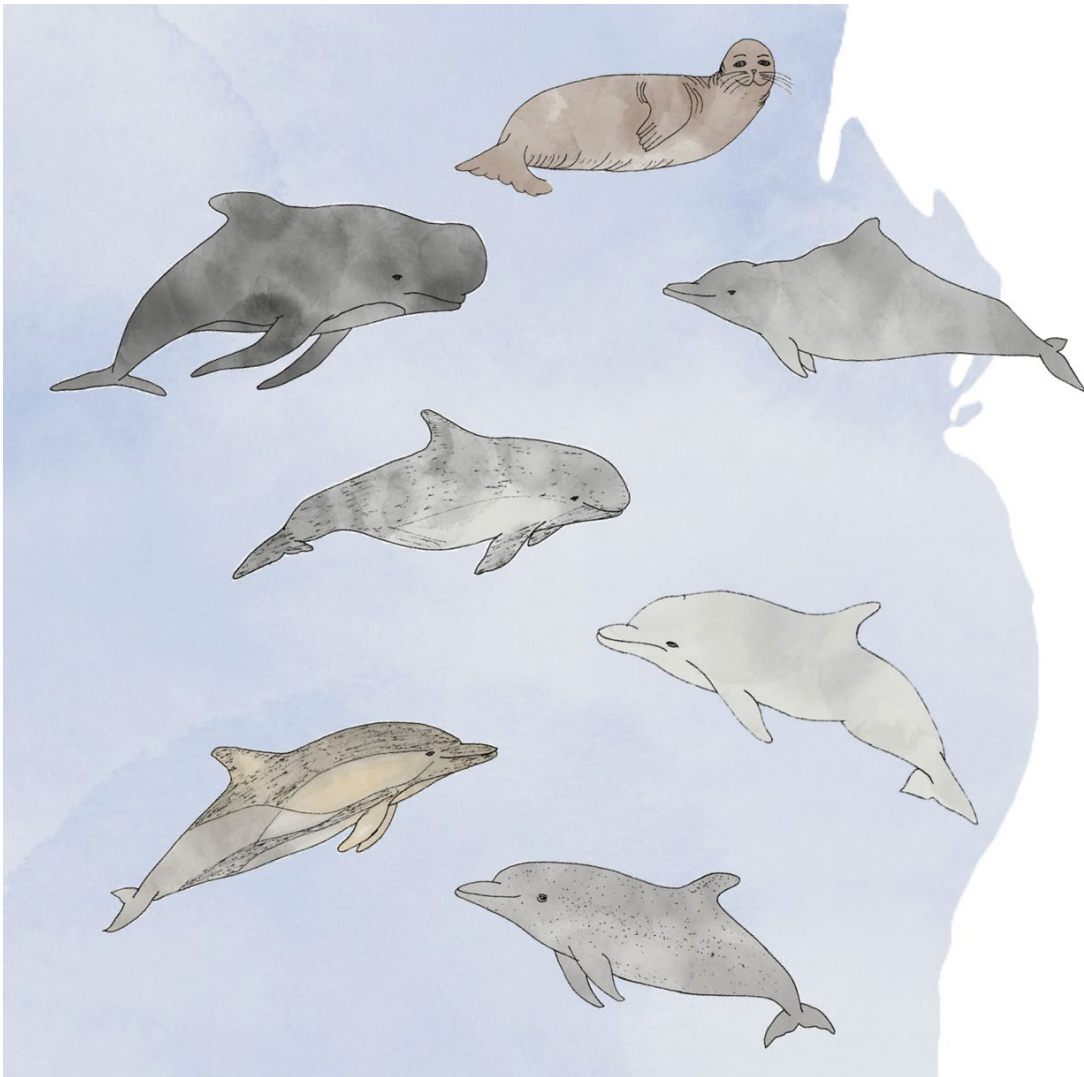


- Riccialdelli, L., Newsome, S.D., Fogel, M.L. and Goodall, R.N.P. 2010. Isotopic assessment of prey and habitat preferences of a cetacean community in the southwestern South Atlantic Ocean. *Marine Ecology Progress Series*, 418, 235-248.
- Rodríguez, D.H., Dassis, M., de León, A.P., Barreiro, C., Farenga, M., Bastida, R.O., Davis, R.W. 2013. Foraging strategies of southern sea lion females in the La Plata river estuary (Argentina-Uruguay). *Deep Sea Research Part II: Topical Studies in Oceanography*, 88, 120-130.
- Roman, J. and Ester, J.A. 2018. Ecology. In *Encyclopedia of Marine Mammals* (third edition), eds. Würsig, B., Thewissen, J.G.M. and Kovacs, K.M., 299-303. San Diego: Academic Press.
- Rubenstein, D.R. and Hobson, K.A. 2004. From birds to butterflies: animal movement patterns and stable isotopes. *Trends in Ecology and Evolution*, 19(5), 256-263. doi:10.1016/j.tree.2004.03.017.
- Saporiti, F., Bearhop, S., Vales, D.G., Silva, L., Zenteno, L., Tavares, M., Crespo, E.A. and Cardona, L. 2016. Resource partitioning among air-breathing marine predators: are body size and mouth diameter the major determinants?. *Marine Ecology*, 37(5), 957-969. doi:10.1111/maec.12304.
- Secchi, E.R., Botta, S., Wiegand, M.M., Lopez, L.A., Fruet, P.F., Genoves, R.C. and Di Tullio, J.C. 2017. Long-term and gender-related variation in the feeding ecology of common bottlenose dolphins inhabiting a subtropical estuary and the adjacent marine coast in the western South Atlantic. *Marine Biology Research*, 13(1), 121-134.
- Schoeninger, M.J. 2010. Chapter 15: Toward a  $\delta^{13}\text{C}$  Isoscape for Primates. In *Isoscapes: Understanding movement, pattern, and process on Earth through isotope mapping*, eds. West, J.B., Bowen, G.J., Dawson, T.E. and Tu, K.P., 319-333. Dordrecht: Springer Science & Business Media. doi:10.1007/978-90-481-3354-3\_15.
- Seyboth, E., Botta, S. and Secchi, E. 2018. Using chemical elements to the study of trophic and spatial ecology in marine mammals of the Southwestern Atlantic Ocean. In *Advances in Marine Vertebrate Research in Latin America: Technological Innovation and Conservation*, pp.221-248.
- Skedros, J. G., Knight, A. N., Clark, G. C., Crowder, C. M., Dominguez, V. M., Qiu, S., Mulhern, D. M., Donahue, S. W., Busse, B., Hulsey, B. I. and Zedda, M. 2013. Scaling of Haversian canal surface area to secondary osteon bone volume in ribs and limb bones. *American Journal of Physical Anthropology*, 151(2), 230-244.
- Smith, E., P., 2020. Ending reliance on statistical significance will improve environmental inference and communication. *Estuaries and Coasts*, 43, 1-6.
- Tellechea, J.S., Perez, W., Olsson, D., Lima, M. and Norbis, W. 2017. Feeding habits of franciscana dolphins (*Pontoporia blainvillei*): echolocation or passive listening?. *Aquatic Mammals*, 43(4), 430-438. doi:10.1578/AM.43.4.2017.430.
- Troina, G.C., Dehairs, F., Botta, S., Di Tullio, J.C., Elskens, M. and Secchi, E.R. 2020. Zooplankton-based  $\delta^{13}\text{C}$  and  $\delta^{15}\text{N}$  isoscapes from the outer continental shelf and slope in the subtropical western South Atlantic. *Deep Sea Research Part I: Oceanographic Research Papers*, 159, p.103235. <https://doi.org/10.1016/j.dsr.2020.103235>.
- Troina, G.C., Riekenberg, P., van der Meer, M.T., Botta, S., Dehairs, F. and Secchi, E.R. 2021. Combining isotopic analysis of bulk-skin and individual amino acids to investigate the trophic position and foraging areas of multiple cetacean species in



- the western South Atlantic. *Environmental Research*, 201, p.111610. <https://doi.org/10.1016/j.envres.2021.111610>.
- Tomaszewicz, C.N.T., Seminoff, J.A., Avens, L., Goshe, L.R., Rguez-Baron, J.M., Peckham, S.H., and Kurle, C.M. 2018. Expanding the coastal forager paradigm: long-term pelagic habitat use by green turtles *Chelonia mydas* in the eastern Pacific Ocean. *Marine Ecology Progress Series*, 587, 217-234.
- Wells, R.S. and Scott, M.D. 2018. Bottlenose dolphin, *Tursiops truncatus*, common bottlenose dolphin. In *Encyclopedia of Marine Mammals* (third edition), eds. Würsig, B., Thewissen, J.G.M. and Kovacs, K.M., 118-125. San Diego: Academic Press.
- Wang, M.C., Shao, K.T., Huang, S.L. and Chou, L.S. 2011. Food partitioning among three sympatric odontocetes (*Grampus griseus*, *Lagenodelphis hosei*, and *Stenella attenuata*). *Marine Mammal Science*, 28(2), E143-E157.
- Wickert, J.C., von Eye, S.M., Oliveira, L.R. and Moreno, I.B. 2016. Revalidation of *Tursiops gephyreus* Lahille, 1908 (Cetartiodactyla: Delphinidae) from the southwestern Atlantic Ocean. *Journal of Mammalogy*, 97(6), 1728–1737.
- Yoshida, N. and Miyazaki, N. 1991. Oxygen isotope correlation of cetacean bone phosphate with environmental water. *Journal of Geophysical Research: Oceans*, 96(C1), 815–820.

### 3.2. Article 2: “Fine-tuning the isotopic niche of a marine mammal community through a multi-element approach and variable spatial scales”



**Cani, A., Cardona, L., Aguilar, Á., Borrell, A. and Drago, M. 2024.** Fine-tuning the isotopic niche of a marine mammal community through a multi-element approach and variable spatial scales. *Estuarine, Coastal and Shelf Science*, 298, p.108641. <https://doi.org/10.1016/j.ecss.2024.108641>





## **Fine-tuning the isotopic niche of a marine mammal community through a multi-element approach and variable spatial scales**

### **ABSTRACT**

It is commonly assumed that the resolution of the isotopic niche of consumers can be improved with a larger number of chemical elements, but this is only true if steep environmental gradients exist at the appropriate spatial scale. Off Mauritania, the  $\delta^{13}\text{C}$  value is a useful proxy to understand the distribution of marine mammals along the inshore-offshore gradient, and the  $\delta^{15}\text{N}$  value to assess their trophic position. Here, the incorporation of  $\delta^{18}\text{O}$  values as an independent habitat tracer largely improved the resolution of the isotopic niche, because the  $\delta^{18}\text{O}$  gradients, mostly reflecting marked salinity gradients, spanned over broad spatial scales when compared to the home range of marine mammals. On the contrary,  $\delta^{34}\text{S}$  values did not improve much the resolution of the isotopic niche at the species level, although it was useful to identify individuals relying on food webs associated with anoxic sediments, such as seagrass meadows. This is because the  $\delta^{34}\text{S}$  gradient in the area develops over a small spatial scale, compared to the home range of the considered species. This study provides new insights into the use of a multi-element approach in isotopic ecology, and improves the understanding of habitat partitioning between the considered marine mammal species off North Western Africa.

**Keywords:** stable isotopes, upwelling, marine mammals, niche partition, habitat use.



## INTRODUCTION

The precise characterization of a species' niche is critical in ecology as it provides a convenient approach to a variety of questions regarding resource availability, habitat use, and geographic distribution, both at the population and community levels (Newsome et al., 2010). However, marine mammals and other elusive species are difficult to study in the wild and their niches are often characterized through parameters such as stable isotope ratios, fatty acid profiles or contaminant levels (Newsome et al., 2010; Ramos and González-Solís, 2012). This is because these intrinsic tracers, stored in animal tissues through time, integrate information on diet composition and habitat use, although this information can only be interpreted if environmental gradients and their temporal and spatial scales are known.

Stable isotope ratios report the relative abundance of the heavy stable isotope of any chemical element in a sample, compared to that in a standard, and are usually reported in the so called  $\delta$  notation (Bond and Hobson, 2012). The stable isotope ratios of carbon (C), nitrogen (N), sulphur (S) and oxygen (O) are commonly used in ecology as intrinsic biogeochemical markers, as they inform about both the trophic and spatial components of the niche (Rubenstein and Hobson, 2004; Newsome et al., 2010; Ramos and González-Solís, 2012). Accordingly, the isotopic niche of a species is defined as the area in the  $\delta$ -space where the values of the population concentrate (Newsome et al., 2010) and is best characterized by the convex hull and standard ellipse areas in a given biplot (Syväranta et al., 2013).

Stable isotopes of C and N have been widely used to study the foraging ecology of marine mammal species worldwide, because they can be measured with a small sample of any tissue (Newsome et al., 2010; Ben-David and Flaherty, 2012; Drago et al., 2021). The C stable isotope ratio ( $^{13}\text{C}/^{12}\text{C}$ ;  $\delta^{13}\text{C}$ ) in animal tissues directly reflects that of their diet and, in aquatic ecosystems, it discriminates accurately between benthic primary producers and phytoplankton (Post, 2002; Newsome et al., 2010). On the other hand, the N stable isotope ratio ( $^{15}\text{N}/^{14}\text{N}$ ;  $\delta^{15}\text{N}$ ) shows a considerable trophic enrichment due to the preferential excretion of the light isotope ( $^{14}\text{N}$ ), and hence, allows inferring the trophic position of a species (Post, 2002; Rubenstein and Hobson, 2004; Ramos and González-Solís, 2012). When combined,  $\delta^{13}\text{C}$  and  $\delta^{15}\text{N}$  values are usually indicative of niche partitioning between species at a local spatial scale (Newsome et al., 2010; Ben-David and Flaherty, 2012; Pinela et al., 2010; Graham et al., 2010; Botta et al., 2012; Costa et al., 2020; Drago et al., 2021). However, characterizing the isotopic niche of a species



using only these two values may fail to capture all the dimensions that make up the isotopic space of an ecosystem (Ramos and González-Solís, 2012; Cani et al., 2023). For this reason, there is an increasing interest in using the stable isotope ratios of other chemical elements, such as S and O (Rossman et al., 2016; Drago et al., 2020; Cani et al., 2023).

The S stable isotope ratio ( $^{34}\text{S}/^{32}\text{S}$ ;  $\delta^{34}\text{S}$ ) reflects the sources of inorganic S available to primary producers (Peterson et al., 1985), and it is mostly applied in combination with  $\delta^{13}\text{C}$  and  $\delta^{15}\text{N}$  values to improve the analysis on habitat use (Rossman et al., 2016; Borrell et al., 2021; García-Vernet et al., 2021). In general, marine phytoplankton is characterized by high  $\delta^{34}\text{S}$  values, whereas seagrasses and mangroves, growing on hypoxic or anoxic sediments, are characterized by much lower  $\delta^{34}\text{S}$  values because of the intense discrimination against the heavier isotope ( $^{34}\text{S}$ ) during sulphate reduction (Peterson, 1999; Croisetière et al., 2009). Likewise, terrestrial particulate organic matter is also characterized by low  $\delta^{34}\text{S}$  values (Peterson, 1999). On the other hand, the O stable isotope ratio ( $^{18}\text{O}/^{16}\text{O}$ ;  $\delta^{18}\text{O}$ ) is commonly used as a habitat tracer in terrestrial ecology, since its distribution can be predicted according to the hydrological cycle and the local geology (Trueman et al., 2012). In the marine environment, there is a positive and linear correlation between the  $\delta^{18}\text{O}$  values and the salinity of the water (Gat, 1996; Conroy et al., 2014), therefore being a useful descriptor of habitat use in areas with strong salinity gradients (Belem et al., 2019; Drago et al., 2020).

It should be noted that, in positive estuaries, where the salinity increases toward oceanic waters (Pritchard, 1952), the  $\delta^{34}\text{S}$  and  $\delta^{18}\text{O}$  gradients are usually generated by the same process, i.e., the freshwater run-off also transporting particulate organic matter from continental origin (Peterson, 1999; Belem et al., 2019). As a result, both  $\delta^{34}\text{S}$  and  $\delta^{18}\text{O}$  values vary similarly on a broad spatial scale, from tens to hundreds of kilometres (Cani et al., 2023). However, the  $\delta^{34}\text{S}$  and  $\delta^{18}\text{O}$  gradients may be uncoupled in negative estuaries, where intense evaporation exceeds the freshwater input nearshore (Pritchard, 1952) and, thus, generates a salinity gradient independent from the freshwater input. In this scenario, the primary source of  $\delta^{34}\text{S}$  variation is the sulphate reduction in sediments, hence, the two gradients are generated by independent processes (Peterson, 1999; Belem et al., 2019).

The Parc National du Banc d'Arguin (PNBA), in Mauritania (Figure 3.1.A), offers a representative example of a negative estuary where the high temperatures and aridity of a desert climate, combined with limited water exchange with the adjoining Atlantic



Ocean, create a strong offshore/inshore salinity and a  $\delta^{18}\text{O}$  gradient year-round (Figure 3.5.B; Wolff et al., 1993). Conversely, no offshore/inshore  $\delta^{34}\text{S}$  gradient is expected to exist in the PNBA as a result of the almost complete absence of freshwater run-off, and negligible wind-driven inputs of terrestrial particulate organic matter from the adjoining sparsely vegetated desert (Pottier et al., 2021). Here, the existence of patches of anoxic sediments covered by seagrasses (Pottier et al., 2021) is the only source of variability in  $\delta^{34}\text{S}$  values of the fishes and sea turtles inhabiting the Parc (Cardona et al., 2009). However, nothing is known about the variation of these values in marine mammals.

Mauritanian waters support a diverse community of marine mammals that includes tropical, subtropical and boreal species (Robineau and Vely, 1998). This is not only because the Mauritanian coast represents a transition zone between the tropical and subtropical waters of the Northeastern Atlantic Ocean (Pelegri et al., 2017), but also because of the existence of two important upwelling areas, constantly enhancing coastal primary production and increasing habitat heterogeneity (Figure 3.5.A; Cropper et al., 2014).

In a previous study, Pinela et al., (2010) used  $\delta^{13}\text{C}$  values to segregate several species of marine mammals along the offshore/inshore gradient off Mauritania, and  $\delta^{15}\text{N}$  values to assess their trophic positions. Here,  $\delta^{18}\text{O}$  values were incorporated to better discriminate between species using water masses of contrasting salinity, and  $\delta^{34}\text{S}$  values to identify those species tightly linked to seagrass meadows.

## METHODS

### *Study Area*

The Islamic Republic of Mauritania is located at the Northwestern coast of Africa, between 16 – 22° N and 16 – 18° W (Figure 3.5.A). This is an area of hydrological complexity due to the strong winds and currents that create almost constant upwelling events throughout the year (Sevrin-Reyssac, 1993; Robineau and Vely, 1998).

On the northern parts of the Mauritanian coast, the salty, cold, and nutrient-rich waters of the Canary Current flow southward reaching the Cape Blanc Peninsula at around 21° N. According to Cropper et al., (2014), this area belongs to the “Permanent Annual Upwelling Zone” (Figure 3.5.A), where southward trade winds produce the offshore advection of surface waters, which are replaced by the colder and nutrient-rich subsurface waters, creating strong and permanent upwelling events along the coast. Consequently, part of these upwelled waters enters the PNBA, located south of Cape



Blanc, and are transported southward across the tidal flats, eventually returning to the open ocean (Figure 3.5.B; Wolff and Smith, 1990). However, the influence of the upwelling decreases significantly towards the inner parts of the PNBA, where the shallow seas and the tidal changes decrease the intensity of the water circulation, thus increasing the transport time inside the bay (Wolff et al., 1993). Here, the influence of the Sahara winds creates conditions of particularly high salinities and temperatures, especially in the intertidal mudflats and channels covered by benthic primary producers, such as seagrasses and macroalgae (Figure 3.5.B; Wolff and Smith, 1990; Araujo and Campredon, 2016; Pottier et al., 2021).

From the south, the seasonal trade winds produce a series of upwelling events, especially during winter, in the “Mauritania-Senegalese Upwelling Zone” (Figure 3.5.A; Cropper et al., 2014). Here, the less salty, warmer, and nutrient-poorer Mauritanian Current (MC) flows northward along the Mauritanian coast bringing warmer surface waters up to about 20° N (Mittelstaedt, 1991; Fischer et al., 2016). Similarly, a subsurface current noted as the Poleward Under-Current (PUC; Figure 3.5.A), almost indistinguishable from the Mauritanian Current, flows northward along the shelf break and reaches farther north than the surface waters, increasing in salinity as it mixes with the Canary Current off Cape Blanc (Figure 3.5.B; Peña-Izquierdo et al., 2012). The combination of these two northward currents creates the MC-PUC system (Figure 3.5.A).

West of the upwelling areas off the Mauritanian shelf, the Cape Verde Frontal Zone appears as a boundary between the Canary Current and the MC-PUC system (Figure 3.5.A; Zenk et al., 1991; Meunier et al., 2012). This boundary is not spatially fixed, but it is rather defined by the location of the 36 isohaline at the 150 m depth (Zenk et al., 1991). Hence, the interaction between the coastal upwelling and this frontal zone becomes complex and dynamic, especially as the two water masses may be upwelled and laterally mixed within this zone (Meunier et al., 2012). Furthermore, the variable contributions of salinity and temperature to the density create a weak and unstable density front with mesoscale variability; the destabilization of this front often results in the formation of mesoscale eddies off Cape Blanc (Meunier et al., 2012).

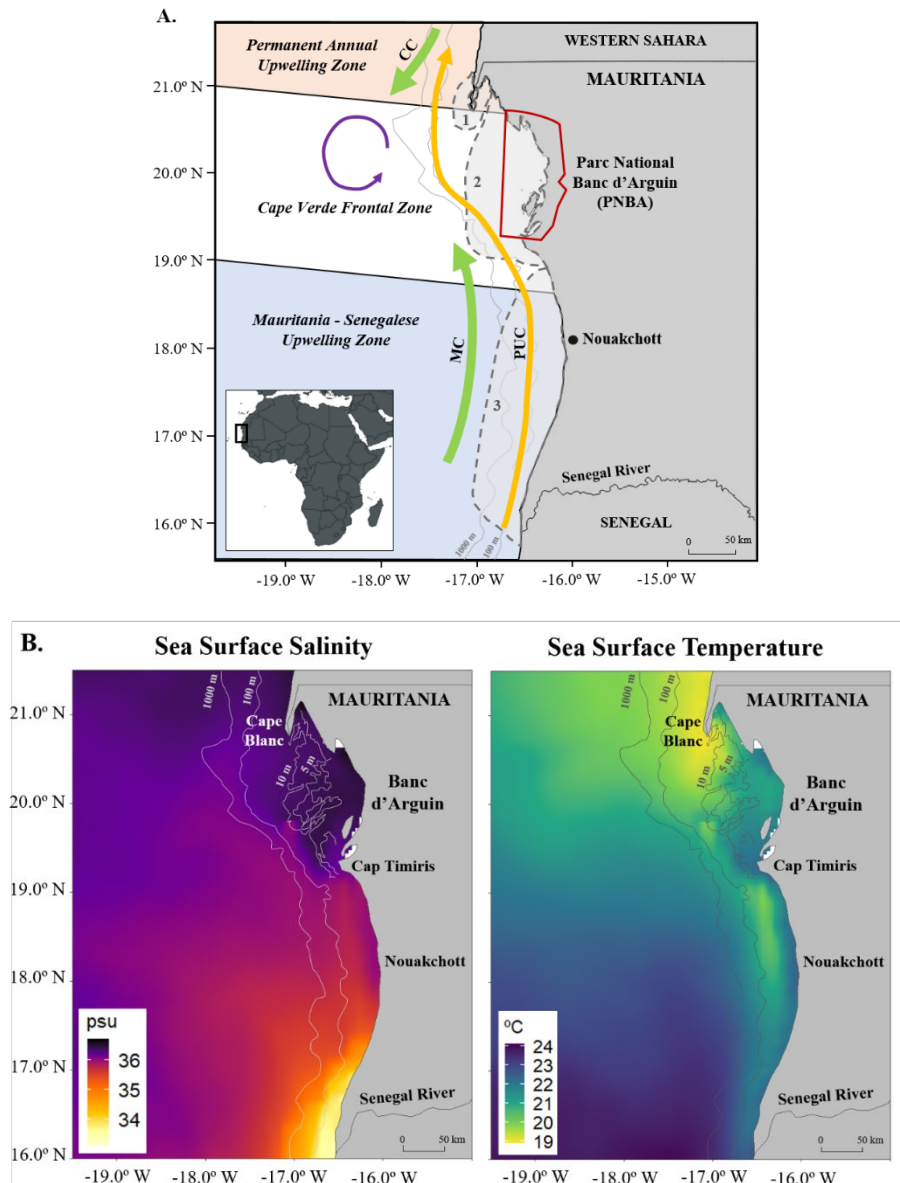


**Figure 3.5.** **A.** Study area showing the upwelling zones (Cropper et al., 2014) and main habitat types (Legibre, 1991; Pottier et al., 2021) found along the Mauritanian coast: (1) Rocky cliffs and scattered, tide-dependent sandy beaches and patches of seagrass beds (*Cymodocea nodosa*). (2) Tidal mudflats, unvegetated in the northern region, and covered by seagrasses and mangroves in the southern region. (3) Sandy beach with scattered sublittoral seagrass patches, deltaic zones and ancient lagoons. The limits of the PNBA are denoted by the red contour. Green arrows indicate the general direction of the two major currents reaching the area: the Canary Current (CC) and the Mauritanian Current (MC). The yellow arrow represents the along-slope Poleward Under-Current (PUC), and the purple arrow represents the Cape Verde Frontal Zone. **B.** Annual mean sea surface salinity (practical salinity units, psu) and sea surface temperature (°C) off the Mauritanian coast in 1993, according to Copernicus.



Different habitat types are found along the Mauritanian coast (Figure 3.5.A). The Cape Blanc Peninsula and the northern part of the PNBA, are mostly rocky cliffs with scattered, tide-dependent sandy beaches with patchy seagrass beds, mostly *Cymodocea nodosa*. The inshore regions of the PNBA constitute a unique ecosystem, with intertidal areas composed by shallow mudflats, crossed by channels covered with patches of seagrass beds, mostly dominated by *Zostera noltrii* and *Cymodocea nodosa*, and mangrove forests in the southern parts. On the other hand, the coast of Nouakchott, known as the “Grande Plage”, is composed mainly of sandy beaches with scattered sublittoral seagrass patches (Lebigre, 1991; Pottier et al., 2021; Pinela et al., 2010).

The tidal flats inside the PNBA (Figure 3.5.A) are relatively isolated, producing differences in the underwater climate along the bay. For instance, the water temperature and salinity vary with season and location, and they can be several degrees higher on the eastern slope compared to the west, as well as on the north-south gradient (Figure 3.5.B; Sevrin-Reyssac, 1993). Hence, average temperature and salinity values of 16 – 20 °C and 35 – 36, respectively, can be found on the northern areas, where the cold ocean waters first enter the bay, and reach up to 25 – 29° C and around 38 – 40, respectively, towards the southern parts due to the isolation of the coastal waters and the high evaporation rates (Figure 3.5.B; Wolff and Smith, 1990; Sevrin-Reyssac, 1993). However, temperature and salinity values higher than 35 °C and 38, respectively, have been recorded at the tidal flats and shallower pools during low tides (Wolff and Smith, 1990; Dedah, 1993; Sevrin-Reyssac, 1993). On the contrary, salinity on the southern coast is lower due to the influence of the MC and the Senegal River, with values lower than 20 at the estuary basin and reaching 35 – 36 around Nouakchott (Figure 3.5.B; Chevalier et al., 2014).

In this region, the marine mammal fauna is of particular interest. In the North, the Cape Blanc Peninsula holds the largest extant subpopulation of the endangered Mediterranean monk seal, *Monachus monachus*, whereas another critically endangered species, the Atlantic humpback dolphin, *Sousa teuszii*, inhabits the shallow areas and intertidal mudflats of the PNBA (Figure 3.5.A; Collins et al., 2017; Karamanlidis and Dendrinou, 2015). Other coastal species, such as the harbour porpoise, *Phocoena phocoena*, are often seen in the colder waters around Cape Blanc and in the northern fringe of the PNBA, while the most commonly reported species, the bottlenose dolphin *Tursiops truncatus*, can be found all over the Mauritanian coast and even in offshore areas (Figure 3.5.B; Robineau and Vely, 1998). Moreover, oceanic species such as the Atlantic spotted dolphin, *Stenella frontalis* are present offshore in the warmer tropical waters



brought up by the Mauritanian Current (Figure 3.5.B; Robineau and Vely, 1998; Herzing and Perrin, 2018), whereas the long-finned pilot whale, *Globicephala melas* prefers the cold temperate waters of the Canary Current, and the common dolphin, *Delphinus delphis*, the second most commonly reported species in the area, is often found in deep waters offshore but is also seen in coastal areas (Figure 3.5.B; Robineau and Vely, 1998; Olson, 2018).

### **Sampling**

Bone samples from 68 individuals, pertaining to seven marine mammal species, were collected along the coast of the Islamic Republic of Mauritania, from 1994 to 1997: Atlantic humpback dolphin *Sousa teuszii* (n = 3), bottlenose dolphin *Tursiops truncatus* (n = 15), harbour porpoise *Phocena phocena* (n = 15), long-finned pilot whale *Globicephala melas* (n = 3), Atlantic spotted dolphin *Stenella frontalis* (n = 5), common short-beak dolphin *Delphinus delphis* (n = 15), and Mediterranean monk seal *Monachus monachus* (n = 12). In all cases, samples were taken from the skull of dead stranded individuals and deposited at the scientific collection of the Faculty of Biology of the University of Barcelona (Spain). Only complete skulls found in good condition without evidence of weathering were selected to ensure no post-mortem alteration of the stable isotope ratios due to long-term exposure to the environmental conditions (Nelson et al., 1986). Additionally, the amount of carbonate in the samples was measured (Supp. Table 2) to assess the risk of precipitation of environmental carbonates (see below).

There is no information about the cause of death of these individuals, but it is assumed that in most cases was due to natural causes (Pinela et al., 2010), with a few cases of potential mortality caused by fishing interactions (Nieri et al., 1999). Although the age and standard length of the individuals were mostly unknown, the condylobasal length of each skull was measured and the degree of fusion of the premaxilla with the maxilla was determined to ensure that only adult specimens were analyzed (Mo et al., 2009). Small fragments of the skull were sampled from the auditory bulla in the case of the Mediterranean monk seals, and from the pterygoid in the case of cetaceans, to avoid damaging the skulls for subsequent studies. Furthermore, bone tissue has a relatively slow turnover rate, thus the values reported here integrate several years of information on the habitat use of each individual (Hobson et al., 2010; Schoeninger 2010; Fahy et al., 2017).



### ***Stable Isotope Analysis***

Stable isotope ratios of C and N were compiled from Pinela et al., (2010) and Drago et al., (2021). Additional bone samples from the same specimens were collected for O and S stable isotope analysis. Bone samples were cleaned with distilled water, dried in a stove at 60°C for 36 h, ground into a fine powder using a mortar and pestle, and split in two aliquots, one for  $\delta^{18}\text{O}$  analysis and the other one for  $\delta^{34}\text{S}$  analysis.

Prior to  $\delta^{18}\text{O}$  analysis, the inorganic matrix of the bone was obtained by soaking the bone powder with 30% hydrogen peroxide ( $\text{H}_2\text{O}_2$ ) for 48 h in partially covered vials at 4 °C, to remove any organic compounds and prevent the precipitation of secondary carbonate. The samples were then rinsed repeatedly with deionized (Milli-Q) water and treated with 1 M of calcium acetate–acetic acid buffer for another 24 h to remove any diagenetic carbonate. Finally, they were carefully rinsed again with Milli-Q water and dried for 24 h and left to dry in an oven at 50°C for another 24 hours (Koch et al., 1997). A Kiel III Carbonate Device preparation system (Thermo Electron-Dual Inlet, Thermo Fisher Scientific, Bremen, Germany) linked to a model MAT-25‰ gas source mass spectrometer (Thermo Fisher Scientific, Bremen, Germany) was used for these analyses. Approximately 1.0 mg of each treated bone sample was weighed and dissolved in 100% phosphoric acid at 70 °C with concurrent cryogenic trapping of  $\text{CO}_2$  and  $\text{H}_2\text{O}$ . The  $\text{CO}_2$  was then admitted to the mass spectrometer for analysis. International isotope secondary standards distributed by the International Atomic Energy Agency (IAEA) of known  $^{18}\text{O}/^{16}\text{O}$  ratios, in relation to the Vienna Pee Dee Belemnite (V-PDB) calcium carbonate were used. These consisted of the NBS-19 and NBS-18 calcite standard, with  $\delta^{18}\text{O}$  values of -2.20‰ and -23.2‰, respectively, relative to V-PDB. These two isotopic reference materials were employed once every six analysed samples in order to recalibrate the system and compensate for any measurement drift over time. The analytical precision of  $\delta^{18}\text{O}$  values tested by replicate analyses was  $\pm 0.05\%$  (standard deviation). Because  $\delta^{18}\text{O}$  values in animal studies are more commonly presented relative to the Vienna Standard Mean Oceanic Water (V-SMOW) index,  $\delta^{18}\text{O}$  values were converted from PDB to SMOW according to the following equation (Koch et al., 1997):

$$\delta^{18}\text{O}_{(\text{SMOW})} = [\delta^{18}\text{O}_{(\text{PDB})} \times 1.03086] + 30.86 \quad (1)$$

The integrity of the samples for the  $\delta^{18}\text{O}$  analysis was assessed by estimating the percentage of carbonate (weight) of the samples (Suppl. Table 2), taking into account that the carbonate contents of well preserve mammalian bones, including those of cetaceans,



ranges from 1.31 to 6.52 % (Sponheimer and Lee-Thorp, 1999; Nemliher et al., 2004; Munro et al., 2008).

No pre-treatment was applied to the crushed bone prior to  $\delta^{34}\text{S}$  analysis, to avoid removing amino acids that contain this element (Nehlich, 2015). Approximately 10 mg of each sample was weighed into a tin capsule and a catalyst (vanadium pentoxide  $\text{V}_2\text{O}_5$ ) was added to accelerate the combustion and reduce variability (Nehlich and Richards, 2009). Samples were loaded and combusted at  $1030^\circ\text{C}$  and analysed with an Elemental Analyzer (Carlo Erba 1108) coupled to a Delta Plus XP mass spectrometer through a ConFlow III interface (both from Thermofisher). International isotope secondary standards distributed by the International Atomic Energy Agency (IAEA) of known  $^{34}\text{S}/^{32}\text{S}$  ratios, in relation to the Vienna- Canyon Diablo Troilite (VCDT) were used. These consisted in barium sulphate (NBS-127:  $\delta^{34}\text{S} = +21.2\text{‰}$ , IAEA SO-5:  $\delta^{34}\text{S} = +0.5\text{‰}$  and IAEA SO-6:  $\delta^{34}\text{S} = -34.1\text{‰}$ ) and YCEM ( $\delta^{34}\text{S} = +12.8$ ), and they were employed once every 12 samples. Analytical precision for repeat measurements of the reference material, run in parallel with the bone samples, was 0.1 ‰.

Stable isotope abundances are expressed in delta ( $\delta$ ) notation, with the relative variations of stable isotope ratios expressed in per mil (‰) deviations from predefined international standards, and they were calculated as:

$$\delta^j\text{X} = \left[ \left( \frac{^j\text{X}}{^i\text{X}} \right)_{\text{sample}} \right] / \left[ \left( \frac{^j\text{X}}{^i\text{X}} \right)_{\text{standard}} \right] - 1 \quad (2)$$

where  $^j\text{X}$  is the heavier isotope ( $^{13}\text{C}$ ,  $^{15}\text{N}$ ,  $^{18}\text{O}$  or  $^{34}\text{S}$ ), and  $^i\text{X}$  is the lighter isotope ( $^{12}\text{C}$ ,  $^{14}\text{N}$ ,  $^{16}\text{O}$  or  $^{32}\text{S}$ ) in the analytical sample and international measurement standard (Bond and Hobson 2012).

All the stable isotope analyses were performed at the Centres Científics i Tecnològics (CCiT-UB) of the University of Barcelona, Spain.

### ***Data analysis***

Normality was tested by means of the Shapiro-Wilk test, and homoscedasticity by means of the Levene test. As the distribution of the stable isotope ratios often departed from normality, and variances were often heteroscedastic, the non-parametric Kruskal-Wallis test, followed by Dunn's post-hoc test with the Holm correction for multiple comparisons, were used for further analysis (Chen et al., 2017).

In order to estimate the isotopic niche width and niche overlap between the considered marine mammal species, the standard ellipse area in two-dimensional plots



( $\delta^{18}\text{O}-\delta^{13}\text{C}$ ,  $\delta^{18}\text{O}-\delta^{15}\text{N}$  and  $\delta^{13}\text{C}-\delta^{15}\text{N}$ ) were calculated using the package “SIBER” (Stable Isotope Bayesian Ellipses; Jackson et al., 2011). Partitioning among  $\delta^{34}\text{S}$  values was not considered here because differences between species were not statistically significant. Two complementary approaches were used to estimate the isotopic niche width (Jackson et al., 2011). The standard ellipse areas corrected for small sample size (SEAc) were used to plot the isotopic niche of each species within the isotopic space (isospace) and to calculate the overlap among species, and the Bayesian standard ellipse areas (SEAb) were used to obtain an unbiased estimate of the isotopic niche width with 95% credibility intervals (Supp. Table 1).

Spatiotemporal trends in SST ( $^{\circ}\text{C}$ ) and SSS (practical salinity) used in Figure 3.5.B were sourced from the Global Ocean Physics and Biogeochemistry Reanalyses (GLOBAL\_MULTIYEAR\_PHY\_001\_030) of the EU Copernicus Marine Environment Monitoring Service (<https://marine.copernicus.eu/>).

All statistical analyses and plots were carried out using R Statistical Software v 4.1.2 (R Core Team, 2021).

Finally, in order to confirm the results obtained in the present study, the inferences on the geographic distribution of each marine mammal species, derived from their isotopic niche, were compared with that derived from a variety of sources: sighting and stranding reports from ship-based surveys (Figure 3.9; Fraser, 1973; Duguy, 1975; Maigret et al., 1976; Maigret, 1980a; Maigret, 1980b; Maigret, 1981; Smeenk et al., 1992; Vely et al., 1995; Robineau and Vely, 1998; Nieri et al., 1999; Tulp and Leopold, 2004; Gazo and Aguilar, 2005; Camphuysen et al., 2013; Weir and Collins, 2015; Russell et al., 2018; Camphuysen, 2021; Camphuysen et al., 2022; Samba Bilal et al., 2023), sightings from shore (González et al., 1997), sightings from fishing vessels (University of Barcelona database), and electronic tracking of individuals (Gazo and Aguilar, 2005). This was done by combining the location of the sightings and strandings with the salinity and temperature maps built for the area (Figure 3.5.B), as well as the distribution of the main benthic primary producers (Pottier et al., 2021).

## RESULTS

The carbonate contents of all the samples analysed in this study fell within the range reported for well-preserved mammalian bone (1.31 to 6.52 %), except for one sample belonging to a bottlenose dolphin, which had a slightly lower carbonate percentage (1.00; Suppl. Table 2). It should be noted that bottlenose dolphins presented



the widest range of carbonate percentage (1.00 – 5.28 %), but the  $\delta^{18}\text{O}$  values of the individuals at both extremes of this range were similar (Suppl. Table 2), thus suggesting the absence of influence of the amount of carbonate on the  $\delta^{18}\text{O}$  values and ruling out the presence of environmental carbonates in the samples with the highest carbonate contents.

Statistically significant differences existed between the considered marine mammal species for  $\delta^{18}\text{O}$  values ( $X^2 = 32.37$ ,  $p < 0.001$ ),  $\delta^{13}\text{C}$  ( $X^2 = 39.63$ ,  $p < 0.001$ ), and  $\delta^{15}\text{N}$  ( $X^2 = 33.77$ ,  $p < 0.001$ ), but not for  $\delta^{34}\text{S}$  values ( $X^2 = 57.23$ ,  $p = 0.455$ ). Nevertheless, a remarkable individual variability in  $\delta^{34}\text{S}$  values was observed in all species, especially in bottlenose dolphins, harbour porpoises, Mediterranean monk seals, and Atlantic humpback dolphins. Furthermore, several individuals of each of the aforementioned species had  $\delta^{34}\text{S}$  values lower than 15 ‰ (Figure 3.6), whereas all individuals of common dolphins, spotted Atlantic dolphins and long-finned pilot whales stayed above this threshold (Figure 3.6).

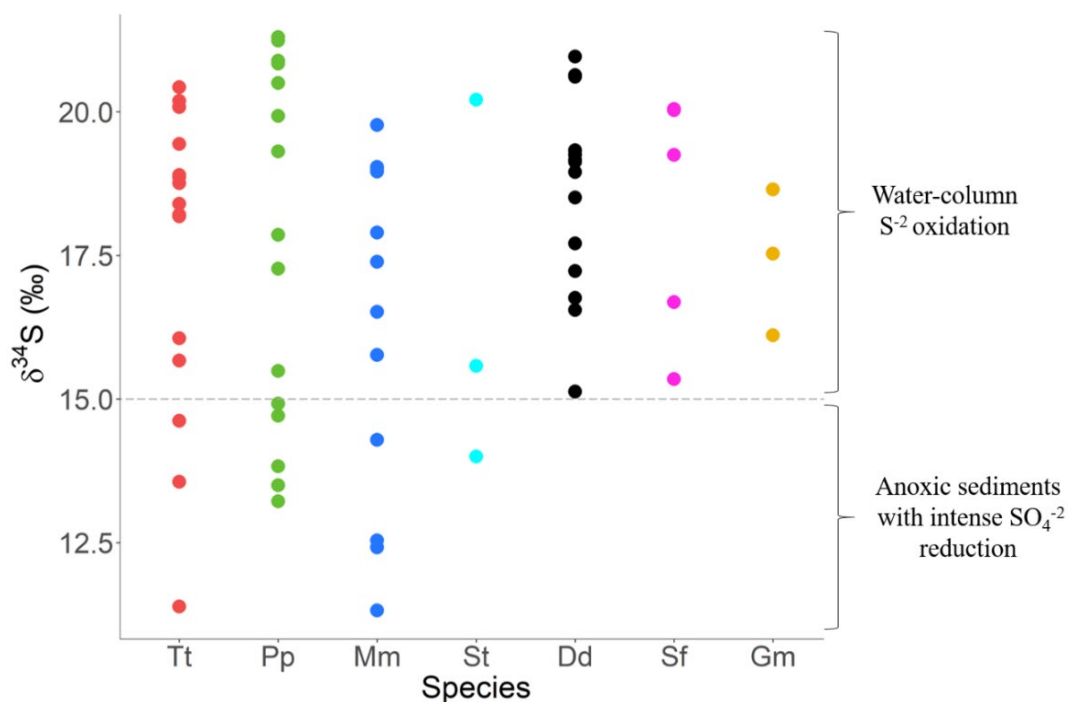


**Figure 3.6.** Scatterplot of the sulphur stable isotope ratios ( $\delta^{34}\text{S}$ ) for the considered marine mammal species from Mauritania. The dotted grey line indicates the approximate transition between the two environmental conditions described on the right. Species: common dolphin (Dd;  $n = 15$ ), bottlenose dolphin (Tt;  $n = 15$ ), harbour porpoise (Pp;  $n = 15$ ), Mediterranean monk seal (Mm;  $n = 12$ ), Atlantic humpback dolphin (St;  $n = 3$ ), Atlantic spotted dolphin (Sf;  $n = 5$ ) and long-finned pilot whale (Gm;  $n = 3$ ).



According to the  $\delta^{18}\text{O}$ ,  $\delta^{13}\text{C}$  and  $\delta^{15}\text{N}$  values, distinct isotopic niches can be found between the considered species. On one side, Atlantic spotted dolphins and Mediterranean monk seals presented the lowest mean  $\delta^{18}\text{O}$  values, whereas common dolphins and Atlantic humpback dolphins showed the highest values (Figure 3.7). On the other hand, Atlantic humpback dolphins, Mediterranean monk seals, bottlenose dolphins and harbour porpoises showed the highest mean  $\delta^{13}\text{C}$  values, while common dolphins had the lowest values (Figure 3.7). Additionally, common dolphins and Atlantic spotted dolphins showed the lowest mean  $\delta^{15}\text{N}$  values, and Mediterranean monk seals had the highest values (Figure 3.7).

The above-mentioned differences suggest that Atlantic humpback dolphins, Mediterranean monk seals, Atlantic spotted dolphins, and common dolphins had unique, distinct isotopic niches (Figure 3.8; Table 3.2). On the contrary, bottlenose dolphins had an extremely broad isotopic niche, encompassing those of harbour porpoises and long-finned pilot whales in the three considered dimensions ( $\delta^{18}\text{O}$ ,  $\delta^{13}\text{C}$  and  $\delta^{15}\text{N}$ ) (Figure 3.8; Table 3.2). The latter two species also showed similar isotopic niches on the  $\delta^{18}\text{O}$  and  $\delta^{13}\text{C}$  axes, but long-finned pilot whales had higher  $\delta^{15}\text{N}$  values. Moreover, the distribution of the species according to the boat-based sighting reports agrees with this interpretation, as Atlantic humpback dolphins were restricted to the PNBA, Mediterranean monk seals, harbour porpoises and long-finned pilot whales occurred mostly off Cape Blanc, Atlantic spotted dolphins and common dolphins inhabited mostly the continental slope and oceanic waters, and bottlenose dolphins occurred everywhere, from the innermost areas of the PNBA to oceanic waters beyond the continental shelf (Figure 3.9).

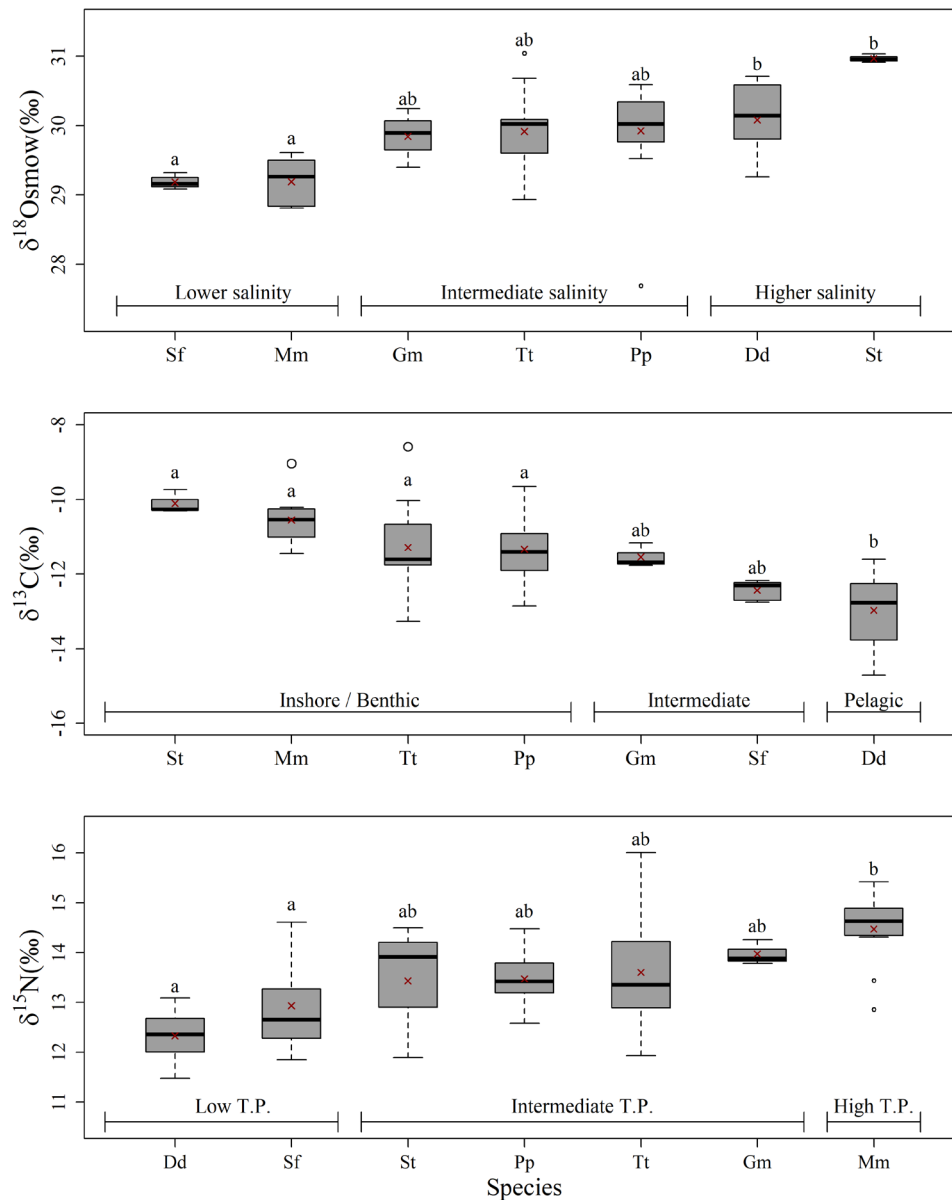


**Figure 3.7.** Boxplots of the stable isotope ratios ( $\delta^{18}\text{O}$ ,  $\delta^{13}\text{C}$ ,  $\delta^{15}\text{N}$ ) for the considered marine mammal species from Mauritania. Species with different superscript letters are statistically different in their mean values, according to the Dunn's test of multiple comparisons and Kruskal-Wallis rank sums test with Holm's method for the correction for multiple comparisons. Boxes represent the first and third quartile, lines the median, "x" the mean, and whiskers the 95% confidence interval. Species: common dolphin (Dd;  $n = 15$ ), bottlenose dolphin (Tt;  $n = 15$ ), harbour porpoise (Pp;  $n = 15$ ), Mediterranean monk seal (Mm;  $n = 12$ ), Atlantic humpback dolphin (St;  $n = 3$ ), Atlantic spotted dolphin (Sf;  $n = 5$ ) and long-finned pilot whale (Gm;  $n = 3$ ).

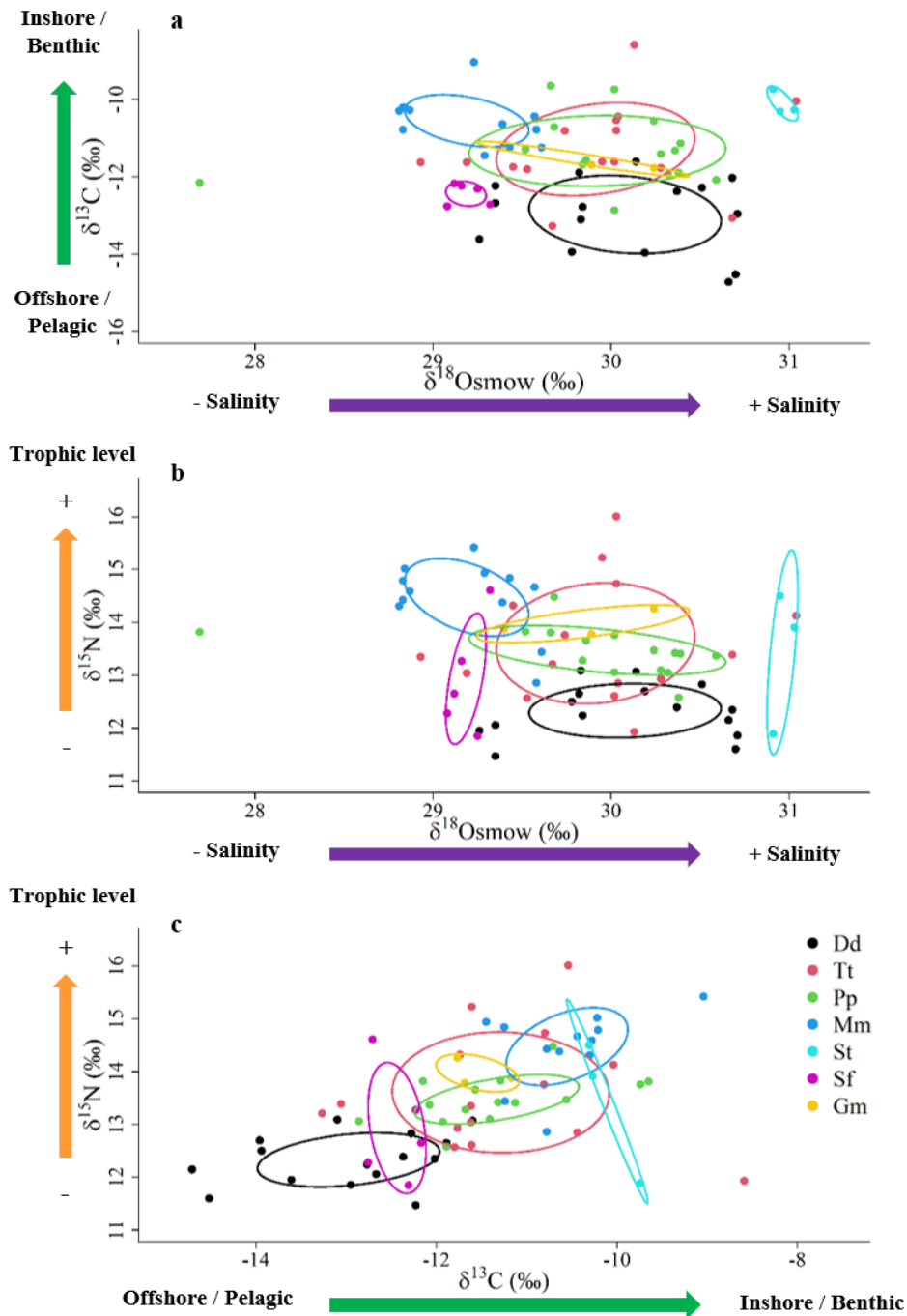
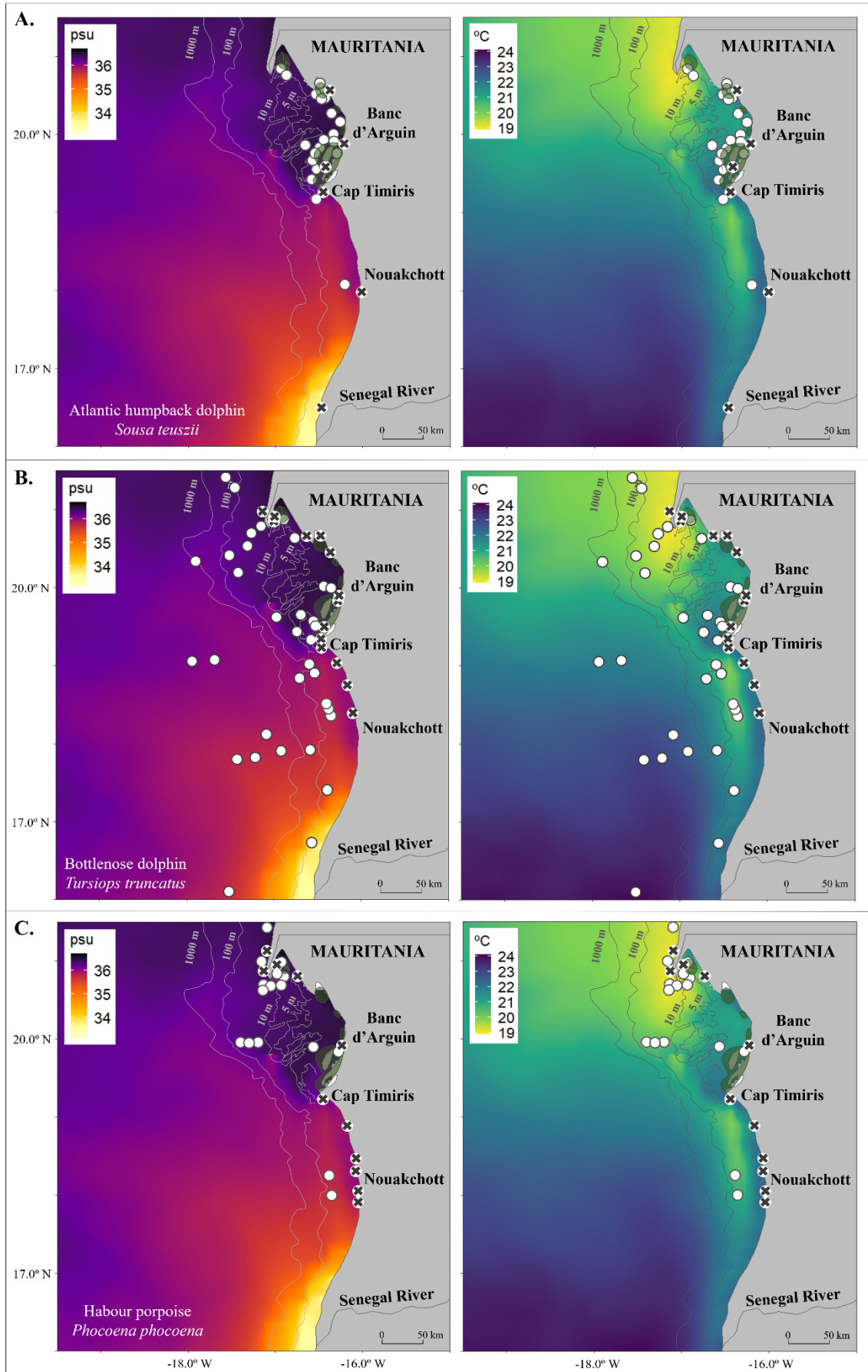


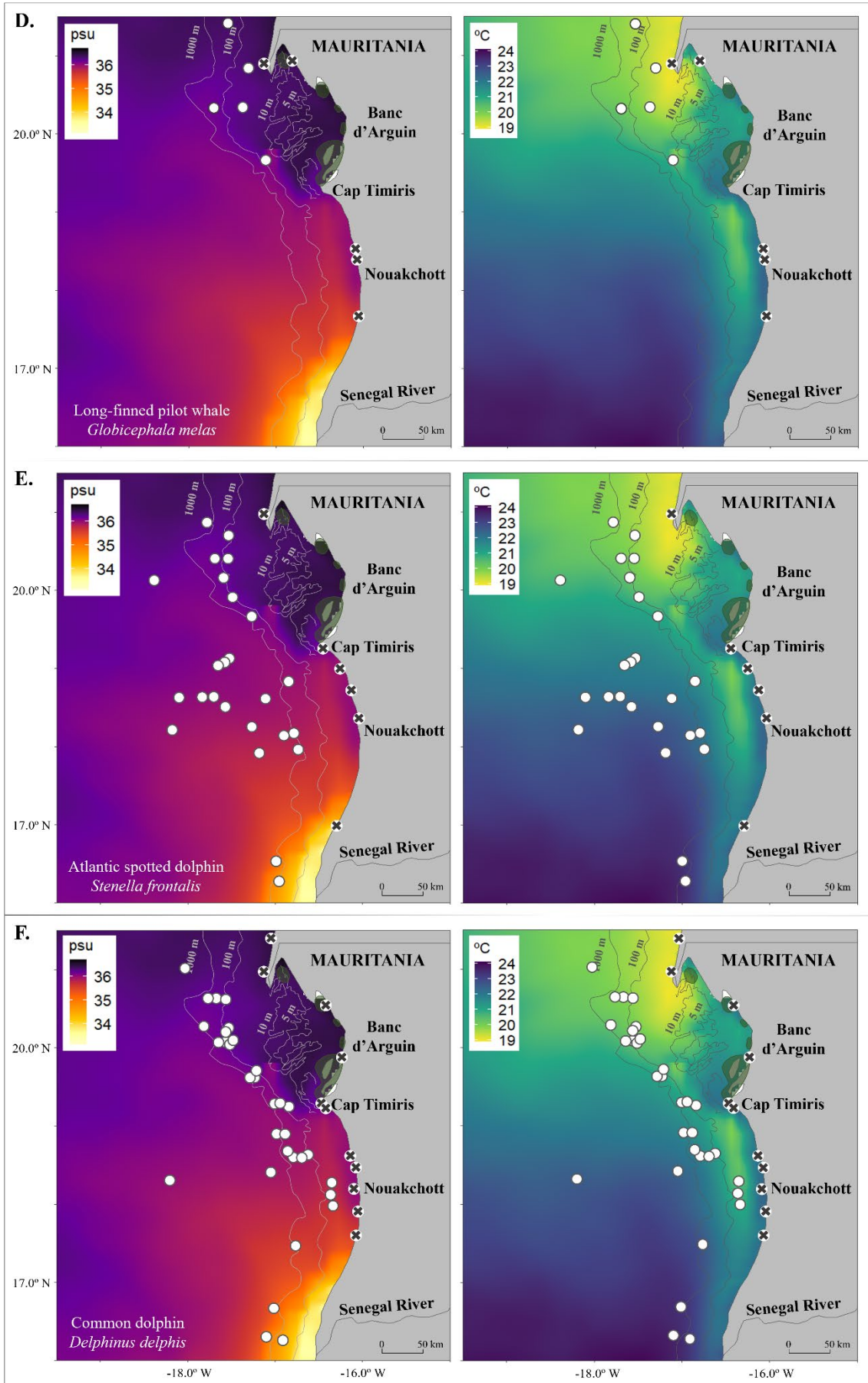
**Figure 3.8.** Standard ellipses corrected for small sample size (SEAc) in the isospace ( $\delta^{18}\text{O}_{\text{SMOW}}$ ,  $\delta^{13}\text{C}$  and  $\delta^{15}\text{N}$ ) of the marine mammal species from Mauritania. The colored arrows indicate the general interpretation of the respective isotopic values for each element, where green corresponds to carbon ( $\delta^{13}\text{C}$ ), purple to oxygen ( $\delta^{18}\text{O}$ ) and orange to nitrogen ( $\delta^{15}\text{N}$ ). Species: common dolphin (Dd;  $n = 15$ ), bottlenose dolphin (Tt;  $n = 15$ ), harbour porpoise (Pp;  $n = 15$ ), Mediterranean monk seal (Mm;  $n = 12$ ), Atlantic humpback dolphin (St;  $n = 3$ ), Atlantic spotted dolphin (Sf;  $n = 5$ ) and long-finned pilot whale (Gm;  $n = 3$ ).



**Table 3.2.** Percentage of overlapped area between each pair of marine mammal species for the different combinations of stable isotope values (isospaces) shown in Figure 3.8, calculated with the R package “SIBER”. In each case, the “% Overlap 1” indicates the percentage of the isotopic niche area of “Species 1” overlapped with the isotopic niche area of “Species 2” for a given pair of species and isospace, and vice versa for “% Overlap 2”. Only the species pairs that showed constant overlap in all analysed dimensions were considered to use a similar isospace in Mauritanian waters. Species: common dolphin (Dd; n = 15), bottlenose dolphin (Tt; n = 15), harbour porpoise (Pp; n = 15), Mediterranean monk seal (Mm; n = 12), Atlantic humpback dolphin (St; n = 3), Atlantic spotted dolphin (Sf; n = 5) and long-finned pilot whale (Gm; n = 3).

Species (1 vs 2)	$\delta^{18}\text{O}$ vs $\delta^{13}\text{C}$ (% Overlap)		$\delta^{18}\text{O}$ vs $\delta^{15}\text{N}$ (% Overlap)		$\delta^{13}\text{C}$ vs $\delta^{15}\text{N}$ (% Overlap)	
	1	2	1	2	1	2
Dd vs Tt	12.76	10.51	17.10	7.42	0.00	0.00
Dd vs Pp	6.49	5.31	0.00	0.00	0.00	0.00
Dd vs Mm	0.00	0.00	0.00	0.00	0.00	0.00
Dd vs St	0.00	0.00	0.00	0.00	0.00	0.00
Dd vs Sf	0.00	0.00	0.00	0.00	26.55	34.66
Dd vs Gm	0.00	0.00	0.00	0.00	0.00	0.00
Tt vs Pp	82.32	81.76	39.26	84.10	26.46	99.93
Tt vs Mm	1.90	5.70	2.35	6.43	15.69	48.29
Tt vs St	0.00	0.00	0.00	0.00	2.44	25.00
Tt vs Sf	0.00	0.00	0.00	0.00	5.41	19.78
Tt vs Gm	11.15	88.06	22.98	93.26	10.82	99.93
Pp vs Mm	5.40	16.31	3.66	4.68	8.36	6.81
Pp vs St	0.00	0.00	0.00	0.00	0.00	0.00
Pp vs Sf	0.00	0.00	2.83	7.19	1.36	1.32
Pp vs Gm	12.46	99.10	19.81	37.54	10.46	25.58
Mm vs St	0.00	0.00	0.00	0.00	8.54	28.47
Mm vs Sf	0.00	0.00	5.04	10.03	0.00	0.00
Mm vs Gm	2.62	6.90	6.07	8.99	0.97	2.90
St vs Sf	0.00	0.00	0.00	0.00	0.00	0.00
St vs Gm	0.00	0.00	0.00	0.00	0.00	0.00
Sf vs Gm	0.00	0.00	1.99	1.48	0.00	0.00





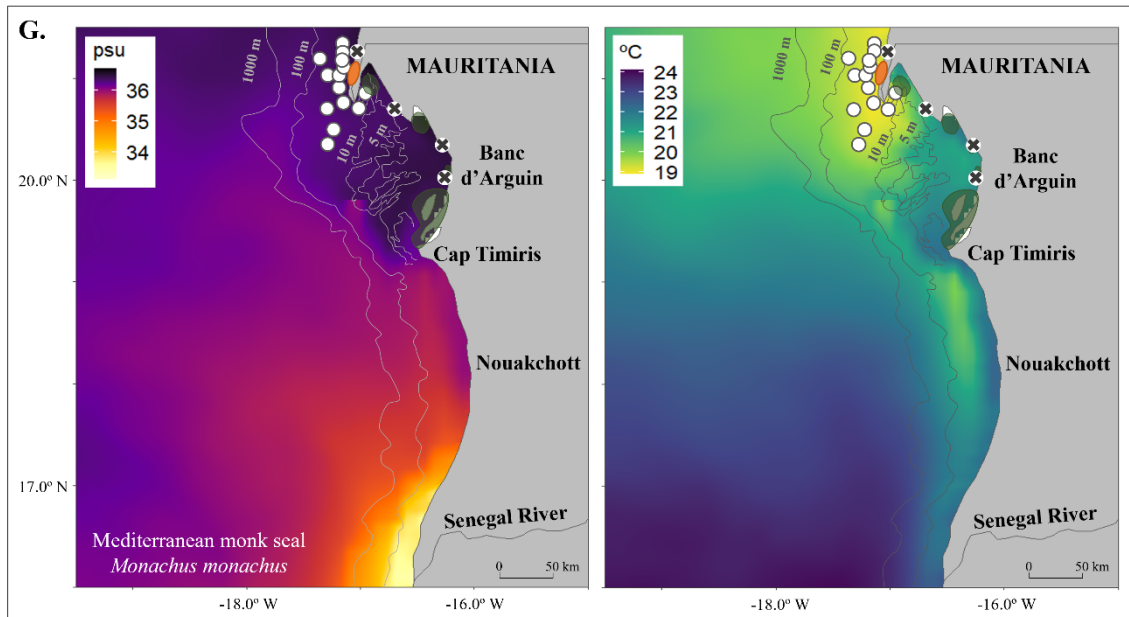


**Figure 3.9.** Sighting and stranding reports for the considered marine mammal species along the Mauritanian coast (Fraser, 1973; Duguay, 1975; Maigret et al., 1976; Maigret, 1980a; Maigret, 1980b; Maigret, 1981; Smeenk et al., 1992; Vely et al., 1995; Robineau and Vely, 1998; Nieri et al., 1999; Tulp and Leopold, 2004; Gazo and Aguilar, 2005; Camphuysen et al., 2013; Weir and Collins, 2015; Russell et al., 2018; Camphuysen, 2021; Camphuysen et al., 2022; Samba Bilal et al., 2023), placed over the annual mean sea surface salinity (left) and temperature (right) in the area. In each case, the species name is written in the bottom-left corner of the salinity map, each white point corresponds to at least one sighting, the white points with a dark “X” show the stranding locations, and the green oval shades represent the location of the main benthic primary producers inside the Parc National du Banc d’Arguin (Pottier et al., 2021). The orange region shown in subfigure G. represents the position of “Las Cuevecillas”, the location of the main haul-out caves for Mediterranean monk seals.

## DISCUSSION

It is commonly assumed that the resolution of the isotopic niche of consumers improves when considering a larger number of chemical elements. This has elicited a progressively increasing interest in multi-element approaches in isotopic ecology (Rossman et al., 2016; Borrell et al., 2021; García-Vernet et al., 2021; Cani et al., 2023). Nevertheless, resolution is expected to improve only if steep environmental gradients exist at the appropriate spatial scale, as highlighted by the present study. Here, incorporating  $\delta^{18}\text{O}$  values certainly improved our understanding on niche partitioning



between the marine mammals occurring off Northwestern Africa (Figure 3.7; Figure 3.8), but the  $\delta^{34}\text{S}$  values were not as useful to distinguish between species (Figure 3.6). It should be noted, however, that individual variability in  $\delta^{34}\text{S}$  values was high, which suggested a heterogeneous environment, but in this case, the intraspecific variability was as large as the interspecific variability. This is because the process generating a heterogeneous distribution of  $\delta^{34}\text{S}$  values in prey species operates at a much smaller spatial scale than the home range of the considered species.

Conversely, major salinity gradients exist at a geographical scale compatible with that of the home ranges of the considered marine mammal species (Figure 3.9; Wolff and Smith, 1990; Klenz et al., 2018). The region is characterized by the existence of several water masses with very distinct physical and chemical properties (Peña-Izquierdo et al., 2012). To the best of our knowledge, *in situ* measurements of the  $\delta^{18}\text{O}$  values of sea water in the study region are missing, but using the  $\delta^{18}\text{O}$ /Salinity relationship reported by Schmidt (1999) for the upper ocean layer (< 250 m) and the salinity values reported for each area within the study region, it was possible to estimate the  $\delta^{18}\text{O}$  values of each water mass. It should be noted that both the temperature and the balance between evaporation and precipitation can affect the  $\delta^{18}\text{O}$  values of surface waters, but the latter is often the main driver of their distribution (Conroy et al., 2014). Hence, the positive and linear correlation existing between the  $\delta^{18}\text{O}$  values and the salinity of the water (Conroy et al., 2014; Belem et al., 2019) facilitates the isotopic distinction between water masses.

From the North, the Canary Current flows southward bringing salty, cold, and nutrient-rich waters with a high phytoplankton growth rate (Peña-Izquierdo et al., 2012; Cropper et al., 2014; Pelegrí et al., 2017). Usual salinity values for this current are between 35 – 37 (Wolff and Smith, 1990), which corresponds to estimated  $\delta^{18}\text{O}$  values of 0.3 – 1.3 ‰, according to the Schmidt (1999) equation. Nevertheless, when reaching the shallow waters of Banc d'Arguin, salinity values increase up to 38 – 40 (Wolff and Smith, 1990), corresponding to  $\delta^{18}\text{O}$  values of 1.8 – 2.8 ‰, according to the Schmidt (1999) equation. From the South, two currents flow northward, one as the less salty, warmer, and oligotrophic Mauritanian Current (MC) on the surface, and another as the along-slope subsurface Poleward Undercurrent (PUC), forming the MC-PUC system (Figure 3.5.A). Both of these currents share similar properties, but the PUC reaches farther North, beyond Cape Blanc, and shows a slight salinity increase as it mixes with the Canary Current (Peña-Izquierdo et al., 2012). In this case, due to the influence of the Senegal River at the southernmost coast of Mauritania, surface water salinity values can



be lower than 30 inside the estuary (Chevalier et al., 2014), which corresponds to  $\delta^{18}\text{O}$  values lower than  $-2.2\text{‰}$  according to the Schmidt (1999) equation. On the other hand, at the coast of Nouakchott and all along the “Grande Plage”, salinity oscillate between 33 and 36 (Chevalier et al., 2014) corresponding to  $\delta^{18}\text{O}$  values between  $-0.7$  and  $0.8\text{‰}$ , according to the Schmidt (1999) equation. Moreover, between  $19^\circ\text{N}$  and  $21^\circ\text{N}$ , the highly dynamic Cape Verde Frontal Zone represents the mixing area between the Canary Current and the MC-PUC system (Figure 3.5.A), with a marked thermohaline indicating the limit between the two water masses (Zenk et al., 1991; Peña-Izquierdo et al., 2012).

In general, a difference in  $\delta^{18}\text{O}$  values of at least  $4.0\text{‰}$  seems to exist between areas such as Banc d’Arguin and the Senegal River estuary, whereas the averaged difference between the Canary Current and the Mauritanian Current is  $0.8\text{‰}$ , and between the Banc d’Arguin and the two currents is  $1.5$  and  $2.3\text{‰}$ , respectively. The largest difference found for the  $\delta^{18}\text{O}$  values in the bone of the marine mammals analysed here was  $3.3\text{‰}$ , between an Atlantic humpback dolphin and a harbour porpoise, but several species had mean differences of more than  $0.8\text{‰}$ , such as the common dolphin compared to the Mediterranean monk seal and the Atlantic spotted dolphin, and the Atlantic humpback dolphin with the rest of the considered species. Hence, considering that the  $\delta^{18}\text{O}$  composition of the biogenic apatite of marine mammal bones is strongly correlated with that of body water (Barrick et al., 1992; Newsome et al., 2010), the above reported differences likely indicate the use of distinct water masses by the different species, which is further discussed in the latter section.

It is worth mentioning, however, that Clementz and Koch (2001) reported a near  $2.0\text{‰}$   $^{18}\text{O}$ -enrichment in cetaceans compared to pinnipeds that were assumed to use identical water masses, although they were unable to provide an explanation for that offset. Furthermore, in this study the stable isotope ratios of monk seals were analyzed in the tympanic bulla while those of cetaceans were analyzed in the pterygoid bone, which might introduce an additional confounding factor when comparing the stable isotope values from the two sample sets. Previous research has shown homogeneous  $\delta^{13}\text{C}$  and  $\delta^{15}\text{N}$  values across the skull bones of pinnipeds (Riofrío-Lazo and Aurióles-Gamboa, 2013; Clark et al., 2017), while finding significant differences between bones from the skull, the axial and the appendicular skeletons of marine mammals due to differences in turnover rates (Clark et al., 2017; Bas et al., 2019). No comparable studies are available on the variability of  $\delta^{18}\text{O}$  values across skeletal elements, but the periotic bone has a much lower water content than other bones in cetaceans (Honda et al., 1984) and it is likely to



have a lower turnover rate. Hence, the  $\delta^{18}\text{O}$  values of the auditory bulla of pinnipeds and the pterygoid of cetaceans might integrate dietary information over different time windows and hence, caution is necessary when comparing the stable isotope ratios reported here for monk seals and those of cetaceans.

In any case, when combining the  $\delta^{18}\text{O}$  gradient reported above with the  $\delta^{13}\text{C}$  gradient caused by on-shore/off-shore differences in the type of primary producers, further differentiations come to light. In Mauritania, coastal primary producers, such as seagrasses and macroalgae, have higher  $\delta^{13}\text{C}$  values than phytoplankton (Cardona et al., 2009; Carlier et al., 2015). The same is also true for coastal and offshore consumers, with the highest  $\delta^{13}\text{C}$  values found in the inhabitants of seagrass meadows (Cardona et al., 2009; Pinela et al., 2010). Moreover,  $\delta^{13}\text{C}$  values can also assist in recognizing the influence of the upwelling in the system, since phytoplankton originated from these oceanographic phenomena and the resulting nutrient increase in surface waters tend to have higher  $\delta^{13}\text{C}$  values than the oceanic phytoplankton, but still lower than benthic primary producers (Carlier et al., 2015).

Overall, high  $\delta^{18}\text{O}$  values are associated with the influence of the Canary Current, as well as areas with high evaporation rates such as the PNBA (Figure 3.5), whereas the  $\delta^{13}\text{C}$  values depend mostly on the primary source of C (Belem et al., 2019; Carlier et al., 2015; Drago et al., 2021). Likewise,  $\delta^{15}\text{N}$  values seem to be a good proxy to determine the trophic position in this ecosystem, with consumers generally showing higher  $\delta^{15}\text{N}$  values than their respective prey (Cardona et al., 2009; Pinela et al., 2010).

On the other hand, the variation of  $\delta^{34}\text{S}$  values in marine waters depends mostly on the source of inorganic S and the oxidative state of the environment (Peterson et al., 1985). For instance, coastal primary producers often use  $^{34}\text{S}$ -depleted sulphides ( $\text{S}^{-2}$ ) produced in anoxic sediments, which results in low  $\delta^{34}\text{S}$  values similar to those found in terrestrial organic matter (Peterson et al., 1985; Peterson, 1999). However, inputs of terrestrial particulate organic matter are negligible in desert regions and, hence, the sulphate ( $\text{SO}_4^{-2}$ ) reduction in anoxic sediments is the only process generating a drop in  $\delta^{34}\text{S}$  values in the area (Peterson, 1999). This is particularly true at the PNBA, where some of the main benthic primary producers are often associated with low  $\delta^{34}\text{S}$  values. This is the case of the seagrass *Cymodocea nodosa* (Cardona et al., 2009), the saltmarshes *Spartina* sp. (Peterson et al., 1985) and mangroves (Velasquez-Vacca et al., 2023). Nevertheless, the limited distribution of these benthic primary producers along the Mauritanian coast (Lebigre, 1991; Pottier et al., 2021) suggests a mismatch between the



spatial scale of  $\delta^{34}\text{S}$  gradients (few kilometers) and the range of marine mammal movements (tens to hundreds of kilometers). Outside the PNBA, the intense bio-turbation and sediment resuspension induced by the upwelling events along the coast generate more oxidizing conditions in deeper sediment layers, and thus resulting in coastal  $\delta^{34}\text{S}$  values resembling those of oxidative marine waters (Zopfi et al., 2008; Diaz et al., 2012). Hence, the presence of scattered seagrass patches (Pottier et al., 2021) likely explains why some individuals of the four species inhabiting coastal areas (Mediterranean monk seals, harbour porpoises, bottlenose dolphins and Atlantic humpback dolphins) had  $\delta^{34}\text{S}$  values lower than 15 ‰, an indicative of foraging in areas with intense  $\text{SO}_4^{2-}$  reduction (Figure 3.6; Peterson et al., 1985), even though the average values of their populations did not differ from those of oceanic species (common dolphins, Atlantic spotted dolphins and long-finned pilot whales). In this scenario,  $\delta^{34}\text{S}$  values do not allow to discriminate between species, but are useful to identify individuals foraging consistently on  $^{34}\text{S}$ -depleted prey and hence linked to anoxic sediments (i.e. seagrass meadows).

### ***Habitat preferences of marine mammals***

The Atlantic humpback dolphin is an endemic species to the shallow areas of the western African coast, from Western Sahara to Angola, with limited exchange between populations (Weir and Collins, 2015). The IUCN Red List of Threatened Species (International Union for Conservation of Nature) catalogues the species as “Critically Endangered”, with a decreasing trend in population size (Collins et al., 2017). In Mauritania, most sightings are clustered inside the PNBA, especially around the islands, and only occasional records of the species exist southward along the coast of Nouakchott (Figure 3.9, A; Collins, 2015; Weir and Collins, 2015). Even with a small sample size, the consistency of the isotopic values of this species agrees with the almost exclusive use of the inner PNBA as feeding grounds, although a larger sample size would be advised to confirm these results more robustly.

On the other hand, bottlenose dolphins are described as the most common cetacean species in Mauritanian waters, since they are broadly distributed along the coast, both in nearshore and offshore areas, as well as inside the PNBA (Figure 3.9, B; Robineau and Vely, 1998; Tulp and Leopold, 2004; Camphuysen et al., 2013; Russell et al., 2018; Camphuysen et al., 2022). Their wide range of  $\delta^{13}\text{C}$  and  $\delta^{15}\text{N}$  values previously led Pinela et al., (2010) to suggest the possible existence of two ecotypes in the area, one with coastal and one with oceanic habits. The same was suggested by Van Waerebeek et al., (2016)



based on several reports of bottlenose dolphins in association with short-finned pilot whales in pelagic habitats, and the year-round presence of the species in coastal areas of less than 14 m depth. This ecotype differentiation is further supported in the present study by the large intraspecific variation of  $\delta^{18}\text{O}$  and  $\delta^{13}\text{C}$  values (Figure 3.7; Figure 3.8). For instance, out of the analysed marine mammal species, only the three Atlantic Humpback dolphins and one bottlenose dolphin seemed to consistently use the saltiest areas of the PNBA as foraging grounds, presenting the highest  $\delta^{18}\text{O}$  values of the study with also high  $\delta^{13}\text{C}$  values (Figure 3.8). By contrast, other individuals of the bottlenose dolphin showed intermediate  $\delta^{18}\text{O}$  values with a wide range of  $\delta^{13}\text{C}$  values, which can encompass the coastal areas off Cape Blanc, as well as the Cape Verde Frontal Zone off the PNBA, with the influence of both coastal primary producers and phytoplankton. In addition, a few individuals had some of the lowest  $\delta^{18}\text{O}$  and  $\delta^{13}\text{C}$  values (Figure 3.8), indicating the constant use of low salinity areas with high influence of oceanic phytoplankton, such as the MC-PUC system off the coast of Nouakchott (Figure 3.8; Figure 3.9, B). Furthermore, the variability of  $\delta^{34}\text{S}$  values amongst this population agrees with the presence of scattered seagrass meadows and other benthic primary producers along the Mauritanian coast. This intraspecific variation found here for the bottlenose dolphin suggests not only the presence of two ecotypes, one coastal and one offshore, but also that within the coastal ecotype, some individuals likely remain inside the PNBA for extended periods of time.

Likewise, the isotopic niche of harbour porpoises and long-finned pilot whales seem to fit the isotopic landscape described for consumers foraging near and offshore the Cape Blanc Peninsula, respectively (Figure 3.9, C and D). Most harbour porpoises analysed here had high  $\delta^{13}\text{C}$  and  $\delta^{18}\text{O}$  values, indicating an extensive use of coastal areas with high salinity, such as the northern coast of Mauritania, which agrees with the local sightings of the species and their reported coastal habits and preference for cold temperate waters (Figure 3.9, C; Bjørge and Tolley, 2018). There are also several sightings of the species offshore the PNBA and within the neritic zone, and only a few detections inside the Parc, which explains the large intraspecific variation of  $\delta^{34}\text{S}$ ,  $\delta^{18}\text{O}$  and  $\delta^{13}\text{C}$  values (Figure 3.6; Figure 3.7; Robineau and Vely, 1998; Camphuysen, 2021; Camphuysen et al., 2022). Furthermore, the lowest  $\delta^{18}\text{O}$  value found in this study belonged to a harbour porpoise, and even though it was an isolated individual, it agrees with the use of low salinity areas in the southern parts of the Mauritanian coast (Figure 3.5.B). This might be an indication of an overlap between the Mauritanian population and the individuals observed further south in Senegalese waters (Ridgway et al., 1998; Fontaine et al., 2014).



Moreover, long-finned pilot whales showed a partial overlap with harbour porpoises in all the considered isospaces, especially for the  $\delta^{18}\text{O}$  values (Figure 3.8; Table 3.2), suggesting the use of similar water masses (i.e., the Canary Current). Regardless, the lower mean  $\delta^{13}\text{C}$  value of the former indicates a more offshore/pelagic feeding, consistent with the local sighting reports and their preference for cold-temperate waters (Figure 3.7; Figure 3.9, D). However, a larger sample size is needed to confirm these results. It is believed that Mauritania marks the southernmost limit of the species' distribution in the northeastern Atlantic, but since they are easy to confuse with the more common short-finned pilot whales, there are only few confirmed sightings of the species in the area (Robineau and Vely, 1998; Olson, 2018).

The last two cetacean species considered here, the Atlantic spotted dolphin, and the common dolphin, presented the lowest mean  $\delta^{13}\text{C}$  and  $\delta^{15}\text{N}$  values, and the highest mean  $\delta^{34}\text{S}$  values (Figure 3.6; Figure 3.7), typical from offshore/pelagic species. In fact, all sightings of these two species occurred either close or offshore the 100 m isobath (Figure 3.9, E and F), but the large differentiation in  $\delta^{18}\text{O}$  values between them suggests the preferential use of different water masses as their main foraging grounds (Figure 3.7; Figure 3.8). On one side, the low  $\delta^{18}\text{O}$  values of the Atlantic spotted dolphins indicate the use of lower salinity areas from the South Atlantic Central Water, here as the Mauritanian Current, which is consistent with their known preference for warm tropical waters (Figure 3.9, E; Herzog and Perrin, 2018). In contrast, the higher  $\delta^{18}\text{O}$  values and the wider range of  $\delta^{13}\text{C}$  values found for common dolphins suggest the use of higher salinity areas influenced by the Canary Current, either with upwelling-derived or oceanic phytoplankton (Figure 3.9, F). However, the lower  $\delta^{18}\text{O}$  values of some of these individuals indicate an overlap with the isotopic niche of the Atlantic spotted dolphins, something that is also evident in the reported sightings (Figure 3.9, E and F). In general, both species tend to inhabit deep waters close to the continental shelf break, but common dolphins often venture into coastal areas and do not seem to be bothered as much by changes in water temperature (Aguilar, personal observation; Robineau and Vely, 1998; Camphuysen et al., 2022).

Lastly, the Cape Blanc Peninsula (Figure 3.5) shelters one of the two remaining large aggregations of the Mediterranean monk seal worldwide (Littnan et al., 2018), with the species currently listed as “Vulnerable” in the IUCN Red List of Threatened Species (Karamanlidis et al., 2023). Unlike cetaceans, the area used by Mediterranean monk seals is mainly linked to the location of their haul-out caves (Figure 3.9, G). Thus, their



distribution along the coast extends from Tarf el Guerguerat in Western Sahara (21° 11' N, 17° 01' W) to the tip of Cape Blanc (González et al., 1997) with scattered sightings further south and along the eastern coast of the Peninsula, such as at the tip of Cansado (20° 51' N, 17° 00' W) (Maigret, 1981; Camphuysen et al., 2013; Camphuysen et al., 2022). However, a large part of this population concentrates in “Las Cuevecillas”, an area located about 35 km north of the tip of Cape Blanc and where the main haul-out caves are placed (Figure 3.9, G; González et al., 1997). All samples here analyzed were collected along this latter segment of coastline.

Little is known about the diet and offshore behaviour of Mediterranean monk seals in Mauritanian waters. The species is generally described as opportunistic coastal feeder (Karamanlidis et al., 2016), but the determination of its feeding habitat is complex due to a large intrapopulation variation. Juveniles and some reproductive males maintaining aquatic territories in front of the haul-out sites used by the females (Pastor et al., 2011) remain near the coast and feed in close neighboring waters, whilst adult females and some adult males periodically engage in foraging trips to a distance of at least 40 km offshore (Gazo and Aguilar, 2005). However, despite the distance travelled, such foraging trips rarely exceed 40 – 50 m depth (Gazo and Aguilar, 2005) because in this region the topography of the seafloor is quite flat and the continental slope is located far from shore (Figure 3.5; Krastel et al., 2006; Karamanlidis et al., 2016). In fact, the high  $\delta^{13}\text{C}$  values found for this species (Figure 3.7) is consistent with a benthic feeding, and the presence of individuals with  $\delta^{34}\text{S}$  values lower than the 15 ‰ threshold (Figure 3.6) indicates that at least part of the population is using a foraging ground associated with seagrass meadows. This could be the Lévrier Bay, although sightings in this location are sparse (Figure 3.9, G; Maigret, 1981; González et al., 1997). Alternatively, there might be some seagrass patches or another unknown source of low  $\delta^{34}\text{S}$  values in the benthic areas along the continental slope off Cape Blanc. Given that the maximum diving depth recorded in the area (100 m for an adult male, and 78 m for a lactating female) (Gazo and Aguilar, 2005), is considerably lower than those recorded in the Mediterranean Sea (Karamanlidis et al., 2016), it is possible that the species is using most of the upper continental shelf as foraging grounds. In addition, the high  $\delta^{15}\text{N}$  values indicate that they are feeding at higher trophic levels than the rest of the considered species (Figure 3.7; Figure 3.8; Pinela et al., 2010). On the other hand, the low  $\delta^{18}\text{O}$  values of monk seals compared to those of cetaceans are odd, considering that the main water mass reaching their known foraging grounds is the salty Canary Current (Figure 3.5; Gazo and Aguilar, 2005; Peña-Izquierdo



et al., 2012). A possible explanation is the 2.0 ‰ offset between  $\delta^{18}\text{O}$  values in pinnipeds and cetaceans reported by Clementz and Koch (2001). If this was true, monk seals would not be using less salty waters than cetaceans, but would overlap in distribution with most of them, except with Atlantic spotted dolphins. This confounding factor should be considered in future studies comparing  $\delta^{18}\text{O}$  values between these two groups of marine mammals.

### **Conclusions**

Overall, the addition of  $\delta^{18}\text{O}$  values to the Mauritanian isotopic landscape in the present study allowed to distinguish between marine mammal species according to their use of the different water masses reaching the area. This is because the spatial scale of distribution of the salinity gradient is appropriate in this case, and thus,  $\delta^{18}\text{O}$  values worked effectively as a complementary habitat tracer for the  $\delta^{13}\text{C}$  and  $\delta^{15}\text{N}$  values, improving the resolution of the isotopic niches. Meanwhile, the  $\delta^{34}\text{S}$  values were more useful to identify individuals associated with anoxic sediments, since the scale of variation of the  $\delta^{34}\text{S}$  gradient in the area was smaller and did not encompass the whole scale of movements of marine mammals. This study provides new insights into the use of multi-element approach in isotopic ecology, and improves the understanding of habitat partitioning between the considered marine mammal species in the eastern North Atlantic Ocean.

### **REFERENCES**

- Araujo, A. and Campredon, P. 2016. Banc d'Arguin (Mauritania). *The Wetland Book: II: Distribution, Description, and Conservation*, 1319-1332.
- Barrick, R.E., Fischer, A.G., Kolodny, Y., Luz, B. and Bohaska, D. 1992. Cetacean bone oxygen isotopes as proxies for Miocene ocean composition and glaciation. *Palaios*, 7(5), 521-531. <https://doi.org/10.2307/3514849>.
- Bas, M., Garcia, N.A., Crespo, E.A. and Cardona, L. 2019. Intraskelletal variability in stable isotope ratios of C and N among pinnipeds and cetaceans. *Marine Mammal Science*, 36(1), 375-385. <https://doi.org/10.1111/mms.12644>.
- Belem, A.L., Caricchio, C., Albuquerque, A.L.S., Venancio, I.M., Zucchi, M., Santos, T.H.R. and Alvarez, Y.G. 2019. Salinity and stable oxygen isotope relationship in the Southwestern Atlantic: constraints to paleoclimate reconstructions. *Anais da Academia Brasileira de Ciências*, 91.
- Ben-David, M. y Flaherty, E.A. 2012. Stable isotopes in mammalian research: a beginner's guide. *Journal of Mammalogy*, 93(2), 312-328, doi: 10.1644/11-MAMM-S-166.1.

- Bjørge, A. and Tolley, K.A. 2018. Habor porpoise. In *Encyclopedia of Marine Mammals* (third edition), eds. Würsig, B., Thewissen, J.G.M. and Kovacs, K.M., 448-451. San Diego: Academic Press.
- Bond, A.L. and Hobson, K.A. 2012. Reporting stable-isotope ratios in ecology: Recommended terminology, guidelines and best practices. *Waterbirds*, 35(2), 324-331.
- Borrell, A., Gazo, M. Aguilar, A., Raga, J.A., Degollada, E., Gozalbes, P. y García-Vernet, R. 2021. Niche partitioning amongst northwestern Mediterranean cetaceans using stable isotopes. *Progress in Oceanography*, 193, 102559, ISSN 0079-6611.
- Botta, S., Hohn, A.A., Macko, S.A. and Secchi, E.R. 2012. Isotopic variation in delphinids from the subtropical western South Atlantic. *Journal of the Marine Biological Association of the United Kingdom*, 92(8), 1689-1698.
- Camphuysen, C.J., van Spanje, T.M. and Verdaat, J.P. 2013. *Ship-based seabird and marine mammal surveys off Mauritania, Nov-Dec 2012: cruise report*. NIOZ, 72.
- Camphuysen, C.J. 2021. Vulnerable wildlife concentrations at the Mauritanian Shelf. A preliminary atlas of vulnerability to surface pollutants. Royal Netherlands Institute for Sea Research (NIOZ), The Netherlands, 45.
- Camphuysen, C.J., Schreurs, T.A.W. and Bilal, A.S. 2022. Ship-based seabird and marine mammal surveys off Mauritania, 17 February-1 March 2022. *Royal Netherlands Institute for Sea Research (NIOZ), Den Burg, Texel and the Institut Mauritanien de Recherche Océanographique et des Pêche (IMROP), Nouadhibou*, pp.73.
- Cani, A., Cardona, L., Valdivia, M., González, E.M. and Drago, M. 2023. Niche Partitioning Among Marine Mammals Inhabiting a Large Estuary as Revealed by Stable Isotopes of C, N, S, and O. *Estuaries and Coasts*, 46(4), 1083-1097, <https://doi.org/10.1007/s12237-023-01193-y>.
- Cardona, L., Revelles, M., Parga, M.L., Tomás, J., Aguilar, A., Alegre, F., Raga, A. and Ferrer, X. 2009. Habitat use by loggerhead sea turtles *Caretta caretta* off the coast of eastern Spain results in a high vulnerability to neritic fishing gear. *Marine Biology*, 156, 2621-2630, doi: 10.1007/s00227-009-1288-9.
- Carrier, A., Chauvaud, L., van Der Geest, M., Le Loc'h, F., Le Duff, M., Vernet, M., Raffray, J., Diakhaté, D., Labrosse, P., Wagué, A. and Le Goff, C. 2015. Trophic connectivity between offshore upwelling and the inshore food web of Banc d'Arguin (Mauritania): New insights from isotopic analysis. *Estuarine, Coastal and Shelf Science*, 165, 149-158. <http://dx.doi.org/10.1016/j.ecss.2015.05.001>.
- Chen, S.Y., Feng, Z. and Yi, X. 2017. A general introduction to adjustment for multiple comparisons. *Journal of thoracic disease*, 9(6), 1725-1729. doi:10.21037/jtd.2017.05.34.
- Chevalier, C., Pagano, M., Corbin, D. and Arfi, R. 2014. The salinity responses of tropical estuaries to changes in freshwater discharge, tidal mixing and geomorphology: case study of the man-affected Senegal River Estuary (West Africa). *Marine and Freshwater Research*, 65(11), 987-1002, doi: 10.1071/MF13169.
- Ciner, B., Wang, Y. and Parker, W. 2016. Oxygen isotopic variations in modern cetacean teeth and bones: implications for ecological, paleoecological, and paleoclimatic studies. *Science Bulletin*, 61(1), pp.92-104. <https://doi.org/10.1007/s11434-015-0921-x>.
- Clark, C.T., Horstmann, L. and Misarti, N. 2017. Quantifying variability in stable carbon and nitrogen isotope ratios within the skeletons of marine mammals of the suborder Caniformia. *Journal of Archaeological Science: Reports*, 15, 393-400. <http://dx.doi.org/10.1016/j.jasrep.2017.09.007>.



- Clementz, M.T. and Koch, P.L. 2001. Differentiating aquatic mammal habitat and foraging ecology with stable isotopes in tooth enamel. *Oecologia*, 129, 461-472. DOI 10.1007/s004420100745.
- Collins, T. 2015. Re-assessment of the Conservation Status of the Atlantic Humpback Dolphin, *Sousa teuszii* (Kükenthal, 1892), Using the IUCN Red List Criteria. In *Advances in marine biology*, Academic Press, 72, 47-77.
- Collins, T., Braulik, G.T. and Perrin, W. 2017. *Sousa teuszii* (errata version published in 2018). *The IUCN Red List of Threatened Species 2017*: e.T20425A123792572. <https://dx.doi.org/10.2305/IUCN.UK.2017-3.RLTS.T20425A50372734.en>. Accessed on 15 December 2023.
- Conroy, J.L., Cobb, K.M., Lynch-Stieglitz, J. and Polissar, P.J. 2014. Constraints on the salinity–oxygen isotope relationship in the central tropical Pacific Ocean. *Marine Chemistry*, 161, 26-33.
- Costa, A.F., Botta, S., Siciliano, S. and Giarrizzo, T. 2020. Resource partitioning among stranded aquatic mammals from Amazon and Northeastern coast of Brazil revealed through Carbon and Nitrogen Stable Isotopes. *Scientific reports*, 10(1), 1-13.
- Croisetière, L., Hare, L., Tessier, A. and Cabana, G. 2009. Sulphur stable isotopes can distinguish trophic dependence on sediments and plankton in boreal lakes. *Freshwater Biology*, 54(5), 1006-1015.
- Cropper, T.E., Hanna, E. and Bigg, G.R., 2014. Spatial and temporal seasonal trends in coastal upwelling off Northwest Africa, 1981–2012. *Deep Sea Research Part I: Oceanographic Research Papers*, 86, 94-111, <http://dx.doi.org/10.1016/j.dsr.2014.01.007>.
- Dedah, S.o. 1993. Wind, surface water temperature, surface salinity and pollution in the area of the Banc d'Arguin, Mauritania. In: Wolff, W.J., van der Land, J., Nienhuis, P.H., de Wilde, P.A.W.J. (eds) *Ecological Studies in the Coastal Waters of Mauritania. Developments in Hydrobiology*, 86 (86), 9-19, Springer, Dordrecht, [https://doi.org/10.1007/978-94-011-1986-3\\_2](https://doi.org/10.1007/978-94-011-1986-3_2).
- Diaz, R., Moreira, M., Mendoza, U., Machado, W., Böttcher, M.E., Santos, H., Belém, A., Capilla, R., Escher, P. and Albuquerque, A.L. 2012. Early diagenesis of sulfur in a tropical upwelling system, Cabo Frio, southeastern Brazil. *Geology*, 40(10), 879-882.
- Drago, M., Valdivia, M., Bragg, D., González, E.M., Aguilar, A. y Cardona, L. 2020. Stable oxygen isotopes reveal habitat use by marine mammals in the Río de la Plata estuary and adjoining Atlantic Ocean. *Estuarine, Coastal and Shelf Science*, Volume 238, 106708, ISSN 0272-7714, <https://doi.org/10.1016/j.ecss.2020.106708>.
- Drago, M., Signaroli, M., Valdivia, M., González, E.M., Borrell, A., Aguilar, A. and Cardona, L. 2021. The isotopic niche of Atlantic, biting marine mammals and its relationship to skull morphology and body size. *Scientific Reports*, 11(1), 1-14.
- Duguy, R. 1975. Contribution à l'étude des mammifères marins de la côte nord-ouest Afrique. *Revue des Travaux de l'Institut des Pêches maritimes*, 39(3), 321-332.
- Fahy, G.E., Deter, C., Pitfield, R., Miskiewicz, J.J., and Mahoney, P. 2017. Bone deep: variation in stable isotope ratios and histomorphometric measurements of bone remodelling within adult humans. *Journal of Archaeological Science*, 87, 10-16.
- Feng, D., Tütken, T., Löffler, N., Tröster, G. and Pack, A. 2022. Isotopically anomalous metabolic oxygen in marine vertebrates as physiology and atmospheric proxy. *Geochimica et Cosmochimica Acta*, 328, 85-102. <https://doi.org/10.1016/j.gca.2022.05.008>.

- Fischer, G., Romero, O., Merkel, U., Donner, B., Iversen, M., Nowald, N., Ratmeyer, V., Ruhland, G., Klann, M. and Wefer, G. 2016. Deep ocean mass fluxes in the coastal upwelling off Mauritania from 1988 to 2012: variability on seasonal to decadal timescales. *Biogeosciences*, 13(10), 3071-3090, doi:10.5194/bg-13-3071-2016.
- Fontaine, M.C., Roland, K., Calves, I., Austerlitz, F., Palstra, F.P., Tolley, K.A., Ryan, S., Ferreira, M., Jauniaux, T., Llavona, A. and Öztürk, B. 2014. Postglacial climate changes and rise of three ecotypes of harbour porpoises, *Phocoena phocoena*, in western Palearctic waters. *Molecular ecology*, 23(13), 3306-3321.
- Fraser, F.C. 1973. Record of a dolphin (*Sousa teuszii*) from the coast of Mauritania. *Transactions of the New York Academy of Sciences*, 35(2), 132-135.
- García-Vernet, R., Borrell, A., Víkingsson, G., Halldórsson, S.D. and Aguilar, A., 2021. Ecological niche partitioning between baleen whales inhabiting Icelandic waters. *Progress in Oceanography*, 199, p.102690, <https://doi.org/10.1016/j.pocean.2021.102690>.
- Gat, J.R. 1996. Oxygen and hydrogen isotopes in the hydrologic cycle. *Annual Review of Earth and Planetary Sciences*, 24(1), 225-262.
- Gazo, M. and Aguilar, A. 2005. Maternal attendance and diving behavior of a lactating Mediterranean monk seal. *Marine Mammal Science*, 21(2), 340-345.
- González, L. M., Aguilar, A., López-Jurado, L. F. and Grau, E. 1997. Status and distribution of the Mediterranean monk seal *Monachus monachus* on the Cabo Blanco Peninsula (Western Sahara-Mauritania) in 1993-1994. *Biol. Conserv.*, 80, 225-233.
- Graham, B.S., Koch, P.L., Newsome, S.D., McMahon, K.W. and Aurioles, D. 2010. Using isoscapes to trace the movements and foraging behavior of top predators in oceanic ecosystems. In *Isoscapes: understanding movement, pattern, and process on earth through isotope mapping*, 299-318.
- Herzing, D.L. and Perrin, W.F. 2018. Atlantic spotted dolphin. In *Encyclopedia of Marine Mammals* (third edition), eds. Würsig, B., Thewissen, J.G.M. and Kovacs, K.M., 40-42. San Diego: Academic Press.
- Hobson, K.A., Barnett-Johnson, R. and Cerling, T. 2010. Chapter 13: Using Isoscapes to Track Animal Migration. In *Isoscapes: Understanding movement, pattern, and process on Earth through isotope mapping*, eds. West, J.B., Bowen, G.J., Dawson, T.E. and Tu, K.P., 273-298. Dordrecht: Springer Science & Business Media.
- Honda, K., Fujise, Y., Itano, K. and Tatsukawa, R. 1984. Composition of chemical components in bone of striped dolphin, *Stenella coeruleoalba*: distribution characteristics of heavy metals in various bones. *Agricultural and biological chemistry*, 48(3), 677-683. <https://doi.org/10.1080/00021369.1984.10866203>.
- Jackson, A.L., Inger, R., Parnell, A.C. and Bearhop, S. 2011. Comparing isotopic niche widths among and within communities: SIBER Stable Isotope Bayesian Ellipses in R. *Journal of Animal Ecology*, 80(3), 595–602.
- Karamanlidis, A. and Dendrinou, P. 2015. *Monachus monachus* (errata version published in 2017). *The IUCN Red List of Threatened Species 2015*: e.T13653A117647375. <https://dx.doi.org/10.2305/IUCN.UK.2015-4.RLTS.T13653A45227543.en>. Accessed on 27 March 2023.
- Karamanlidis, A.A., Dendrinou, P., De Larrinoa, P.F., Gücü, A.C., Johnson, W.M., Kiraç, C.O. and Pires, R. 2016. The Mediterranean monk seal *Monachus monachus*: status, biology, threats, and conservation priorities. *Mammal Review*, 46(2), 92-105.



- Karamanlidis, A.A., Dendrinis, P., Fernandez de Larrinoa, P., Kıraç, C.O., Nicolaou, H. & Pires, R. 2023. *Monachus monachus*. *The IUCN Red List of Threatened Species* 2023: e.T13653A238637039. Accessed on 15 December 2023.
- Klenz, T., Dengler, M. and Brandt, P. 2018. Seasonal variability of the Mauritania Current and hydrography at 18 N. *Journal of Geophysical Research: Oceans*, 123(11), 8122-8137.
- Koch, P.L., Tuross, N., Fogel, M.L. 1997. The effects of sample treatment and diagenesis on the isotopic integrity of carbonate in biogenic hydroxyapatite. *Journal of Archaeological Science*, 24(5), 417–429.
- Krastel, S., Wynn, R.B., Hanebuth, T.J., Henrich, R., Holz, C., Meggers, H., Kuhlmann, H., Georgiopoulou, A. and Schulz, H.D. 2006. Mapping of seabed morphology and shallow sediment structure of the Mauritania continental margin, Northwest Africa: some implications for geohazard potential. *Norwegian Journal of Geology*, 86(3), 163-176.
- Lebigre, J.M. 1991. Les marais maritimes de Mauritanie: Protection et valorisation. Les cahiers d'outre-mer 44 (176), 379–400, <https://doi.org/10.3406/caoum.1991.3413>.
- Littnan, C., Karamanlidis, A. and Dendrinis, P. 2018. Monk seals. In *Encyclopedia of Marine Mammals* (third edition), eds. Würsig, B., Thewissen, J.G.M. and Kovacs, K.M., 618-622. San Diego: Academic Press.
- Maigret, J. 1980a. Données nouvelles sur l'écologie du *Sousa teuszii* (Cetacea, Delphinidae) de la côte ouest africaine. *Bulletin de l'Institut Français d'Afrique Noire*, 42A (3), 619-633.
- Maigret, J. 1980b. Les mammifères marins des côtes de Mauritanie. Etat des observations en 1980. *Bulletin du Centre National de Recherches Océanographiques et des Pêches*, Nouadhibou, 9(1), 130-152.
- Maigret, J. 1981. Les mammifères marins des côtes de Mauritanie. 2<sup>o</sup> Rapport annuel des observations signalées en 1981. *Bulletin du Centre National de Recherches Océanographiques et des Pêches*, Nouadhibou, 10(1), 81-85.
- Maigret, J., Trotignon, J. and Duguy, R. 1976. Observations de Cétacés sur les Côtes de Mauritanie (1971-1975). *ICES, Comité des Mammifères Marins CM*, (4), 7.
- Meunier, T., E. D. Barton, B. Barreiro, and R. Torres. 2012. Upwelling filaments off Cap Blanc: Interaction of the NW African upwelling current and the Cape Verde frontal zone eddy field?. *J. Geophys. Res.*, 117, C08031, doi:10.1029/2012JC007905.
- Mittelstaedt, E. 1991. The ocean boundary along the northwest African coast: Circulation and oceanographic properties at the sea surface. *Progress in Oceanography*, 26(4), 307-355.
- Mo, G., Zotti, A., Agnesi, S., Finoia, M.G., Bernardini, D. and Cozzi, B. 2009. Age classes and sex differences in the skull of the Mediterranean monk seal, *Monachus monachus* (Hermann, 1779). A study based on bone shape and density. *The Anatomical Record: Advances in Integrative Anatomy and Evolutionary Biology*, 292(4), 544-556.
- Munro, L.E., Longstaffe, F.J. and White, C.D., 2008. Effects of heating on the carbon and oxygen-isotope compositions of structural carbonate in bioapatite from modern deer bone. *Palaeogeography, Palaeoclimatology, Palaeoecology*, 266(3-4), pp.142-150. <https://doi.org/10.1016/j.palaeo.2008.03.026>.
- Nehlich, O. and Richards, M.P. 2009. Establishing collagen quality criteria for sulphur isotope analysis of archaeological bone collagen. *Archaeological and Anthropological Sciences*, 1(1), 59-75.

- Nehlich, O. 2015. The application of sulphur isotope analyses in archaeological research: a review. *Earth-Science Reviews*, 142, 1-17.
- Nelson, B.K., DeNiro, M.J., Schoeninger, M.J., De Paolo, D.J. and Hare, P.E. 1986. Effects of diagenesis on strontium, carbon, nitrogen and oxygen concentration and isotopic composition of bone. *Geochimica et Cosmochimica Acta*, 50(9), pp.1941-1949.
- Nemliher, J.G., Baturin, G.N., Kallaste, T.E. and Murdmaa, I.O., 2004. Transformation of hydroxyapatite of bone phosphate from the ocean bottom during fossilization. *Lithology and Mineral Resources*, 39, 468-479. <https://doi.org/10.1023/B:LIMI.0000040736.62014.2d>.
- Newsome, S.D., Clementz, M.T. y Koch, P.L. 2010. Using stable isotope biogeochemistry to study marine mammal ecology. *Mar Mam Sc*, 26, 509-572, <https://doi.org/10.1111/j.1748-7692.2009.00354.x>.
- Nieri, M., Grau, E., Lamarche, B. and Aguilar, A., 1999. Mass mortality of Atlantic spotted dolphins (*Stenella frontalis*) caused by a fishing interaction in Mauritania. *Marine Mammal Science*, 15(3), 847-854.
- Olson, P.A. 2018. Pilot whales. In *Encyclopedia of Marine Mammals* (third edition), eds. Würsig, B., Thewissen, J.G.M. and Kovacs, K.M., 701-705. San Diego: Academic Press.
- Pastor, T., Cappozzo, H. L., Grau, E., Amos, W., Aguilar, A. 2011. The mating system of the Mediterranean monk seal in the Western Sahara. *Mar. Mamm. Sci.* 27(4): E302-320.
- Pelegrí, J.L., Peña-Izquierdo, J., Machín, F., Meiners, C. and Presas-Navarro, C., 2017. Oceanography of the Cape Verde basin and Mauritanian slope waters. *Deep-sea ecosystems off Mauritania: research of marine biodiversity and habitats in the Northwest African margin*, 119-153.
- Peña-Izquierdo, J., Pelegrí, J.L., Pastor, M.V., Castellanos, P., Emelianov, M., Gasser, M., Salvador, J. and Vázquez-Domínguez, E., 2012. The continental slope current system between Cape Verde and the Canary Islands. *Sci. Mar*, 76, 65-78.
- Peterson, B.J.; Howarth, R.W. and Garritt, R.H. 1985. Multiple Stable Isotopes Used to Trace the Flow of Organic Matter in Estuarine Food Webs. *Science*, 227(4692), 1361–1363, doi:10.1126/science.227.4692.1361.
- Peterson, B.J. 1999. Stable isotopes as tracers of organic matter input and transfer in benthic food webs: a review. *Acta oecologica*, 20(4), 479-487.
- Pinela, A., Borrell, A., Cardona, L. y Aguilar, A. 2010. Stable isotopes reveals habitat partitioning among marine mammals off the NW African coast and unique trophic niches for two globally threatened species. *Mar Eco Prog Series*, Vol. 416. 295-306, 10.3354/meps08790.
- Post, D.M. 2002. Using stable isotopes to estimate trophic position: models, methods, and assumptions. *Ecology*, 83(3), 703-718.
- Pottier, A., Catry, T., Trégarot, E., Maréchal, J.P., Fayad, V., David, G., Cheikh, M.S. and Failler, P., 2021. Mapping coastal marine ecosystems of the National Park of Banc d'Arguin (PNBA) in Mauritania using Sentinel-2 imagery. *International Journal of Applied Earth Observation and Geoinformation*, 102, p.102419, <https://doi.org/10.1016/j.jag.2021.102419>.
- Pritchard, D.W., 1952. Estuarine hydrography. In *Advances in geophysics*, Elsevier, 1, 243-280.
- R Core Team, 2021. R: A Language and Environment for Statistical Computing. R Foundation for Statistical Computing, Vienna. <https://www.R-project.org>. Accessed 13 June 2022.

- Ramos, R. y González-Solís, J. 2012. Trace me if you can: the use of intrinsic biogeochemical markers in marine top predators. *Frontiers in Ecology and the Environment*, 10: 258-266, <https://doi.org/10.1890/110140>.
- Ridgway, S.H., Harrison, R. and Harrison, R.J. (eds.) 1998. *Handbook of marine mammals: the second book of dolphins and the porpoises*. Elsevier, 486 pp.
- Riofrío-Lazo, M. and Aurióles-Gamboa, D. 2013. Timing of isotopic integration in marine mammal skull: comparative study between calcified tissues. *Rapid Communications in Mass Spectrometry*, 27(9), 1076-1082, <https://doi.org/10.1002/rcm.6556>.
- Robineau, D. and Vely, M. 1998. Les cétacés des côtes de Mauritanie (Afrique du Nord-ouest). Particularités et variations spatio-temporelles de répartition: Rôle des facteurs océanographiques. *Revue d'Ecologie, Terre et Vie, Société nationale de protection de la nature*, 53 (2), 123-152, hal-03529162.
- Rossmann, S., Ostrom, P.H., Gordon, F. and Zipkin, E.F. 2016. Beyond carbon and nitrogen: guidelines for estimating three-dimensional isotopic niche space. *Ecology and Evolution*, 6(8), 2405-2413, doi: 10.1002/ece3.2013.
- Rubenstein, D.R. y Hobson, K.A. 2004. From birds to butterflies: animal movement patterns and stable isotopes. *TRENDS in Ecology and Evolution*, 19(5), doi:10.1016/j.tree.2004.03.017.
- Russell, G., Sánchez-Cabanes, A. and Nimak-Wood, M. 2018. The autumn occurrence and spatial distribution of cetaceans in the waters of Mauritania during a geophysical survey in 2012. *African Journal of Marine Science*, 40(4), 371-381.
- Samba Bilal, A., Wagne, M.M., Wagué, A., Dia, A. and Van Waerebeek, K. 2023. The Cetaceans of Mauritania, West Africa: a concise zoogeographical review with two new species records. *Journal of Animal Diversity*, 5(1), 1-35.
- Schmidt, G.A. 1999. Error analysis of paleosalinity calculations. *Paleoceanography*, 14(3), 422-429. <https://doi.org/10.1029/1999PA900008>.
- Schoeninger, M.J. 2010. Chapter 15: Toward a  $\delta^{13}\text{C}$  Isoscape for Primates. In *Isoscapes: Understanding movement, pattern, and process on Earth through isotope mapping*, eds. West, J.B., Bowen, G.J., Dawson, T.E. and Tu, K.P., 319-333. Dordrecht: Springer Science & Business Media. doi: 10.1007/978-90-481-3354-3\_15.
- Séon, N., Brasseur, I., Scala, C., Tacail, T., Catteau, S., Fourel, F., Vincent, P., Lécuyer, C., Suan, G., Charbonnier, S. and Vinçon-Laugier, A. 2023. Determination of water balance maintenance in *Orcinus orca* and *Tursiops truncatus* using oxygen isotopes. *Journal of Experimental Biology*, 226(23), jeb245648. <https://doi.org/10.1242/jeb.245648>.
- Sevrin-Reyssac, J. 1993. Hydrology and underwater climate of the Banc d'Arguin, Mauritania: a review. In *Ecological Studies in the Coastal Waters of Mauritania: Proceedings of a Symposium held at Leiden, The Netherlands 25–27 March 1991*, Springer Netherlands, 1-8.
- Smeenk, C., Leopold, M.F. and Addink, M.J. 1992. Note on the harbour porpoise *Phocoena phocoena* in Mauritania, West Africa. *Lutra*, (35), 98-104.
- Sponheimer, M. and Lee-Thorp, J.A. 1999. Alteration of enamel carbonate environments during fossilization. *Journal of Archaeological Science*, 26(2), 143-150. <https://doi.org/10.1006/jasc.1998.0293>.
- Syväranta, J., Lensu, A., Marjomäki, T.J., Oksanen, S. and Jones, R.I. 2013. An empirical evaluation of the utility of convex hull and standard ellipse areas for assessing population niche widths from stable isotope data. *PloS one*, 8(2), p.e56094., doi:10.1371/journal.pone.0056094.



- Tulp, I. and Leopold, M.F. 2004. Marine mammals and seabirds in Mauritanian waters: pilot study April 2004, No. 04.020, RIVO *Biologie en Ecologie*, 42.
- Trueman, C.N., MacKenzie, K.M. and Palmer, M.R., 2012. Identifying migrations in marine fishes through stable-isotope analysis. *Journal of Fish Biology*, 81(2), 826-847, doi:10.1111/j.1095-8649.2012.03361.x.
- Van Waerebeek, K., Ofori-Danson, P.K., Debrah, J., Collins, T., Djiba, A. and Samba Ould Bilal, A. 2016. On the status of the common bottlenose dolphin *Tursiops truncatus* in western Africa, with emphasis on fisheries interactions, 1947-2015. *Document SC/66b/SM19 presented to the Scientific Committee of the International Whaling Commission, Bled, Slovenia*, 20.
- Velasquez-Vacca, A., Seminoff, J.A., Jones, T.T., Balazs, G.H. and Cardona, L. 2023. Isotopic ecology of Hawaiian green sea turtles (*Chelonia mydas*) and reliability of  $\delta^{13}\text{C}$ ,  $\delta^{15}\text{N}$ , and  $\delta^{34}\text{S}$  analyses of unprocessed bone samples for dietary studies. *Marine Biology*, 170(7), 81, <https://doi.org/10.1007/s00227-023-04232-1>.
- Vely, M., Dia, A.T. and N'diaye, R. 1995. Premières données concernant l'inventaire des mammifères marins du Parc National du Banc d'Arguin. Rapport CIRAD-EMVT N° 015, *Union Européenne et CIRAD-EMVT eds*.
- Weir, C.R. and Collins, T. 2015. A review of the geographical distribution and habitat of the Atlantic humpback dolphin (*Sousa teuszii*). *Advances in Marine Biology*, 72, 79-117.
- Wolff, W.J. and Smit, C.J. 1990. The Banc d'Arguin, Mauritania, as an environment for coastal birds. *Ardea*, 78(1), 17-38.
- Wolff, W.J., Van der Land, J., Nienhuis, P.H. and De Wilde, P.A.W.J., 1993. The functioning of the ecosystem of the Banc d'Arguin, Mauritania: a review. *Hydrobiologia*, 258, 211-222.
- Zenk, W., Klein, B. and Schroder, M. 1991. Cape Verde frontal zone. *Deep Sea Research Part A. Oceanographic Research Papers*, 38, S505-S530.
- Zenteno, L., Crespo, E., Goodall, N., Aguilar, A., de Oliveira, L., Drago, M., Secchi, E.R., Garcia, N. and Cardona, L. 2013. Stable isotopes of oxygen reveal dispersal patterns of the South American sea lion in the southwestern Atlantic Ocean. *Journal of Zoology*, 291(2), 119-126. <https://doi.org/10.1111/jzo.12051>.
- Zopfi, J., Böttcher, M.E. and Jørgensen, B.B. 2008. Biogeochemistry of sulfur and iron in Thioploca-colonized surface sediments in the upwelling area off central Chile. *Geochimica et Cosmochimica Acta*, 72(3), 827-843.

**3.3. Article 3: “The journey of loggerhead turtles from the Northwest Atlantic to the Mediterranean Sea as recorded by the stable isotope ratios of O, C and N of their bones”**



**Cani, A., Besén, C., Carreras, C., Pascual, M. and Cardona, L.** 2024. The journey of loggerhead turtles from the Northwest Atlantic to the Mediterranean Sea as recorded by the stable isotope ratios of O, C and N of their bones. *Marine Environmental Research*, p.106851. <https://doi.org/10.1016/j.marenvres.2024.106851>





## The journey of loggerhead turtles from the Northwest Atlantic to the Mediterranean Sea as recorded by the stable isotope ratios of O, C and N of their bones

### ABSTRACT

Loggerhead turtles, *Caretta caretta*, born on the nesting beaches of the Northwest Atlantic Ocean (US eastern coast) undertake a transoceanic migration immediately after birth, traveling eastward in association with the Gulf Stream and reaching the coasts of Europe and northwestern Africa when two or three years old and 20-30 cm in curve carapace length. Once there, they may remain in the eastern Atlantic or enter the Mediterranean Sea before eventually returning to the western Atlantic several years later. However, the timing of entry into the Mediterranean and the length of the period spent inside are poorly known. To study this, skeletochronology was combined with the analysis of the stable isotope ratios of oxygen ( $\delta^{18}\text{O}$ ), carbon ( $\delta^{13}\text{C}$ ) and nitrogen ( $\delta^{15}\text{N}$ ) in the cortical bone of the humerus of 31 juvenile loggerhead turtles of Northwest Atlantic origin found dead stranded in the Balearic Islands. Incremental bone layers were sampled to assess changes in habitat through the movement across isotopically distinct water masses and the existence of any ontogenetic change in the diet. Although the incremental layers corresponding to the very first years of live were missing in all individuals, the wide range of  $\delta^{18}\text{O}$  values of the remaining layers suggested that these juveniles moved between water masses differing in salinity, from the eastern Atlantic, the western Mediterranean, and the much saltier eastern Mediterranean, without any consistent temporal pattern. Nevertheless, upon reaching ten years old, loggerhead turtles seem to settle in low salinity areas of the western Mediterranean, such as the Algerian Basin or the Alboran Sea, likely preparing for their return towards their natal beaches in the Northwest Atlantic. Finally, the changes observed in the  $\delta^{13}\text{C}$  and  $\delta^{15}\text{N}$  values were small, suggesting only minor ontogenetic changes in their diet throughout the analysed life stages.

**Keywords:** Bioapatite; *Caretta caretta*; Habitat use; Salinity; Skeletochronology.



## INTRODUCTION

The loggerhead turtle, *Caretta caretta*, is the most common sea turtle species in the Mediterranean Sea (Casale et al., 2018), where individuals from three distinct Regional Management Units can be found: the Mediterranean, the Northwest Atlantic and, to a lesser extent, the Eastern Atlantic (Clusa et al., 2014; Wallace et al., 2023). Loggerhead turtles hatching on the nesting beaches of the Northwest Atlantic disperse along the Gulf Stream (Figure 3.10) and reach the coasts of Europe and northwestern Africa when two or three years old and 20-30 cm in curved carapace length (CCL) (Hays and Marsh, 1997; Bolten et al., 2003; Mansfield et al., 2014). Experimental evidence indicates that these juveniles exhibit directional swimming to remain within the North Atlantic Subtropical Gyre (Lohmann et al., 2001; Lohmann et al., 2012), although some might drift out of the mainstream in association with gyre currents and meso-scale eddies (Mansfield et al., 2014). Eventually, these juvenile loggerhead turtles will reach the Azores, Madeira and the Canary Islands (Monzón-Argüello et al., 2009; Mansfield et al., 2009; Mansfield et al., 2014) and some will remain several years in the eastern Atlantic (Varo-Cruz et al., 2016; Freitas et al., 2019; Chambault et al., 2019; Chambault et al., 2021) before returning to the Northwest Atlantic when 40-60 cm CCL (Bolten et al., 2003; McClellan and Read, 2007; Mansfield et al., 2009).

During their stay in the eastern Atlantic Ocean, some of the juvenile loggerhead turtles of Northwestern Atlantic origin may enter the Mediterranean Sea (Clusa et al., 2014), where the strong and permanent eastward current at the Strait of Gibraltar (Figure 3.10) will prevent them from returning to the East Atlantic until they are approximately 60 cm CCL (Revelles et al., 2007a). However, the entry of juvenile loggerhead turtles in the Mediterranean Sea seems to be a rare event, as only one out of 64 individuals (size range = 23.4 – 94.6 cm CCL) satellite tracked in the Northeast Atlantic entered the Mediterranean Sea during the tracking period [Canary Islands: n = 24 (Varo-Cruz et al., 2016); Azores: n = 28 (Chambault et al., 2019); Madeira: n = 10 (Freitas et al., 2019); Bay of Biscay: n = 22 (Chambault et al., 2021)]. The rarity of such event is, in fact, surprising, considering that juveniles from the Northwest Atlantic population prevail over juveniles of Mediterranean origin in some of the Mediterranean foraging grounds with the highest density of loggerhead turtles in the Mediterranean Sea (Clusa et al., 2014; DiMatteo et al., 2022). Hence, a better understanding on the timing of entry of these juveniles in the Mediterranean Sea is necessary to understand the relevance of this region as a developmental habitat for the Northwestern Atlantic loggerhead turtle population, to



assess the significance of the bycatch mortality in the area (de Quevedo et al., 2013) and to predict future changes in the make-up of Mediterranean foraging grounds, especially in a context of environmental changes influencing both the weakening of the Gulf Stream (Piecuch and Beal, 2023) and the Azores current (Frazão et al., 2022) and the inflow across the Strait of Gibraltar (Soto-Navarro et al., 2020).

The use of indirect techniques such as stable isotope analysis has largely increased in the last decades, since they can be informative about a variety of factors such as diet, trophic position, migration patterns and habitat use (Rubenstein and Hobson, 2004). For instance, the oxygen stable isotope ratio ( $\delta^{18}\text{O}$ ) in animal tissues reflects that of the water mass where they feed, thus allowing to differentiate between individuals foraging in isotopically distinct areas (Yoshida and Miyazaki, 1991; Rubenstein and Hobson, 2004; Newsome et al., 2010; Ben-David and Flaherty, 2012). In addition, the periosteal bone of the humerus of sea turtles exhibits annual growth bands, also known as incremental layers, which can be used to assess the age of an individual as well as sampled for stable isotope analysis (Snover et al., 2010; Ramirez et al., 2015; Turner Tomaszewicz et al., 2017a). Thus, assessing the  $\delta^{18}\text{O}$  ratio across the incremental layers of the bone should allow tracking the movement of sea turtles across isotopically distinct water masses.

The Mediterranean Sea has a negative water balance due to an excess of evaporation over precipitation and river runoff, which results in a decrease of sea level, compensated by the entry of Atlantic surface waters through the Strait of Gibraltar (Millot and Taupier-Letage, 2005; Soto-Navarro et al., 2020). This process creates a marked and predictable salinity gradient inside the Mediterranean Sea, increasing eastward from the Strait of Gibraltar and reaching the point of maximum salinity at the Levantine Sea (Figure 3.10) (Brasseur et al., 1996; Millot and Taupier-Letage, 2005). Similarly, regions with an excess of evaporation also present higher  $\delta^{18}\text{O}$  values in surface waters due to the preferential evaporation of the water molecules carrying the lighter  $^{16}\text{O}$  isotope and the resultant concentration of water molecules carrying the heavier  $^{18}\text{O}$  isotope (Sharp, 2017), which creates a positive and linear correlation between salinity and  $\delta^{18}\text{O}$  values (Gat, 1996; Conroy et al., 2014). Therefore, the  $\delta^{18}\text{O}$  values of Mediterranean surface waters reflect the same gradual increase as those of salinity from the Strait of Gibraltar to the eastern basin (Figure 3.10) (LeGrande and Smith, 2006) and this relationship facilitates the use of the  $\delta^{18}\text{O}$  as a habitat tracer to analyse animal movement, distribution and habitat use within the Mediterranean Sea (Belem et al., 2019; Cani et al., 2024).



Additionally, the carbon ( $\delta^{13}\text{C}$ ) and nitrogen ( $\delta^{15}\text{N}$ ) stable isotope ratios have been widely used to study the trophic ecology of marine animals (Newsome et al., 2010; Ramos and González-Solís, 2012). The former indicates the primary source of carbon in the diet, with generally higher  $\delta^{13}\text{C}$  values observed in benthic and coastal species and lower values found in pelagic and offshore consumers, whereas the latter increases consistently along the food web due to the trophic enrichment and thus allows for the assessment of trophic position of species or individuals (Rubenstein and Hobson, 2004; Newsome et al., 2010). Hence, the  $\delta^{13}\text{C}$  and  $\delta^{15}\text{N}$  values can be potentially used to identify changes in the diet and trophic position of loggerhead turtles (Cardona et al., 2014).

The present study uses the  $\delta^{18}\text{O}$ ,  $\delta^{13}\text{C}$  and  $\delta^{15}\text{N}$  values of incremental layers in the humerus of loggerhead turtles, previously confirmed to be of Northwestern Atlantic origin through genetic analysis (Clusa et al., 2014), found dead stranded in the Balearic Islands to assess the timing of entry into the Mediterranean Sea, analyse their movements across isotopically distinct water masses and identify any ontogenetic changes in the diet during their stay in developmental habitats.

## METHODS

### *Study area*

The Gulf Stream is one of the main currents of the North Atlantic Ocean, playing an important role on water circulation and climate for the northern hemisphere (Palter, 2015). It flows northwards along the coast of Florida until around  $35^\circ\text{N}$ , where it separates from the continental slope and moves eastward towards the Azores to form the North Atlantic Current and the Azores Current (Figure 3.10) (Fofonoff, 1981; Schmitz Jr. and McCartney, 1993). The latter then turns into the Canary Current, which flows southward along the western coast of South Africa and then returns to the western North Atlantic as the North Equatorial Current (Figure 3.10). However, part of the Azores Current reaches the Strait of Gibraltar and enters the Mediterranean Sea as the Algerian Current, circulating in a counter-clockwise direction through the entire basin and getting continuously transformed into a denser water mass that will eventually sink and outflow back into the eastern North Atlantic (Figure 3.10) (Fofonoff, 1981; Schmitz Jr. and McCartney, 1993; Millot and Taupier-Letage, 2005).

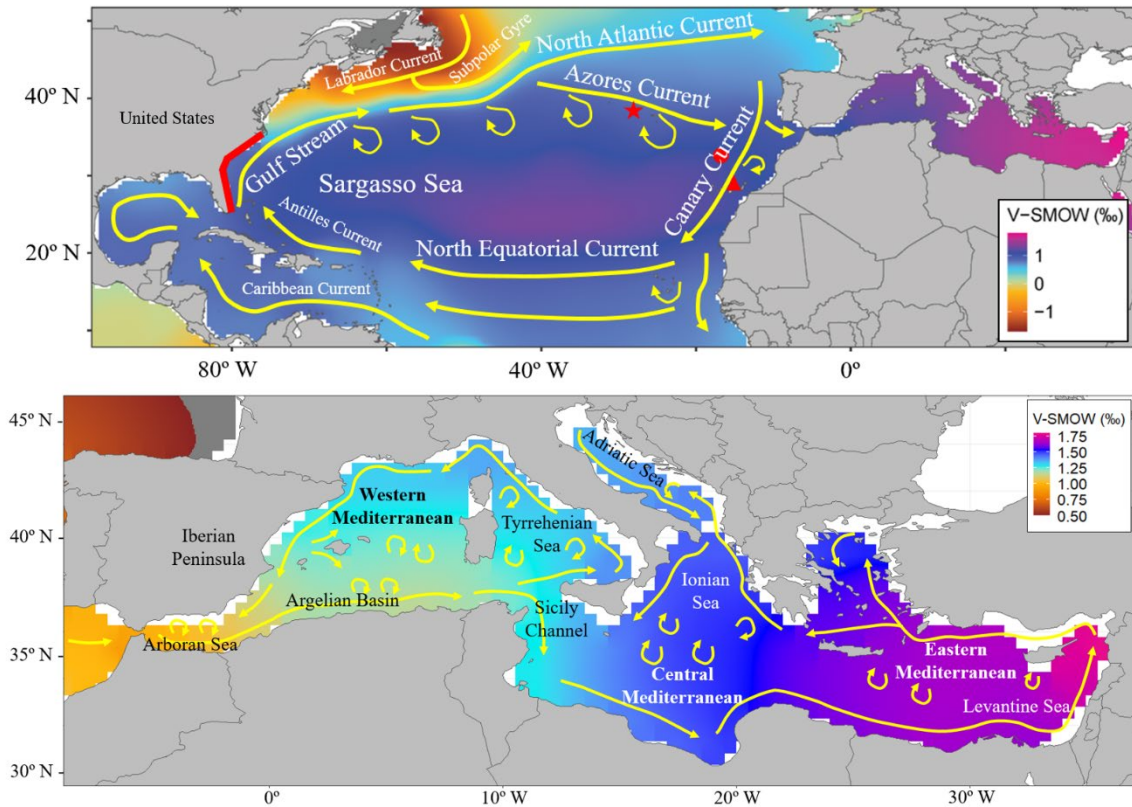


**Figure 3.10.** Main currents of the North Atlantic Ocean (above) and the Mediterranean Sea (below); background colours represent the sea surface mean  $\delta^{18}\text{O}$  values as indicated by the corresponding scale. Yellow arrows show the general path of the local currents, including gyres and meso-scale eddies. Red features in the top panel show, from left to right, the position of the nesting beaches of the Northwestern Atlantic (thick line), the Azores (star), Madeira (circle) and the Canary Islands (triangle). Sea surface  $\delta^{18}\text{O}$  values were obtained from LeGrande and Schmidt (2006) (data available at: <https://data.giss.nasa.gov/o18data/grid.html>).

The Mediterranean Sea is a semi-enclosed system divided into three main basins according to their location and properties: western, central and eastern basins (Figure 3.10) (Millot and Taupier-Letage, 2005). The western basin is characterized by a constant inflow of fresher Atlantic surface waters from the Strait of Gibraltar in the southwest, passing through the Alboran Sea and the Algerian Basin (Figure 3.10). Part of these Atlantic waters stay within the boundaries of the western basin, moving northwards through the Tyrrhenian Sea, reaching the coasts of the Iberian Peninsula from the north and closing the western Mediterranean gyre at the Alboran Sea (Figure 3.10) (Millot and Taupier-Letage, 2005). At the same time, another part of these waters continues



alongslope the Algerian Basin towards the central basin through the Strait of Sicily, eventually reaching the Levantine Sea and becoming part of the eastern Mediterranean gyre (Figure 3.10). As it circulates, the higher evaporation rate in the eastern Mediterranean increases the salinity and hence the density of this water mass, causing its sinking at specific zones in the northern parts of each basin (Millot and Taupier-Letage, 2005).

Figure 3.10 shows an isoscape of the study area for the  $\delta^{18}\text{O}$  values of the upper 5 m of seawater, based on the estimations made by LeGrande and Smith (LeGrande and Smith, 2006), which combined direct observations with regional estimates of the  $\delta^{18}\text{O}$  to salinity relationship.

### ***Sampling***

Humeri of 31 loggerhead turtles stranded or incidentally caught off the Balearic Islands between 2002 and 2007, and previously confirmed to be of Northwestern Atlantic origin through individual assignments using genetic analysis (Clusa et al., 2014), were selected from the tissue bank of the University of Barcelona. For all individuals, the curved carapace length (CCL) notch-to-notch was measured when necropsied for samples. More recent samples were not included in the analysis because the recent colonization of the western Mediterranean since 2010 by nesting females of both Mediterranean and Northwest Atlantic origin (Carreras et al., 2018; Luna-Ortiz et al., 2024; Cardona et al., 2024) have dampened the resolution of mitochondrial haplotypes and microsatellites for individual assignation to regional management units.

Two contiguous cross sections made in between the deltopectoral crest and the narrowest part of the right humerus of each individual were used (Zug et al., 1986; Goshe et al., 2020). The first cross section, of approximately 5 mm thick along the longitudinal axis of the bone, was decalcified with 5 % nitric acid for 3-4 days (Bjorndal et al., 2000) and subsequently dehydrated and fixed in paraffin wax according to the protocol described by Durfort (1987) as follows: 12 hours immersion in 70 % ethanol, 12 hours in 90 % ethanol, 12 hours in 100 % ethanol, 5 hours in 100 % chloroform, 5 hours in chloroform saturated with paraffin and, lastly, 5 hours in the oven while submerged in paraffin. The decalcified and dehydrated samples were then embedded in paraffin wax using a paraffin dispenser and left at room temperature to solidify. Histological sections of 10-20  $\mu\text{m}$  thick were obtained using a Rotary Microtome and placed on a glass slide for the posterior Hematoxylin-Eosin staining (Cardiff et al., 2014). Each stained section



was observed using an Olympus SZX10 Stereo Microscope and analysed with the cellSens Imaging Software to identify the incremental layers in the cortical bone. At least two stained sections were used per sample to confirm the continuity of the observed incremental layers, which were counted twice by two independent readers each time (LC, AC or CB). Counts matched in 25 samples and for the five samples that differed the last count performed was used.

The second cross section, of approximately 3 cm thick along the longitudinal axis of the humerus, was affixed to a surface and used to obtain the powdered bone samples for the stable isotope analysis using a hand drill with a fine diamond tip (Figure 3.11, a), obtaining between 2.0-3.0 mg of powdered bone for each sampled layer. Two ( $n = 17$ ) or three ( $n = 14$ ) layers between 2-3 mm deep were sampled from each humerus (Figure 3.11, a), with a total of 76 samples. The resulting bone powder was homogenized and weighted as explained in subsection 2.3.

The cortical bone of a turtle's humerus is formed by periosteal deposition, and the innermost incremental layers, corresponding to the earlier years of life and remaining closer to the medullar bone, often suffer an endosteal resorption (Zug et al., 1986). For this reason, the estimation of the age of each individual resulted from the sum of the total number of incremental layers observed, and the estimated number of reabsorbed layers (Suppl. Table 1), which was calculated using the regression equation derived from the correction-factor protocol described by Parham and Zug (1997). Briefly, for each humerus, the diameter of the resorption core was measured, which included the medullar cavity and any endosteal bone deposited in the area of resorption where incremental layers were lost (Zug et al., 1986; Piovano et al., 2011). The correction-factor protocol (Parham and Zug, 1997) was chosen since it was the method that showed the least variation and that adjusted best to the observed pattern of bone growth in loggerhead turtles. Moreover, it provides a direct estimation of the relationship between the resorption core radius and the number of lost layers based on an empirically derived relationship. This regression equation was derived from a subsample of small turtles with CCL < 70 cm and a few larger individuals added to establish a growth trajectory; thus, it accounts for the different distribution of the incremental layers in the cortical bone as the individual grows, since the outermost layers (those corresponding to the last years of the turtle's life) tend to be closer together than the innermost layers (those corresponding to the earlier years of the turtle's life). The regression equation used for this purpose was as follows:



$$\# \text{ Lost layers} = (r_{rc} - 0.407)/0.75 \quad (1)$$

where  $r_{rc}$  is the radius of the resorption core, obtained by dividing the measured diameter by two (Parham and Zug, 1997).

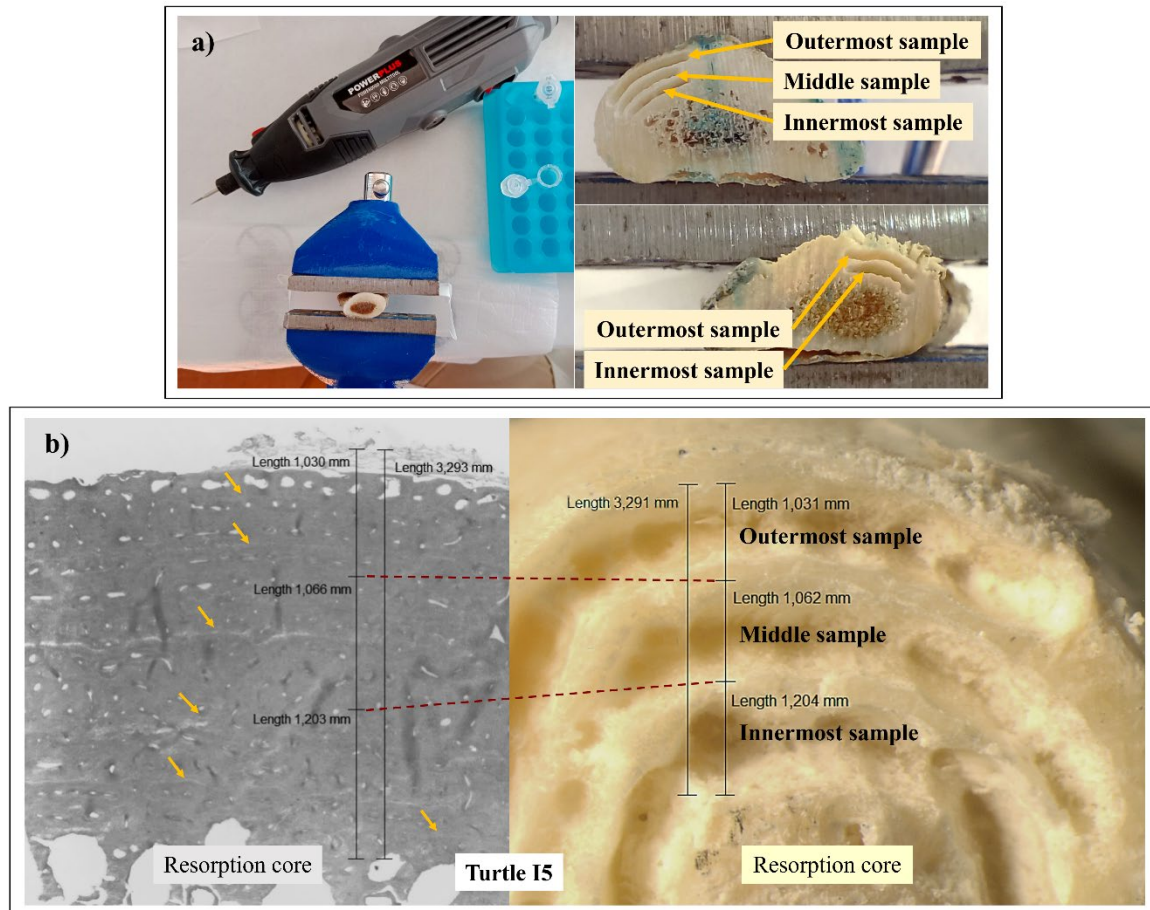


**Figure 3.11.** **a)** Bone sampling of three (outermost, middle and innermost) or two (outermost and innermost) layers from the second cross-section of the humerus. **b)** Example of the method for cross-referencing the position of each observed incremental layer (yellow arrows on the left) to that of the contiguous section of the same bone that was sampled for stable isotope analysis (the colour of this image was edited to better show the incremental layers).

The ages covered by each sampled bone layer were determined by cross-referencing the position of each sample (i.e., where the bone powder was obtained for stable isotope analysis) with that of the counted incremental layers after the staining procedure, based on the measurements between sampled layers and using the outermost part of the bone and the resorption core as references (Figure 3.11, b). When more than



one year was covered by the same sample, the highest age of the estimated range was assigned (Table 3.3). Finally, it was not possible to determine the age of turtle A20, since the poor condition of the bone hindered the observation and counting of the incremental layers; thus, this individual was not considered for the age-related analysis. However, for discussion purposes, we assumed that turtle A20 was approximately eight years old, based on the mean of the ages estimated for turtles of similar CCL (A8 and I4; Table 3.3).

### ***Stable isotope analysis***

#### ***- Oxygen stable isotopes***

Between 1.5- 2.0 mg of each of the homogenized bone samples were soaked in 30% hydrogen peroxide (H<sub>2</sub>O<sub>2</sub>) for 48 h to remove any organic compounds, and then rinsed repeatedly with deionized (Milli-Q) water and treated with 1 M of calcium acetate–acetic acid buffer for another 24 h to remove any diagenetic carbonate. Finally, they were carefully rinsed again with Milli-Q water and dried for 24 h and left to dry in an oven at 50°C for another 24 hours (Koch et al., 1997).

Approximately 1.0 mg of each treated bone sample was weighed and dissolved in 100 % phosphoric acid at 70 °C with concurrent cryogenic trapping of CO<sub>2</sub> and H<sub>2</sub>O. The CO<sub>2</sub> was then admitted to a Finnigan MAT 252 Isotope Ratio Mass Spectrometer (IRMS) with Kiel III Carbonate Analysis Device (Thermo Fisher Scientific) to obtain the isotopic ratio. Two internal isotopic reference materials, RC-1 and CECC with δ<sup>18</sup>O values relative to the Vienna Pee Dee Belemnite (V-PDB) calcium carbonate of -2.08 ‰ and -17.56 ‰, respectively, were employed once every five analysed samples in order to recalibrate the system and compensate for any measurement drift over time. Internationally certified isotope secondary standards distributed by the International Atomic Energy Agency (IAEA) of known <sup>18</sup>O/<sup>16</sup>O ratios were then used to confirm the results. These consisted of the NBS-19, NBS-18 and IAEA 603 calcite standard, with δ<sup>18</sup>O values of -2.20 ‰, -23.2 ‰ and -2.37 ‰, respectively, relative to V-PDB. The analytical precision of δ<sup>18</sup>O tested by replicate analyses was ±0.04 ‰ (standard deviation). Because δ<sup>18</sup>O values in animal studies are more commonly presented relative to the Vienna Standard Mean Oceanic Water (V-SMOW) index, δ<sup>18</sup>O values were converted from V-PDB to V-SMOW according to the following equation (Cardona et al., 2014):

$$\delta^{18}\text{O}_{(\text{SMOW})} = [\delta^{18}\text{O}_{(\text{PDB})} \times 1.03086] + 30.86 \quad (2)$$



### - *Carbon and nitrogen stable isotopes*

Approximately 1.0 mg of each of the homogenized bone samples were weighted and encapsulated in tin capsules (3.3 x 5 mm) for  $\delta^{13}\text{C}$  and  $\delta^{15}\text{N}$  determination. No pre-treatment was applied since the lipid content of the cortical bone of sea turtles is low (Turner Tomaszewicz et al., 2015). Samples were combusted at 900 °C using a Delta V Advantage isotope ratio mass spectrometer with a Flash IRMS elemental analyzer and CONFLO IV interface (Thermo Fisher Scientific). Isotopic reference materials of known  $^{13}\text{C}/^{12}\text{C}$  ratios were: IAEA CH7 ( $\delta^{13}\text{C} = -32.15 \text{ ‰}$ ), UCGEMA SC ( $\delta^{13}\text{C} = -13.21 \text{ ‰}$ ), UCGEMA CH ( $\delta^{13}\text{C} = -22.08 \text{ ‰}$ ), fructose ( $\delta^{13}\text{C} = -10.80 \text{ ‰}$ ), and USGS 62 ( $\delta^{13}\text{C} = -14.79 \text{ ‰}$ ). Isotopic reference materials of known  $^{15}\text{N}/^{14}\text{N}$  ratios were: UCGEMA CH ( $\delta^{15}\text{N} = -4.81 \text{ ‰}$ ), IAEA N1 ( $\delta^{15}\text{N} = 0.40 \text{ ‰}$ ), UCGEMA P ( $\delta^{15}\text{N} = 7.60 \text{ ‰}$ ), UCGEMA SC ( $\delta^{15}\text{N} = 12.40 \text{ ‰}$ ), IAEA 600 ( $\delta^{15}\text{N} = 1.00 \text{ ‰}$ ), USGS 62 ( $\delta^{15}\text{N} = 20.17$ ). All these isotopic reference materials were used at the beginning and at the end of the whole run and different combinations of two of them were used to recalibrate the system once every 16 samples, in order to compensate for any measurement drift over time. Analytical precision for repeated measurements of the reference material, run in parallel with the bone samples, was 0.4 ‰ for  $\delta^{13}\text{C}$  and 0.3 ‰ for  $\delta^{15}\text{N}$ .

### *Data analysis*

All statistical analyses and plots were carried out using R Statistical Software v 4.1.2 (R Core Team, 2021). Normality was assessed through the Lilliefors test and homoscedasticity by means of the Levene test. All data was confirmed to follow a normal distribution, except age ( $D = 0.186$ ,  $p < 0.001$ ), thus, parametric and non-parametric tests were applied accordingly. The relationship between the  $\delta^{18}\text{O}$ ,  $\delta^{13}\text{C}$  and  $\delta^{15}\text{N}$  values of each sampled incremental layer and their corresponding estimated age was determined with Kendall's rank correlation (tau) and an adjusted Generalized Additive Model (GAM) with the isotopic ratios as the response variable, the age as the explanatory variable to which a smoothing spline was included in order to capture non-linear relationships, and the individual's ID as a random factor.

Two-dimensional plots were built using the package "SIBER" (Stable Isotope Bayesian Ellipses) (Jackson et al., 2011) to estimate the isotopic niche width and overlaps between the different ages for the  $\delta^{13}\text{C}$  and  $\delta^{15}\text{N}$  isotopic space (isospace). Most age classes were analysed independently, but animals of 3 and 4 years old and those ranging 12-15 years old were pooled together, respectively, because sample size was too small to



calculate the standard ellipses using SIBER (Jackson et al., 2011). The isotopic niche width was estimated as the standard ellipse area of each age class, corrected for small sample size (SEAc) (Jackson et al., 2011). This approach was preferred over the Bayesian estimate of the standard ellipse because allows plotting the isotopic niche of each species within the isospace and to calculate the overlap among species. Moreover, the relationship between the SEAc in the  $\delta^{13}\text{C}$ - $\delta^{15}\text{N}$  isospace and age was further analysed with Kendall's rank correlation ( $\tau$ ) and an adjusted Generalized Additive Model (GAM), with the SEAc as the response variable and the age as the explanatory variable.

In addition, the magnitude of the difference between the  $\delta^{18}\text{O}$ ,  $\delta^{13}\text{C}$  and  $\delta^{15}\text{N}$  values of the outermost, the middle (when applicable), and the innermost incremental layer per individual was compared with the magnitude of the difference of known environmental values of the North Atlantic Ocean and the Mediterranean Sea, to analyse changes in the habitat use over time (Figure 3.13). For this, the differences in  $\delta^{18}\text{O}$  values between incremental layers of each turtle were compared to the isospace presented in Figure 3.10, based on the estimations made by LeGrande & Smith (2006) and available at the Global Seawater Oxygen Isotope Database (<https://data.giss.nasa.gov/o18data/>). Considering the endosteal resorption of the innermost incremental layers explained above, and thus the loss of the information about the first years of life corresponding to the time spent in the Gulf Stream, only the surface waters between Azores and the European/Northeast African coast were considered. In this case, the magnitude of the difference between the lowest  $\delta^{18}\text{O}$  values found at the nearby North Atlantic waters (0.80 ‰) and the highest values found at the Easternmost part of the Mediterranean (1.80 ‰) is  $\pm 1.00$  ‰. Furthermore, a mean increase of 0.25 ‰ was found between Mediterranean regions (i.e., Strait of Gibraltar and Alboran Sea, western Mediterranean basin, central Mediterranean basin, and eastern Mediterranean basin). Hence, only those individuals with a difference larger than  $\pm 0.25$  ‰ between incremental layers were considered to have moved between regions, whereas those with a difference larger than  $\pm 1.00$  ‰ were likely to move from one side to the other of the Mediterranean Sea. The direction of these migrations for each individual was determined by the sign of the value (e.g., positive differences indicate movement towards waters with higher  $\delta^{18}\text{O}$  values, and vice versa).

Regarding the  $\delta^{13}\text{C}$  values, the difference between layers was compared to the difference between the mean values of the oceanic particulate organic matter (-23.1 ‰) and the neritic seagrass *Posidonia oceanica* (-13.0 ‰) off the Balearic Islands, according to Cardona et al., (2007), which is  $\pm 10.1$  ‰. The direction of the movement was also



determined by the sign of the value (e.g., positive differences indicate movements towards oceanic waters with lower  $\delta^{13}\text{C}$  values, and vice versa). Finally, the  $\delta^{15}\text{N}$  values were compared to  $\pm 3.4$  ‰, the mean trophic fractionation in aquatic food webs according to Post (2002).

Finally, Straight Carapace Length (SCL) values reported in the literature were converted to Curved Carapace Length (CCL) using the following unpublished equation, derived by the authors for loggerhead turtles found in the Mediterranean Sea:

$$CCL = [SCL + 0.129] / 0.926 \quad (3)$$

## RESULTS

The curved carapace length (CCL) of the 31 analysed loggerhead turtles ranged from 28.0 to 80.6 cm, with a mean value of  $55.4 \pm 11.5$  cm CCL (Table 3.3). The age when stranded was estimated for 30 turtles, as it was not possible for individual A20, and ranged from 4 to 15 years old with a mean of  $8.3 \pm 2.7$  years old (Table 3.3). Bone sampling for the stable isotope analysis of these 30 individuals yielded 74 samples, with sample ages ranging from 3 to 15 years old ( $7.1 \pm 2.6$  years old; Table 3.3). In addition, each sampled layer covered between one and four years of a turtle's life, because of large differences in layer thickness. In most cases (54.1 %), each layer corresponded to two consecutive years, others (21.6 %) to only one year, and the rest corresponded to three and four years (17.6 % and 6.8 %, respectively).

When pooled together, the  $\delta^{18}\text{O}$  values obtained for the incremental layers of the humerus of the analysed individuals ranged from 30.9 to 34.5 ‰ ( $32.9 \pm 0.8$  ‰; Table 3.3; Figure 3.12, a). Therefore, the maximum difference between the bone  $\delta^{18}\text{O}$  values was 3.6 ‰, which is considerably larger than the estimated difference between the  $\delta^{18}\text{O}$  ratio of surface waters for the study area (1.00 ‰; see Methods), hence suggesting the use of isotopically different water masses between individuals. Furthermore, the  $\delta^{18}\text{O}$  values of the incremental layers corresponding to less than 10 years old, which included 29 turtles, were considerably scattered, whereas those of 10 years and older, which included 10 turtles, were clustered around a lower mean  $\delta^{18}\text{O}$  value (Figure 3.12, a). The age of the incremental layers and their respective  $\delta^{18}\text{O}$  values were negatively correlated (Kendall's rank correlation:  $\tau = -0.24$ ,  $z = -2.83$ ,  $p = 0.004$ ) and the adjusted GAM, which accounted for 80.3 % of the variability in the data, suggested a predominantly linear relationship between the two variables (GAM model:  $R^2(\text{adj}) = 0.67$ ,  $\text{GCV} = 0.36$ ,



Scale est. = 0.21; Figure 3.12, a). Furthermore, 24 out of the 31 considered turtles showed differences equal or larger than  $\pm 0.25$  ‰ between at least two of the analysed incremental layers (Table 3.3; Suppl. Table 2), which is the estimated difference in the  $\delta^{18}\text{O}$  ratio of surface waters between Mediterranean basins (see Methods; Figure 3.13) and thus indicates the use of water masses with distinct  $\delta^{18}\text{O}$  values throughout the analysed periods.

On the other hand, when analysing individual movement patterns, four different scenarios appeared. First, 17 turtles had the highest  $\delta^{18}\text{O}$  value in their innermost incremental layer compared to the middle and/or outermost ones (Table 3.3; Suppl. Table 2; Suppl. Figure 1), suggesting a continuous movement from  $^{18}\text{O}$ -enriched to  $^{18}\text{O}$ -depleted waters. However, four of them (A1, I5, A15, A28) also showed a decrease in the  $\delta^{18}\text{O}$  value of their middle layer compared to the other two, seemingly going from  $^{18}\text{O}$ -enriched to  $^{18}\text{O}$ -depleted and back to  $^{18}\text{O}$ -enriched waters. On the contrary, a second group of four turtles (A10, M11, A20, A35), three of which were estimated to be six and seven years old, showed the highest  $\delta^{18}\text{O}$  value in their outermost incremental layer compared to the middle and/or innermost ones (Table 3.3; Suppl. Table 2; Suppl. Figure 1), suggesting the movement from  $^{18}\text{O}$ -depleted to  $^{18}\text{O}$ -enriched waters during the analysed period. A third group of three turtles (I4, M19, A18) showed the highest  $\delta^{18}\text{O}$  value in their middle layer and similarly low values in their outermost and innermost incremental layers (Table 3.3; Suppl. Table 2; Suppl. Figure 1), indicating the movement from a  $^{18}\text{O}$ -depleted to a  $^{18}\text{O}$ -enriched region and back to a  $^{18}\text{O}$ -depleted region. Finally, the remaining seven turtles had a difference smaller than  $\pm 0.25$  ‰ between all the analysed incremental layers and hence, they were considered to be similar. This included two of the oldest turtles analysed in this study, A39 and M17, estimated to be 13 and 15 years old, respectively, when stranded. They both showed similarly low  $\delta^{18}\text{O}$  values between the analysed incremental layers, covering around seven years (from 7 to 13 years old) for the former and nine years (from 7 to 15 years old) for the latter (Table 3.3; Suppl. Table 2; Suppl. Figure 1).

In addition to what is mentioned above, five turtles (A19, A15, A13, A28, A22) belonging to the first two groups and with an estimated age between 8 and 13 years old, showed differences larger than  $\pm 1.00$  ‰ between at least two of the analysed incremental layers (Table 2; Figure 3.13, a), a change that seemed to occur in about two years for four of these individuals (Table 3.3; Suppl. Table 2; Suppl. Figure 1).



On the other hand, the  $\delta^{13}\text{C}$  values obtained for the incremental layers of the considered turtles ranged from -16.7 to -14.4 ‰ ( $-15.5 \pm 0.4$  ‰; Suppl. Table 4) and showed no significant correlation with the corresponding estimated age (Kendall's rank correlation:  $\tau = -0.08$ ,  $z = -0.90$ ,  $p = 0.37$ ; Figure 3.12, b). In this case, the maximum difference between the highest and the lowest  $\delta^{13}\text{C}$  values for the analysed incremental layers was 2.3 ‰ and between layers of the same individual was 1.2 ‰, both considerably smaller than the estimated difference between oceanic and neritic habitats in the study area ( $\pm 10.1$  ‰; see Methods; Figure 3.13), thus suggesting that all the considered turtles relied on a similar diet which seemed to remain stable during the studied period.

Conversely, the  $\delta^{15}\text{N}$  values of all incremental layers ranged from 11.04 to 7.05 ‰ ( $9.1 \pm 0.8$  ‰; Suppl. Table 5), with less variability and higher values in those over 9 years old (Figure 3.12, c). However, no statistically significant correlation was observed between the  $\delta^{15}\text{N}$  values and the corresponding age (Kendall's rank correlation:  $\tau = 0.15$ ;  $z = 1.75$ ;  $p = 0.08$ ; Figure 3.12, c). Here, the maximum difference observed between incremental layers of the same individual was 2.3 ‰ (Suppl. Table 2), which is smaller than the mean estimated trophic enrichment of 3.4 ‰ per trophic level (see Methods; Figure 3.13), suggesting no changes in trophic position during the studied period. Nevertheless, the  $\delta^{15}\text{N}$  values of all samples combined covered a range of about 4.00 ‰, which can suggest that some individuals might be using regions with different  $\delta^{15}\text{N}$  baselines.

Finally, the standard ellipses of the analysed age classes largely overlapped within the  $\delta^{13}\text{C} - \delta^{15}\text{N}$  isospace, with the ellipses of the youngest age classes encompassing those of the older ones (Figure 3.14, a). Furthermore, the standard ellipse area (SEAc) decreased significantly with age (Kendall's rank correlation:  $\tau = -0.86$ ,  $z = -2.97$ ,  $p = 0.003$ ) and the adjusted GAM, which accounted for 89.3 % of the variability in the data, suggested linear relationship between the SEAc and age (GAM model:  $R^2(\text{adj}) = 0.88$ ,  $\text{GCV} = 0.05$ ,  $\text{Scale est.} = 0.04$ ; Figure 3.14, b).



**Table 3.3.** Oxygen stable isotope ratio ( $\delta^{18}\text{O}$ ), estimated age and years covered for each sampled incremental layer for all the considered individuals.

Turtle ID	CCL (cm)	Age	Cortical bone samples								
			Innermost layer			Middle layer			Outermost layer		
			$\delta^{18}\text{O}_{\text{SMOW}}$ (‰)	Age	Years covered	$\delta^{18}\text{O}_{\text{SMOW}}$ (‰)	Age	Years covered	$\delta^{18}\text{O}_{\text{SMOW}}$ (‰)	Age	Years covered
A4	28.00	4	32.75	3	2	-	-	-	33.00	4	1
M12	36.00	5	34.47	4	2	-	-	-	34.38	5	1
A10	41.83	6	33.50	4	2	-	-	-	33.20	6	2
A36	43.00	6	32.09	4	2	32.01	7	2	32.78	6	2
M11	45.94	6	33.66	4	1	33.19	5	1	32.78	6	1
M15	47.50	6	33.38	4	2	-	-	-	33.52	6	2
M7	47.62	8	32.50	6	3	-	-	-	33.19	8	2
A8	48.50	7	33.48	5	2	-	-	-	33.73	7	2
A20	48.50	*8	33.84	-	-	-	-	-	33.18	-	-
I4	48.67	9	32.87	5	2	33.53	7	2	32.79	9	2
M19	50.00	7	32.75	4	1	33.43	5	1	32.92	7	2
M14	52.00	7	32.20	5	3	-	-	-	33.04	7	2
A7	52.65	7	33.21	5	2	-	-	-	33.01	7	2
A1	53.00	7	32.86	4	1	32.39	6	2	32.79	7	1
A19	53.46	7	31.88	4	2	31.90	6	2	32.87	7	1
A14	54.00	9	31.86	6	4	-	-	-	32.77	9	3
A23	54.00	8	32.03	5	2	32.38	7	2	32.34	8	1
A21	54.22	6	33.63	5	2	-	-	-	33.74	6	1
A35	57.40	10	32.58	7	4	-	-	-	32.29	10	3
A13	58.50	10	32.62	6	3	32.02	8	2	33.83	10	2
A6	59.00	7	33.79	5	1	34.11	6	1	34.13	7	1
I5	59.00	9	33.45	5	2	32.66	7	2	33.44	10	3
A32	61.50	8	33.43	6	3	-	-	-	33.36	8	2
A29	62.00	8	33.76	6	2	-	-	-	34.31	8	2
A18	66.80	9	33.30	5	1	33.67	7	2	33.28	9	2
A26	67.00	9	31.31	7	3	-	-	-	31.63	9	2
A15	69.00	10	32.78	6	2	31.02	8	2	32.59	10	2
A39	70.00	13	31.89	9	3	-	-	-	32.05	13	4
A22	70.85	14	30.87	10	4	-	-	-	32.19	14	4
M17	76.00	15	31.98	9	3	31.86	12	3	31.99	15	3
A28	80.64	14	32.47	10	3	31.73	12	2	33.21	14	2

\*assumed on the basis of the age of turtles of similar CCL

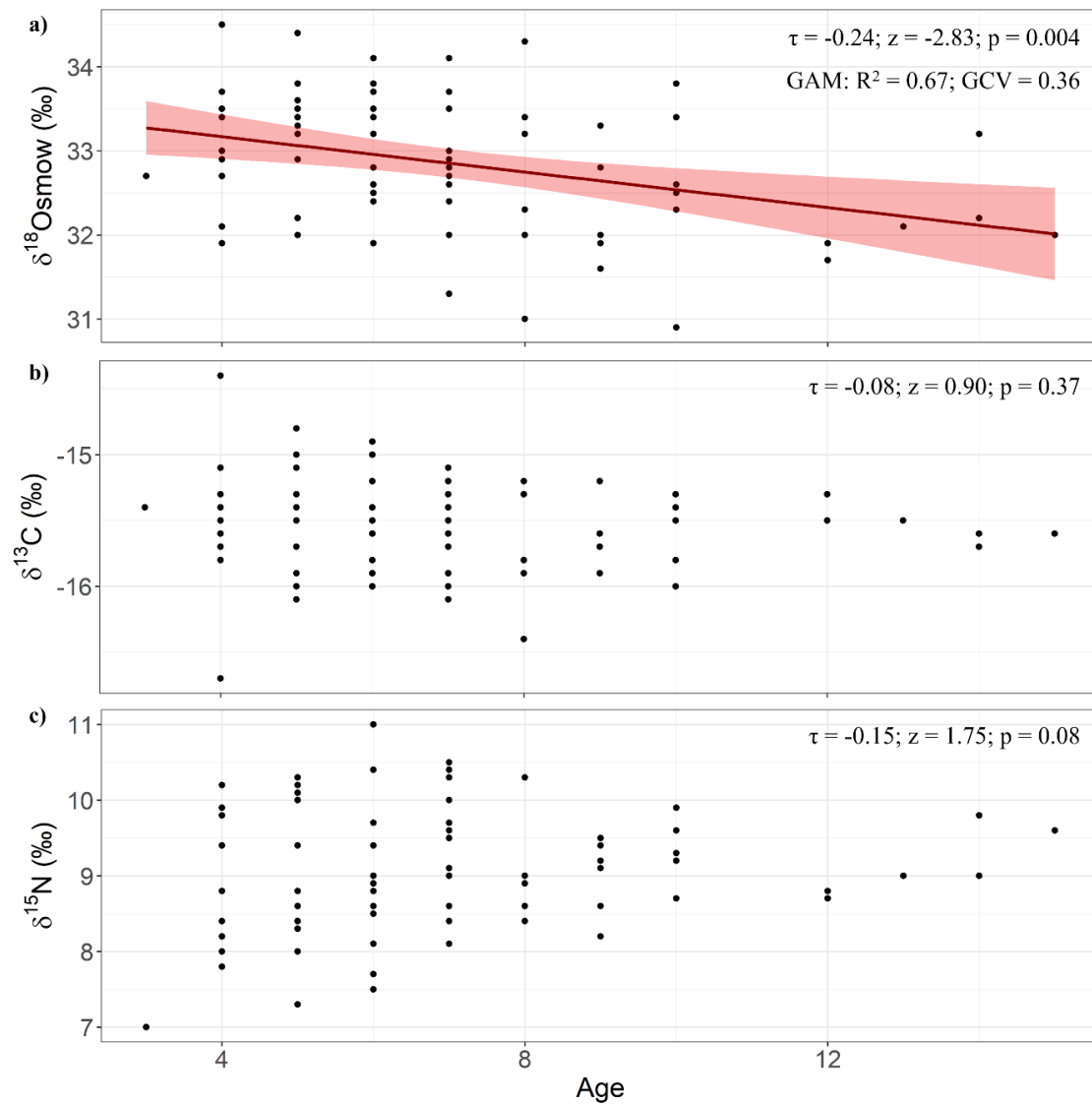


**Figure 3.12.** Individual (a)  $\delta^{18}\text{O}$ , (b)  $\delta^{13}\text{C}$  and (c)  $\delta^{15}\text{N}$  values for each of the analysed incremental layer and the respective estimated age (with all individuals pooled together), including the statistics for the Kendall's rank correlation ( $\tau$ ) and a visual representation of the only adjusted generalized additive model (GAM) that showed a good fit (a), with the mean tendency (dark red line) and the respective 95 % confidence interval (light red shaded area).

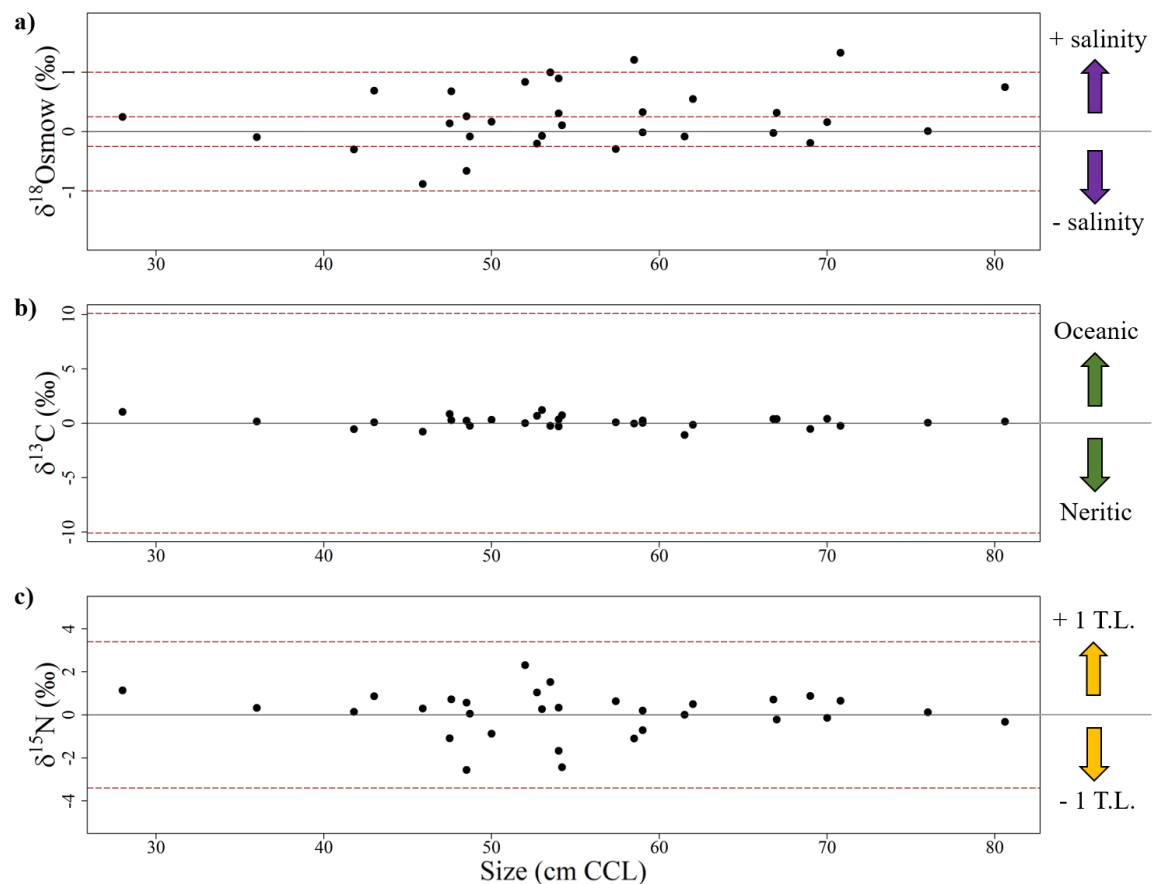


**Figure 3.13.** Differences between the stable isotope ratios of the outermost and the innermost analysed incremental layers for each of the considered loggerhead turtles ( $n = 31$ ) and their environmental interpretation. Each turtle is represented in each panel by a single black dot. The horizontal solid line within each panel denotes no change over time. The dashed red line at  $\pm 0.25$  ‰ in panel “a” shows the mean difference between adjacent regions of the Mediterranean Sea and that at  $\pm 1.00$  ‰ shows the difference between the Northeast Atlantic Ocean and the eastern Mediterranean Sea (LeGrande and Smith, 2006). The dashed red line at  $\pm 10.1$  ‰ in panel “b” represents the difference between the oceanic particulate organic matter and the neritic seagrass *Posidonia oceanica* off the Balearic Islands (Cardona et al., 2007). The dashed red line at  $\pm 3.4$  ‰ in panel “c” denotes changes corresponding to one trophic level (T.L.), according to the mean trophic fractionation in aquatic ecosystems (Post, 2002).

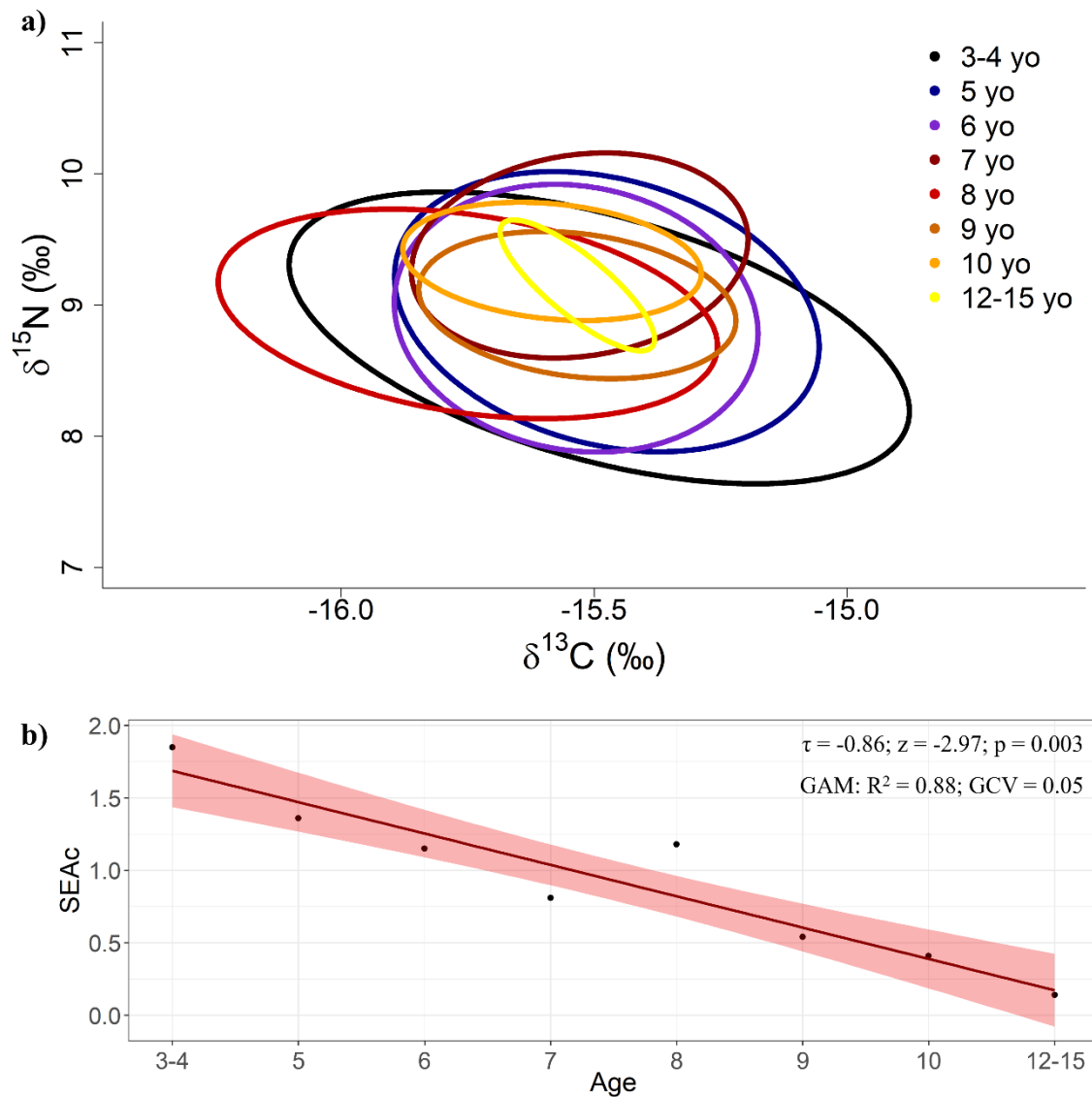


**Figure 3.14. a)** Standard ellipses containing 40 % of the data within the  $\delta^{13}\text{C}$  -  $\delta^{15}\text{N}$  isospace of eight age classes of loggerhead turtles observed in the study. Individual values are not shown. Sample sizes are as follows: 3-4 years old (n = 10), 5 years old (n = 12), 6 years old (n = 14), 7 years old (n = 14), 8 years old (n = 6), 9 years old (n = 6), 10 years old (n = 6), and 12-15 years old (n = 6). **b)** Relationship between the standard ellipse area corrected for small sample size (SEAc) from the top panel and the estimated age, showing the statistics for the Kendall's rank correlation ( $\tau$ ) and a visual representation of the adjusted generalized additive model (GAM), with the mean trend (dark red line) and the respective 95 % confidence interval (light red shaded area).



## DISCUSSION

The evidence here reported revealed that the loggerhead turtles of Northwestern Atlantic origin found dead stranded in the Balearic Islands exhibited a broad variability in the  $\delta^{18}\text{O}$  values of their bones, both across incremental layers of the same individual and across individuals. Variability was particularly high when turtles were under nine years old and decreased thereafter. These results indicate that the 29 turtles of which an incremental layer younger than 10 years old was identified inhabited a diversity of water masses of different salinities as early juveniles, before settling in lower salinity areas such as the Algerian Basin after reaching 10 years or older. Moreover, the temporal pattern of change was also extremely variable, suggesting that the entry to the Mediterranean Sea may happen at any time after their arrival to the Northeast Atlantic Ocean. On the other hand, the  $\delta^{13}\text{C}$  and  $\delta^{15}\text{N}$  values of the incremental layers also exhibited a broader variability during the first 6 years of life, although mean values suggested only minor ontogenetic changes in the diet during the analysed period.

### *The $\delta^{18}\text{O}$ in Mediterranean surface waters*

The loggerhead turtles analysed in the present study exhibited four major patterns of individual movement during the time recorded in the cortical bone of the humerus: 1) movement from  $^{18}\text{O}$ -enriched to  $^{18}\text{O}$ -depleted waters ( $n = 17$ ), with some of them ( $n = 4$ ) returning to  $^{18}\text{O}$ -enriched waters; 2) movement from  $^{18}\text{O}$ -depleted to  $^{18}\text{O}$ -enriched waters ( $n = 4$ ), which is the expected pattern from turtles that recently entered the Mediterranean Sea from the Northeast Atlantic Ocean (Figure 3.10); 3) movement from  $^{18}\text{O}$ -depleted to  $^{18}\text{O}$ -enriched and back to  $^{18}\text{O}$ -depleted waters ( $n = 3$ ), and 4) long-term residence in  $^{18}\text{O}$  depleted waters ( $n = 7$ ).

As described in the introduction, water circulation in the Mediterranean Sea is mostly driven by an excess of evaporation over precipitation and river runoff, which results in a decrease of sea level inside the Mediterranean and the permanent eastward flow of surface water from the Atlantic through the Strait of Gibraltar (Millot and Taupier-Letage, 2005). The constant input of less salty Atlantic waters to the west and the higher evaporation rate of surface waters to the east due to higher environmental temperatures, create a marked and predictable salinity gradient that allows to divide the Mediterranean Sea into four regions as follows: (1) Strait of Gibraltar and Alboran Sea, (2) western basin, (3) central basin, and (4) eastern basin (Figure 3.10). Furthermore, the preferential evaporation of water molecules carrying  $^{16}\text{O}$  atoms causes a local enrichment of  $^{18}\text{O}$  in seawater (Sharp,



2017), producing a positive and linear correlation between the salinity and the  $\delta^{18}\text{O}$  ratio in surface waters (Conroy et al., 2014; Belem et al., 2019) and thus allowing the isotopic distinction between water masses.

According to the estimations made by LeGrande & Smith (2006) and represented in Figure 3.10, the  $\delta^{18}\text{O}$  values of Mediterranean surface waters show a similar gradual increase from the Strait of Gibraltar towards the eastern basin as the salinity, with a mean increase of 0.25 ‰ from one region to the next. Hence, if the difference in  $\delta^{18}\text{O}$  values across the incremental layers of a turtle is larger than this absolute value, it can be an indicative of movement between regions with different salinities. Moreover, a mean increase of 1.00 ‰ or larger represents the absolute difference between Atlantic waters and the eastern Mediterranean (LeGrande and Smith, 2006) and hence, if this was the only source of variability for the  $\delta^{18}\text{O}$  values of bone tissue, the expected range of  $\delta^{18}\text{O}$  values in the incremental layers of the population should be equal or lower than 1.00 ‰.

#### ***Variability of $\delta^{18}\text{O}$ between incremental layers***

In this context, 24 out of the 31 considered turtles showed differences equal or larger than 0.25 ‰ between incremental layers (Table 3.3; Suppl. Table 2), with six individuals (A10, M11, A20, A35, I4, A18) having the lowest  $\delta^{18}\text{O}$  values in their outermost layer. Three of these turtles died when they were six or seven years old and hence, they would have had to cross the Atlantic Ocean and reach the saltier regions of the Mediterranean Sea in less than four years after birth, stranding at the Balearic Islands after spending at least one year in a less salty region. The plausibility of that trip is supported by satellite telemetry data from previous studies. First, Lagrangian drifters indicate that the trans-Atlantic drift time for early juvenile turtles from the Northwest Atlantic found in the United Kingdom was between 1.80 and 3.75 years (Hays and Marsh, 1997). Second, satellite-tracked head-started early juveniles ranging 12.8-19.9 cm CCL and 3.5-9 months old spent less than one year to reach the Azores after being released off southeast Florida (Mansfield et al., 2014). Third, some satellite-tracked head-started early juveniles ranging 18.1-25.0 cm CCL and 9-13 months old released off Spain drifted into the eastern Mediterranean after only a few months, although most individuals remained within the western Mediterranean (Abalo-Morla et al., 2023). This evidence suggests that loggerhead turtles from the Northwest Atlantic Ocean can potentially reach the eastern Mediterranean Sea in less than four years, thus supporting the interpretation stated above. On the other hand, the permanent eastward flow of surface water in the Channel of Sicily



may retain them within the central and eastern basins until they grow large enough to swim counter-current (Cardona and Hays, 2018). This would explain why all the loggerhead turtles analysed here with evidence of re-entering the western Mediterranean from the eastern basin are larger than 40 cm CCL, the minimum carapace length required to swim counter-current along the Channel of Sicily (Cardona and Hays, 2018).

On the contrary, 17 individuals between 5-13 years old had the highest  $\delta^{18}\text{O}$  values in the outermost incremental layer, yet they were all recovered dead off the Balearic Islands, indicating that they moved from a less salty region several months before their death. However, only three of those turtles showed evidence of the use of saltier areas in older-age incremental layers, whereas for the remaining 14 individuals, the pattern is consistent with an arrival to the western Mediterranean from the Atlantic between the formation of the innermost and the outermost incremental layers. Furthermore, five individuals (A19, A15, A13, A28 and A22) between 8-13 years old showed differences large enough (+ 1.00 ‰) to indicate movement from areas with high influence of Atlantic waters towards the saltiest parts of the eastern Mediterranean. Three of them (A15, A13, A28) showed this large difference twice in the analysed periods, probably changing regions every two years, approximately, and seemingly moving from the eastern to the western basin and back.

In addition, two of the oldest turtles of the study (A39 and M17; 70.0 and 76.0 cm CCL, respectively), estimated to be 13 and 15 years old when stranded, were the only ones that showed similarly low  $\delta^{18}\text{O}$  values for the whole analysed period, which in this case corresponded to the last seven and nine years, respectively, before stranding. This is a strong indication of several years of foraging in the southern part of the western Mediterranean, likely at the Algerian Basin, and is consistent with the use of these area as an important foraging ground for the species, as revealed recently through satellite telemetry of 103 loggerhead turtles which included post-hatchlings, juveniles and adults of both sexes (22.8-83.0 cm CCL) (Abalo-Morla et al., 2022).

Finally, amongst all the  $\delta^{18}\text{O}$  values obtained here, there were three notably lower than the rest. Two of them corresponded to the innermost sampled layers of two different individuals (A26 and A22) from when they were eight and nine years old. Hence, it is possible that these low values correspond to their time in the Atlantic Ocean, in which case they would have delayed their entrance to the Mediterranean Sea after spending several years in the eastern Atlantic. By contrast, the third low value belonged to the middle layer of turtle A15, and the values of the innermost and the outermost sampled



layers of this individual were distinctively higher, with a difference of -1.76 and +1.57 ‰, respectively, which is much larger than the estimated for the Mediterranean basin ( $\pm 1.00$  ‰). Similar changes were also found in other three turtles (+1.82 ‰, +1.48 ‰ and +1.33 ‰ for turtles A13, A28 and A22, respectively), which suggests that there are likely other factors affecting the  $\delta^{18}\text{O}$  values of bone carbonate in loggerhead turtles. These factors are discussed in the next section.

### ***Sources of variability in bone $\delta^{18}\text{O}$ values***

An important shortcoming to consider is that the isotopic composition of seawater is not the only factor influencing the isotopic values of bone tissue in sea turtles. The  $\delta^{18}\text{O}$  value of bone carbonate (bioapatite) is given by that of the body water from which carbonate precipitates, which depends on the magnitude and isotopic composition of the different oxygen fluxes into and out of the body, the isotopic fractionations associated with metabolism, and the temperature at which it forms (Luz et al., 1984; Kohn, 1996; Kohn and Cerling, 2002).

Sea turtles have two main sources of oxygen that can influence the  $\delta^{18}\text{O}$  values of their tissues. One is the metabolic water produced through cellular respiration using the atmospheric  $\text{O}_2$ , which is enriched in  $^{18}\text{O}$  compared to seawater due to the Dole effect (Luz et al., 1984; Luz and Barkan, 2011), and the other one is the ingested seawater, either by direct drinking or from their prey (Jones et al., 2009). Given that sea turtles drink seawater regularly (Reina et al., 2002) and the diet of oceanic loggerhead turtles is dominated by jelly plankton with a very high water content (Cardona et al., 2012), the contribution of metabolic water to the body water of sea turtles is minimal (Jones et al., 2009) and therefore, the  $\delta^{18}\text{O}$  values of bone carbonate are expected to reflect mostly those of the water mass where they live (Séon et al., 2023). Nevertheless, the range of  $\delta^{18}\text{O}$  values reported here for the analysed loggerhead turtles is much broader than the range expected for seawater within the study area (3.60 vs 1.00 ‰, respectively). Furthermore, the difference between adjacent incremental layers was, in some cases, as large as 1.82 ‰, also much larger than the estimated range of variability within the whole Mediterranean basin and the adjoining Atlantic Ocean (1.30 ‰). This leads to the conclusion that other processes must be affecting the  $\delta^{18}\text{O}$  values during the formation of bone carbonate in sea turtles.

The  $\delta^{18}\text{O}$  fractionation factor between body water and carbonate during bioapatite precipitation is temperature dependent (Sharp, 2017; Coulson et al., 2008) when isotopic



equilibrium between carbonate and water is reached (Kim and O'Neil, 1997). Due to the ectothermic nature of turtles, at higher environmental temperatures their body temperature also increases, causing a decrease in the carbonate-water fractionation factor during bioapatite precipitation and producing carbonates with a more similar  $^{18}\text{O}$  content to that of the body water used during precipitation (Kim and O'Neil, 1997; Kohn and Cerling, 2002), which in this case is primarily the  $^{18}\text{O}$ -enriched ingested seawater. Another consequence of the increased body temperature, assuming a regular food and water intake, is an increase in the metabolic rate of the turtle and, therefore, in the turnover rate of body water, which can accelerate bioapatite precipitation (i.e., bone tissue grows faster) and in turn affect the isotopic balance between body water and carbonate, producing bioapatite out of isotopic equilibrium with body water. In this case, the reaction becomes less dependent on the temperature and could alter the resultant  $\delta^{18}\text{O}$  values (Kim and O'Neil, 1997).

On the contrary, the exposure to cold temperatures causes a significant reduction on the metabolic rate, food intake and  $\text{O}_2$  consumption in sea turtles (Hochscheid et al., 2004). In this case, the turnover rate of body water and thus the precipitation of bioapatite will be slower and more likely to reach isotopic equilibrium with body water. Hence, if food and water intake are not limiting and the evaporation rate in surface waters is lower due to lower temperatures, the bioapatite produced during this period will likely have lower  $\delta^{18}\text{O}$  values than that produced in warmer waters (Kim and O'Neil, 1997).

On the other hand, if the turtle remains in a state of low metabolic activity due to low food availability, or even reach a fasting state, the effect over the  $\delta^{18}\text{O}$  values of bioapatite will be the opposite. Oceanic juvenile loggerhead turtles alternate periods of high food availability with extended periods of fasting (Bjorndal et al., 2003), during which they rely on their fat stores to obtain energy (Jones et al., 2009) and thus, metabolic water is expected to become the dominant influx of water in their bodies unless they increase the drinking rate. As mentioned above, metabolic water is enriched in  $^{18}\text{O}$  compared to seawater (Luz and Barkan, 2011) and animals relying on lipid-rich diets, as well as those with irregular access to food or subjected to fasting, tend to be enriched in  $^{18}\text{O}$  (Jones et al., 2009; Séon et al., 2023). In addition, the eastern Mediterranean is highly oligotrophic (Bosc et al., 2004), which results in a scarcity of oceanic loggerhead turtles in the area (DiMatteo et al., 2022). Therefore, if the juvenile loggerhead turtles of Northwestern Atlantic origin entering the eastern Mediterranean (Clusa et al., 2014) have less access to food and fast more frequently than those remaining in the western



Mediterranean, they would exhibit an additional increase in their  $\delta^{18}\text{O}$  values, operating in synergy with a higher sea surface temperature and evaporation rate (measured as salinity) in the eastern basin (Millot and Taupier-Letage, 2005) to considerably expand the range of  $\delta^{18}\text{O}$  values in bone carbonate compared to seawater.

From the above follows that regional differences in water temperature and food availability may have an impact on the  $\delta^{18}\text{O}$  values of sea turtle's bone carbonate, since they both affect the metabolic rate and hence, the turnover rate of the body water used in bioapatite precipitation. In the Mediterranean Sea, salinity, sea surface temperature and food availability change along the west-east axis, reinforcing the eastward increase in the  $\delta^{18}\text{O}$  values of sea turtles bone carbonate, but this is not necessarily true elsewhere. Thus, researchers should keep in mind these other sources of variability when using  $\delta^{18}\text{O}$  as a habitat tracer in sea turtles. Another caveat to be considered is that incremental layers formed during fasting periods are narrower than those formed in feasting periods and hence contribute with a smaller amount of carbonate when assessing the  $\delta^{18}\text{O}$  value of samples integrating several incremental layers.

#### ***Trophic ecology according to bone $\delta^{13}\text{C}$ and $\delta^{15}\text{N}$***

In general, the changes observed in the  $\delta^{13}\text{C}$  and  $\delta^{15}\text{N}$  values between incremental layers were small and suggested only minor ontogenetic changes in the diet of these juvenile loggerhead turtles during their journey through the Mediterranean Sea, with a tendency to reduce the isotopic niche area as they grow older. This is consistent with movement patterns previously observed for loggerhead turtles in the Mediterranean Sea, as the movement of turtles smaller than 40 cm CCL is highly dependent on current velocity (Revelles et al., 2007a), whereas larger turtles can actively remain in more favourable areas (Eckert et al., 2008).

Considering that the bone samples used in the present study are from the early 2000's, we considered the environmental conditions of the Mediterranean Sea of that time for the following discussions. On one hand, the range of  $\delta^{13}\text{C}$  values obtained for the considered turtles (from -16.7 to -14.4 ‰) is consistent to that of potential pelagic prey such as gelatinous plankton (from -17.6 to -15.7 ‰) and small pelagic and mesopelagic fishes (from -16.4 to -15.9 ‰) from foraging grounds off the Balearic Islands (Cardona et al., 2007), after accounting for the diet-to-tissue fractionation reported for the cortical bone of sea turtles ( $2.1 \pm 0.6$  ‰) (Turner Tomaszewicz et al., 2017b). This similarity suggests the use of mostly oceanic habitats. Furthermore, the variability observed



between individuals could be explained by the horizontal distribution of  $\delta^{13}\text{C}$  values in surface waters within and between Mediterranean basins. Pierre (1999) found that the northern margins of both the eastern and western Mediterranean, known as regions of deep-water formation, present the lowest  $\delta^{13}\text{C}$  values because of the input of  $^{13}\text{C}$ -depleted  $\text{CO}_2$  from deeper waters especially during winter, whereas the highest values are found in the Alboran Sea and southern Algerian Basin. However, the range of values in both basins was similar and the maximum differences reported for the western and eastern Mediterranean were small (0.43 and 0.41 ‰, respectively) (Pierre, 1999), which explains the little variability observed in our data.

Regarding the  $\delta^{15}\text{N}$  values, those of the studied loggerhead turtles ranged between 7.05-11.04 ‰ and stomach content analysis of pelagic loggerhead turtles off the Balearic Islands had previously revealed gelatinous plankton and pelagic fishes as their main prey (Revelles et al., 2007b). The  $\delta^{15}\text{N}$  values of gelatinous plankton from the Balearic Islands in the early 2000's ranged 3.9-5.6 ‰ and those of small pelagic and mesopelagic fishes from the same area and period ranged 8.7-10.2 ‰ (Cardona et al., 2007). As the diet-to-tissue discrimination factor for the cortical bone of sea turtles is  $5.1 \pm 1.1$  ‰ (Eckert et al., 2008), the  $\delta^{15}\text{N}$  of the diet of loggerhead turtles should range 1.95-5.4 ‰, suggesting that gelatinous zooplankton was the staple food of the loggerhead turtles analyzed during the life stages recorded in their bone tissue, a conclusion consistent with the results of a previous mixing model based on the  $\delta^{13}\text{C}$  and  $\delta^{15}\text{N}$  values of epidermis (Cardona et al., 2007). Another possibility is that these differences are caused by the higher  $\delta^{15}\text{N}$  values of the particulate organic matter in the surface waters of the western basin, especially towards the Alboran Sea (Pantoja et al., 2002). If this was the case, it would agree with the previously discussed tendency to settle in areas of lower salinity of the western Mediterranean as they reach ten years of age.

Lastly, the tendency to reduce the isotopic niche area is mostly driven by a lower variability in incremental layers older than 9 years old. This indicates either a more consistent diet over time, a greater fidelity to the same water mass, or both, in older turtles.

### ***Conclusions***

Our results suggest that loggerhead turtles born at the nesting beaches of the Northwest Atlantic do not follow just one straight path towards the Mediterranean Sea, and the wide range of  $\delta^{18}\text{O}$  values found for these turtles, especially in those younger than



nine years old, do not indicate any specific temporal pattern in their movements. This agrees with the observations of Mansfield et al., (2014), where some satellite tracked neonate loggerhead turtles released off their natal beaches in Florida travelled out of the Gulf Stream and towards the Sargasso Sea in association with meso-scale eddies and remained there for different periods of time, while others seemed to swim directly towards the eastern Atlantic (Mansfield et al., 2014). This uneven dispersion of neonates while crossing the Atlantic explains the non-systematic entry of juvenile loggerhead turtles into the Mediterranean Sea as well as the variability of  $\delta^{18}\text{O}$  values in turtles of similar size and age. Similar variations in the timing of ontogenic habitat shifts were observed in juvenile loggerhead turtles from the North Pacific (Turner Tomaszewicz et al., 2017a). Moreover, the observed tendency to settle in lower salinity areas as they grow older than 10 years old does not seem to be related to their distribution as juveniles. Available satellite data suggests that individuals larger than 57 cm CCL are more likely to remain within the Alboran Sea and the adjacent Algerian Basin (Eckert et al., 2008), and they can already leave the Mediterranean and start their journey back to the Northwestern Atlantic before reaching 68 cm CCL (Moncada et al., 2010). According to our estimations, all turtles estimated to be 10 years or older had a CCL larger than 57 cm. Certainly, the exact time of their departure is highly variable and likely depends on factors that are mostly unknown but may include the availability of food resources and good environmental conditions (Eckert et al., 2008).

## REFERENCES

- Abalo-Morla, S., Belda, E.J., March, D., Revuelta, O., Cardona, L., Giralt, S., Crespo-Picazo, J.L., Hochscheid, S., Marco, A., Merchán, M. and Sagarminaga, R. 2022. Assessing the use of marine protected areas by loggerhead sea turtles (*Caretta caretta*) tracked from the western Mediterranean. *Global Ecology and Conservation*, 38, p.e02196. <https://doi.org/10.1016/j.gecco.2022.e02196>
- Abalo-Morla, S., Muñoz-Mas, R., Tomás, J. and Belda, E.J., 2023. Factors driving dispersal and habitat use of loggerhead sea turtle post-hatchlings and its conservational implications. *Marine Biology*, 170(12), p.155. <https://doi.org/10.1007/s00227-023-04285-2>
- Belem, A.L., Caricchio, C., Albuquerque, A.L.S., Venancio, I.M., Zucchi, M., Santos, T.H.R. and Alvarez, Y.G. 2019. Salinity and stable oxygen isotope relationship in the Southwestern Atlantic: constraints to paleoclimate reconstructions. *Anais da Academia Brasileira de Ciências*, 91, p.e20180226. <https://doi.org/10.1590/0001-3765201920180226>
- Ben-David, M. and Flaherty, E.A. 2012. Stable isotopes in mammalian research: a beginner's guide. *Journal of Mammalogy*, 93(2), pp.312-328. <https://doi.org/10.1644/11-MAMM-S-166.1>

- Bjorndal, K.A., Bolten, A.B. and Martins, H.R. 2000. Somatic growth model of juvenile loggerhead sea turtles *Caretta caretta*: duration of pelagic stage. *Marine Ecology Progress Series*, 202, pp.265-272. doi:10.3354/meps202265
- Bjorndal, K.A., Bolten, A.B., Dellinger, T., Delgado, C. and Martins, H.R., 2003. Compensatory growth in oceanic loggerhead sea turtles: response to a stochastic environment. *Ecology*, 84(5), pp.1237-1249. [https://doi.org/10.1890/0012-9658\(2003\)084\[1237:CGIOLS\]2.0.CO;2](https://doi.org/10.1890/0012-9658(2003)084[1237:CGIOLS]2.0.CO;2)
- Bolten, A.B. 2003. Active swimmers-passive drifters: the oceanic juvenile stage of loggerheads in the Atlantic system. In: Bolten, A.B., Witherington, B.E. (Eds.), *Loggerhead Sea Turtles*. Smithsonian Institution Press, Washington, D.C., pp.63–78.
- Bosc, E., Bricaud, A. and Antoine, D. 2004. Seasonal and interannual variability in algal biomass and primary production in the Mediterranean Sea, as derived from 4 years of SeaWiFS observations. *Global Biogeochemical Cycles*, 18(1), GB1005, pp.1-17. <https://doi.org/10.1029/2003GB002034>
- Brasseur, P., Beckers, J.M., Brankart, J.M. and Schoenauen, R., 1996. Seasonal temperature and salinity fields in the Mediterranean Sea: Climatological analyses of a historical data set. *Deep Sea Research Part I: Oceanographic Research Papers*, 43(2), pp.159-192. [https://doi.org/10.1016/0967-0637\(96\)00012-X](https://doi.org/10.1016/0967-0637(96)00012-X)
- Cani, A., Cardona, L., Aguilar, Á., Borrell, A. and Drago, M., 2024. Fine-tuning the isotopic niche of a marine mammal community through a multi-element approach and variable spatial scales. *Estuarine, Coastal and Shelf Science*, 298, p.108641. <https://doi.org/10.1016/j.ecss.2024.108641>
- Cardiff, R.D., Miller, C.H. and Munn, R.J. 2014. Manual hematoxylin and eosin staining of mouse tissue sections. *Cold Spring Harbor Protocols*, 2014(6), pp.655-658. doi:10.1101/pdb.prot073411
- Cardona, L., Revelles, M., Sales, M., Aguilar, A. and Borrell, A. 2007. Meadows of the seagrass *Posidonia oceanica* are a significant source of organic matter for adjoining ecosystems. *Marine Ecology Progress Series*, 335, pp.123-131. doi:10.3354/meps335123
- Cardona, L., Álvarez de Quevedo, I., Borrell, A. and Aguilar, A. 2012. Massive consumption of gelatinous plankton by Mediterranean apex predators. *PloS one*, 7(3), p.e31329. <https://doi.org/10.1371/journal.pone.0031329>
- Cardona, L., Clusa, M., Eder, E., Demetropoulos, A., Margaritoulis, D., Rees, A.F., Hamza, A.A., Khalil, M., Levy, Y., Türkozan, O., Marín, I. and Aguilar, A. 2014. Distribution patterns and foraging ground productivity determine clutch size in Mediterranean loggerhead turtles. *Marine Ecology Progress Series*, 497, 229-241. <https://doi.org/10.3354/meps10595>
- Cardona, L. and Hays, G.C. 2018. Ocean currents, individual movements and genetic structuring of populations. *Marine biology*, 165, pp.1-10. <https://doi.org/10.1007/s00227-017-3262-2>
- Cardona, L., Abalo-Morla, S., Cani, A., Feliu-Tena, B., Izaguirre, N., Tomás, J. and Belda, E.J. 2024. Identifying the foraging grounds of the new loggerhead turtle nesters in the western Mediterranean. *Aquatic Conservation: Marine and Freshwater Ecosystems*, 34(1), p.e4059. <https://doi.org/10.1002/aqc.4059>
- Carreras, C., Pascual, M., Tomás, J., Marco, A., Hochscheid, S., Castillo, J.J., Gozalbes, P., Parga, M., Piovano, S. and Cardona, L. 2018. Sporadic nesting reveals long distance colonisation in the philopatric loggerhead sea turtle (*Caretta caretta*). *Scientific reports*, 8(1), pp.1435. <https://doi.org/10.1038/s41598-018-19887-w>

- Casale, P., Broderick, A.C., Camiñas, J.A., Cardona, L., Carreras, C., Demetropoulos, A., Fuller, W.J., Godley, B.J., Hochscheid, S., Kaska, Y. and Lazar, B. 2018. Mediterranean Sea turtles: current knowledge and priorities for conservation and research. *Endangered species research*, 36, pp.229-267. <https://doi.org/10.3354/esr0090>
- Chambault, P., Baudena, A., Bjorndal, K.A., Santos, M.A., Bolten, A.B. and Vandeperre, F. 2019. Swirling in the ocean: Immature loggerhead turtles seasonally target old anticyclonic eddies at the fringe of the North Atlantic gyre. *Progress in oceanography*, 175, pp.345-358. <https://doi.org/10.1016/j.pocean.2019.05.005>
- Chambault, P., Gaspar, P. and Dell'Amico, F. 2021. Ecological trap or favorable habitat? First evidence that immature sea turtles may survive at their range-limits in the North-East Atlantic. *Frontiers in Marine Science*, 8, p.736604. <https://doi.org/10.3389/fmars.2021.736604>
- Clusa, M., Carreras, C., Pascual, M., Gaughran, S.J., Piovano, S., Giacoma, C., Fernández, G., Levy, Y., Tomás, J., Raga, J.A. and Maffucci, F. 2014. Fine-scale distribution of juvenile Atlantic and Mediterranean loggerhead turtles (*Caretta caretta*) in the Mediterranean Sea. *Marine Biology*, 161, pp.509-519. <https://doi.org/10.1007/s00227-013-2353-y>
- Coulson, A.B., Kohn, M.J., Shirley, M.H., Joyce, W.G. and Barrick, R.E. 2008. Phosphate–oxygen isotopes from marine turtle bones: Ecologic and paleoclimatic applications. *Palaeogeography, Palaeoclimatology, Palaeoecology*, 264(1-2), pp.78-84. <https://doi.org/10.1016/j.palaeo.2008.04.008>
- Conroy, J.L., Cobb, K.M., Lynch-Stieglitz, J. and Polissar, P.J. 2014. Constraints on the salinity–oxygen isotope relationship in the central tropical Pacific Ocean. *Marine Chemistry*, 161, pp.26-33.
- de Quevedo, I.A., San Félix, M. and Cardona, L. 2013. Mortality rates in by-caught loggerhead turtle *Caretta caretta* in the Mediterranean Sea and implications for the Atlantic populations. *Marine Ecology Progress Series*, 489, pp.225-234. <https://doi.org/10.3354/meps10411>
- DiMatteo, A., Cañadas, A., Roberts, J., Sparks, L., Panigada, S., Boisseau, O., Moscrop, A., Fortuna, C.M., Lauriano, G., Holcer, D. and Peltier, H. 2022. Basin-wide estimates of loggerhead turtle abundance in the Mediterranean Sea derived from line transect surveys. *Frontiers in Marine Science*, 9, p.930412. <https://doi.org/10.3389/fmars.2022.930412>
- Durfort, M. 1987. Algunes tècniques d'obtenció de preparacions d'estructures i de teixits animals. Seminaris d'Estudis Universitaris. Institució Catalana d'Història Natural. pp.27.
- Eckert, S.A., Moore, J.E., Dunn, D.C., van Buiten, R.S., Eckert, K.L. and Halpin, P.N. 2008. Modeling loggerhead turtle movement in the Mediterranean: importance of body size and oceanography. *Ecological Applications*, 18(2), pp.290-308. <https://doi.org/10.1890/06-2107.1>
- Fofonoff, N.P. 1981. Chapter 4: The Gulf Stream. In: Warren, B.A. and Wunsch, C. (Eds.), *Evolution of Physical Oceanography: scientific surveys in honor of Henry Stommel*, pp.112-139.
- Frazão, H.C., Prien, R.D., Schulz-Bull, D.E., Seidov, D. and Waniek, J.J. 2022. The forgotten Azores current: A long-term perspective. *Frontiers in Marine Science*, 9, p.842251. <https://doi.org/10.3389/fmars.2022.842251>
- Freitas, C., Caldeira, R. and Dellinger, T., 2019. Surface behavior of pelagic juvenile loggerhead sea turtles in the eastern North Atlantic. *Journal of experimental*

- marine biology and ecology*, 510, pp.73-80.  
<https://doi.org/10.1016/j.jembe.2018.10.006>
- Gat, J.R. 1996. Oxygen and hydrogen isotopes in the hydrologic cycle. *Annual Review of Earth and Planetary Sciences*, 24(1), pp.225-262.
- Goshe, L.R., Avens, L., Snover, M.L. and Hohn, A.A. 2020. Protocol for processing sea turtle bones for age estimation. **NOAA Technical Memorandum NMFS-SEFSC-746**, U.S. Department of Commerce, pp.43. <https://doi.org/10.25923/gqva-9y22>
- Hays, G.C. and Marsh, R. 1997. Estimating the age of juvenile loggerhead sea turtles in the North Atlantic. *Canadian Journal of Zoology*, 75(1), pp.40-46.  
<https://doi.org/10.1139/z97-005>
- Hochscheid, S., Bentivegna, F. and Speakman, J.R. 2004. Long-term cold acclimation leads to high Q10 effects on oxygen consumption of loggerhead sea turtles *Caretta caretta*. *Physiological and Biochemical Zoology*, 77(2), pp.209-222.  
<https://doi.org/10.1086/381472>
- Jackson, A.L., Inger, R., Parnell, A.C. and Bearhop, S. 2011. Comparing isotopic niche widths among and within communities: SIBER Stable Isotope Bayesian Ellipses in R. *Journal of Animal Ecology*, 80(3), pp.595–602.
- Jones, T.T., Hastings, M.D., Bostrom, B.L., Andrews, R.D. and Jones, D.R. 2009. Validation of the use of doubly labeled water for estimating metabolic rate in the green turtle (*Chelonia mydas* L.): a word of caution. *Journal of Experimental Biology*, 212(16), pp.2635-2644. <https://doi.org/10.1242/jeb.029330>
- Kim, S.T. and O'Neil, J.R. 1997. Equilibrium and nonequilibrium oxygen isotope effects in synthetic carbonates. *Geochimica et cosmochimica acta*, 61(16), pp.3461-3475.  
[https://doi.org/10.1016/S0016-7037\(97\)00169-5](https://doi.org/10.1016/S0016-7037(97)00169-5)
- Koch, P.L., Tuross, N. and Fogel, M.L. 1997. The effects of sample treatment and diagenesis on the isotopic integrity of carbonate in biogenic hydroxyapatite. *Journal of Archaeological Science*, 24(5), pp.417–429.  
<https://doi.org/10.1006/jasc.1996.0126>
- Kohn, M.J. 1996. Predicting animal  $\delta^{18}\text{O}$ : accounting for diet and physiological adaptation. *Geochimica et cosmochimica Acta*, 60(23), pp.4811-4829.  
[https://doi.org/10.1016/S0016-7037\(96\)00240-2](https://doi.org/10.1016/S0016-7037(96)00240-2)
- Kohn, M.J. and Cerling, T.E. 2002. Stable isotope compositions of biological apatite. *Reviews in mineralogy and geochemistry*, 48(1), pp.455-488.  
<https://doi.org/10.2138/rmg.2002.48.12>
- LeGrande, A.N., Schmidt, G.A. 2006. Global gridded data set of the oxygen isotopic composition in seawater. *Geophysical Research Letters*, 33(12), pp.1-5.  
<https://doi.org/10.1029/2006GL026011>
- Lohmann, K.J., Cain, S.D., Dodge, S.A. and Lohmann, C.M. 2001. Regional magnetic fields as navigational markers for sea turtles. *Science*, 294(5541), pp.364-366.  
<https://doi.org/10.1126/science.1064557>
- Lohmann, K.J., Putman, N.F. and Lohmann, C.M. 2012. The magnetic map of hatchling loggerhead sea turtles. *Current Opinion in Neurobiology*, 22(2), pp.336-342.  
<https://doi.org/10.1016/j.conb.2011.11.005>
- Luna-Ortiz, A., Marín-Capuz, G., Abella, E., Crespo-Picazo, J.L., Escribano, F., Félix, G., Giralt, S., Tomás, J., Pegueroles, C., Pascual, M. and Carreras, C. 2024. New colonisers drive the increase of the emerging loggerhead turtle nesting in Western Mediterranean. *Scientific Reports*, 14(1), p.1506. <https://doi.org/10.1038/s41598-024-51664-w>
- Luz, B., Kolodny, Y. and Horowitz, M. 1984. Fractionation of oxygen isotopes between mammalian bone-phosphate and environmental drinking water. *Geochimica et*

- Cosmochimica Acta*, 48(8), pp.1689-1693. [https://doi.org/10.1016/0016-7037\(84\)90338-7](https://doi.org/10.1016/0016-7037(84)90338-7)
- Luz, B. and Barkan, E. 2011. The isotopic composition of atmospheric oxygen. *Global Biogeochemical Cycles*, 25(3), pp.14. <https://doi.org/10.1029/2010GB003883>
- Mansfield, K.L., Saba, V.S., Keinath, J.A. and Musick, J.A. 2009. Satellite tracking reveals a dichotomy in migration strategies among juvenile loggerhead turtles in the Northwest Atlantic. *Marine Biology*, 156, pp.2555-2570. <https://doi.org/10.1007/s00227-009-1279-x>
- Mansfield, K.L., Wynneken, J., Porter, W.P. and Luo, J. 2014. First satellite tracks of neonate sea turtles redefine the 'lost years' oceanic niche. *Proceedings of the Royal Society B: Biological Sciences*, 281(1781), pp.20133039. <https://doi.org/10.1098/rspb.2013.3039>
- McClellan, C.M. and Read, A.J. 2007. Complexity and variation in loggerhead sea turtle life history. *Biology Letters*, 3(6), pp.592-594. <https://doi.org/10.1098/rsbl.2007.0355>
- Millot, C. and Taupier-Letage, I. 2005. Circulation in the Mediterranean Sea. In: Saliot, A. (Eds), *The Mediterranean Sea. Handbook of Environmental Chemistry*, Springer, Berlin, Heidelberg, 5K, pp.29-66. <https://doi.org/10.1007/b107143>
- Moncada, F., Abreu-Grobois, F.A., Bagley, D., Bjorndal, K.A., Bolten, A.B., Camiñas, J.A., Ehrhart, L., Muhlia-Melo, A., Nodarse, G., Schroeder, B.A. and Zurita, J. 2010. Movement patterns of loggerhead turtles *Caretta caretta* in Cuban waters inferred from flipper tag recaptures. *Endangered Species Research*, 11(1), pp.61-68. <https://doi.org/10.3354/esr00248>
- Monzón-Argüello, C., Rico, C., Carreras, C., Calabuig, P., Marco, A. and López-Jurado, L.F. 2009. Variation in spatial distribution of juvenile loggerhead turtles in the eastern Atlantic and western Mediterranean Sea. *Journal of Experimental Marine Biology and Ecology*, 373(2), pp.79-86. <https://doi.org/10.1016/j.jembe.2009.03.007>
- Newsome, S.D., Clementz, M.T. and Koch, P.L. 2010. Using stable isotope biogeochemistry to study marine mammal ecology. *Marine Mammal Science*, 26(3), pp.509-572. <https://doi.org/10.1111/j.1748-7692.2009.00354.x>
- Palter, J.B. 2015. The role of the Gulf Stream in European climate. *Annual review of marine science*, 7, pp.113-137. <https://doi.org/10.1146/annurev-marine-010814-015656>
- Pantoja, S., Repeta, D.J., Sachs, J.P. and Sigman, D.M. 2002. Stable isotope constraints on the nitrogen cycle of the Mediterranean Sea water column. *Deep Sea Research Part I: Oceanographic Research Papers*, 49(9), pp.1609-1621. [https://doi.org/10.1016/S0967-0637\(02\)00066-3](https://doi.org/10.1016/S0967-0637(02)00066-3)
- Parham, J.F. and Zug, G.R. 1997. Age and growth of loggerhead sea turtles (*Caretta caretta*) of coastal Georgia: an assessment of skeletochronological age-estimates. *Bulletin of Marine Science*, 61(2), pp.287-304.
- Piecuch, C.G. and Beal, L.M. 2023. Robust weakening of the Gulf Stream during the past four decades observed in the Florida Straits. *Geophysical research letters*, 50(18), p.e2023GL105170. <https://doi.org/10.1029/2023GL105170>
- Pierre, C. 1999. The oxygen and carbon isotope distribution in the Mediterranean water masses. *Marine geology*, 153(1-4), pp.41-55. [https://doi.org/10.1016/S0025-3227\(98\)00090-5](https://doi.org/10.1016/S0025-3227(98)00090-5)
- Piovano, S., Clusa, M., Carreras, C., Giacoma, C., Pascual, M. and Cardona, L. 2011. Different growth rates between loggerhead sea turtles (*Caretta caretta*) of

- Mediterranean and Atlantic origin in the Mediterranean Sea. *Marine Biology*, 158, pp.2577-2587. <https://doi.org/10.1007/s00227-011-1759-7>
- Post, D.M. 2002. Using stable isotopes to estimate trophic position: models, methods, and assumptions. *Ecology*, 83(3), pp.703-718.
- Ramirez, M.D., Avens, L., Seminoff, J.A., Goshe, L.R. and Heppell, S.S. 2015. Patterns of loggerhead turtle ontogenetic shifts revealed through isotopic analysis of annual skeletal growth increments. *Ecosphere*, 6(11), pp.1-17. <https://doi.org/10.1890/ES15-00255.1>
- Ramos, R. and González-Solís, J. 2012. Trace me if you can: the use of intrinsic biogeochemical markers in marine top predators. *Frontiers in Ecology and the Environment*, 10(5), pp.258-266. <https://doi.org/10.1890/110140>
- R Core Team, 2021. R: A Language and Environment for Statistical Computing. R Foundation for Statistical Computing, Vienna. <https://www.R-project.org>. Accessed 26 September 2024.
- Reina, R.D., Jones, T.T. and Spotila, J.R., 2002. Salt and water regulation by the leatherback sea turtle *Dermodochelys coriacea*. *Journal of Experimental Biology*, 205(13), pp.1853-1860. <https://doi.org/10.1242/jeb.205.13.1853>
- Revelles, M., Carreras, C., Cardona, L., Marco, A., Bentivegna, F., Castillo, J.J., de Martino, G., Mons, J.L., Smith, M.B., Rico, C. and Pascual, M. 2007a. Evidence for an asymmetrical size exchange of loggerhead sea turtles between the Mediterranean and the Atlantic through the Straits of Gibraltar. *Journal of Experimental Marine Biology and Ecology*, 349(2), pp.261-271. Doi: 10.1016/j.jembe.2007.05.018
- Revelles, M., Cardona, L., Aguilar, A. and Fernández, G. 2007b. The diet of pelagic loggerhead sea turtles (*Caretta caretta*) off the Balearic archipelago (western Mediterranean): relevance of long-line baits. *Journal of the Marine Biological Association of the United Kingdom*, 87(3), pp.805-813. <https://doi.org/10.1017/S0025315407054707>
- Rubenstein, D.R. and Hobson, K.A. 2004. From birds to butterflies: animal movement patterns and stable isotopes. *Trends in ecology & evolution*, 19(5), pp.256-263. <https://doi.org/10.1016/j.tree.2004.03.017>
- Schmitz Jr., W.J. and McCartney, M.S. 1993. On the north Atlantic circulation. *Reviews of Geophysics*, 31(1), pp.29-49. <https://doi.org/10.1029/92RG02583>
- Séon, N., Brasseur, I., Scala, C., Tacail, T., Catteau, S., Fourel, F., Vincent, P., Lécuyer, C., Suan, G., Charbonnier, S. and Vinçon-Laugier, A. 2023. Determination of water balance maintenance in *Orcinus orca* and *Tursiops truncatus* using oxygen isotopes. *Journal of Experimental Biology*, 226(23), p.jeb245648. <https://doi.org/10.1242/jeb.245648>
- Sharp, Z. 2017. Principles of Stable Isotope Geochemistry, 2nd Edition. University of New Mexico. <https://doi.org/10.25844/h9q1-0p82>
- Snover, M. L., Hohn, A. A., Crowder, L. B., y Macko, S. A. 2010. Combining stable isotopes and skeletal growth marks to detect habitat shifts in juvenile loggerhead sea turtles *Caretta caretta*. *Endangered Species Research*, 13(1), pp.25–31. <https://doi.org/10.3354/esr00311>
- Soto-Navarro, J., Jordá, G., Amores, Á., Cabos, W., Somot, S., Sevault, F., Macías, D., Djurdjevic, V., Sannino, G., Li, L. and Sein, D. 2020. Evolution of Mediterranean Sea water properties under climate change scenarios in the Med-CORDEX ensemble. *Climate Dynamics*, 54, pp.2135-2165. <https://doi.org/10.1007/s00382-019-05105-4>



- Turner Tomaszewicz, C.N., Seminoff, J.A., Ramirez, M.D. and Kurle, C.M. 2015. Effects of demineralization on the stable isotope analysis of bone samples. *Rapid Communications in Mass Spectrometry*, 29(20), pp.1879-1888. <https://doi.org/10.1002/rcm.7295>
- Turner Tomaszewicz, C. N., Seminoff, J. A., Peckham, S. H., Avens, L., y Kurle, C. M. 2017a. Intrapopulation variability in the timing of ontogenetic habitat shifts in sea turtles revealed using  $\delta^{15}\text{N}$  values from bone growth rings. *Journal of Animal Ecology*, 86(3), pp.694–704. <https://doi.org/10.1111/1365-2656.12618>
- Turner Tomaszewicz, C.N., Seminoff, J.A., Price, M. and Kurle, C.M., 2017b. Stable isotope discrimination factors and between-tissue isotope comparisons for bone and skin from captive and wild green sea turtles (*Chelonia mydas*). *Rapid Communications in Mass Spectrometry*, 31(22), pp.1903-1914. <https://doi.org/10.1002/rcm.7974>
- Varo-Cruz, N., Bermejo, J. A., Calabuig, P., Cejudo, D., Godley, B. J., López-Jurado, L. F., Pikesley, S. K., Witt, M. J., y Hawkes, L. A. 2016. New findings about the spatial and temporal use of the Eastern Atlantic Ocean by large juvenile loggerhead turtles. *Diversity and Distributions*, 22 (4), pp.481–492. <https://doi.org/10.1111/ddi.12413>
- Wallace, B.P., Posnik, Z.A., Hurley, B.J., DiMatteo, A.D., Bandimere, A., Rodriguez, I., Maxwell, S.M., Meyer, L., Brenner, H., Jensen, M.P. and LaCasella, E., 2023. Marine turtle regional management units 2.0: an updated framework for conservation and research of wide-ranging megafauna species. *Endangered Species Research*, 52, pp.209-223. <https://doi.org/10.3354/esr01243>
- Yoshida, N. and Miyazaki, N. 1991. Oxygen isotope correlation of cetacean bone phosphate with environmental water. *Journal of Geophysical Research: Oceans*, 96(C1), pp.815–820. <https://doi.org/10.1029/90JC01580>
- Zug, G.R., Wynn, A.H. and Ruckdeschel, C. 1986. Age determination of loggerhead sea turtles, *Caretta caretta*, by incremental growth marks in the skeleton. Smithsonian Contributions to Zoology, Smithsonian Institution Press, City of Washington, 427, pp.1-34.

### 3.4. Article 4: “Identifying the foraging grounds of the new loggerhead turtle nesters in the western Mediterranean”



Cardona, L., Abalo-Morla, S., **Cani, A.**, Feliu-Tena, B., Izaguirre, N., Tomás, J. and Belda, E.J. 2024. Identifying the foraging grounds of the new loggerhead turtle nesters in the western Mediterranean. *Aquatic Conservation: Marine and Freshwater Ecosystems*, 34(1), p.e4059. <https://doi.org/10.1002/aqc.4059>





## Identifying the foraging grounds of the new loggerhead turtle nesters in the western Mediterranean

### Abstract

1. The western Mediterranean Sea has traditionally served as a primary foraging ground for juvenile loggerhead turtles from three distinct regional management units: the Northwestern Atlantic, the Mediterranean, and Cape Verde. Nesting activities were sporadic.
2. Recently, nesting activity on the beaches of eastern Spain has increased, due to warmer sand and water temperatures during the summer months.
3. The study has integrated stable isotope analysis of carbon (C), nitrogen (N), and sulphur (S) with satellite telemetry to identify the foraging grounds of these new colonizers nesting on Spanish beaches.
4. Results indicate that the majority of these adult females forage oceanically in the Algerian Basin, with a few exhibiting distinct stable isotope signals, tentatively associated with foraging in shallow coastal areas in the central Mediterranean Sea.
5. The dominance of oceanic foragers in this new population is noteworthy, given the Algerian Basin's oligotrophic nature. This contrasts with the prevalence of neritic foraging in adult females nesting in the central and eastern Mediterranean Sea.
6. The use of the Algerian Basin as a foraging ground for adult loggerhead turtles exposes them to bycatch from drifting longlines. The authorities should refrain from increasing bluefin quotas imposed on longliners in the Algerian Basin unless the fishery avoids using squid as bait and agrees to deploy hooks deeper than 25 m to reduce loggerhead turtle bycatch.

**Key words:** Algerian Basin, *Caretta caretta*, colonization, foraging grounds, satellite telemetry, stable isotopes.



## INTRODUCTION

Temperature is a major determinant of geographic distribution in animals (Lomolino et al., 2010). As global warming intensifies, many species respond by shifting their distribution range in order to adapt to new environmental conditions (La Sorte & Thompson, 2007; Bebbler, Ramotowski & Gurr, 2013; Kortsch et al., 2015). In recent years, even highly philopatric species like sea turtles (FitzSimmons et al., 1997; Lee, Luschi & Hays, 2007) have expanded into historically colder areas that were once unsuitable for their reproduction. Notably, loggerhead turtles (*Caretta caretta*) have ventured into the western Mediterranean for nesting (Carreras et al., 2018; Cardona et al., 2022; Hochscheid et al., 2022; Mancino, Canestrelli & Mariorano, 2022), while green turtles (*Chelonia mydas*) have been observed nesting in the western Gulf of Mexico (Shaver et al., 2020).

The life history of sea turtles is characterized by natal philopatry (FitzSimmons et al., 1997; Lee, Luschi & Hays, 2007), which seems to be incompatible with the circumtropical distribution of five out of the seven extant species (Wallace et al., 2010). This suggests that these five species are capable of long-distance colonization, although this is likely an infrequent process that operates over long time scales. Distant colonization may result from adults with reduced philopatry (Stewart et al., 2014), individuals reaching sexual maturity while still at their developmental habitats (Carreras et al., 2018), or a combination of these factors, although the process remains poorly understood.

Turtles are imprinted by the magnetic field of their natal beaches (Lohmann, Putman & Lohmann, 2008) and are thereby expected to return to those beaches to nest. However, natal philopatry in sea turtles is imperfect, and some adult females are known to nest on beaches that are several hundreds of kilometers apart, even within the same nesting season (Tucker, 2010; Stewart et al., 2014). This relaxed philopatry can result in a range expansion of hundreds of kilometers and probably explains the recent colonization of green turtles in the northwestern Gulf of Mexico (Shaver et al., 2020). However, this process does not enable colonization of distant areas.

The hatchlings of most sea turtle species disperse across entire ocean basins by following major current systems (Mansfield et al., 2014; Scott, March & Hays, 2014; Briscoe et al., 2016), and they spend several years foraging in areas thousands of kilometers away from where they were born (Carreras et al., 2011; Hawkes et al., 2012; Turner Tomaszewicz et al., 2017; Campos & Cardona, 2019). As they grow older,



juvenile sea turtles migrate to other foraging grounds closer to their natal beaches (Bolten, 2003; Revelles et al., 2007a; Turner Tomaszewicz et al., 2017; Campos & Cardona, 2019). However, the timing of this migration is highly variable, and there is evidence that some turtles reach sexual maturity before moving to the foraging grounds used by the adults of their natal population (Piovano et al., 2011). Eventually, these individuals may mate and nest on nearby beaches (Carreras et al., 2018; Shaver et al., 2020; Cardona et al., 2022; Santidrián Tomillo et al., 2022), thus laying the foundations for a new population if their offspring remains faithful to their own natal beaches, which are distinct from those of their forebears.

During the latter half of the 20<sup>th</sup> century, loggerhead turtles nesting in the Mediterranean Sea was primarily confined to the eastern basin (Casale et al., 2018 and references therein), with occasional low levels of nesting in the central basin (Laurent et al., 1990; Mingozi et al., 2008; Casale et al., 2012; Jribi & Bradai, 2014). While a few isolated nests have been reported in the westernmost part of the Mediterranean Sea since 1870 (Tomás et al., 2008 and references therein), consistent nesting was hindered during this period due to sand temperatures being consistently below 25 °C during most summer months (Pike, 2013; Cardona et al., 2022).

However, in recent years, nesting activity (i.e., the number of nests) in the western Mediterranean Basin has seen a substantial increase (Benabdi & Belmahi, 2020; Hochscheid et al., 2022; Mancino, Canestrelli & Mariorano, 2022). This increase is not solely due to expanded search efforts but rather to the fact that, since 2010, sand temperatures on most beaches in this area have consistently exceeded the threshold for successful incubation of the eggs (25 °C for 80 consecutive days). This temperature change is likely a consequence of global warming (Cardona et al., 2022; Santidrián Tomillo et al., 2022).

Genetic analysis has revealed an admixture of parents from Mediterranean and Atlantic origins on the nesting beaches of the western Mediterranean, dispelling the possibility that these nesting events were remnants of a nearly extinct population decimated by tourism development (Carreras et al., 2018). Satellite tracking of early juveniles from Spanish beaches has shown that most of these individuals remain in the western Mediterranean during the winter months. However, some may drift with prevailing currents to the foraging grounds in the central Mediterranean (Abalo-Morla et al., 2018 and 2023), which are also utilized by hatchlings and early juveniles from the



nesting beaches of the central and eastern Mediterranean Sea (Casale & Mariani, 2014). Conversely, little is known about the habitat used by their parents.

Adult loggerhead turtles nesting in the central and eastern Mediterranean Sea forage primarily on the continental shelf of those regions (Schofield et al., 2013a & 2013b; Haywood et al., 2020). Almpnidou et al., (2022) recently identified several potential neritic foraging grounds for adult loggerhead turtles scattered along the northern shore of the western Mediterranean. However, satellite tracking of non-nesting adult loggerhead turtles incidentally captured in the western Mediterranean has revealed that they are primarily oceanic foragers that extensively use the Algerian Basin (Abalo-Morla et al., 2022a). This region contains one of the highest densities of loggerhead turtles in the entire Mediterranean Sea (DiMatteo et al., 2022) and was previously considered to be solely a juvenile foraging ground (Cardona & Hays, 2018), inhabited mainly by individuals of Atlantic origin (Carreras et al., 2006 & 2011; Clusa et al., 2014). The presence of some adult loggerhead turtles at the oceanic foraging grounds in the Algerian Basin aligns with the hypothesis that certain individuals may reach adulthood while at their juvenile foraging grounds (Piovano et al., 2011). This, in turn, allows some of them to nest on nearby beaches (Carreras et al., 2018) before commencing their return migration to the foraging grounds in their natal region, where they will ultimately settle.

This paper uses stable isotope analysis and satellite telemetry to identify the foraging grounds of female loggerhead turtles currently nesting on Spanish beaches in the Mediterranean. This research aims to investigate the ongoing colonization process of the western Mediterranean basin and test the hypothesis that these nesting females share oceanic foraging grounds with juveniles in the Algerian Basin.

## METHODS

### *Stable isotope analysis*

Previous research has established that stable isotope ratios in sea turtle eggs and hatchlings reflect those of their mothers, allowing characterization of the mothers' foraging grounds (Frankel et al., 2012; Carpentier et al., 2015; Ceriani et al., 2017; Frankel et al., 2012). To this end, epidermis samples were collected from deceased hatchlings originating from 15 nests on Spanish beaches between 2018 and 2020 (one hatchling per nest) and were used to deduce information about their mothers. Additionally, an epidermis sample was collected directly from a nesting female.



Furthermore, epidermis samples were gathered from 58 dead loggerhead turtles found stranded along the Mediterranean coast of eastern mainland Spain (hereafter referred to as the Iberian Peninsula) and the Balearic Islands from 2014 to 2020. This was done to characterize the stable isotope ratios of carbon (C), nitrogen (N), and sulphur (S) in loggerhead turtles foraging in the Gulf of Valencia and the Algerian Basin, which, respectively, correspond to the turtles found on the Mediterranean coast and those in the Balearic Islands (Figure 3.15; Appendix S1). The Iberian Peninsula and the Balearic Islands are treated as distinct regions due to the limited exchange of turtles between them, as indicated by previous research (Revelles et al., 2007a, 2007b & 2008; Eckert et al., 2008; Cardona et al., 2009; Clusa et al., 2014; Abalo-Morla et al., 2022a).

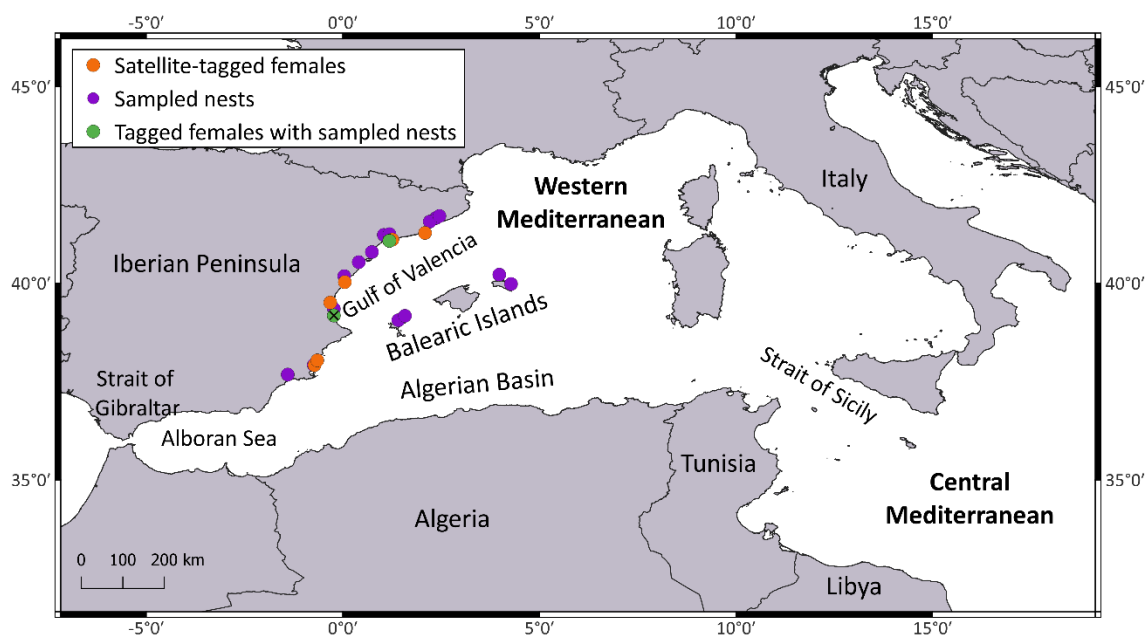


**Figure 3.15.** Distribution of sampled nests and location of satellite-tagged females. The “X” indicates the location of the epidermis sample collected directly from a nesting female, named Victoria.

Skin samples were stored at  $-20^{\circ}\text{C}$ , dried in a laboratory oven at  $50^{\circ}\text{C}$  for 24h, and then cut into small pieces using dissection scissors. Sea turtle epidermis has very low fat content, thus obviating the need for lipid extraction with organic solvents (Bergamo, Botta & Copertino, 2016). Approximately 0.3 mg of dry epidermis were weighed and enclosed in tin capsules (3.3 x 5 mm) for  $\delta^{13}\text{C}$  and  $\delta^{15}\text{N}$  determination. Samples were combusted at  $900^{\circ}\text{C}$ , and the resulting gases were analyzed using an isotope ratio mass spectrometer (Flash 1112 IRMS Delta C Series EA; ThermoFinnigan, Bremen, Germany), coupled to an elemental analyzer (Thermo Fisher Scientific, Milan, Italy).



For  $\delta^{34}\text{S}$  determination, approximately 3 mg of dry epidermis were weighed and placed in tin capsules, with the addition of vanadium pentoxide ( $\text{V}_2\text{O}_5$ ) as a catalyst to expedite the combustion and minimize variability (Nehlich & Richards, 2009). These samples were combusted at 1,035 °C, and the gases analyzed with an Elemental Analyzer (Carlo Erba 1108) coupled to a Delta Plus XP mass spectrometer via a ConFlow III interface (both from Thermofisher) at Centres Científics i Tecnològics (CCiT-UB) of the University of Barcelona, Spain. Isotopic reference materials were used every 12 samples for calibration, achieving a precision of 0.3 ‰ for  $\delta^{13}\text{C}$ , 0.2 ‰ for  $\delta^{15}\text{N}$ , and 0.1 ‰ for  $\delta^{34}\text{S}$ . Details regarding these materials can be found in the Supplementary Information (Appendix S2).

Stable isotope abundances were denoted in delta ( $\delta$ ) notation, with relative variations expressed as per mil (‰) deviations from established international standards. The calculation is as follows:

$$\delta^j\text{X} = \left[ \frac{(^j\text{X}/^i\text{X})_{\text{sample}}}{(^j\text{X}/^i\text{X})_{\text{standard}}} \right] - 1 \quad (1)$$

where  $^j\text{X}$  represents the heavier isotope ( $^{13}\text{C}$ ,  $^{15}\text{N}$ , or  $^{34}\text{S}$ ), while  $^i\text{X}$  represents the lighter isotope ( $^{12}\text{C}$ ,  $^{14}\text{N}$ , or  $^{32}\text{S}$ ) in both the analytical sample and the international measurement standard. The international standards that we applied were Vienna Pee Dee Belemnite (VPDB) calcium carbonate for  $\delta^{13}\text{C}$  values, atmospheric nitrogen for  $\delta^{15}\text{N}$  values, and Vienna-Canyon Diablo Troilite (VCDT) for  $\delta^{34}\text{S}$  values.

The stable isotope ratios of dead stranded turtles from the Iberian Peninsula and the Balearic Islands were compared using the Wilcoxon-Mann-Whitney U test, due to their departure from normality, as determined by the Shapiro-Wilk test. Similarly, the stable isotope ratios of hatchlings from the Iberian Peninsula and the Balearic Islands were compared using the Wilcoxon-Mann-Whitney U test. For these comparisons, no mother-to-hatchling fractionation was assumed for the  $\delta^{34}\text{S}$  values, and the  $\delta^{13}\text{C}$  and  $\delta^{15}\text{N}$  values of nesting females were calculated from those of hatchling epidermises using the following equations (Frankel et al., 2012):

$$\delta^{13}\text{C}_{\text{female}} = 0.51 \times \delta^{13}\text{C}_{\text{hatchling}} - 7.38 \quad (2)$$

$$\delta^{15}\text{N}_{\text{female}} = 1.02 \times \delta^{15}\text{N}_{\text{hatchling}} - 1.02 \quad (3)$$

Two-dimensional plots were built using the package “SIBER” (Stable Isotope Bayesian Ellipses; Jackson et al., 2011) to assess isotopic niche width and overlaps between groups, which include nesting females, individuals stranded in the Balearic Islands, and those stranded in the Iberian Peninsula. These assessments were conducted based on different pairs of stable isotope ratios. Standard ellipse areas corrected for small



sample size (SEAc) were used to represent each species' isotopic niche within the isotopic space and to calculate species overlap (Jackson et al., 2011).

All statistical analyses and plots related to stable isotope analysis were conducted using R Statistical Software version 4.1.2 (R Core Team 2021).

### *Satellite telemetry*

Satellite tracking data from seven female loggerhead turtles were utilized. These turtles were opportunistically tagged during nesting events on Spanish Mediterranean beaches between 2016 and 2022 (see Figure 3.15 and Table 1). One of the turtles, Mascletà, was tagged during two different nesting seasons, in 2016 and 2020, with each track being analyzed independently. It should be noted that only two females (Victoria and Mascletà 2020) shared both stable isotope and satellite telemetry data, making the two datasets complementary.

Location data were obtained through the Argos satellite system. We also employed state-space models (SSM), which are widely used and versatile statistical tools for deriving position estimates from observed data, which they accomplish specifically by accounting for measurement errors and variability in the movement dynamics (Jonsen, Flemming & Myers, 2005; Jonsen, Myers & James, 2007; Jonsen et al., 2013). These models have previously been applied to modelling the movements of marine animals, including sea turtles (Jonsen, Myers & James, 2007; Hoenner et al., 2012). A hierarchical switching state-space model (hDCRWS) was fitted to the data in order to provide position estimates at regular 12-hour intervals, along with associated behavioral states (Jonsen, Myers & James, 2007; Jonsen, 2016; Christiansen et al., 2016). The “bsam” R-package (Jonsen, Flemming & Myers, 2005) within R version 3.4.3 (R Core Team, 2019) was used for this analysis. Two Markov Chain Monte Carlo (MCMC) chains were run for 120,000 iterations. The first 60,000 samples were discarded as a burn-in. To reduce sample autocorrelation, we retained every 10th sample from the remaining 60,000 samples, which were all assumed to have occurred after the convergence of each chain. Thus, these model parameters and estimated locations were calculated using a total of 12,000 MCMC samples. Using a time-step of 12 hours, two daily locations during the tracking period were generated from the posterior means of the resultant distributions.



**Table 3.4.** Details of satellite-tracked nesting females. This table provides: Argos ID number, name, CCL (curved carapace length), CCW (curved carapace width), date of deployment, deployment coordinates (latitude and longitude), date of the end of monitoring, attachment method (epoxy resin or silicone), tag brand (SIRTRACK, DesertStar, or Wildlife Computers), type of tag (solar-powered PPT, SPOT, FASTLOC GPS), and the institutions involved in satellite-tagging and data acquisition (FO: Fundació Ocenogràfic, UV: Universitat de València, GVA: Generalitat de la Comunitat Valenciana, UPV: Universitat Politècnica de València, UVic: Universitat de Vic, UB: Universitat de Barcelona, CRAM: Fundació para la Conservació y Recuperació de Animals Marins, E: Eucrante Association, C:Chelonia Association). “NA” indicates not available data, and “\*” indicates turtles with tags that are still transmitting data. Satellite-tracking data for turtles Ana, Maria, Mascletà 2016, and Yaiza are publicly accessible at the EMODNet repository (Abalo-Morla et al., 2022b).

Argos ID	Name	CCL (cm)	CCW (cm)	Deployment date	Latitude	Longitude	End monitoring date	Attachment method	Tag brand	Type tag	Institutions
160303	Mascletà 2016	61	77	24/06/2016	41.28	2.09	21/08/2016	Silicone	DesertStar	Solar PTT	CRAM, UPV, C
33052	Yaiza	79	72.5	27/06/2018	39.51	-0.32	03/01/2019	Epoxy	Wildlife Computers	SPOT	FO, UV, GVA, UPV, E
60623	Maria	79	NA	30/06/2018	40.03	0.05	15/07/2018	Epoxy	Wildlife Computers	SPOT	FO, UV, GVA, UPV, E
36422	Ana	80	76	08/07/2018	37.92	-0.72	15/11/2018	Epoxy	SIRTRACK	SPOT	FO, UV, GVA, UPV, E
84260	Mascletà 2020	60	NA	16/07/2020	41.08	1.18	13/09/2020	Epoxy	SIRTRACK	FASTLOC GPS	UB, UVic, UPV, UV
222027	Victoria	87	82	30/07/2020	39.18	-0.23	13/12/2022*	Epoxy	SIRTRACK	FASTLOC GPS	FO, UV, GVA, UPV, E
222028	Elena	NA	NA	10/07/2021	41.11	1.26	30/09/2021	Epoxy	SIRTRACK	FASTLOC GPS	UVic, UV, UPV y CRAM
232741	Catherine	80	73	26/07/2022	38.04	-0.65	11/12/2022*	Epoxy	SIRTRACK	FASTLOC GPS	FO, UV, GVA, UPV, E



### *Analysis of foraging behavior*

Location data from the first month following satellite tagging were excluded from the analysis, due to the observed change in female behavior during the nesting season (June – August) compared to the rest of the year. Research indicates that females tend to reduce feeding activity during the nesting season (Miller, 1997; Hays et al., 2002; Hays, 2008) and remain in close proximity to the nesting beach during consecutive nesting events, which is known as the “internesting period” (Zbinden et al., 2007). In line with the approach of Lydersen et al., (2020), we employed a hierarchical switching state-space model (hDCRWS) to differentiate between two behavioral states: transiting and areas of restricted search (ARS). We estimated the mean behavioral state for each location, taking into account all of the bimodal MCMC samples, which were assigned values of 1 (transiting) or 2 (ARS) for the behavioral state (Jonsen et al., 2007; Lydersen et al., 2020). Subsequently, we applied the same cut-off points as in previous studies, defining locations with mean behavioral estimates below 1.25 as indicative of transiting/migratory behavior, those with estimates above 1.75 as representing ARS patches, and locations with mean behavioral estimates between 1.25 and 1.75 as “uncertain,” signifying a lack of sufficient information to distinguish between behaviors in these cases (Jonsen et al., 2007; Lydersen et al., 2020).

To identify distinct movement phases, the trajectories of the turtles were divided into segments characterized by homogeneous behavior using Guéguen’s method (2001 and 2009) via the “adehabitatLT” R-package (Calenge, 2006). Independence of the residuals from the trajectory segmentation was assessed using the Wald and Wolfowitz test (Wald & Wolfowitz, 1943). To identify the core use areas for each female, we employed the Brownian Bridge approach of the kernel method, which was implemented in the “adehabitatHR” package (Horne et al., 2007). Core use areas for each female were defined as the 50% Kernel Utilization Distribution (KUD). The results were then overlaid to identify any overlapping core areas.

The protocols and procedures employed in this study underwent ethical review in accordance with Directive 2010/63/EU, and they were approved by Universitat Politècnica de València. The satellite tagging of females was authorized by the Spanish Ministry for the Ecological Transition and the Demographic Challenge (Ministerio para la Transición Ecológica y el Reto Demográfico) under the following permit numbers: DIV/BDM/AUTSPP/38/2017, SGPM/BDM/AUTSPP/26/2019,



SGPM/BDM/AUTSPP/23/2020,  
SGBTM/BDM/AUTSPP/44/2022.

SGBTM/BDM/AUTSPP/43/2021

and

## RESULTS

### *Isotopic characterization of nesting female feeding areas*

Stranded individuals from the Iberian Peninsula and the Balearic Islands exhibited no significant differences in the distribution of their  $\delta^{34}\text{S}$  values (Figure 3.16; Wilcoxon-Mann-Whitney Test:  $U = 367.5$ ,  $P = 0.549$ ,  $n_1 = 30$ ,  $n_2 = 27$ ). However, they did differ in the distribution of their  $\delta^{13}\text{C}$  and  $\delta^{15}\text{N}$  values. Specifically, individuals depleted in  $^{13}\text{C}$  or  $^{15}\text{N}$  were more prevalent in the Iberian Peninsula compared to the Balearic Islands (see Figure 3.16; Wilcoxon-Mann-Whitney Test,  $n_1 = 30$ ,  $n_2 = 27$ ;  $\delta^{13}\text{C}$ :  $U = 237.5$ ,  $P = 0.007$ ;  $\delta^{15}\text{N}$ :  $U = 108.0$ ,  $P < 0.001$ ). As a result, the standard ellipses of the turtles stranded in these two regions showed only slight overlap in the  $\delta^{13}\text{C}$ - $\delta^{15}\text{N}$  and  $\delta^{15}\text{N}$ - $\delta^{34}\text{S}$  isospaces (Figure 3.17; Table 2), thus confirming that turtles from these regions indeed used different foraging grounds.

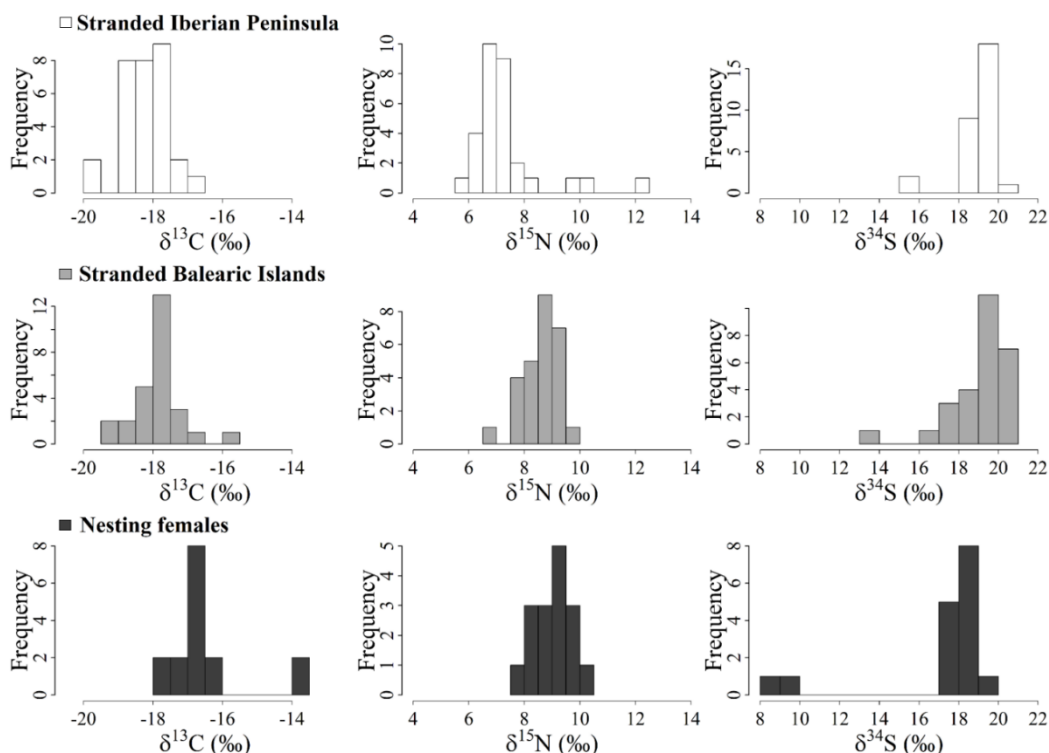


**Figure 3.16.** Stable isotope ratios of C, N, and S of stranded loggerhead turtles from the Iberian Peninsula and the Balearic Islands; and of nesting females from the Spanish Mediterranean coast, as inferred from their hatchlings.



The stable isotopes ratios of C, N, and S in nesting females from both the Iberian Peninsula and the Balearic Islands, as inferred from their hatchlings (Table 2), did not show statistically significant differences (Wilcoxon-Mann-Whitney Test;  $n_1 = 12$ ,  $n_2 = 4$ ;  $\delta^{13}\text{C}$ :  $U = 32.0$ ,  $P = 0.379$ ;  $\delta^{15}\text{N}$ :  $U = 11.0$ ,  $P = 0.115$ ;  $\delta^{34}\text{S}$ :  $U = 29.0$ ,  $P = 0.544$ ). Consequently, all nesting females were pooled together for further analysis. Additionally, genetic analysis revealed that each nest was laid by a distinct female (Carreras, unpublished data), thus eliminating concerns of pseudo-replication. The distribution of  $\delta^{13}\text{C}$  values in nesting females differed significantly from that of stranded turtles in both areas (Wilcoxon-Mann-Whitney test; Iberian Peninsula:  $U = 17.0$ ,  $P < 0.001$ ,  $n_1 = 16$ ,  $n_2 = 30$ ; Balearic Islands:  $U = 45.0$ ,  $P < 0.001$ ,  $n_1 = 16$ ,  $n_2 = 27$ ), due to the presence of two nesting females with highly enriched  $^{13}\text{C}$  values (Table 2; Figure 3.17). The same pattern held true for the  $\delta^{34}\text{S}$  values, with the same two nesting females showing notable depletion in  $^{34}\text{S}$  (Figure 3.17; Wilcoxon-Mann-Whitney test; Iberian Peninsula:  $U = 408.0$ ,  $P < 0.001$ ,  $n_1 = 16$ ,  $n_2 = 30$ ; Balearic Islands:  $U = 345.0$ ,  $P = 0.001$ ,  $n_1 = 16$ ,  $n_2 = 27$ ). In contrast, the distribution of  $\delta^{15}\text{N}$  values in nesting females significantly differed from that of the turtles stranded on the Iberian Peninsula (Figure 3.17; Wilcoxon-Mann-Whitney test; Iberian Peninsula:  $U = 49.0$ ,  $P < 0.001$ ,  $n_1 = 16$ ,  $n_2 = 30$ ), but not from those females stranded on the Balearic Islands (Figure 3.17; Wilcoxon-Mann-Whitney test,  $U = 153.5$ ,  $P = 0.116$ ,  $n_1 = 16$ ,  $n_2 = 27$ ). As a result, the standard ellipse of the nesting females showed no overlap with the standard ellipse of the turtles stranded on the Iberian Peninsula in two of the three considered isospaces, while the third had less than a 2% overlap (Table 3; Figure 3.17). However, the standard ellipse of the nesting females partially overlapped with those of the turtles stranded on the Balearic Islands in all three isospaces, although the overlap was limited due to the presence of two nesting females with enriched  $^{13}\text{C}$  and depleted  $^{34}\text{S}$  (Figure 3.17).



**Table 3.5.** Stable isotope ratios (‰) in hatchlings from Spanish Mediterranean beaches and the inferred ratios in their mothers, according to Frankel et al., (2012) for  $\delta^{13}\text{C}$  and  $\delta^{15}\text{N}$ . No mother-to-hatchling fractionation was assumed for the  $\delta^{34}\text{S}$  values. The values obtained directly from a nesting female are denoted by \*.

ID	Nesting location	Year	$\delta^{13}\text{C}$		$\delta^{15}\text{N}$		$\delta^{34}\text{S}$
			hatchlings	females	hatchlings	females	
ENV. 1	Iberian Peninsula	2019	-18.0	-16.6	9.8	9.0	18.8
ENV. 2	Iberian Peninsula	2020	-18.3	-16.7	10.4	9.5	19.0
ENV. 3	Iberian Peninsula	2019	-17.7	-16.4	10.0	9.1	18.4
ENC. 1	Iberian Peninsula	2020	-18.7	-16.9	8.9	8.1	19.0
ENC. 2	Iberian Peninsula	2018	-20.6	-17.9	10.2	9.4	18.3
ENC. 3	Iberian Peninsula	2018	-20.3	-17.7	9.6	8.8	18.0
ENC. 4	Iberian Peninsula	2018	-12.7	-13.9	8.9	8.1	9.4
ENC. 5	Iberian Peninsula	2020	-12.9	-14.0	9.2	8.3	8.0
ENC. 6	Iberian Peninsula	2020	-18.6	-16.9	9.8	9.0	17.2
ENM. 1	Iberian Peninsula	2020	-18.7	-16.9	8.7	7.9	18.5
ENM. 2	Iberian Peninsula	2020	-18.4	-16.7	10.4	9.6	18.0
EVLC. 1*	Iberian Peninsula	2020	-	-16.6	-	9.2	19.1
ENB. 1	Balearic Islands	2019	-17.6	-16.4	10.2	9.4	18.0
ENB. 2	Balearic Islands	2020	-18.8	-16.9	10.9	10.1	17.9
ENB. 3	Balearic Islands	2020	-19.1	-17.1	9.5	8.7	18.5
ENB. 4	Balearic Islands	2020	-19.0	-17.1	10.7	9.9	17.9

**Table 3.6.** Overlap between the standard ellipses of loggerhead turtles stranded along the coasts of the Iberian Peninsula and Balearic Islands, and nesting females, as shown in Figure 3.17. Overlap is reported as the percentage of the standard ellipse area of each group enclosed in the standard ellipse of the other group.

Pairs (1 vs 2)	$\delta^{13}\text{C} - \delta^{15}\text{N}$		$\delta^{13}\text{C} - \delta^{34}\text{S}$		$\delta^{34}\text{S} - \delta^{15}\text{N}$	
	(% Overlap)		(% Overlap)		(% Overlap)	
	1	2	1	2	1	2
<b>Stranded Iberian Peninsula vs. Stranded Balearic Islands</b>	18.59	29.17	71.55	46.01	21.70	19.16
<b>Stranded Iberian Peninsula vs. Nesting females</b>	0.00	0.00	0.00	0.00	1.95	0.89
<b>Stranded Balearic Islands vs. Nesting females</b>	14.75	10.89	26.49	16.56	44.64	23.09

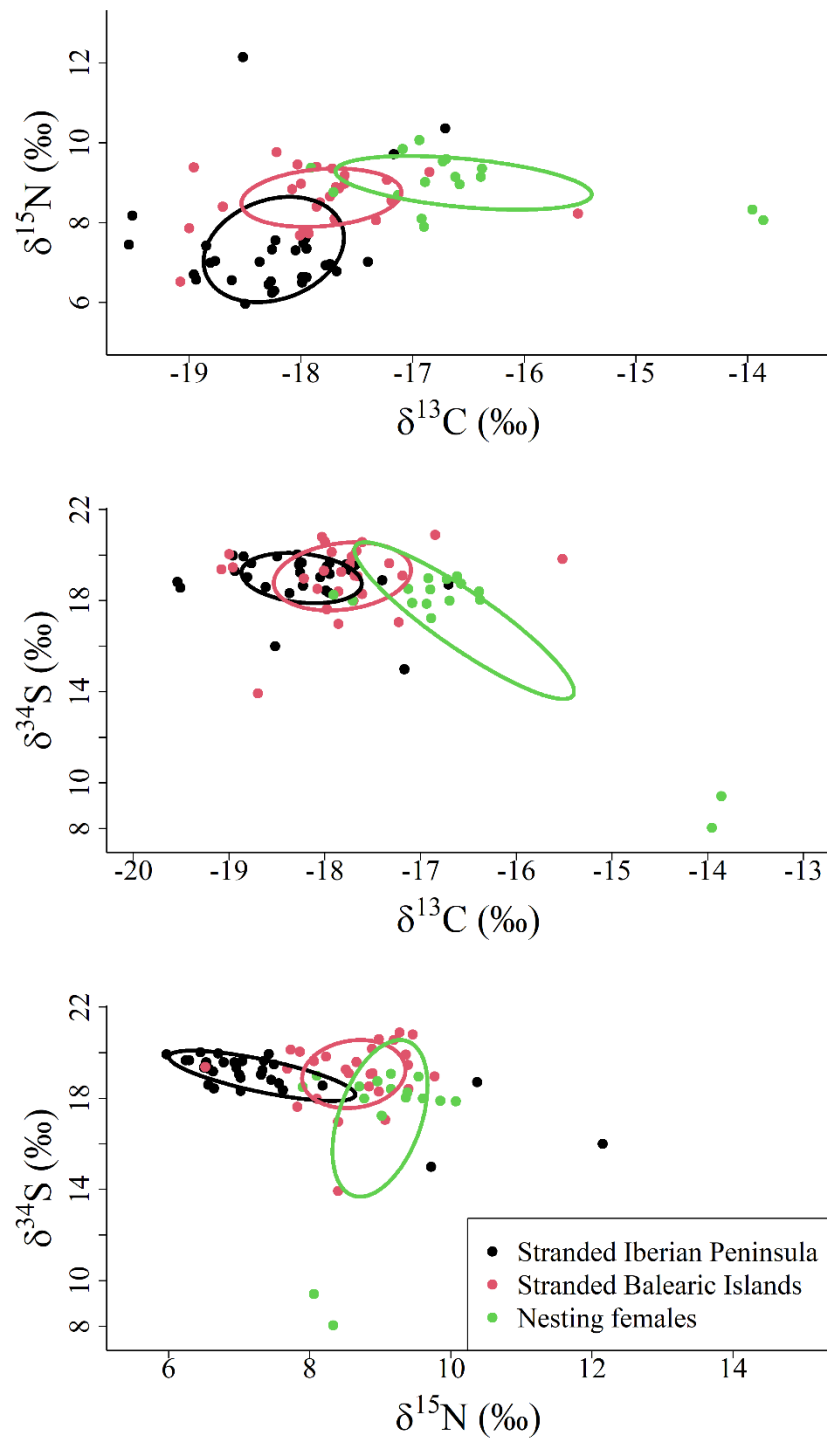


**Figure 3.17.** Standard ellipses of loggerhead turtles stranded along the coasts of the Iberian Peninsula and Balearic Islands, and nesting females, all corrected for small sample size (SEAc). The relative overlap values are reported in Table 3.



### *Satellite telemetry*

Ana and Catherine were tagged in southeastern Spain, a region directly facing the Algerian Basin (Figure 3.18). They initially traveled southward and then shifted eastward, spending most of their tracking time in the western part of the Algerian Basin. The remaining females (Victoria, Maria, Mascletà in 2016 and 2020, Elena and Yaiza) were tagged along the eastern Spanish coast (see Figure 3.18). Notably, Victoria initially ventured to the easternmost part of the Alboran Sea, moved eastward toward the Strait of Sicily, spent 3.5 months in the central Mediterranean, and eventually returned to the Algerian Basin. Maria remained close to the deployment location, but transmission was lost 15 days after tagging. The other three turtles moved to the central Algerian Basin after tagging, although following two distinct routes. Mascletà was tagged in two different years (2016 and 2020) at beaches 88 km apart. In both years, she initially moved eastward across the Balearic Sea and along the northern rim of the Balearic Islands, later traveling southward to the central part of the Algerian Basin. Elena was tagged on a beach near the nesting sites used by Mascletà for nesting in 2016 and 2020, and she followed a similar route. In contrast, Yaiza was tagged at a more southerly beach and traveled eastward along the southern rim of the Balearic Islands, ultimately reaching the central part of the Algerian Basin (Fig. 1).

The seven adult females spent most of their tracking time (92.3% of daily locations) in areas deeper than 200 m, indicating that they remained predominantly in the oceanic domain. Additionally, Kernel analysis demonstrated that the central Algerian Basin was the most frequently utilized area by all of them (see Figure 3.19).

Four turtles (Ana, Elena, Yaiza and Victoria) clearly exhibited alternation between behavioral states (migratory vs. ARS) during tracking (Figure 3.18). However, resolution was poor for Catherine and Mascletà in both 2016 and 2020 and, therefore, behavioral states could not be reliably assigned to them. Trajectory segmentation provided support for the hypothesis that all turtles, except Catherine, alternated between faster and slower movement phases. The validity of this approach was confirmed by the independence of the residuals from these segmentations (Wald and Wolfowitz test,  $P > 0.05$ ; see Figure 3.20). Fast movement model phases (characterized by high average displacement) correspond to traveling, while slow movement model phases (characterized by low average displacement) correspond to foraging or resting.

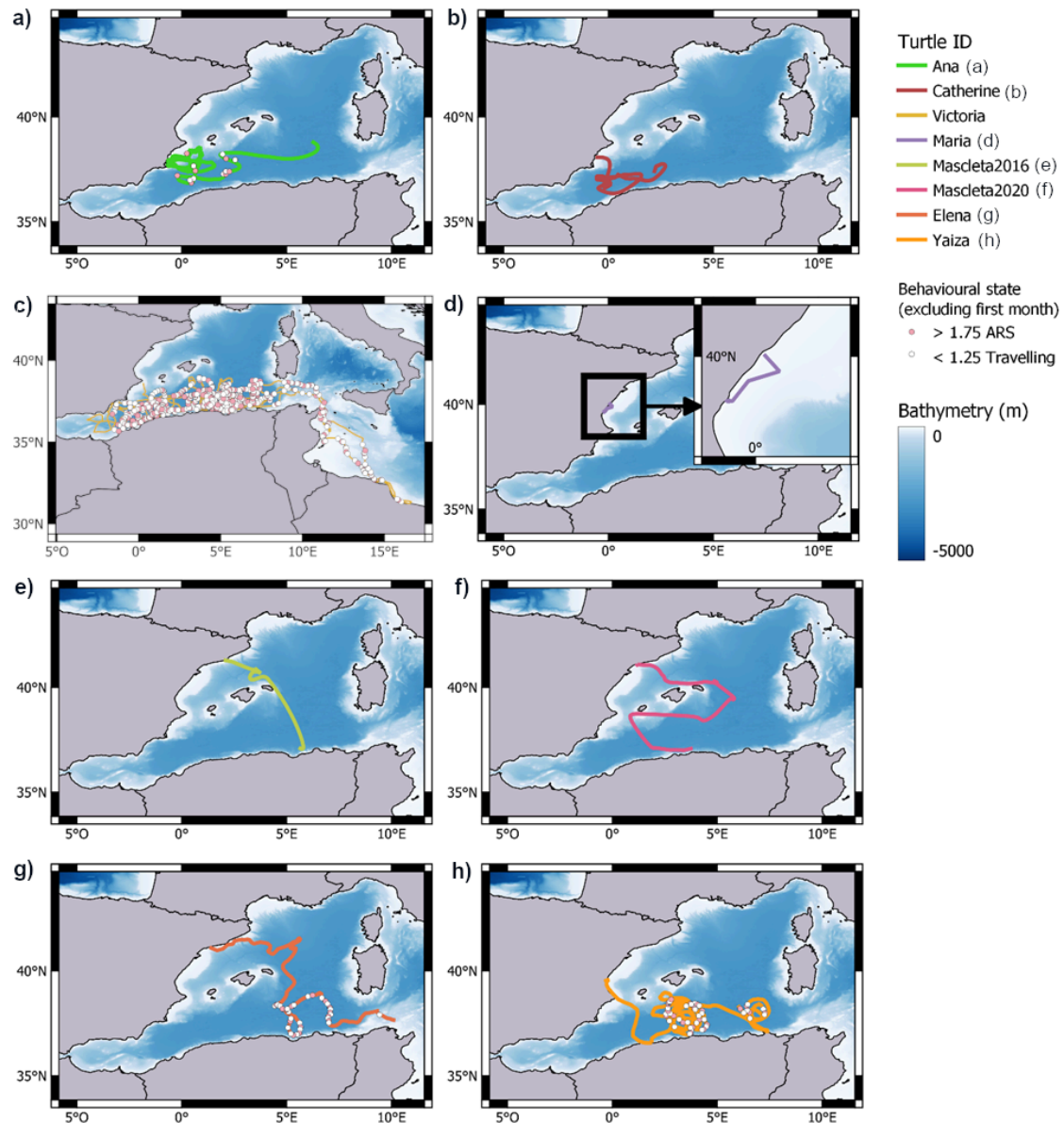


**Figure 3.18.** Tracks of the seven female loggerhead turtles satellite-tracked from Spanish nesting beaches during the entire tracking period. The blue background reveals bathymetry. Behavioral states (traveling, mean behavioral estimate below 1.25; and area restricted search, mean behavioral estimate above 1.75) after the first month of tagging are denoted by white (traveling) and pink (foraging) symbols, respectively. Behavioral states during the first month after tagging were not considered. Locations with mean behavioral estimates between 1.25 and 1.75 were considered “uncertain” and were not plotted.

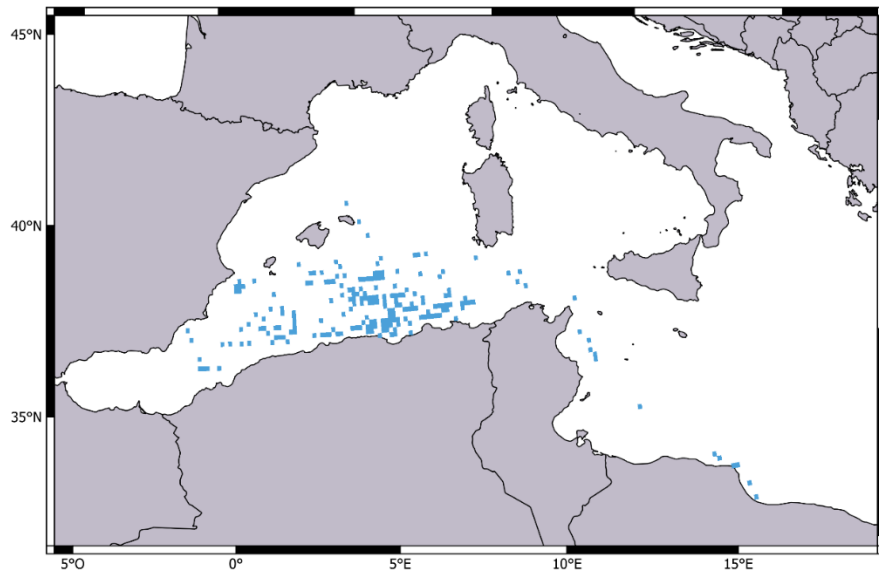


**Figure 3.19.** Estimates of Kernel habitat use obtained by the Brownian Bridge method at 50% KUD.

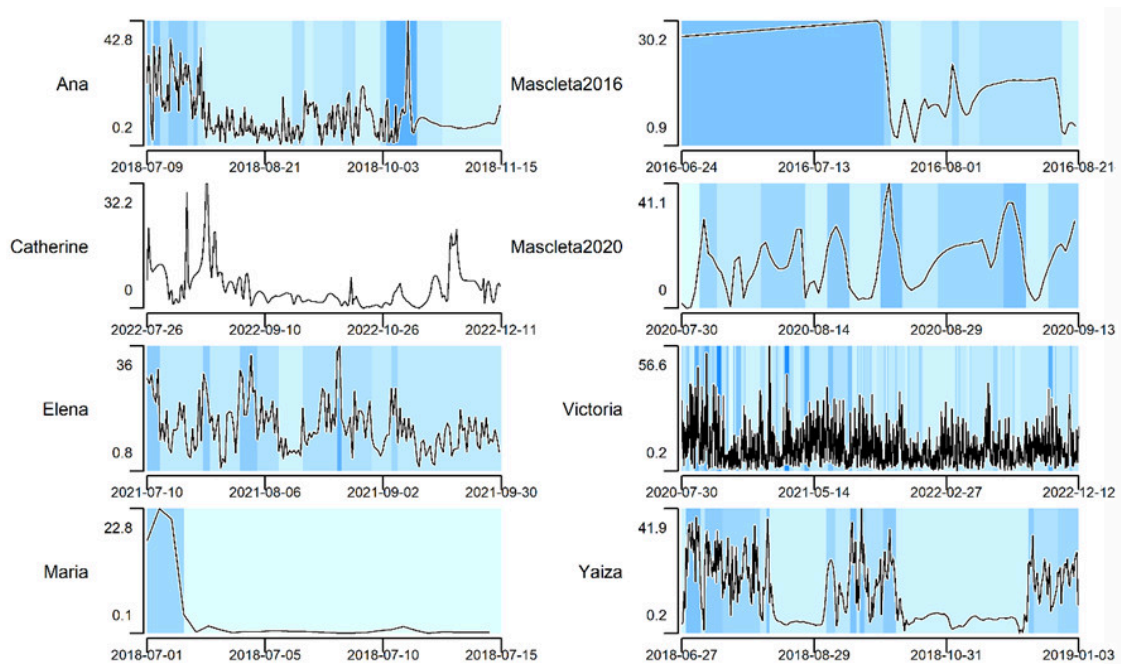


**Figure 3.20.** Results of the movement segmentation analysis covering the entire tracking period for each turtle. The figure shows mean travel distance in km (y-axis), which varies for each turtle, and over time (x-axis). Background colors highlight phases differing by average travel speed, with more intense blues indicating a greater average distance traveled per time unit, thus representing a faster movement phase, while lighter blues represent smaller distances traveled. White background denotes no differences.



## DISCUSSION

The combined evidence from stable isotope analysis and satellite telemetry reported in this study reveals that females currently nesting on the Mediterranean coast of Spain are oceanic foragers, predominantly utilizing the Algerian Basin. It should be noted that the two analyzed datasets contained only two females who shared both stable isotope and satellite telemetry data (Victoria and Mascletà 2020). This limited overlap is due to the wide distribution of nests along the Spanish Mediterranean coast, making it challenging for researchers to reach nesting events before the females depart from the beach, and because dead hatchlings do not occur at some nests. The complementarity of these two data sets addresses the challenges posed by the small sample size, a consequence of the very recent colonization of Spanish beaches by nesting females, which in turn has led to a relatively small number of nesting events recorded annually on these shores, with fewer than 11 nests per year until 2022 (Cardona et al., 2022; Hochscheid et al., 2022).

Stable isotope ratios in the epidermis of sea turtles integrate dietary information over several months (Reich, Bjørndal & Martínez del Río, 2008). Therefore, the presence of statistically significant differences in the stable isotope ratios of C, N, and S of the loggerhead turtles stranded on the Iberian Peninsula and the Balearic Islands indicates that they have been utilizing distinct foraging grounds during the months immediately preceding their demise. Interestingly, the isotopic niche of nesting females differed significantly from that of loggerhead turtles stranded along the coast of the Iberian Peninsula, but this niche partially overlapped with that of loggerhead turtles stranded in the Balearic Islands, thus suggesting that the females nesting on the Mediterranean beaches of Spain and the turtles stranded in the Balearic Islands share foraging grounds.

The differences in the isotopic niches of loggerhead turtles stranded on the Iberian Peninsula and the Balearic Islands are consistent with previous satellite telemetry data, which have consistently shown limited exchange of loggerhead turtles between these two areas (Cardona et al., 2005; Revelles et al., 2007b, 2007c & 2008; Eckert et al., 2008; Cardona et al., 2009; Abalo-Morla et al., 2022a). These findings can be attributed to the close association between the movements of oceanic loggerhead turtles in the western Mediterranean and the general circulation pattern of sea surface waters (Cardona & Hays, 2018). However, it is worth noting that the prevalence of oceanic foragers among the nesting females sampled on Spanish beaches is remarkable, even though the small sample size limits the accuracy of estimating their proportion. Adult loggerhead turtles can



exhibit either neritic or oceanic foraging behaviors (Hatase, Omuta & Tsukamoto, 2010), with the prevalence of oceanic foragers being higher in regions with abundant primary productivity (Hawkes et al., 2006; Rees et al., 2010; Ceriani et al., 2012; Eder et al., 2012). Published data indicate that approximately 98% of female loggerhead turtles nesting in the central and eastern Mediterranean are neritic foragers (Zbinden et al., 2008 & 2011; Schofield et al., 2013a & 2013b; Haywood et al., 2020), which aligns with the generally oligotrophic nature of the Mediterranean Sea. Primary productivity in the Algerian Basin is slightly higher than in the Ionian Sea and the Levantine Basin, and, furthermore, it has increased over recent decades (Colella et al., 2016). This increased productivity might explain why oceanic foragers are more frequently found in the Algerian Basin than in the central and eastern Mediterranean. However, primary productivity is much higher in the neritic habitats along the coast of the Iberian Peninsula, where suitable foraging grounds exist and are used by juvenile loggerhead turtles (Cardona et al., 2009; Almpanidou et al., 2022; Abalo-Morla et al., 2022a). The reason why these neritic foraging grounds are not utilized by nesting females remains unknown, but it could be related to their Atlantic origin, as discussed further below.

The Algerian Basin is primarily inhabited by loggerhead turtles that originate from nesting beaches in the northwestern Atlantic Ocean, with a predominant origin in southern Florida (Carreras et al., 2006 & 2011; Clusa et al., 2014). As early juveniles, they drift eastward along the Gulf Stream (Mansfield et al., 2014), and some eventually enter the Mediterranean Sea, where they typically remain until they reach an average straight carapace length (SCL) of 54.5 cm (Revelles et al., 2007a). At this size, they are capable of overcoming the permanent eastward current at the Straits of Gibraltar and return to the western Atlantic Ocean (Eckert et al., 2008; Revelles et al., 2008; Cejudo et al., 2006). It is worth noting that, during their sojourn in the Mediterranean Sea, most of these loggerhead turtles of North Atlantic origin prefer to remain within the Algerian Basin (Clusa et al., 2014), where they exhibit oceanic foraging behaviors (Revelles et al., 2007b, 2007c & 2008). Furthermore, some individuals delay their return to the Atlantic Ocean, reaching adulthood while still in the Mediterranean Sea (Piovano et al., 2011), and even nesting on Spanish and Italian beaches in the western Mediterranean (Carreras et al., 2018). This suggests that the prevalence of oceanic foraging behavior among females nesting on Spanish beaches may be attributed to the early sexual maturity of individuals of Atlantic origin, who persistently inhabit the juvenile foraging grounds in the western Mediterranean.



However, this explanation does not account for the distinctive isotopic niche observed in some of the females nesting on Spanish beaches, characterized by elevated  $\delta^{13}\text{C}$  and reduced  $\delta^{34}\text{S}$  values, which suggest foraging in an isotopically distinct area. Seagrasses growing in anoxic sediments of sheltered bays are known for their high  $\delta^{13}\text{C}$  and low  $\delta^{34}\text{S}$  values (Peterson, 1999). Some adult loggerhead turtles foraging in coastal habitats in the central and eastern Mediterranean exhibit significant enrichments in  $^{13}\text{C}$  and depletions in  $^{34}\text{S}$  (Haywood et al., 2020), a pattern akin to the two isotopically distinct females nesting in Spain, as mentioned above. Notably, one of the nesting females tracked by satellite in this study (Victoria) spent 3.5 months in coastal habitats within the central Mediterranean, yet her stable isotope ratios did not display enrichments in  $^{13}\text{C}$  or depletions in  $^{34}\text{S}$ . While enclosed bays with seagrass meadows also exist along the coasts of the Iberian Peninsula and Balearic Islands, none of the loggerhead turtles found dead in those areas and analyzed here exhibited the same level of  $^{13}\text{C}$  enrichment and  $^{34}\text{S}$  depletion as these two distinct nesting females. As a result, our current knowledge does not provide a clear identification of these distinct foraging grounds, and further research is necessary to identify their location and characteristics.

### ***Implications for conservation***

The cumulative evidence presented in this study indicates that the majority of female loggerhead turtles nesting on recently colonized Mediterranean beaches in Spain predominantly forage in oceanic habitats within the western Mediterranean Sea. This diverges from the typical foraging ecology observed in females nesting in the eastern Mediterranean Basin, where they are mostly neritic foragers (Zbinden et al., 2008 & 2011; Schofield et al., 2013a & 2013b; Haywood et al., 2020). As to whether or not a similar oceanic foraging pattern applies to females nesting in the recently colonized beaches of western Italy (Hochscheid et al., 2022), this remains a topic that requires further investigation. Additionally, it remains uncertain whether this oceanic behavior is exclusive to females of North Atlantic origin and whether they transition to neritic foraging as they grow older.

What is clear is that the Algerian Basin is a region where most of the longline fishing effort within the entire Mediterranean Sea is concentrated (Taconet, Kroodsmá and Fernandes, 2021). In the 1990s, Spanish drifting longlines captured as many as 20,000 loggerhead turtles annually, posing a significant threat to these turtles in the region (Álvarez de Quevedo, San Félix & Cardona, 2013). Over the past decade, a dramatic



reduction in bycatch levels has occurred in the western Mediterranean Sea (Báez et al., 2019). Despite this, the density of turtles at-sea (DiMatteo et al., 2022) and nest counts at major nesting beaches (Casale et al., 2018, Ceriani et al., 2019) have either remained stable or slightly increased. The decline in bycatch levels was driven by operational changes in the Spanish longline fleet, which shifted its focus from bluefin tuna to swordfish as their main target species due to new regulations. They now deploy longlines deeper than 200 m (Báez et al., 2019), effectively keeping the turtles using the surface waters out of reach (Álvarez de Quevedo, San Félix & Cardona, 2013).

In this case, a simple operational change in a critical human activity, such as fishing, has produced a positive impact on this species in the region. Global warming has certainly improved the thermal conditions for the nesting of loggerhead turtles in Spanish beaches (Cardona et al., 2022), but increased survival in the oceanic foraging grounds of the Algerian Basin has probably increased the number of adults present in the region. However, this progress could potentially be reversed in the near future if fishing quotas increase and fishermen revert to targeting bluefin tuna in surface waters. If that were to happen, the bycatch of sea turtles would once again surge, putting the survival of adults currently involved in the ongoing colonization of the western Mediterranean at risk. For this reason, any potential increase in the bluefin tuna quotas for the longline fleet in the western Mediterranean should be accompanied by measures aimed at reducing loggerhead turtle bycatch, such as avoiding the use of squid as bait and deploying hooks deeper than 25 m (Swimmer et al., 2017), which must be considered by all countries involved in the fishery. Furthermore, bycatch in other fisheries should also be reduced, as adult loggerhead turtles are often captured incidentally by artisanal fisheries operating off Morocco and Algeria (Belmahi et al., 2020; Mghili et al., 2023). Considering that regional population estimates for the Mediterranean population are likely to be considerably overestimated (Rees et al., 2020), the conservation of any adult loggerhead turtle is more important than previously thought.

## REFERENCES

- Abalo-Morla, S., Marco, A., Tomás, J., Revuelta, O., Abella, E., Marco, V., Crespo-Picazo, J.L., Fernández, C., Valdés, F., Arroyo, M.D.C. and Montero, S. 2018. Survival and dispersal routes of head-started loggerhead sea turtle (*Caretta caretta*) post-hatchlings in the Mediterranean Sea. *Marine Biology*, 165, pp.1-17. <https://doi.org/10.1007/s00227-018-3306-2>

- Abalo-Morla, S., Belda, E.J., March, D., Revuelta, O., Cardona, L., Giralt, S., Crespo-Picazo, J.L., Hochscheid, S., Marco, A., Merchán, M. and Sagarminaga, R. 2022a. Assessing the use of marine protected areas by loggerhead sea turtles (*Caretta caretta*) tracked from the western Mediterranean. *Global Ecology and Conservation*, 38, pp.e02196. <https://doi.org/10.1016/j.gecco.2022.e02196>
- Abalo-Morla, S., Belda, E.J., Tomás, J., Crespo-Picazo, J.L., Marco, A. and Revuelta, O. 2022b. Satellite-tracking dataset of loggerhead sea turtles tracked from western Mediterranean. *Data in Brief*, 43, p.108432. <https://doi.org/10.1016/j.dib.2022.108432>
- Abalo-Morla, S., Muñoz Más, R., Tomás, J., Belda, E. 2023. Factors driving dispersal and habitat use of loggerhead turtle post-hatchlings and its conservation implications. *Marine Biology*, 170, pp.155. <https://doi.org/10.1007/s00227-023-04285-2>
- Almpanidou, V., Tsapalou, V., Chatzimentor, A., Cardona, L., Claro, F., Hostetters, P., Kaska, Y., Liu, W., Mansui, J., Miliou, A., Pietroluongos, G., Sacchi, J., Sezgin, C., Sözbilen, D. and Mazaris, A.D. 2022. Foraging grounds of adult loggerhead sea turtles across the Mediterranean Sea: key sites and hotspots of risk. *Biodiversity Conservation*, 31, pp.143-160. <https://doi.org/10.1007/s10531-021-02326-0>
- Álvarez de Quevedo, I., San Félix, M. and Cardona, L. 2013. Mortality rates in by-caught loggerhead turtle *Caretta caretta* in the Mediterranean Sea and implications for the Atlantic populations. 2013. *Marine Ecology Progress Series*, 489, pp.225–234. <https://doi.org/10.3354/meps10411>
- Báez, J.C., García-Barcelona, S., Camiñas, J.A. and Macías, D. 2019. Fishery strategy affects the loggerhead sea turtle mortality trend due to the longline bycatch. *Fisheries Research*, 212, pp.21-28. <https://doi.org/10.1016/j.fishres.2018.11.032>
- Bebber, D.P., Ramotowski, M.A. and Gurr, S.J. 2013. Crop pests and pathogens move polewards in a warming world. *Nature climate change*, 3(11), pp.985-988. <https://doi.org/10.1038/nclimate1990>
- Belmahi, A.E., Belmahi, Y., Benabdi, M., Bouziani, A.L., Darna, S.A., Boulash, Y., Bendoula, M., Bouderbala, M. 2020. First study of sea turtle strandings in Algeria (western Mediterranean) and associated threats: 2016-2017. *Herpetozoa*, 33, pp. 113-120. <https://doi.org/10.3897/herpetozoa.33.e48541>
- Benabdi, M. and Belmahi, A.E. 2020. First record of loggerhead turtle (*Caretta caretta*) nesting in the Algerian coast (southwestern Mediterranean). *Journal of the Black Sea/Mediterranean Environment*, 26(1), pp.100-105.
- Bergamo, T.F., Botta, S. and Copertino, M. 2016. Lipid extraction in stable isotope analyses of juvenile sea turtle skin and muscle. *Aquatic Biology*, 25, pp.1–6. <https://doi.org/10.3354/ab00652>
- Bolten, A.B. 2003. Active swimmers-passive drifters: the oceanic juvenile stage of loggerheads in the Atlantic system. In: Bolten, A.B., Witherington, B.E. (Eds.), *Loggerhead Sea Turtles*. Smithsonian Institution Press, Washington, D.C., pp.63–78.
- Briscoe, D.K., Parker, D.M., Balazs, G.H., Kurita, M., Saito, T., Okamoto, H., Rice, M., Polovina, J.J. and Crowder, L.B. 2016. Active dispersal in loggerhead sea turtles (*Caretta caretta*) during the ‘lost years’. *Proceedings of the Royal Society B: Biological Sciences*, 283(1832), p.20160690. <https://doi.org/10.1098/rspb.2016.0690>

- Calenge, C. 2006. The package “adehabitat” for the R software: a tool for the analysis of space and habitat use by animals. *Ecological modelling*, 197(3-4), pp.516-519. <https://doi.org/10.1016/j.ecolmodel.2006.03.017>.
- Campos, P. and Cardona, L. 2019. Individual variability in the settlement of juvenile green turtles in the western South Atlantic Ocean: relevance of currents and somatic growth rate. *Marine Ecology Progress Series*, 614, pp.173-182. <https://doi.org/10.3354/meps12909>
- Cardona, L., Revelles, M., Carreras, C., San Félix, M., Gazo, M. and Aguilar, A. 2005. Western Mediterranean immature loggerhead turtles: habitat use in spring and summer assessed through satellite tracking and aerial surveys. *Marine Biology*, 147, pp.583-591. <https://doi.org/10.1007/s00227-005-1578-9>
- Cardona, L., Revelles, M., Parga, M.L., Tomás, J., Aguilar, A., Alegre, F., Raga, A. and Ferrer, X. 2009. Habitat use by loggerhead sea turtles *Caretta caretta* off the coast of eastern Spain results in a high vulnerability to neritic fishing gear. *Marine Biology*, 156, pp.2621-2630. <https://doi.org/10.1007/s00227-009-1288-9>
- Cardona, L. and Hays, G.C. 2018. Ocean currents, individual movements and genetic structuring of populations. *Marine biology*, 165, pp.1-10. <https://doi.org/10.1007/s00227-017-3262-2>
- Cardona, L., San Martín, J., Benito, L., Tomás, J., Abella, E., Eymar, J., Aguilera, M., Esteban, J.A., Tarragó, A. and Marco, A. 2022. Global warming facilitates the nesting of the loggerhead turtle on the Mediterranean coast of Spain. *Animal Conservation*, 26(3), pp.365-380. <https://doi.org/10.1111/acv.12828>
- Carpentier, A.S., Booth, D.T., Arthur, K.E. and Limpus, C.J. 2015. Stable isotope relationships between mothers, eggs and hatchlings in loggerhead sea turtles *Caretta caretta*. *Marine Biology*, 162, pp.783-797. <https://doi.org/10.1007/s00227-015-2624-x>
- Carreras, C., Pont, S., Maffucci, F., Pascual, M., Barcelo, A., Bentivegna, F., Cardona, L., Alegre, F., SanFelix, M., Fernandez, G. and Aguilar, A. 2006. Genetic structuring of immature loggerhead sea turtles (*Caretta caretta*) in the Mediterranean Sea reflects water circulation patterns. *Marine Biology*, 149, pp.1269-1279. <https://doi.org/10.1007/s00227-006-0282-8>
- Carreras, C., Pascual, M., Cardona, L., Marco, A., Bellido, J.J., Castillo, J.J., Tomás, J., Raga, J.A., Sanfélix, M., Fernández, G. and Aguilar, A. 2011. Living together but remaining apart: Atlantic and Mediterranean loggerhead sea turtles (*Caretta caretta*) in shared feeding grounds. *Journal of Heredity*, 102(6), pp.666-677. <https://doi.org/10.1093/jhered/esr089>
- Carreras, C., Pascual, M., Tomás, J., Marco, A., Hochscheid, S., Castillo, J.J., Gozalbes, P., Parga, M., Piovano, S. and Cardona, L. 2018. Sporadic nesting reveals long distance colonisation in the philopatric loggerhead sea turtle (*Caretta caretta*). *Scientific reports*, 8(1), pp.1435. <https://doi.org/10.1038/s41598-018-19887-w>
- Casale, P., Palilla, G., Salemi, A., Napoli, A., Prinzi, M., Genco, L., Bonaviri, D., Mastrogiacomo, A., Oliverio, M. and Valvo, M.L. 2012. Exceptional sea turtle nest records in 2011 suggest an underestimated nesting potential in Sicily (Italy). *Acta Herpetologica*, 7(1), pp.181-188. [https://doi.org/10.13128/Acta\\_Herpetol-10725](https://doi.org/10.13128/Acta_Herpetol-10725)
- Casale, P. and Mariani, P. 2014. The first ‘lost year’ of Mediterranean sea turtles: dispersal patterns indicate subregional management units for conservation. *Marine Ecology Progress Series*, 498, pp.263-274. <https://doi.org/10.3354/meps10640>

- Casale, P., Broderick, A.C., Camiñas, J.A., Cardona, L., Carreras, C., Demetropoulos, A., Fuller, W.J., Godley, B.J., Hochscheid, S., Kaska, Y. and Lazar, B. 2018. Mediterranean sea turtles: current knowledge and priorities for conservation and research. *Endangered Species Research*, 36, pp.229–267. <https://doi.org/10.3354/esr00901>
- Cejudo, D., Varo-Cruz, N., Liria-Loza, A., Castillo, J.J., Bellido, J.J. and López-Jurado, L.F. 2006. Transatlantic migration of juvenile loggerhead turtles (*Caretta caretta* L.) from the Strait of Gibraltar. *Marine Turtle Newsletter*, 114, pp.9-11.
- Ceriani, S.A., Roth, J.D., Evans, D.R., Weishample, J.F., Ehrhart, L.M. 2012. Inferring foraging areas of nesting loggerhead turtles using satellite telemetry and stable isotopes. *PLoS ONE*, 7(9), pp.e45335. <https://doi.org/10.1371/journal.pone.0045335>
- Ceriani, S.A., Weishampel, J.F., Ehrhart, L.M., Mansfield, K.L. and Wunder, M.B. 2017. Foraging and recruitment hotspot dynamics for the largest Atlantic loggerhead turtle rookery. *Scientific reports*, 7(1), pp.16894. <https://doi.org/10.1038/s41598-017-17206-3>
- Ceriani, S. A., P. Casale, M. Brost, E. H. Leone, and B. E. Witherington. 2019. Conservation implications of sea turtle nesting trends: elusive recovery of a globally important loggerhead population. *Ecosphere*, 10(11), pp.e02936. <https://doi.org/10.1002/ecs2.2936>
- Christiansen, F., Putman, N.F., Farman, R., Parker, D.M., Rice, M.R., Polovina, J.J., Balazs, G.H. and Hays, G.C. 2016. Spatial variation in directional swimming enables juvenile sea turtles to reach and remain in productive waters. *Marine Ecology Progress Series*, 557, pp.247-259. <https://doi.org/10.3354/meps11874>.
- Colella, S., Falcini, F., Rinaldi, E., Sammartino, M. and Santoleri, R. 2016. Mediterranean Ocean Colour Chlorophyll Trends. *PLoS ONE*, 11(6), pp.e0155756. <https://doi.org/10.1371/journal.pone.0155756>
- Clusa, M., Carreras, C., Pascual, M., Gaughran, S.J., Piovano, S., Giacoma, C., Fernández, G., Levy, Y., Tomás, J., Raga, J.A. and Maffucci, F. 2014. Fine-scale distribution of juvenile Atlantic and Mediterranean loggerhead turtles (*Caretta caretta*) in the Mediterranean Sea. *Marine Biology*, 161, pp.509-519. <https://doi.org/10.1007/s00227-013-2353-y>
- DiMatteo, A., Cañadas, A., Roberts, J., Sparks, L., Panigada, S., Boisseau, O., Moscrop, A., Fortuna, C.M., Lauriano, G., Holcer, D., Peltier, H., Ridoux, V., Raga, J.A., Tomás, J., Broderick, A.C., Godley, B.J., Haywood, J., March, D., Snape, R., Sagarminaga, R. and Hochscheid, S. 2022. Basin-wide estimates of loggerhead turtle abundance in the Mediterranean Sea derived from line transect surveys. *Frontiers in Marine Science*, 9, p.930412. <https://doi.org/10.3389/fmars.2022.930412>
- Eckert, S.A., Moore, J.E., Dunn, D.C., van Buiten, R.S., Eckert, K.L. and Halpin, P.N. 2008. Modeling loggerhead turtle movement in the Mediterranean: importance of body size and oceanography. *Ecological Applications*, 18(2), pp.290-308. <https://doi.org/10.1890/06-2107.1>
- Eder, E., Ceballos, A., Martins, S., Pérez-García, H., Marín, I., Marco, A. and Cardona, L. 2012. Foraging dichotomy in loggerhead sea turtles *Caretta caretta* off northwestern Africa. *Marine Ecology Progress Series*, 470, pp.113-122. <https://doi.org/10.3354/meps10018>
- FitzSimmons, N.N., Limpus, C.J., Norman, J.A., Goldizen, A.R., Miller, J.D. and Moritz, C. 1997. Philopatry of male marine turtles inferred from mitochondrial DNA

- markers. *Proceedings of the National Academy of Sciences*, 94(16), pp.8912-8917. <https://doi.org/10.1073/pnas.94.16.8912>
- Frankel, N.S., Vander Zanden, H.B., Reich, K.J., Williams, K.L. and Bjorndal, K.A. 2012. Mother– offspring stable isotope discrimination in loggerhead sea turtles *Caretta caretta*. *Endangered Species Research*, 17(2), pp.133-138. <https://doi.org/10.3354/esr00412>
- Guéguen, L. 2001. Segmentation by maximal predictive partitioning according to composition biases. In: Gascuel, O., Sagot, MF. (Eds), *Computational Biology. JOBIM 2000. Lecture Notes in Computer Science*, Springer Berlin Heidelberg, pp.32-44. [https://doi.org/10.1007/3-540-45727-5\\_4](https://doi.org/10.1007/3-540-45727-5_4)
- Hatase, H., Omuta, K. and Tsukamoto, K. 2010. Oceanic residents, neritic migrants: a possible mechanism underlying foraging dichotomy in adult female loggerhead turtles (*Caretta caretta*). *Marine Biology*, 157, pp.1337-1342. <https://doi.org/10.1007/s00227-010-1413-9>
- Hawkes, L.A., Broderick, A.C., Coyne, M.S., Godfrey, M.H., Lopez-Jurado, L.F., Lopez-Suarez, P., Merino, S.E., Varo-Cruz, N. and Godley, B.J. 2006. Phenotypically linked dichotomy in sea turtle foraging requires multiple conservation approaches. *Current Biology*, 16(10), pp.990-995. <https://doi.org/10.1016/j.cub.2006.03.063>
- Hawkes, L.A., Tomás, J., Revuelta, O., León, Y.M., Blumenthal, J.M., Broderick, A.C., Fish, M., Raga, J.A., Witt, M.J. and Godley, B.J. 2012. Migratory patterns in hawksbill turtles described by satellite tracking. *Marine Ecology Progress Series*, 461, pp.223-232. <https://doi.org/10.3354/meps09778>
- Hays, G.C., Broderick, A.C., Glen, F. and Godley, B.J. 2002. Change in body mass associated with long-term fasting in a marine reptile: the case of green turtles (*Chelonia mydas*) at Ascension Island. *Canadian Journal of Zoology*, 80(7), pp.1299-1302. <https://doi.org/10.1139/z02-110>
- Hays, G.C. 2008. Sea turtles: a review of some key recent discoveries and remaining questions. *Journal of Experimental Marine Biology and Ecology*, 356(1-2), pp.1-7. <https://doi.org/10.1016/j.jembe.2007.12.016>
- Haywood, J.C., Fuller, W.J., Godley, B.J., Margaritoulis, D., Shutler, J.D., Snape, R.T., Widdicombe, S., Zbinden, J.A. and Broderick, A.C. 2020. Spatial ecology of loggerhead turtles: Insights from stable isotope markers and satellite telemetry. *Diversity and Distributions*, 26(3), pp.368-381. <https://doi.org/10.1111/ddi.13023>
- Hoenner, X., Whiting, S.D., Hindell, M.A. and McMahon, C.R. 2012. Enhancing the use of Argos satellite data for home range and long distance migration studies of marine animals. *PLoS One*, 7(7), pp.e40713. <https://doi.org/10.1371/journal.pone.0040713>
- Hochscheid, S., Maffucci, F., Abella, E., Bradai, M.N., Camedda, A., Carreras, C., Claro, F., de Lucia, G.A., Jribi, I., Mancusi, C. and Marco, A. 2022. Nesting range expansion of loggerhead turtles in the Mediterranean: phenology, spatial distribution, and conservation implications. *Global Ecology and Conservation*, 38, pp.e02194. <https://doi.org/10.1016/j.gecco.2022.e02194>
- Horne, J.S., Garton, E.O., Krone, S.M. and Lewis, J.S. 2007. Analyzing animal movements using Brownian bridges. *Ecology*, 88(9), pp.2354-2363. <https://doi.org/10.1890/06-0957.1>
- Jackson, A.L., Inger, R., Parnell, A.C. and Bearhop, S. 2011. Comparing isotopic niche widths among and within communities: SIBER Stable Isotope Bayesian Ellipses

- in R. *Journal of Animal Ecology*, 80(3), pp.595-602. <https://doi.org/10.1111/j.1365-2656.2011.01806.x>
- Jonsen, I.D., Flemming, J.M. and Myers, R.A. 2005. Robust state–space modeling of animal movement data. *Ecology*, 86(11), pp.2874-2880. <https://doi.org/10.1890/04-1852>
- Jonsen, I.D., Myers, R.A. and James, M.C. 2007. Identifying leatherback turtle foraging behaviour from satellite telemetry using a switching state-space model. *Marine Ecology Progress Series*, 337, pp.255-264. <https://doi.org/10.3354/meps337255>
- Jonsen, I.D., Basson, M., Bestley, S., Bravington, M.V., Patterson, T.A., Pedersen, M.W., Thomson, R., Thygesen, U.H. and Wotherspoon, S.J. 2013. State-space models for bio-loggers: A methodological road map. *Deep Sea Research Part II: Topical Studies in Oceanography*, 88, pp.34-46. <https://doi.org/10.1016/j.dsr2.2012.07.008>
- Jonsen, I.D. 2016. Joint estimation over multiple individuals improves behavioural state inference from animal movement data. *Scientific reports*, 6(1), pp.20625. <https://doi.org/10.1038/srep20625>
- Jribi, I. and Bradai, M. N. 2014. Sex ratio estimations of loggerhead sea turtle hatchlings at Kuriat Islands, Tunisia: can minor nesting sites contribute to compensate globally female-biased sex ratio? *The Scientific World Journal*, 2014, pp.1-8. <https://doi.org/10.1155/2014/419410>
- Kortsch, S., Primicerio, R., Fossheim, M., Dolgov, A.V., Aschan, M. 2015. Climate change alters the structure of arctic marine food webs due to poleward shifts of boreal generalists. *Proceedings of the Royal Society B: Biological Sciences*, 282(1814), pp.20151546. <https://doi.org/10.1098/rspb.2015.1546>
- Laurent, L., Nouira, S., Jeudy De Grissac, A. and Bradai, M.N. 1990. Les tortues marines de Tunisie: Premières données. *Bulletin de la Société Herpétologique de France*, 53, pp.1-17.
- La Sorte, F.A. and Thompson III, F.R. 2007. Poleward shifts in winter ranges of North American birds. *Ecology*, 88(7), pp.1803-1812. <https://doi.org/10.1890/06-1072.1>
- Lee, P.L., Luschi, P. and Hays, G.C. 2007. Detecting female precise natal philopatry in green turtles using assignment methods. *Molecular ecology*, 16(1), pp.61-74. <https://doi.org/10.1111/j.1365-294X.2006.03115.x>
- Lohmann, K.J., Putman, N.F. and Lohmann, C.M. 2008. Geomagnetic imprinting: A unifying hypothesis of long-distance natal homing in salmon and sea turtles. *Proceedings of the National Academy of Sciences*, 105(49), pp.19096-19101. <https://doi.org/10.1073/pnas.080185910>
- Lomolino, M.V., Riddle, B.R., Whittaker, R.J. and Brown, J.H. 2010. Biogeography. Sunderland, MA: Sinauer Associates, 385, pp.878.
- Lydersen, C., Vacquié-Garcia, J., Heide-Jørgensen, M.P., Øien, N., Guinet, C. and Kovacs, K.M. 2020. Autumn movements of fin whales (*Balaenoptera physalus*) from Svalbard, Norway, revealed by satellite tracking. *Scientific Reports*, 10(1), pp.16966. <https://doi.org/10.1038/s41598-020-73996-z>
- Mancino, C., Canestrelli, D. and Mariorano, L. 2022. Going west: Range expansion for loggerhead sea turtles in the Mediterranean Sea under climate change. *Global Ecology and Conservation*, 38, pp.e02264. <https://doi.org/10.1016/j.gecco.2022.e02264>
- Mansfield, K.L., Wyneken, J., Porter, W.P. and Luo, J. 2014. First satellite tracks of neonate sea turtles redefine the ‘lost years’ oceanic niche. *Proceedings of the*

- Royal Society B: Biological Sciences*, 281(1781), pp.20133039. <https://doi.org/10.1098/rspb.2013.3039>
- Miller, J.D. 1997. Reproduction in sea turtles. In: *The Biology of Sea Turtles*, Lutz, P.L. and Musick, J.A. (Eds), *Volume I*, pp.51–81.
- Mingozzi, T., Masciari, G., Paolillo, G., Pisani, B., Russo, M. and Massolo, A. 2008. Discovery of a regular nesting area of loggerhead turtle *Caretta caretta* in southern Italy: a new perspective for national conservation. *Biodiversity and Conservation in Europe*, 7, pp.277-299. [https://doi.org/10.1007/978-1-4020-6865-2\\_20](https://doi.org/10.1007/978-1-4020-6865-2_20)
- Mghili, B., Benhardouze, W., Akissou, M., Tiwari, M. 2023. Sea turtle strandings along the Northwestern Moroccan coast: Spatio-temporal distribution and main threats. *Ocean and Coastal Management*, 237, pp.106539. <https://doi.org/10.1016/j.ocecoaman.2023.106539>
- Nehlich, O. and Richards, M.P. 2009. Establishing collagen quality criteria for sulphur isotope analysis of archaeological bone collagen. *Archaeological and Anthropological Sciences*, 1, pp.59-75. <https://doi.org/10.1007/s12520-009-0003-6>
- Peterson, B.J. 1999. Stable isotopes as tracers of organic matter input and transfer in benthic food webs: a review. *Acta oecologica*, 20(4), pp.479-487. [https://doi.org/10.1016/S1146-609X\(99\)00120-4](https://doi.org/10.1016/S1146-609X(99)00120-4)
- Pike, D.A. 2013. Climate influences the global distribution of sea turtle nesting. *Global Ecology and Biogeography*, 22(5), pp.555–566. <https://doi.org/10.1111/geb.12025>
- Piovano, S., Clusa, M., Carreras, C., Giacoma, C., Pascual, M. and Cardona, L. 2011. Different growth rates between loggerhead sea turtles (*Caretta caretta*) of Mediterranean and Atlantic origin in the Mediterranean Sea. *Marine Biology*, 158, pp.2577-2587. <https://doi.org/10.1007/s00227-011-1759-7>
- R Core Team. 2019. R: A language and environment for statistical computing. R Foundation for Statistical Computing, Vienna, Austria. <https://www.R-project.org/>
- Rees, A.F., Al Saady, S., Broderick, A.C., Coyne, M.S., Papathanasopoulou, N. and Godley, B.J. 2010. Behavioural polymorphism in one of the world's largest populations of loggerhead sea turtles *Caretta caretta*. *Marine Ecology Progress Series*, 418, pp.201-212. <https://doi.org/10.3354/meps08767>
- Rees, A.F., Theodorou, P., Margaritoulis, D. 2020. Clutch frequency for loggerhead turtles (*Caretta caretta*) nesting in Kyparissia Bay, Greece. *Herpetological Conservation and Biodiversity*, 15, pp.131-138.
- Reich, K.J., Bjorndal, K.A. and Martínez del Río, C. 2008. Effects of growth and tissue type on the kinetics of <sup>13</sup>C and <sup>15</sup>N incorporation in a rapidly growing ectotherm. *Oecologia*, 155, pp.651-663. <https://doi.org/10.1007/s00442-007-0949-y>
- Revelles, M., Carreras, C., Cardona, L., Marco, A., Bentivegna, F., Castillo, J.J., De Martino, G., Mons, J.L., Smith, M.B., Rico, C. and Pascual, M. 2007a. Evidence for an asymmetrical size exchange of loggerhead sea turtles between the Mediterranean and the Atlantic through the Straits of Gibraltar. *Journal of Experimental Marine Biology and Ecology*, 349(2), pp.261-271. <https://doi.org/10.1016/j.jembe.2007.05.018>
- Revelles, M., Cardona, L., Aguilar, A., San Félix, M. and Fernández, G. 2007b. Habitat use by immature loggerhead sea turtles in the Algerian Basin (western

- Mediterranean): swimming behaviour, seasonality and dispersal pattern. *Marine Biology*, 151, pp.1501-1515. <https://doi.org/10.1007/s00227-006-0602-z>
- Revelles, M., Isern-Fontanet, J., Cardona, L., San Félix, M., Carreras, C. and Aguilar, A. 2007c. Mesoscale eddies, surface circulation and the scale of habitat selection by immature loggerhead sea turtles. *Journal of Experimental Marine Biology and Ecology*, 347(1-2), pp.41-57. <https://doi.org/10.1016/j.jembe.2007.03.013>
- Revelles, M., Camiñas, J.A., Cardona, L., Parga, M.L., Tomás, J., Aguilar, A., Alegre, F., Raga, A., Bertolero, A., Oliver, G. 2008. Tagging reveals limited exchange of immature loggerhead sea turtles (*Caretta caretta*) between regions in the western Mediterranean. *Sci. Mar.* 72(3), pp.511-518. <http://hdl.handle.net/10550/2336>
- Scott, R., March, R. and Hays, G.C. 2014. Ontogeny of long distance migration. *Ecology*, 95(10), pp.2840-2850. <https://doi.org/10.1890/13-2164.1>
- Shaver, D.J., Frandsen, H.R., George, J.A. and Gredzens, C. 2020. Green Turtle (*Chelonia mydas*) nesting underscores the importance of protected areas in the Northwestern Gulf of Mexico. *Frontiers in Marine Science*, 7, pp.673. <https://doi.org/10.3389/fmars.2020.00673>
- Santidrián Tomillo, P., Tomás, J., Marco, A., Panagopoulou, A. and Tavecchia, G. 2022. Environmental changes in the Mediterranean Sea could facilitate the western expansion of loggerhead turtles. *Marine Ecology Progress Series*, SHIFtav1, pp.1-17. <https://doi.org/10.3354/meps14149>
- Schofield, G., Scott, R., Dimadi, A., Fossette, S., Katselidis, K.A., Koutsoubas, D., Lilley, M.K., Pantis, J.D., Karagouni, A.D. and Hays, G.C. 2013a. Evidence-based marine protected area planning for a highly mobile endangered marine vertebrate. *Biological Conservation*, 161, pp.101-109. <https://doi.org/10.1016/j.biocon.2013.03.004>
- Schofield, G., Dimadi, A., Fossette, S., Katselidis, K.A., Koutsoubas, D., Lilley, M.K., Luckman, A., Pantis, J.D., Karagouni, A.D. and Hays, G.C. 2013b. Satellite tracking large numbers of individuals to infer population level dispersal and core areas for the protection of an endangered species. *Diversity and Distributions*, 19(7), pp.834-844. <https://doi.org/10.1111/ddi.12077>
- Stewart, K.R., Martin, K.J., Johnson, C., Desjardin, N., Eckert, S.A. and Crowder, L.B. 2014. Increased nesting, good survival and variable site fidelity for leatherback turtles in Florida, USA. *Biological conservation*, 176, pp.117-125. <https://doi.org/10.1016/j.biocon.2014.05.008>
- Swimmer, Y., Gutierrez, A., Bigelow, K., Barceló, C., Schroeder, B., Keene, K., Shattenkirk, K. and Foster, D.G. 2017. Sea turtle bycatch mitigation in US longline fisheries. *Frontiers in Marine Science*, 4, pp.260. <https://doi.org/10.3389/fmars.2017.00260>
- Taconet, M., Kroodsma, D., and Fernandes, J.A. 2019. Global Atlas of AIS-based fishing activity - Challenges and opportunities. Rome, FAO. (also available at [www.fao.org/3/ca7012en/ca7012en.pdf](http://www.fao.org/3/ca7012en/ca7012en.pdf))
- Tomás, J., Gazo, M., Álvarez, C., Gozalbes, P., Perdiguero, D., Raga, J.A. and Alegre, F. 2008. Is the Spanish coast within the regular nesting range of the Mediterranean loggerhead sea turtle (*Caretta caretta*)?. *Journal of the Marine Biological Association of the United Kingdom*, 88(7), pp.1509-1512. <https://doi.org/10.1017/S0025315408001768>
- Turner Tomaszewicz, C.N., Seminoff, J.A., Peckham, S.H., Avens, L. and Kurle, C.M. 2017. Intrapopulation variability in the timing of ontogenetic habitat shifts in sea turtles revealed using  $\delta^{15}\text{N}$  values from bone growth rings. *Journal of Animal Ecology*, 86(3), pp.694-704. <https://doi.org/10.1111/1365-2656.12618>



- Tucker, A.D. 2010. Nest site fidelity and clutch frequency of loggerhead turtles are better elucidated by satellite telemetry than by nocturnal tagging efforts: implications for stock estimation. *Journal of Experimental Marine Biology and Ecology*, 383(1), pp.48-55. <https://doi.org/10.1016/j.jembe.2009.11.009>
- Wald, A. and Wolfowitz, J. 1943. An exact test for randomness in the non-parametric case based on serial correlation. *The Annals of Mathematical Statistics*, 14(4), pp.378-388. <https://doi.org/10.1214/aoms/1177731358>
- Wallace, B., DiMatteo, A.D., Hurley, B.J., Finkbein, E.M., Bolten, A.B., Chaloupka, M.Y., Hutchison, B.J., Abreu-Grobois, F.A., Amorocho, D., Bjorndal, K.A., Bourjea, J., Bowe, B.W., Briseño Dueñas, R., Casale, P., Choudhury, B.C., Costa, A., Dutton, P.H., Fallabrino, A., Girard, A., Girondot, M., Godfrey, M.H., Hamann, M., López-Mendilaharsu, M., Marcovaldi, M.A., Mortimer, J.A., Musick, J.A., Nel, R., Pilcher, N.J., Seminoff, J.A., Troëng, S., Witherington, B. and Mast, R. B. 2010. Regional management units for marine turtles: a novel framework for prioritizing conservation and research across multiple scales. *PLoS ONE*, 5(12), pp.e15465. <https://doi.org/10.1371/journal.pone.0015465>
- Zbinden, J.A., Aebischer, A., Margaritoulis, D. and Arlettaz, R. 2007. Insights into the management of sea turtle interesting area through satellite telemetry. *Biological Conservation*, 137(1), pp.157-162. <https://doi.org/10.1016/j.biocon.2007.01.022>
- Zbinden, J.A., Aebischer, A., Margaritoulis, D. and Arlettaz, R. 2008. Important areas at sea for adult loggerhead sea turtles in the Mediterranean Sea: satellite tracking corroborates findings from potentially biased sources. *Marine Biology*, 153, pp.899-906. <https://doi.org/10.1007/s00227-007-0862-2>
- Zbinden, J.A., Bearhop, S., Bradshaw, P., Gill, B., Margaritoulis, D., Newton, J. and Godley, B.J. 2011. Migratory dichotomy and associated phenotypic variation in marine turtles revealed by satellite tracking and stable isotope analysis. *Marine Ecology Progress Series*, 421, pp.291-302. <https://doi.org/10.3354/meps08871>



## **3.5. Summary of Results**







### 3.5.1. Community level characterization of the isotopic niche

Significant differences were found among marine mammal species from Río de la Plata estuary for the  $\delta^{13}\text{C}$ ,  $\delta^{15}\text{N}$ ,  $\delta^{34}\text{S}$  and  $\delta^{18}\text{O}$  values, which allowed to use different combinations of these four intrinsic tracers to characterize the isotopic niche of the considered species. On one hand, significant differences were found between females and males for South American sea lions and South American fur seals, and hence, they were analysed separately. However, the constant partial overlap between sexes of the same species in all the considered isospaces suggested some similarities between their isotopic niches. In addition, franciscana dolphins and Burmeister's porpoises overlapped in their  $\delta^{13}\text{C}$ ,  $\delta^{15}\text{N}$  and  $\delta^{34}\text{S}$  values but largely differed in their  $\delta^{18}\text{O}$  values, with the porpoises showing significantly higher values which suggests the use of saltier waters. On the other hand, the isotopic niche of false killer whales overlapped with that of most of the considered species, particularly with South American fur seals (both females and males) and franciscana dolphins. Furthermore, the wide range of values found for this species suggested the possible existence of two ecotypes of false killer whales using isotopically different regions within the estuary. Finally, Fraser's dolphins presented the highest  $\delta^{18}\text{O}$  and  $\delta^{34}\text{S}$  values, the lowest  $\delta^{13}\text{C}$  and  $\delta^{15}\text{N}$  values and only showed a small but constant overlap in isotopic niche with that of false killer whales. In this case, adding the  $\delta^{34}\text{S}$  and  $\delta^{18}\text{O}$  values to those of  $\delta^{13}\text{C}$  and  $\delta^{15}\text{N}$  improved the characterization of niche partitioning among the marine mammal species from Río de la Plata.

In Mauritanian waters, significant differences were found among marine mammal species for the  $\delta^{13}\text{C}$ ,  $\delta^{15}\text{N}$  and  $\delta^{18}\text{O}$  values but not for the  $\delta^{34}\text{S}$  values. However, the latter allowed to identify high levels of individual variability for those species found nearshore, such as bottlenose dolphins, harbour porpoises, Mediterranean monk seals, and Atlantic humpback dolphins. The largest overlaps in isotopic niches were between bottlenose dolphins, harbour porpoises and long-finned pilot whales, with the former encompassing most of the area covered by the latter two. In fact, the wide range of values found for bottlenose dolphins indicated the existence of at least two ecotypes of this species in the area. On the other hand, common dolphins and Atlantic spotted dolphins showed a partial overlap for the  $\delta^{13}\text{C}$  and  $\delta^{15}\text{N}$  values but largely differed in the  $\delta^{18}\text{O}$  values. The same was true for Mediterranean monk seals, bottlenose dolphins and Atlantic humpback dolphins, with the latter showing the highest  $\delta^{18}\text{O}$  values among the considered species.



In this case, including the  $\delta^{18}\text{O}$  values allowed for a better definition of the isotopic niche partitioning among marine mammal species in Mauritanian waters, whereas the  $\delta^{34}\text{S}$  values allowed to identify intraspecific differences among each considered population.

### 3.5.2. Species level characterization of the isotopic niche

Differences in the habitat use and foraging ecology among loggerhead turtle individuals were detected by comparing the stable isotope ratios in their bone and skin tissues with those estimated for different regions of the Mediterranean Sea.

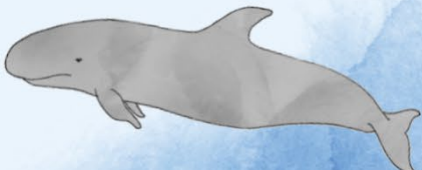
Changes in the isotopic niche of juvenile loggerhead turtles of Northwestern Atlantic origin found at the western Mediterranean Sea were analyzed using the  $\delta^{13}\text{C}$ ,  $\delta^{15}\text{N}$  and  $\delta^{18}\text{O}$  values of different incremental bone layers. First, the layers corresponding to the very first years of life were missing in all the analysed individuals due to the endosteal resorption of the medullar bone; thus, sampled incremental layers corresponded to ages 3 to 15 years old. Second, a broad variability in the  $\delta^{18}\text{O}$  values was found both among incremental layers of the same individual and among individuals, finding a negative and linear correlation between these values and the age. Here, turtles younger than nine years old showed more scattered  $\delta^{18}\text{O}$  values, which suggested the movement between isotopically distinct water masses with no consistent temporal pattern, whereas turtles aged ten years and older were clustered around a lower mean  $\delta^{18}\text{O}$  value. Furthermore, most loggerhead turtles seemed to move following different patterns, either from  $^{18}\text{O}$ -enriched to  $^{18}\text{O}$ -depleted waters or vice versa. However, seven turtles showed no significant changes among incremental layers during the analysed period, including the two oldest turtles of the study that showed similarly low  $\delta^{18}\text{O}$  values for their last seven and nine years of life, respectively. Finally, five individuals showed differences between incremental layers that were larger than the estimated difference for the study area, hence suggesting the influence of other factors over the  $\delta^{18}\text{O}$  values of the bone of these loggerhead turtles. On the other hand, no significant correlation was found between the  $\delta^{13}\text{C}$  values and the age of these individuals, nor between the  $\delta^{15}\text{N}$  values and the age, and differences among incremental layers of the same individual for these two intrinsic tracers did not show significant changes in carbon source or trophic position, respectively, throughout the analysed periods. Nevertheless, when studying the  $\delta^{13}\text{C}$  -  $\delta^{15}\text{N}$  isospace, the standard ellipse area (SEAc) decreased significantly and linearly with the age,



showing large overlaps among all the considered age classes with the standard ellipses of the younger ages encompassing those of older ages.

Lastly, differences in the  $\delta^{13}\text{C}$  and  $\delta^{15}\text{N}$  values were found between juvenile loggerhead turtles stranded along the Iberian Peninsula – assumed to feed neritically along the continental shelf – and those stranded in the Balearic Islands – assumed to feed oceanically at the Algerian Basin. Here, turtles found at the Iberian Peninsula showed lower  $\delta^{13}\text{C}$  and  $\delta^{15}\text{N}$  values compared to those from the Balearic Islands, with only a small overlap in the respective standard ellipses. In contrast, no significant differences were found for the  $\delta^{34}\text{S}$  values of both groups. Based on this, the isotopic niche of female loggerhead turtles that had recently nested in Spanish Mediterranean beaches was closer to that of turtles from the Balearic Islands, thus suggesting that they had foraged mostly at the Algerian Basin. The only exception were two nesting females that were highly enriched in  $^{13}\text{C}$  and highly depleted in  $^{34}\text{S}$ , suggesting the use of a different foraging region during the months prior to nesting.





## **Chapter 4: General Discussion**





## 4. General discussion

Despite the difficulties to properly estimate the trophic discrimination factors between diet and consumer, the stable isotope analysis offers an invaluable opportunity to study distinct aspects of the foraging and spatial ecology of large marine vertebrates. This technique has provided information on a variety of topics including diet and trophic niche, site fidelity, migratory movements, colonisation processes, ontogenetic shifts, intra and interspecific differences, as well as regional variations among species and populations, for both marine mammals and sea turtles (e.g., Borrell et al., 2012; Turner Tomaszewicz et al., 2017b; Drago et al., 2020; Haywood et al., 2020b). In addition, results derived from these studies have been used to inform about local threats and conservation strategies for several marine species and ecosystems worldwide (Newsome et al., 2010; Haywood et al., 2019; Abalo-Morla et al., 2022a).

One of the great advantages of the stable isotope analysis is that it can be complemented by other research techniques. The stable isotopes technique is less precise to geographically locate the studied individuals, but it is a great tool to analyse the resource partitioning and behavioural changes of species at a population and community levels. In addition, these analyses are quite cheap and can be carried out in tissues taken from both alive and dead individuals, which allows to have a larger sample size compared to other techniques that require the capture and release of live animals. For this reason, satellite telemetry data can directly complement and confirm the information on habitat use inferred by the isotopic values with high-resolution tracking of animal movements at an individual level (Newsome et al., 2010). At the same time, the combination of these two techniques can help to overcome the low sample size often associated with the study of large marine vertebrates, as shown in subchapter 3.4. Furthermore, several studies (e.g., Newsome et al., 2010; Bradshaw et al., 2017; Haywood et al., 2020a) have highlighted the importance of combining satellite telemetry with stable isotope analysis and have even encouraged to take a non-invasive sample of tissue from satellite-tracked individuals, when possible, to better understand the spatial ecology of large marine vertebrates both at a species and population level. Other complementary techniques that can be used along with the stable isotopes are genetic analysis to study the connectivity between foraging grounds and rookeries (e.g., Medeiros et al., 2019; Cani et al., 2025 in subchapter 3.3), stomach content analysis to identify ingested taxa (e.g., McCluskey et al., 2021), fatty



acids to analyse the food web structure (e.g., Cardona et al., 2015), the analysis of organic contaminants and trace metals to study the trophic transfer and biomagnification in a population (e.g., Cipro et al., 2012; Pinzone et al., 2019), and direct observations to confirm a species distribution and ethology (e.g., Zabala et al., 2013; Cani et al., 2024 in subchapter 3.2).

Overall, it is important to consider the possible limitations associated with the use of stable isotopes as intrinsic biogeochemical tracers of large marine vertebrates. Nevertheless, it continues to be one of the best approaches in the field of marine ecology, especially when involving elusive species and life stages that are often hard to encounter in the wild. Historically, the  $\delta^{13}\text{C}$  and  $\delta^{15}\text{N}$  ratio have been the most commonly used tracers to study the trophic ecology of marine individuals, but the inclusion of other chemical elements has increased in isotopic research during the last decades, especially when studying the habitat use and migratory patterns of species and individuals (Newsome et al., 2010). Furthermore, the advantages of the inclusion of additional isotopic tracers depend largely on the ecosystem and the species analysed, as discussed in the following subsections.

#### **4.1. Resource partitioning and habitat use**

A common assumption when studying the isotopic niche partitioning among species or individuals is that considering a larger number of habitat tracers will improve the resolution of the analysis. However, as highlighted throughout this study, resolution can only improve under certain conditions. This thesis shows different scenarios where the  $\delta^{13}\text{C}$ ,  $\delta^{15}\text{N}$ ,  $\delta^{34}\text{S}$  and  $\delta^{18}\text{O}$  values can be applied to characterize the habitat use and trophic ecology of large marine vertebrates, both at a community and population level. In addition, those cases where the use of a specific tracer rendered no significant results are discussed and explained, according to available information on the isotopic biogeochemistry of each chemical element, the analysed tissue and the composition of each ecosystem.

Based on the results exposed in chapter 3, one of the most important factors when comparing the isotopic niche of consumers is the presence of steep environmental gradients at the right spatial scale, which must be in accordance with the scale of movement of the considered species and the time period integrated by the analysed tissue. Environmental isotopic gradients result from the interplay between the physicochemical



conditions of the water masses and the metabolic pathways used by the dominant primary producers in each region; hence, they can only occur if different conditions exist within the same study area. Certainly, the stable isotope ratio of each chemical element informs about a specific dimension of the ecosystem and, together, they can show new qualities of the habitat use and trophic ecology of a species or individual, although their interpretation can differ among ecosystems.

In general, a horizontal gradient of isotopic variation can be found between inshore/coastal and offshore/oceanic waters, as well as a vertical gradient between benthic and pelagic regions. The main source of these variations is often the influence of terrestrial inputs of freshwater and particulate organic matter (POM), which bring water molecules and plant detritus with distinct isotopic signatures into coastal areas and also increases the concentration of POM within the water column, decreasing light availability and promoting the formation of anoxic sediments (Peterson et al., 1985; Gat, 1996). Most terrestrial plants with a C3 metabolism are generally  $^{13}\text{C}$ -depleted and use the  $^{34}\text{S}$ -depleted sulphides ( $\text{S}^{2-}$ ) formed under anaerobic conditions in the soil as the primary source of sulphur, and the  $^{18}\text{O}$ -depleted molecules from precipitation as the primary source of water (Peterson and Howarth, 1987; Gat, 1996; Emerson and Hedges, 2008). Furthermore, river water also originates from precipitation, and it often drags  $^{15}\text{N}$ -enriched sewage from nearby cities into coastal areas (Gat, 1996; McClelland and Valiela, 1998). Therefore, river plumes flowing into coastal waters are characterized by POM with low  $\delta^{13}\text{C}$ ,  $\delta^{34}\text{S}$  and  $\delta^{18}\text{O}$  values and high  $\delta^{15}\text{N}$  values. Another differential aspect of coastal areas is the presence of rooted primary producers that often colonize hypoxic and anaerobic sediments (Peterson et al., 1985) and use predominantly the dissolved  $\text{HCO}_3^-$  as their primary source of carbon because the high productivity of coastal systems often limits the dissolved  $\text{CO}_2$  (Newsome et al., 2010; Reinfelder, 2011); thus, they can represent a major source of plant detritus with high  $\delta^{13}\text{C}$  and low  $\delta^{34}\text{S}$  values into the marine food web (Peterson and Howarth, 1987; Emerson and Hedges, 2008).

In contrast, the main primary producer found in marine pelagic waters is phytoplankton, which typically has a C3 metabolism but is more likely to use the dissolved  $\text{CO}_2$  as the primary source of carbon, unless its concentration becomes limiting (Finlay et al., 1999; Falkowski and Raven, 2007; Carlier et al., 2015). In addition, the well-mixed and highly oxidized water column allows the formation of  $^{34}\text{S}$ -enriched sulphates ( $\text{SO}_4^{2-}$ ), which represent the primary source of sulphur in the open ocean



(Peterson et al., 1985; Ben-David and Flaherty, 2012), and the evaporation of surface waters produces an increment in the concentration of water molecules carrying the heavier  $^{18}\text{O}$  isotope (Gat, 1996). Therefore, the organic matter produced by oceanic phytoplankton is characterized by low  $\delta^{13}\text{C}$  and  $\delta^{15}\text{N}$  values and high  $\delta^{34}\text{S}$  and  $\delta^{18}\text{O}$  values. However, as stated above, certain processes such as phytoplankton blooms can limit the concentration of dissolved  $\text{CO}_2$  and alter the isotopic values in pelagic food webs, since the composition of upwelling-derived phytoplankton often differs from that of oceanic phytoplankton (Carlier et al., 2015). For instance, the nutrient input into surface waters during an upwelling event drives primary productivity and commonly favours the growth of diatom species with a C4-like metabolism, resulting in an increase of the  $\delta^{13}\text{C}$  values of phytoplankton (Carlier et al., 2015; Ferreira et al., 2020; Launay et al., 2020). It should be noted that part of the organic matter produced by phytoplankton during these upwelling events is released back into the water as  $^{15}\text{N}$ -depleted dissolved organic matter (DOM), which normally enters directly into the microbial loop and does not influence the isotopic values of consumers in the classic food web analysed in this thesis (Post, 2002; Pontiller et al., 2022).

Meanwhile, it is also important to identify the processes that cause each environmental isotopic gradient, since they can explain the observed relationship – or lack of – among the different chemical elements. For instance, both the  $\delta^{34}\text{S}$  and  $\delta^{18}\text{O}$  gradients can be generated by a constant input of terrestrial POM and freshwater into coastal areas (Gat, 1996; Peterson, 1999), in which case they can show a similar variation within an ecosystem at a broad spatial scale. However, these two gradients can be uncoupled if the  $\delta^{18}\text{O}$  gradient is generated instead by an intense evaporation of surface waters due to high environmental temperatures, or if the primary source of variation for the  $\delta^{34}\text{S}$  values is the presence of benthic primary producers growing in anoxic sediments nearshore (Peterson, 1999; Sharp, 2017). Similar patterns can be seen between the  $\delta^{13}\text{C}$  and  $\delta^{34}\text{S}$  gradients, since they can both originate due to the input of terrestrial plant detritus into coastal areas, but the presence of rooted plants using anoxic sediments, primary producers with C4 and CAM-like metabolisms, as well as the influence of an upwelling event can alter these two gradients in different degrees, serving as alternative sources of variability for the  $\delta^{13}\text{C}$  and  $\delta^{34}\text{S}$  values within an ecosystem. Lastly, the input of sewage into coastal areas often causes an increase of  $\delta^{15}\text{N}$  values in species and



individuals feeding nearby (McClelland and Valiela, 1998; Botto et al., 2011), thus altering the expected increase of  $\delta^{15}\text{N}$  values with each trophic position.

#### **4.2. Characterization of the isotopic niche in a marine mammal community**

The two ecosystems analysed at a community level showed different degrees of significance for each of the biogeochemical tracers given the origin, strength and distribution of the environmental isotopic gradients in each case. The isotopic gradients in Río de la Plata (subchapter 3.1) are mostly generated by (1) the influence of the river input, which brings  $^{13}\text{C}$ - and  $^{34}\text{S}$ -depleted terrestrial detritus and  $^{18}\text{O}$ -depleted freshwater nearshore, (2) the presence of  $^{13}\text{C}$ -enriched and  $^{34}\text{S}$ -depleted salt marsh detritus in the middle reaches of the estuary, and (3) the  $^{13}\text{C}$ -depleted and  $^{34}\text{S}$ -enriched phytoplankton and  $^{18}\text{O}$ -enriched marine waters offshore (Peterson and Howarth, 1987; Guerrero et al., 1997; Connolly et al., 2004; Botto et al., 2011; Belem et al., 2019). Here, the use of the different areas along the estuary basin by the seven marine mammal species analysed was characterized based on the isotopic niche obtained with the combination of the mean  $\delta^{13}\text{C}$ ,  $\delta^{15}\text{N}$ ,  $\delta^{34}\text{S}$  and  $\delta^{18}\text{O}$  values of their bone tissue and the distribution of the environmental isotopic gradients explained above.

In this context, the estuary was divided into three zones according to the predominant plant detritus and salinity values (Figure 2.1, bottom panel; Guerrero et al., 1997; Botto et al., 2011). First, the inner estuary is the zone with the highest influence of river runoff and thus high turbidity and low light availability; it is characterized by a high abundance of terrestrial and freshwater marsh detritus with low  $\delta^{13}\text{C}$  and  $\delta^{34}\text{S}$  values and freshwater with low  $\delta^{18}\text{O}$  values. None of the studied marine mammal species was found to feed in this zone. Second, the estuarine or mixohaline zone has a large influence of salt marsh detritus from nearby coastal areas, characterized by high  $\delta^{13}\text{C}$  and low  $\delta^{34}\text{S}$  values. In this region, the turbidity is lower but the light is still limiting, and a salt wedge is formed due to the partial mixing of the freshwater from the river input at the surface and the marine water entering the estuary at the bottom (Guerrero et al., 1997; Acha et al., 2008). Hence, this zone is characterized by low  $\delta^{18}\text{O}$  values at the top water layers and higher  $\delta^{18}\text{O}$  values at the bottom layers, and it seems to be a highly used area by most of the considered species. Bottlenose dolphins, female and male South American sea lions and female South American fur seals showed isotopic values consistent with the use of



the lower salinity areas of this estuarine zone, although the latter two probably have a more pelagic diet given the lower  $\delta^{13}\text{C}$  values. On the contrary, the low  $\delta^{34}\text{S}$  values of franciscana dolphins and Burmeister's porpoises indicate the influence of terrestrial or marsh plant POM in their diet, whereas the higher  $\delta^{18}\text{O}$  values suggest the use of the marine waters under the salt wedge. Lastly, the marine zone has a greater light availability and allows phytoplankton to become the main carbon source (Botto et al., 2011), which combined with the saltier marine waters and a well-mixed water column result in low  $\delta^{13}\text{C}$  and high  $\delta^{34}\text{S}$  and  $\delta^{18}\text{O}$  values. Only one species, the Fraser's dolphin, presented this combination of values, thus confirming the known offshore habits of this species (Botta et al., 2012). Nevertheless, male South American fur seals and false killer whales showed values in between those expected for the estuarine and the marine zones, suggesting the use of both areas as feeding grounds. However, the wide range of individual isotopic values of false killer whales could also indicate the existence of two ecological groups (ecotypes) of the species in Río de la Plata, one coastal and one oceanic, which was also proposed by Valdivia et al. (2024). Regarding the  $\delta^{15}\text{N}$  values, the Fraser's dolphin showed significantly lower values compared to the other six species, whereas male and female South American sea lions, franciscana dolphins and Burmeister's porpoises showed significantly higher  $\delta^{15}\text{N}$  values. However, the large differences found among species for this tracer are likely an artefact of the sewage input into the estuary (Nagy et al., 2002; Botto et al., 2011).

Meanwhile, the isotopic gradients along the Mauritanian coast (subchapter 3.2) are generated by different processes. The saltier Canary Current brings  $^{18}\text{O}$ -enriched waters from the north, whereas the less salty Mauritanian Current brings  $^{18}\text{O}$ -depleted waters from the south (Peña-Izquierdo et al., 2012; Conroy et al., 2014; Belem et al., 2019). In both cases, the vertical mixing caused by the almost constant upwelling events produces homogenous  $\delta^{34}\text{S}$  values within the water column, both inshore and offshore (Zopfi et al., 2008). Therefore, the only available source of  $^{34}\text{S}$ -depleted values in this area seem to be the scattered patches of benthic primary producers growing in anoxic sediments nearshore (Peterson, 1999; Zenk et al., 1991; Peña-Izquierdo et al., 2012; Pottier et al., 2021). In addition, upwelling-derived phytoplankton is  $^{13}\text{C}$ -enriched compared to oceanic phytoplankton, which allows to identify these two sources of carbon among consumers in the area (Carlier et al., 2015). Furthermore, the extremely high temperatures and shallow seas inside the Parc National du Banc d'Arguin (PNBA; Figure



2.1, right panel) produce highly  $^{18}\text{O}$ -enriched waters and favour the presence of  $^{13}\text{C}$ -enriched benthic primary producers (e.g., seagrasses and mangroves) with variable  $\delta^{34}\text{S}$  values depending on the local redox potential of the sediments where they grow (Conroy et al., 2014; Pottier et al., 2021). In this case, the influence of the two currents with contrasting salinities and the extreme temperatures inside the PNBA allowed to find differences among marine mammal species through the  $\delta^{13}\text{C}$ ,  $\delta^{15}\text{N}$  and  $\delta^{18}\text{O}$  values in their bone tissue, but the presence of year-round upwelling events constantly mixing the water column hindered the use of  $\delta^{34}\text{S}$  values at the community level, but allowed to identify intraspecific differences in habitat use (Zenk et al., 1991; Peña-Izquierdo et al., 2012; Carlier et al., 2015; Pottier et al., 2021).

On one hand, the higher  $\delta^{18}\text{O}$  values found for harbour porpoises and long-finned pilot whales showed a higher affinity for the saltier waters of the Canary Current at the northern coast of Mauritania, but the lower  $\delta^{13}\text{C}$  values of the pilot whales indicated a more offshore/pelagic feeding than the porpoises. On the contrary, the low mean  $\delta^{13}\text{C}$  and  $\delta^{15}\text{N}$  values and the high  $\delta^{34}\text{S}$  values found in all individuals of Atlantic spotted dolphins and common dolphins indicated an offshore/pelagic feeding for both species, although the lower  $\delta^{18}\text{O}$  values of the former suggested a higher affinity to the less salty Mauritanian Current and the higher  $\delta^{18}\text{O}$  values and wider range of  $\delta^{13}\text{C}$  values observed in common dolphins suggested the use of areas with a higher influence of the Canary Current, either with upwelling-derived or oceanic phytoplankton. On the other hand, only two cetacean species seemed to consistently use the saltiest areas of the PNBA, as indicated by the high  $\delta^{18}\text{O}$  and  $\delta^{13}\text{C}$  values of Atlantic Humpback dolphins and some individuals of bottlenose dolphins. However, the wide range of isotopic values found for bottlenose dolphins not only indicated the presence of two ecotypes, one coastal and one oceanic as previously suggested by Pinela et al. (2010) and Van Waerebeek et al. (2016), but also that, within the coastal ecotype, some individuals likely remain inside the PNBA for extended periods of time. Furthermore, the high  $\delta^{13}\text{C}$  values of Mediterranean monk seals suggested a benthic feeding, likely near the haul-out caves found at the north, and the significantly higher  $\delta^{15}\text{N}$  values indicated that they feed at a higher trophic level than the considered cetacean species. Finally, individual variations in the  $\delta^{34}\text{S}$  values of the four species found nearshore – Atlantic Humpback dolphins, bottlenose dolphins, harbour porpoises and Mediterranean monk seals – indicated that some individuals are consistently feeding on  $^{34}\text{S}$ -depleted prey likely associated with anoxic sediments (i.e.,



seagrass meadows). The previous assumptions about habitat use by marine mammals off Mauritania were validated with local sighting and stranding reports for each species in the area (e.g., Robineau and Vely, 1998; Gazo and Aguilar, 2005; Camphuysen, 2021; Camphuysen et al., 2022, among others).

Overall, the addition of complementary habitat tracers such as the  $\delta^{34}\text{S}$  and  $\delta^{18}\text{O}$  values can improve the resolution of the isotopic niche and resource partitioning among marine mammal species of the same community, since they vary independently from the  $\delta^{13}\text{C}$  and  $\delta^{15}\text{N}$  ratios and thus include different dimensions of the ecosystem. However, their use is clearly conditioned by the existence of the respective environmental  $\delta^{34}\text{S}$  and  $\delta^{18}\text{O}$  gradients within the ecosystem of interest and hence, they are not necessarily useful in every system. Therefore, when using stable isotopes as intrinsic biogeochemical tracers it becomes necessary to understand first the physical and chemical processes operating in the ecosystem and how they can affect the formation of environmental isotopic gradients relevant to the study at hand.

### **4.3. Individual characterization of the isotopic niche in sea turtles**

The combination of the  $\delta^{34}\text{S}$  or  $\delta^{18}\text{O}$  values with those of  $\delta^{13}\text{C}$  and  $\delta^{15}\text{N}$  allowed to detect individual differences in loggerhead turtles due to the different environmental conditions found inside the Mediterranean Sea. On one hand, the general counter-clockwise circulation pattern of surface waters along the three Mediterranean basins – western, central and eastern – and the higher evaporation rates of surface waters towards the eastern basin due to higher environmental and sea surface temperatures, constantly transform the fresher Atlantic waters entering through the Strait of Gibraltar into saltier Mediterranean waters, creating a west-east gradient of sea surface salinity (Figure 2.1, top panel; Millot and Taupier-Letage, 2005; Soukissian et al., 2017). Another consequence of the higher evaporation rates at the eastern basin is an increase in the concentration of water molecules carrying the heavier  $^{18}\text{O}$  isotope, because those carrying the lighter  $^{16}\text{O}$  isotope tend to evaporate quicker, thus leaving a pool of surface waters with higher  $\delta^{18}\text{O}$  values compared to those in colder regions with lower evaporation rates (Sharp, 2017). In this case, the west-east gradients of sea surface salinity and  $\delta^{18}\text{O}$  values originate from the same process, which creates a positive and linear correlation between the two factors and allows to make inferences about the habitat use of individuals based on their  $\delta^{18}\text{O}$  values and the salinity changes along the Mediterranean Sea (LeGrande and



Smith, 2006; Conroy et al., 2014). On the other hand, there is little information about the baseline variations of the  $\delta^{13}\text{C}$  and  $\delta^{34}\text{S}$  values along the different Mediterranean basins, but the  $\delta^{15}\text{N}$  values of particulate organic nitrogen (PON) are significantly lower in the central and eastern basins, except for the Adriatic Sea which has unusually high  $\delta^{15}\text{N}$  values due to high inputs of sewage from river systems (Figure 2.1; Pantoja et al., 2002; Zbinden et al., 2011).

Juvenile loggerhead turtles of Northwestern Atlantic origin estimated to be nine years or younger showed a wide range of  $\delta^{13}\text{C}$ ,  $\delta^{15}\text{N}$  and  $\delta^{18}\text{O}$  values in their bone tissue, probably because they have a higher dependence on surface currents for their movements, which causes a greater dispersion throughout the Mediterranean Sea (Revelles et al., 2007a and 2007b). In addition, they could be adopting different feeding strategies depending on their location and the available resources. On the contrary, older individuals (over 10 years old) might be more selective of their prey and foraging area, as shown by the smaller standard ellipse areas and lower  $\delta^{18}\text{O}$  values observed in older loggerhead turtles of the same origin, which suggest a preference for foraging grounds in lower salinity areas, likely in the western Mediterranean (subchapter 3.3). This coincides with the tendency of most adult loggerhead females to forage oceanically in the Algerian Basin, both prior and after nesting in the Iberian Peninsula as shown by the stable isotope ratios of their skin and satellite telemetry data (subchapter 3.4). In this case, the isotopic niche of most of the analysed females showed larger overlaps with that of juveniles stranded at the Balearic Islands, an area frequented by individuals using the oceanic regions of the Algerian Basin and characterized by higher  $\delta^{13}\text{C}$  and  $\delta^{15}\text{N}$  values compared to those stranded at the Iberian Peninsula, where they are more likely to use the neritic areas of the Balearic Sea as feeding grounds (Figure 2.1, top panel; Abalo-Morla et al., 2023). Interestingly, the  $\delta^{34}\text{S}$  values of both groups of stranded turtles and those of most nesting females were similar, except for two nesting females that showed highly  $^{13}\text{C}$ -enriched and  $^{34}\text{S}$ -depleted values, suggesting the use of a different foraging ground. Furthermore, this combination of high  $\delta^{13}\text{C}$  and low  $\delta^{34}\text{S}$  values has only been described for turtles feeding off Tunisia (Haywood et al., 2020a), which is most likely were these two females were feeding since there is evidence of satellite tracked loggerhead turtles crossing the Strait of Sicily some time after nesting in the Iberian Peninsula (subchapter 3.4).



Similar differences in  $\delta^{13}\text{C}$ ,  $\delta^{15}\text{N}$  and  $\delta^{34}\text{S}$  values have been previously reported in loggerhead turtles feeding in other Mediterranean foraging grounds. For instance, Haywood et al. (2020a) reported higher mean  $\delta^{13}\text{C}$  values and lower mean  $\delta^{34}\text{S}$  values in turtles assigned to neritic foraging grounds of the central and eastern Mediterranean compared to those feeding oceanically at the Tunisian Plateau (central basin; Figure 2.1, top panel), while the mean  $\delta^{15}\text{N}$  values of both groups were similar. On the contrary, similar  $\delta^{13}\text{C}$  values were found between individuals caught at the Northern Levantine Sea (eastern basin) and those from the Eastern Ionian Sea (central basin), but in this case, the mean  $\delta^{15}\text{N}$  values of the latter were slightly higher (Haywood et al., 2020b), probably due to the proximity to the Adriatic Sea (Figure 2.1; Zbinden et al., 2011; Haywood et al., 2020a). Overall, there seems to be a general west-east increase of  $\delta^{13}\text{C}$  values in the Mediterranean foraging grounds used by these loggerhead turtles (subchapter 3.4; Haywood et al., 2020a and 2020b), which might be a consequence of the higher primary productivity in the western Mediterranean (Bosc et al., 2004) and the lower  $\delta^{13}\text{C}$  values of oceanic phytoplankton compared to neritic primary producers (Newsome et al., 2010). In the western basin, primary productivity is slightly higher in both oceanic and neritic regions and has been increasing in the last decades, whereas the central and eastern basins have a low primary productivity in oceanic regions but a relatively high chlorophyll concentration in certain neritic areas (Bosc et al., 2004; Colella et al., 2016). This could also explain the prevalence of neritic foragers among adult loggerhead turtles nesting and feeding in the central and eastern Mediterranean basins (Schofield et al., 2013a and 2013b; Haywood et al., 2020a), whereas those from the western basin appear to feed mostly in oceanic regions (subchapter 3.4). On the contrary, mean  $\delta^{15}\text{N}$  values in the epidermis of loggerhead turtles show differences between foraging grounds within the same basin (e.g., Balearic Sea vs Algerian Basin; Eastern Ionian vs Northern Levantine) but seem relatively similar along the different basins – excluding the Adriatic Sea – and the  $\delta^{34}\text{S}$  values only seem to be lower in neritic areas associated with the presence of benthic primary producers (subchapter 3.4; Haywood et al., 2020a and 2020b). Lastly, the isotopic values in the epidermis of loggerhead turtles show possible differences among feeding grounds, but further studies are necessary to integrate this information and evaluate the distribution of these isotopic gradients along the Mediterranean Sea.

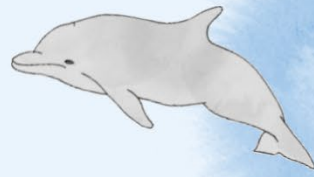
In general, the inclusion of the  $\delta^{34}\text{S}$  or  $\delta^{18}\text{O}$  ratios allowed to refine our understanding of individual specialization and isotopic niches through the identification



---

of areas and resources used by each turtle across the isospace, as they were complementary to the  $\delta^{13}\text{C}$  and  $\delta^{15}\text{N}$  ratios and thus allowed to make inferences about migratory patterns and foraging ecology that would not have been possible otherwise.





## Conclusions



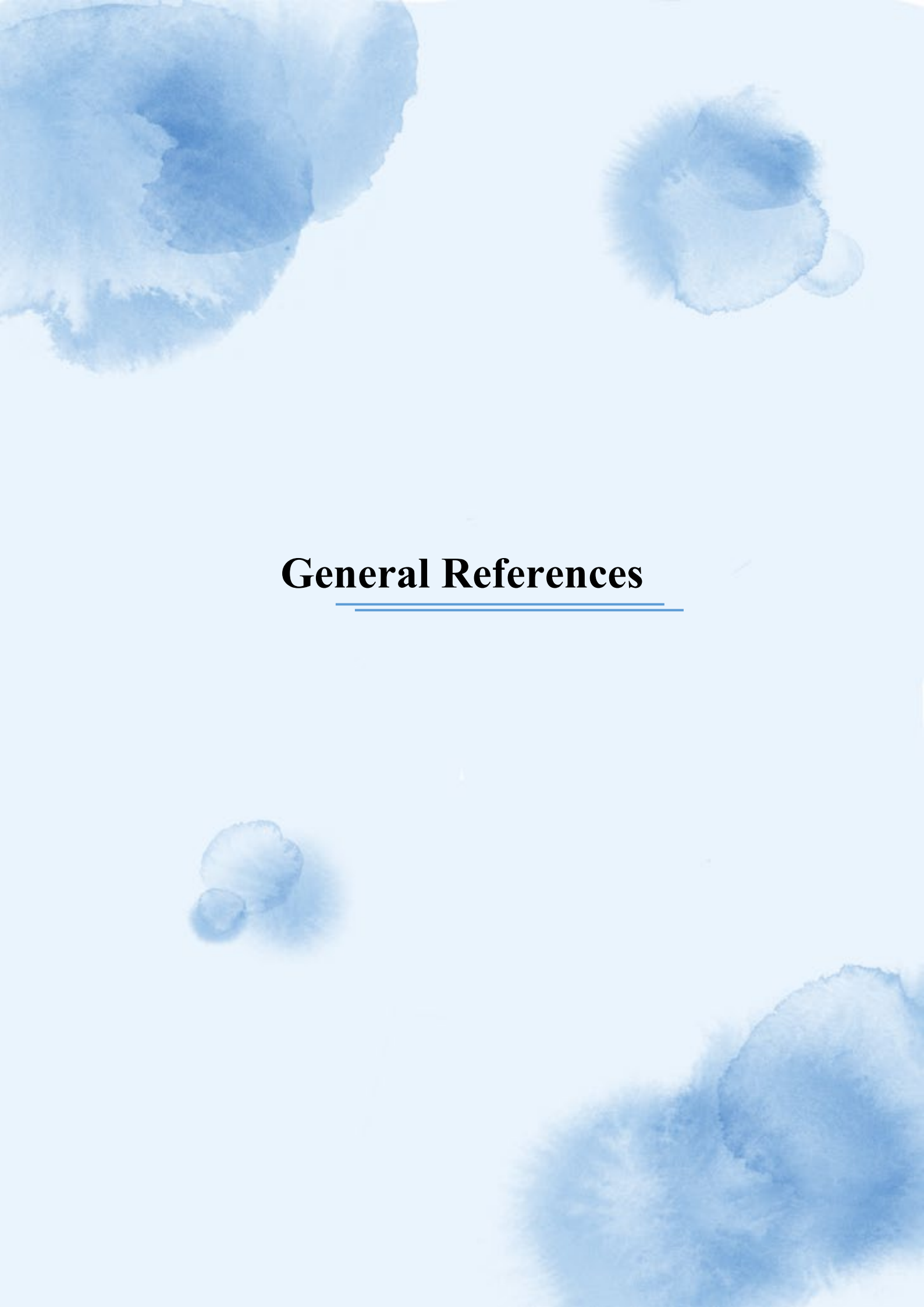




## Conclusions

1. The spatial scale of the environmental isotopic gradients delineating the isospace must be large enough to cover the area used by the species of interest, thus allowing the differentiation of habitats to be reflected in the isotopic values of the individuals' tissues. For large marine vertebrates, those scales span from tens to hundreds of kilometres.
2. Accounting for potential environmental and metabolic confounding factors that affect the isotopic fractionation of a chemical element is critical to ensure that the inferences on habitat use and trophic ecology are robust.
3. A multi-element approach allows for improved resolution of intraspecific individual variability and to better delineate the isotopic niches of sympatric species of large marine vertebrates, compared to the use of only two intrinsic tracers and considering the scale of the environmental isotopic gradients.
4. The  $\delta^{34}\text{S}$  ratio helps to improve the characterization of the isotopic niche of large marine vertebrates inhabiting marine ecosystems with high terrestrial inputs of particulate organic matter and to identify individuals associated with hypoxic or anoxic sediments.
5. The  $\delta^{18}\text{O}$  ratio in bone tissue helps to delineate the isotopic niche of large marine vertebrates inhabiting marine ecosystems with marked salinity gradients, formed by the input of fresh water or by different evaporation rates of surface waters.
6. Marine mammal species can exhibit a fine isotopic niche partitioning when a multi-element approach is adopted, as observed in those from Río de la Plata and off Mauritania.
7. The multi-element approach shows high levels of individual variability in the migration patterns of juvenile loggerhead turtles across the isospace of the Mediterranean Sea, whereas older turtles show a higher specialization towards certain regions and feeding grounds.
8. Inferences about the habitat use and trophic ecology derived from the stable isotope analysis of marine megafauna can be complemented by more direct research techniques such as *in situ* observations, satellite telemetry and genetic analysis, which can also be used to validate the results.





# **General References**





## General references

- Abalo-Morla, S., Muñoz Más, R., Tomás, J., Belda, E. 2023. Factors driving dispersal and habitat use of loggerhead turtle post-hatchlings and its conservation implications. *Marine Biology*, 170, pp.155. <https://doi.org/10.1007/s00227-023-04285-2>
- Acha, E.M., Mianzan, H., Guerrero, R., Carreto, J., Giberto, D., Montoya, N. and Carignan, M. 2008. An overview of physical and ecological processes in the Rio de la Plata Estuary. *Continental shelf research*, 28(13), 1579-1588. DOI:10.1016/j.csr.2007.01.031.
- Araujo, A. and Campredon, P. 2016. Banc d'Arguin (Mauritania). In: *The Wetland Book: II: Distribution, Description, and Conservation*, C.M. Finlayson et al. (eds.), pp.1319-1332. DOI:10.1007/978-94-007-6173-5\_154-1
- Balmer, B.C., Wells, R.S., Howle, L.E., Barleycorn, A.A., McLellan, W.A., Ann Pabst, D., Rowles, T.K., Schwacke, L.H., Townsend, F.I., Westgate, A.J. and Zolman, E.S. 2014. Advances in cetacean telemetry: A review of single-pin transmitter attachment techniques on small cetaceans and development of a new satellite-linked transmitter design. *Marine Mammal Science*, 30(2), pp.656-673. <https://doi.org/10.1111/mms.12072>
- Bas, M., García, N.A., Crespo, E.A. and Cardona, L. 2019. Intraskelletal variability in stable isotope ratios of C and N among pinnipeds and cetaceans. *Marine Mammal Science*, 36(1). DOI:10.1111/mms.12644
- Belem, A.L., Caricchio, C., Albuquerque, A.L.S., Venancio, I.M., Zucchi, M., Santos, T.H.R. and Alvarez, Y.G. 2019. Salinity and stable oxygen isotope relationship in the Southwestern Atlantic: constraints to paleoclimate reconstructions. *Anais da Academia Brasileira de Ciências*, 91(03), p.e20180226. <https://doi.org/10.1590/0001-3765201920180226>
- Ben-David, M. and Flaherty, E.A. 2012. Stable isotopes in mammalian research: a beginner's guide. *Journal of Mammalogy*, 93(2), pp.312-328. <https://doi.org/10.1644/11-MAMM-S-166.1>
- Bergamo, T.F., Botta, S. and Copertino, M. 2016. Lipid extraction in stable isotope analyses of juvenile sea turtle skin and muscle. *Aquatic Biology*, 25, pp.1-6. <https://doi.org/10.3354/ab00652>
- Bligh, E.G. and Dyer, W.J. 1959. A rapid method of total lipid extraction and purification. *Canadian journal of biochemistry and physiology*, 37(8), pp.911-917. <https://doi.org/10.1139/o59-099>
- Bond, A.L. and Hobson, K.A. 2012. Reporting stable-isotope ratios in ecology: recommended terminology, guidelines and best practices. *Waterbirds*, 35(2), pp.324-331. <https://doi.org/10.1675/063.035.0213>
- Borrell, A., Abad-Oliva, N., Gómez-Campos, E., Giménez, J. and Aguilar, A. 2012. Discrimination of stable isotopes in fin whale tissues and application to diet assessment in cetaceans. *Rapid Communications in Mass Spectrometry*, 26(14), pp.1596-1602. <https://doi.org/10.1002/rcm.6267>
- Borrell, A., Gazo, M. Aguilar, A., Raga, J.A., Degollada, E., Gozalbes, P. and García-Vernet, R. 2021. Niche partitioning amongst northwestern Mediterranean cetaceans using stable isotopes. *Progress in Oceanography*, 193, p.102559. <https://doi.org/10.1016/j.pocean.2021.102559>
- Bosc, E., Bricaud, A. and Antoine, D. 2004. Seasonal and interannual variability in algal biomass and primary production in the Mediterranean Sea, as derived from 4 years

- of SeaWiFS observations. *Global Biogeochemical Cycles*, 18(1), GB1005, pp.1-17. <https://doi.org/10.1029/2003GB002034>
- Botta, S., Hohn, A.A., Macko, S.A. and Secchi, E.R. 2012. Isotopic variation in delphinids from the subtropical western South Atlantic. *Journal of the Marine Biological Association of the United Kingdom*, 92(8), pp.1689-1698. <https://doi.org/10.1017/S0025315411000610>
- Botto, F., Gaitán, E., Mianzan, H., Acha, M., Giberto, D., Schiariti, A. and Iribarne, O. 2011. Origin of resources and trophic pathways in a large SW Atlantic estuary: An evaluation using stable isotopes. *Estuarine, Coastal and Shelf Science*, 92(1), 70-77. doi:10.1016/j.ecss.2010.12.014.
- Boyer, E.W. and Howarth, R.W. 2013. Chapter 36: Nitrogen Fluxes from Rivers to the Coastal Oceans. In: Nitrogen in the marine environment (2<sup>nd</sup> edition), eds. Capone, D.G, Bronk, D.A., Mulholland, M.R. and Carpenter, E.J., Elsevier, pp.1565-1587. DOI:10.1016/B978-0-12-372522-6.00036-0
- Bradshaw, P.J., Broderick, A.C., Carreras, C., Inger, R., Fuller, W., Snape, R., Stokes, K.L. and Godley, B.J. 2017. Satellite tracking and stable isotope analysis highlight differential recruitment among foraging areas in green turtles. *Marine Ecology Progress Series*, 582, pp.201-214. <https://doi.org/10.3354/meps12297>
- Brady, A.L., White, C.D., Longstaffe, F.J. and Southam, G. 2008. Investigating intra-bone isotopic variations in bioapatite using IR-laser ablation and micromilling: Implications for identifying diagenesis?. *Palaeogeography, Palaeoclimatology, Palaeoecology*, 266(3-4), pp.190-199. <https://doi.org/10.1016/j.palaeo.2008.03.031>
- Browning, N.E., Dold, C., I-Fan, J. and Worthy, G.A. 2014. Isotope turnover rates and diet–tissue discrimination in skin of ex situ bottlenose dolphins (*Tursiops truncatus*). *Journal of Experimental Biology*, 217(2), pp.214-221. <https://doi.org/10.1242/jeb.093963>
- Camphuysen, C.J. 2021. Vulnerable wildlife concentrations at the Mauritanian Shelf. A preliminary atlas of vulnerability to surface pollutants. Royal Netherlands Institute for Sea Research (NIOZ), The Netherlands, pp.45.
- Camphuysen, C.J., Schreurs, T.A.W. and Bilal, A.S. 2022. Ship-based seabird and marine mammal surveys off Mauritania, 17 February-1 March 2022. *Royal Netherlands Institute for Sea Research (NIOZ), Den Burg, Texel and the Institut Mauritanien de Recherche Océanographique et des Pêche (IMROP), Nouadhibou*, pp.73.
- Canfield, D.E. 2001. Biogeochemistry of sulfur isotopes. *Reviews in mineralogy and geochemistry*, 43(1), pp.607-636. <https://doi.org/10.2138/gsrmg.43.1.607>
- Cani, A., Besén, C., Carreras, C., Pascual, M. and Cardona, L. 2024. The journey of loggerhead turtles from the Northwest Atlantic to the Mediterranean Sea as recorded by the stable isotope ratios of O, C and N of their bones. *Marine Environmental Research*, p.106851. <https://doi.org/10.1016/j.marenvres.2024.106851>
- Carlier, A., Chauvaud, L., van Der Geest, M., Le Loc'h, F., Le Duff, M., Vernet, M., Raffray, J., Diakhaté, D., Labrosse, P., Wagué, A. and Le Goff, C. 2015. Trophic connectivity between offshore upwelling and the inshore food web of Banc d'Arguin (Mauritania): New insights from isotopic analysis. *Estuarine, Coastal and Shelf Science*, 165, pp.149-158. <https://doi.org/10.1016/j.ecss.2015.05.001>
- Cardona, L., Revelles, M., Parga, M.L., Tomás, J., Aguilar, A., Alegre, F., Raga, A. and Ferrer, X. 2009. Habitat use by loggerhead sea turtles *Caretta caretta* off the coast of eastern Spain results in a high vulnerability to neritic fishing gear. *Marine Biology*, 156, pp.2621-2630. <https://doi.org/10.1007/s00227-009-1288-9>

- Cardona, L., Martínez-Iñigo, L., Mateo, R. and González-Solís, J. 2015. The role of sardine as prey for pelagic predators in the western Mediterranean Sea assessed using stable isotopes and fatty acids. *Marine Ecology Progress Series*, 531, pp.1-14. <https://doi.org/10.3354/meps11353>
- Carreto, J.I., Montoya, N.G., Benavides, H.R., Guerrero, R.A., Carignan, M.O. 2003. Characterization of spring phytoplankton communities in the Río de la Plata maritime front using pigment signatures and cell microscopy. *Marine Biology*, 143(5), 1013-1027. <https://doi.org/10.1007/s00227-003-1147-z>
- Carreto, J.I., Montoya, N., Akselman, R., Carignan, M.O., Silva, R.I. and Cucchi Colleoni, D.A. 2008. Algal pigment patterns and phytoplankton assemblages in different water masses of the Río de la Plata maritime front. *Continental Shelf Research*, 28(13), 1589-1606. <https://doi.org/10.1016/j.csr.2007.02.012>
- Cipro, C.V., Bustamante, P., Taniguchi, S. and Montone, R.C. 2012. Persistent organic pollutants and stable isotopes in pinnipeds from King George Island, Antarctica. *Marine Pollution Bulletin*, 64(12), pp.2650-2655. <https://doi.org/10.1016/j.marpolbul.2012.10.012>
- Colella, S., Falcini, F., Rinaldi, E., Sammartino, M. and Santoleri, R. 2016. Mediterranean ocean colour chlorophyll trends. *PloS one*, 11(6), p.e0155756. <https://doi.org/10.1371/journal.pone.0155756>
- Connolly, R.M., Guest, M.A., Melville, A.J. and Oakes, J.M. 2004. Sulfur stable isotopes separate producers in marine food-web analysis. *Oecologia*, 138, pp.161-167. <https://doi.org/10.1007/s00442-003-1415-0>
- Conroy, J.L., Cobb, K.M., Lynch-Stieglitz, J. and Polissar, P.J. 2014. Constraints on the salinity–oxygen isotope relationship in the central tropical Pacific Ocean. *Marine Chemistry*, 161, pp.26-33. <https://doi.org/10.1016/j.marchem.2014.02.001>
- Cushman, J.C. and Borland, A. 2002. Induction of Crassulacean acid metabolism by water limitation. *Plant, cell & environment*, 25(2), pp.295-310. <https://doi.org/10.1046/j.0016-8025.2001.00760.x>
- Cropper, T.E., Hanna, E. and Bigg, G.R. 2014. Spatial and temporal seasonal trends in coastal upwelling off Northwest Africa, 1981–2012. *Deep Sea Research Part I: Oceanographic Research Papers*, 86, pp.94-111, <http://dx.doi.org/10.1016/j.dsr.2014.01.007>
- de Buffrénil, V., Quilhac, A. and Castanet, J. 2021. Cyclical growth and skeletochronology. In: Vertebrate skeletal histology and paleohistology, eds. de Buffrénil, V., de Ricqlès, A.J., Zylberberg, Z. and Padian, K., CRC Press, pp.626-644. <https://doi.org/10.1201/9781351189590>
- DeNiro, M.J. and Epstein, S. 1978. Influence of diet on the distribution of carbon isotopes in animals. *Geochimica et cosmochimica acta*, 42(5), pp.495-506. [https://doi.org/10.1016/0016-7037\(78\)90199-0](https://doi.org/10.1016/0016-7037(78)90199-0)
- DiMatteo, A., Cañadas, A., Roberts, J., Sparks, L., Panigada, S., Boisseau, O., Moscrop, A., Fortuna, C.M., Lauriano, G., Holcer, D. and Peltier, H. 2022. Basin-wide estimates of loggerhead turtle abundance in the Mediterranean Sea derived from line transect surveys. *Frontiers in Marine Science*, 9, p.930412. <https://doi.org/10.3389/fmars.2022.930412>
- Drago, M., Valdivia, M., Bragg, D., González, E.M., Aguilar, A. and Cardona, L. 2020. Stable oxygen isotopes reveal habitat use by marine mammals in the Río de la Plata estuary and adjoining Atlantic Ocean. *Estuarine, Coastal and Shelf Science*, 238, p.106708. <https://doi.org/10.1016/j.ecss.2020.106708>
- Drago, M., Signaroli, M., Valdivia, M., González, E.M., Borrell, A., Aguilar, A. and Cardona, L. 2021. The isotopic niche of Atlantic, biting marine mammals and its

- relationship to skull morphology and body size. *Scientific Reports*, 11(1), p.15147. <https://doi.org/10.1038/s41598-021-94610-w>
- Eckardt, F. 2001. The origin of sulphates: an example of sulphur isotopic applications. *Progress in physical geography*, 25(4), pp.512-519. <https://doi.org/10.1177/030913330102500403>
- Eckert, S.A., Moore, J.E., Dunn, D.C., van Buiten, R.S., Eckert, K.L. and Halpin, P.N. 2008. Modeling loggerhead turtle movement in the Mediterranean: importance of body size and oceanography. *Ecological Applications*, 18(2), pp.290-308. <https://doi.org/10.1890/06-2107.1>
- Emerson, S. and Hedges, J. 2008. Chemical oceanography and the marine carbon cycle. Cambridge University Press, pp.470.
- Fahy, G.E., Deter, C., Pitfield, R., Miszkiewicz, J.J. and Mahoney, P. 2017. Bone deep: variation in stable isotope ratios and histomorphometric measurements of bone remodelling within adult humans. *Journal of Archaeological Science*, 87, pp.10-16. <https://doi.org/10.1016/j.jas.2017.09.009>
- Falkowski, P.G. and Raven, J.A. 2007. Aquatic photosynthesis (2<sup>nd</sup> edition). Princeton University Press, pp.488.
- Ferreira, A., Sá, C., Silva, N., Beltrán, C., Dias, A.M. and Brito, A.C. 2020. Phytoplankton response to nutrient pulses in an upwelling system assessed through a microcosm experiment (Algarrobo Bay, Chile). *Ocean & coastal management*, 190, p.105167. <https://doi.org/10.1016/j.ocecoaman.2020.105167>
- Finlay, J.C., Power, M.E. and Cabana, G. 1999. Effects of water velocity on algal carbon isotope ratios: implications for river food web studies. *Limnology and Oceanography*, 44(5), pp.1198-1203. <https://doi.org/10.4319/lo.1999.44.5.1198>
- Fischer, G., Romero, O., Merkel, U., Donner, B., Iversen, M., Nowald, N., Ratmeyer, V., Ruhland, G., Klann, M. and Wefer, G. 2016. Deep ocean mass fluxes in the coastal upwelling off Mauritania from 1988 to 2012: variability on seasonal to decadal timescales. *Biogeosciences*, 13(10), pp.3071-3090. <https://doi.org/10.5194/bg-13-3071-2016>
- Florin, S.T., Felicetti, L.A. and Robbins, C.T. 2010. The biological basis for understanding and predicting dietary-induced variation in nitrogen and sulphur isotope ratio discrimination. *Functional Ecology*, 25(3), pp.519-526. <https://doi.org/10.1111/j.1365-2435.2010.01799.x>
- Fofonoff, N.P. 1981. Chapter 4: The Gulf Stream. In: Warren, B.A. and Wunsch, C. (Eds.), *Evolution of Physical Oceanography: scientific surveys in honor of Henry Stommel*, pp.112-139.
- Framiñan, M.B. and Brown, O.B. 1996. Study of the Río de la Plata turbidity front, Part 1: spatial and temporal distribution. *Continental Shelf Research*, 16(10), pp.1259-1282.
- Francioso, A., Baseggio Conrado, A., Mosca, L. and Fontana, M. 2020. Chemistry and biochemistry of sulfur natural compounds: Key intermediates of metabolism and redox biology. *Oxidative Medicine and Cellular Longevity*, 2020(1), p.8294158. <https://doi.org/10.1155/2020/8294158>
- Fuentes, M.M., McMichael, E., Kot, C.Y., Silver-Gorges, I., Wallace, B.P., Godley, B.J., Brooks, A.M., Ceriani, S.A., Cortés-Gómez, A.A., Dawson, T.M. and Dodge, K.L. 2023. Key issues in assessing threats to sea turtles: knowledge gaps and future directions. *Endangered Species Research*, 52, pp.303-341. <https://doi.org/10.3354/esr01278>
- García-Vernet, R., Borrell, A., Víkingsson, G., Halldórsson, S.D. and Aguilar, A. 2021. Ecological niche partitioning between baleen whales inhabiting Icelandic

- waters. *Progress in Oceanography*, 199, p.102690.  
<https://doi.org/10.1016/j.pocean.2021.102690>
- Gat, J.R. 1996. Oxygen and hydrogen isotopes in the hydrologic cycle. *Annual Review of Earth and Planetary Sciences*, 24(1), pp.225-262.  
<https://doi.org/10.1146/annurev.earth.24.1.225>
- Gazo, M. and Aguilar, A. 2005. Maternal attendance and diving behavior of a lactating Mediterranean monk seal. *Marine Mammal Science*, 21(2), 340-345.
- Guerrero, R.A., Acha, E.M., Framin, M.B. and Lasta, C.A. 1997. Physical oceanography of the Río de la Plata Estuary, Argentina. *Continental shelf research*, 17(7), pp.727-742. [https://doi.org/10.1016/S0278-4343\(96\)00061-1](https://doi.org/10.1016/S0278-4343(96)00061-1)
- Hays, G.C. and Hawkes, L.A. 2018. Satellite tracking sea turtles: Opportunities and challenges to address key questions. *Frontiers in Marine Science*, 5, pp.432.  
<https://doi.org/10.3389/fmars.2018.00432>
- Hays, G.C. and Scott, R. 2013. Global patterns for upper ceilings on migration distance in sea turtles and comparisons with fish, birds and mammals. *Functional Ecology*, 27(3), pp.748-756. <https://doi.org/10.1111/1365-2435.12073>
- Haywood, J.C., Fuller, W.J., Godley, B.J., Shutler, J.D., Widdicombe, S. and Broderick, A.C. 2019. Global review and inventory: how stable isotopes are helping us understand ecology and inform conservation of marine turtles. *Marine Ecology Progress Series*, 613, pp.217-245. <https://doi.org/10.3354/meps12889>
- Haywood, J.C., Fuller, W.J., Godley, B.J., Margaritoulis, D., Shutler, J.D., Snape, R.T., Widdicombe, S., Zbinden, J.A. and Broderick, A.C. 2020a. Spatial ecology of loggerhead turtles: Insights from stable isotope markers and satellite telemetry. *Diversity and Distributions*, 26(3), pp.368-381. <https://doi.org/10.1111/ddi.13023>
- Haywood, J.C., Casale, P., Freggi, D., Fuller, W.J., Godley, B.J., Lazar, B., Margaritoulis, D., Rees, A.F., Shutler, J.D., Snape, R.T. and Swain-Diaz, N.R. 2020b. Foraging ecology of Mediterranean juvenile loggerhead turtles: insights from C and N stable isotope ratios. *Marine Biology*, 167(3), p.28.  
<https://doi.org/10.1007/s00227-020-3647-5>
- Hobson, K.A. 1999. Tracing origins and migration of wildlife using stable isotopes: a review. *Oecologia*, 120, pp.314-326. <https://doi.org/10.1007/s004420050865>
- Hobson, K.A. and Clark, R.G. 1992. Assessing avian diets using stable isotopes I: turnover of  $^{13}\text{C}$  in tissues. *The Condor*, 94(1), pp.181-188.  
<https://doi.org/10.2307/1368807>
- Hobson, K.A., Barnett-Johnson, R. and Cerling, T. 2010. Chapter 13: Using Isoscapes to Track Animal Migration. In *Isoscapes: Understanding movement, pattern, and process on Earth through isotope mapping*, eds. West, J.B., Bowen, G.J., Dawson, T.E. and Tu, K.P., 273-298. Dordrecht: Springer Science & Business Media.
- Hoefs, J. 2018. Stable isotope geochemistry (8<sup>th</sup> edition). *Springer*, Göttingen, Germany, pp.437. <https://doi.org/10.1007/978-3-030-77692-3>
- Hussey, N.E., Kessel, S.T., Aarestrup, K., Cooke, S.J., Cowley, P.D., Fisk, A.T., Harcourt, R.G., Holland, K.N., Iverson, S.J., Kocik, J.F. and Mills Flemming, J.E. 2015. Aquatic animal telemetry: a panoramic window into the underwater world. *Science*, 348(6240), p.1255642. <https://doi.org/10.1126/science.1255642>
- Jackson, A.L., Inger, R., Parnell, A.C. and Bearhop, S. 2011. Comparing isotopic niche widths among and within communities: SIBER Stable Isotope Bayesian Ellipses in R. *Journal of Animal Ecology*, 80(3), pp.595-602.  
<https://doi.org/10.1111/j.1365-2656.2011.01806.x>
- Jones, T.T., Hastings, M.D., Bostrom, B.L., Andrews, R.D. and Jones, D.R. 2009. Validation of the use of doubly labeled water for estimating metabolic rate in the

- green turtle (*Chelonia mydas* L.): a word of caution. *Journal of Experimental Biology*, 212(16), pp.2635-2644. <https://doi.org/10.1242/jeb.029330>
- Kiddon, J., Bender, M.L., Orchardo, J., Caron, D.A., Goldman, J.C. and Dennett, M. 1993. Isotopic fractionation of oxygen by respiring marine organisms. *Global Biogeochemical Cycles*, 7(3), pp.679-694. <https://doi.org/10.1029/93GB01444>
- Kingsbury, B.A. and Robinson, N.J. 2016. Movement patterns and telemetry. In: *Reptile ecology and conservation: A handbook of techniques*, eds. Kenneth Dodd Jr., C., Oxford University Press, pp.110-121.
- Kirsanow, K. and Tuross, N. 2011. Oxygen and hydrogen isotopes in rodent tissues: Impact of diet, water and ontogeny. *Palaeogeography, Palaeoclimatology, Palaeoecology*, 310(1-2), pp.9-16. <https://doi.org/10.1016/j.palaeo.2011.03.022>
- Koch, P.L., Tuross, N. and Fogel, M.L. 1997. The effects of sample treatment and diagenesis on the isotopic integrity of carbonate in biogenic hydroxylapatite. *Journal of Archaeological Science*, 24(5), pp.417-429. <https://doi.org/10.1006/jasc.1996.0126>
- Larkum, A.W.D., Davey, P.A., Kuo, J., Ralph, P.J. and Raven, J.A. 2017. Carbon-concentrating mechanisms in seagrasses. *Journal of Experimental Botany*, 68(14), pp.3773-3784. <https://doi.org/10.1093/jxb/erx206>
- Launay, H., Huang, W., Maberly, S.C. and Gontero, B. 2020. Regulation of carbon metabolism by environmental conditions: a perspective from diatoms and other chromalveolates. *Frontiers in Plant Science*, 11, p.1033. <https://doi.org/10.3389/fpls.2020.01033>
- Layman, C.A., Araujo, M.S., Boucek, R., Hammerschlag-Peyer, C.M., Harrison, E., Jud, Z.R., Matich, P., Rosenblatt, A.E., Vaudo, J.J., Yeager, L.A. and Post, D.M. 2012. Applying stable isotopes to examine food-web structure: an overview of analytical tools. *Biological reviews*, 87(3), pp.545-562. <https://doi.org/10.1111/j.1469-185X.2011.00208.x>
- Lebigre, J.M. 1991. Les marais maritimes de Mauritanie: Protection et valorisation. Les cahiers d'outre-mer 44 (176), 379–400, <https://doi.org/10.3406/caoum.1991.3413>
- LeGrande, A.N., Schmidt, G.A. 2006. Global gridded data set of the oxygen isotopic composition in seawater. *Geophysical Research Letters*, 33(12), pp.1-5. <https://doi.org/10.1029/2006GL026011>
- Liu, D., Ma, Q., Valiela, I., Anderson, D.M., Keesing, J.K., Gao, K., Zhen, Y., Sun, X. and Wang, Y. 2020. Role of C4 carbon fixation in *Ulva prolifera*, the macroalga responsible for the world's largest green tides. *Communications Biology*, 3(1), p.494. <https://doi.org/10.1038/s42003-020-01225-4>
- Liu, T., Chan, A.W. and Abbatt, J.P. 2021. Multiphase oxidation of sulfur dioxide in aerosol particles: Implications for sulfate formation in polluted environments. *Environmental Science & Technology*, 55(8), pp.4227-4242. <https://doi.org/10.1021/acs.est.0c06496>
- Lorrain, A., Savoye, N., Chauvaud, L., Paulet, Y.M. and Naulet, N. 2003. Decarbonation and preservation method for the analysis of organic C and N contents and stable isotope ratios of low-carbonated suspended particulate material. *Analytica Chimica Acta*, 491(2), pp.125-133. [https://doi.org/10.1016/S0003-2670\(03\)00815-8](https://doi.org/10.1016/S0003-2670(03)00815-8)
- Luz, B. and Barkan, E. 2011. The isotopic composition of atmospheric oxygen. *Global Biogeochemical Cycles*, 25(3), pp.14. <https://doi.org/10.1029/2010GB003883>
- MacLeod, N.A. and Barton, D.R. 1998. Effects of light intensity, water velocity, and species composition on carbon and nitrogen stable isotope ratios in periphyton.

- Canadian Journal of Fisheries and Aquatic Sciences*, 55(8), pp.1919-1925.  
<https://doi.org/10.1139/f98-075>
- Matthews, B. and Mazumder, A. 2004. A critical evaluation of intrapopulation variation of  $\delta^{13}\text{C}$  and isotopic evidence of individual specialization. *Oecologia*, 140, pp.361-371. <https://doi.org/10.1007/s00442-004-1579-2>
- Matthews, C.J., Longstaffe, F.J. and Ferguson, S.H. 2016. Dentine oxygen isotopes ( $\delta^{18}\text{O}$ ) as a proxy for odontocete distributions and movements. *Ecology and Evolution*, 6(14), pp.4643-4653. <https://doi.org/10.1002/ece3.2238>
- McClelland, J.W. and Valiela, I. 1998. Changes in food web structure under the influence of increased anthropogenic nitrogen inputs to estuaries. *Marine Ecology Progress Series*, 168, pp.259-271. DOI:10.3354/meps168259
- McCluskey, S.M., Sprogis, K.R., London, J.M., Bejder, L. and Loneragan, N.R. 2021. Foraging preferences of an apex marine predator revealed through stomach content and stable isotope analyses. *Global Ecology and Conservation*, 25, p.e01396. <https://doi.org/10.1016/j.gecco.2020.e01396>
- McCutchan Jr, J.H., Lewis Jr, W.M., Kendall, C. and McGrath, C.C. 2003. Variation in trophic shift for stable isotope ratios of carbon, nitrogen, and sulfur. *Oikos*, 102(2), pp.378-390. <https://doi.org/10.1034/j.1600-0706.2003.12098.x>
- Medeiros, L., Monteiro, D.S., Botta, S., Proietti, M.C. and Secchi, E.R. 2019. Origin and foraging ecology of male loggerhead sea turtles from southern Brazil revealed by genetic and stable isotope analysis. *Marine Biology*, 166, pp.1-14. <https://doi.org/10.1007/s00227-019-3524-2>
- Meunier, T., Barton, E.D., Barreiro, B. and Torres, R. 2012. Upwelling filaments off Cap Blanc: Interaction of the NW African upwelling current and the Cape Verde frontal zone eddy field?. *Journal of Geophysical Research: Oceans*, 117(C08031), pp.18. <https://doi.org/10.1029/2012JC007905>
- Michener, R. H. and Lajtha, K. 2007. *Stable isotopes in ecology and environmental science*. Second Edition. Malden: Blackwell publishing, pp.594.
- Millot, C. and Taupier-Letage, I. 2005. Circulation in the Mediterranean Sea. In: Saliot, A. (Eds), *The Mediterranean Sea. Handbook of Environmental Chemistry*, Springer, Berlin, Heidelberg, 5K, pp.29-66. <https://doi.org/10.1007/b107143>
- Miloslavich, P., Klein, E., Díaz, J.M., Hernández, C.E., Bigatti, G., Campos, L., Artigas, F., Castillo, J., Penchaszadeh, P.E., Neill, P.E., Carranza, A., Retana, M.V., Díaz de Astarloa, J.M., Lewis, M., Yorrio, Y., Piriz, M.L., Rodríguez, D., Yoneshigue-Valentin, Y., Gamboa, L., Martín, A. 2011. Marine biodiversity in the Atlantic and Pacific coasts of South America: knowledge and gaps. *PLoS One*, 6(1), p.e14631. <https://doi.org/10.1371/journal.pone.0014631>
- Mittelstaedt, E. 1991. The ocean boundary along the northwest African coast: Circulation and oceanographic properties at the sea surface. *Progress in Oceanography*, 26(4), pp.307-355. [https://doi.org/10.1016/0079-6611\(91\)90011-A](https://doi.org/10.1016/0079-6611(91)90011-A)
- Modest, M., Irvine, L., Andrews-Goff, V., Gough, W., Johnston, D., Nowacek, D., Pallin, L., Read, A., Moore, R.T. and Friedlaender, A. 2021. First description of migratory behavior of humpback whales from an Antarctic feeding ground to a tropical calving ground. *Animal Biotelemetry*, 9(1), pp.1-16. <https://doi.org/10.1186/s40317-021-00266-8>
- Mooney, H.A. 2004. Stable isotopes and biosphere-atmosphere interactions: processes and biological controls, eds. L.B. Flanagan, J.R. Ehleringer and D.E. Pataki, Elsevier, pp.400.

- Nagy, G.J., Gómez-Erache, M., López, C.H. and Perdomo, A.C. 2002. Distribution patterns of nutrients and symptoms of eutrophication in the Rio de la Plata River Estuary System. In: Nutrients and Eutrophication in Estuaries and Coastal Waters, eds. E. Orive, M. Elliott & V.N. de Jonge, *Hydrologia* 475/476, Kluwer Academic Publishers, Netherlands, pp.125-139.
- Nehlich, O. 2015. The application of sulphur isotope analyses in archaeological research: a review. *Earth-Science Reviews*, 142, 1-17. <https://doi.org/10.1016/j.earscirev.2014.12.002>
- Newsome, S.D., Koch, P.L., Etnier, M.A. and Auriolles-Gamboa, D. 2006. Using carbon and nitrogen isotope values to investigate maternal strategies in northeast Pacific otariids. *Marine Mammal Science*, 22(3), pp.556-572. <https://doi.org/10.1111/j.1748-7692.2006.00043.x>
- Newsome, S.D., Clementz, M.T. and Koch, P.L. 2010. Using stable isotope biogeochemistry to study marine mammal ecology. *Marine Mammal Science*, 26(3), pp.509-572. <https://doi.org/10.1111/j.1748-7692.2009.00354.x>
- Newton, W.E. 2007. Chapter 8 - Physiology, biochemistry, and molecular biology of nitrogen fixation. In: Biology of the nitrogen cycle, eds. Bothe, H., Ferguson, S. and Newton, W.E., Elsevier, pp.109-129. <https://doi.org/10.1016/B978-044452857-5.50009-6>
- Palter, J.B. 2015. The role of the Gulf Stream in European climate. *Annual review of marine science*, 7, pp.113-137. <https://doi.org/10.1146/annurev-marine-010814-015656>
- Pantoja, S., Repeta, D.J., Sachs, J.P. and Sigman, D.M. 2002. Stable isotope constraints on the nitrogen cycle of the Mediterranean Sea water column. *Deep Sea Research Part I: Oceanographic Research Papers*, 49(9), pp.1609-1621. [https://doi.org/10.1016/S0967-0637\(02\)00066-3](https://doi.org/10.1016/S0967-0637(02)00066-3)
- Pecquerie, L., Nisbet, R.M., Fablet, R., Lorrain, A. and Kooijman, S.A. 2010. The impact of metabolism on stable isotope dynamics: a theoretical framework. *Philosophical Transactions of the Royal Society B: Biological Sciences*, 365(1557), pp.3455-3468. <https://doi.org/10.1098/rstb.2010.0097>
- Pelegrí, J.L., Peña-Izquierdo, J., Machín, F., Meiners, C. and Presas-Navarro, C. 2017. Oceanography of the Cape Verde Basin and Mauritanian Slope Waters. In: Ramos, A., Ramil, F., Sanz, J. (eds) Deep-Sea Ecosystems Off Mauritania. Springer, Dordrecht, pp.119-153. [https://doi.org/10.1007/978-94-024-1023-5\\_3](https://doi.org/10.1007/978-94-024-1023-5_3)
- Peña-Izquierdo, J., Pelegrí, J.L., Pastor, M.V., Castellanos, P., Emelianov, M., Gasser, M., Salvador, J. and Vázquez-Domínguez, E. 2012. The continental slope current system between Cape Verde and the Canary Islands. *Sci. Mar*, 76, pp.65-78.
- Peterson, B.J.; Howarth, R.W. and Garritt, R.H. 1985. Multiple Stable Isotopes Used to Trace the Flow of Organic Matter in Estuarine Food Webs. *Science*, 227(4692), pp.1361-1363. DOI:10.1126/science.227.4692.1361.
- Peterson, B.J. and Howarth, R.W. 1987. Sulfur, carbon, and nitrogen isotopes used to trace organic matter flow in the salt-marsh estuaries of Sapelo Island, Georgia 1. *Limnology and oceanography*, 32(6), pp.1195-1213.
- Peterson, B.J. and Fry, B. 1987. Stable isotopes in ecosystem studies. *Annual review of ecology and systematics*, pp.293-320.
- Peterson, B.J. 1999. Stable isotopes as tracers of organic matter input and transfer in benthic food webs: a review. *Acta oecologica*, 20(4), pp.479-487.
- Pfeiffer, C.J. and Jones, F.M. 1993. Epidermal lipid in several cetacean species: ultrastructural observations. *Anatomy and embryology*, 188, pp.209-218. <https://doi.org/10.1007/BF00188213>

- Pierella Karlusich, J.J., Pelletier, E., Lombard, F., Carsique, M., Dvorak, E., Colin, S., Picheral, M., Cornejo-Castillo, F.M., Acinas, S.G., Pepperkok, R. and Karsenti, E. 2021. Global distribution patterns of marine nitrogen-fixers by imaging and molecular methods. *Nature communications*, 12(1), pp.4160. <https://doi.org/10.1038/s41467-021-24299-y>
- Pinela, A., Borrell, A., Cardona, L. y Aguilar, A. 2010. Stable isotopes reveals habitat partitioning among marine mammals off the NW African coast and unique trophic niches for two globally threatened species. *Mar Eco Prog Series*, 416, pp.295-306. <https://doi.org/10.3354/meps08790>
- Pinzone, M., Acquarone, M., Huyghebaert, L., Sturaro, N., Michel, L.N., Siebert, U. and Das, K. 2017. Carbon, nitrogen and sulphur isotopic fractionation in captive juvenile hooded seal (*Cystophora cristata*): Application for diet analysis. *Rapid Communications in Mass Spectrometry*, 31(20), pp.1720-1728. <https://doi.org/10.1002/rcm.7955>
- Pinzone, M., Damseaux, F., Michel, L.N. and Das, K. 2019. Stable isotope ratios of carbon, nitrogen and sulphur and mercury concentrations as descriptors of trophic ecology and contamination sources of Mediterranean whales. *Chemosphere*, 237, p.124448. <https://doi.org/10.1016/j.chemosphere.2019.124448>
- Pontiller, B., Martínez-García, S., Joglar, V., Amnebrink, D., Pérez-Martínez, C., González, J.M., Lundin, D., Fernández, E., Teira, E. and Pinhassi, J. 2022. Rapid bacterioplankton transcription cascades regulate organic matter utilization during phytoplankton bloom progression in a coastal upwelling system. *The ISME Journal*, 16(10), pp.2360-2372. <https://doi.org/10.1038/s41396-022-01273-0>
- Post, D.M. 2002. Using stable isotopes to estimate trophic position: models, methods, and assumptions. *Ecology*, 83(3), pp.703-718. [https://doi.org/10.1890/0012-9658\(2002\)083\[0703:USITET\]2.0.CO;2](https://doi.org/10.1890/0012-9658(2002)083[0703:USITET]2.0.CO;2)
- Pottier, A., Catry, T., Trégarot, E., Maréchal, J.P., Fayad, V., David, G., Cheikh, M.S. and Failler, P. 2021. Mapping coastal marine ecosystems of the National Park of Banc d'Arguin (PNBA) in Mauritania using Sentinel-2 imagery. *International Journal of Applied Earth Observation and Geoinformation*, 102, p.102419, <https://doi.org/10.1016/j.jag.2021.102419>
- Pritchard, D.W. 1952. Estuarine hydrography. In *Advances in geophysics*, Vol. 1, Elsevier, pp.243-280.
- R Core Team. 2021. R: A Language and Environment for Statistical Computing. R Foundation for Statistical Computing, Vienna. <https://www.R-project.org>.
- Ramos, R. and González-Solís, J. 2012. Trace me if you can: the use of intrinsic biogeochemical markers in marine top predators. *Frontiers in Ecology and the Environment*, 10(5), pp.258-266. <https://doi.org/10.1890/110140>
- Raoult, V., Phillips, A.A., Nelson, J., Niella, Y., Skinner, C., Tilcock, M.B., Burke, P.J., Szpak, P., James, W.R. and Harrod, C. 2024. Why aquatic scientists should use sulfur stable isotope ratios ( $\delta^{34}\text{S}$ ) more often. *Chemosphere*, p.141816. <https://doi.org/10.1016/j.chemosphere.2024.141816>
- Raven, J.A., Johnston, A.M., Kübler, J.E., Korb, R., McInroy, S.G., Handley, L.L., Scrimgeour, C.M., Walker, D.I., Beardall, J., Vanderklift, M. and Fredriksen, S. 2002. Mechanistic interpretation of carbon isotope discrimination by marine macroalgae and seagrasses. *Functional Plant Biology*, 29(3), pp.355-378.

- Raven, J. A., and Beardall, J. 2003. Carbon acquisition mechanisms of algae: Carbon dioxide diffusion and CO<sub>2</sub> concentrating mechanisms. *Photosynthesis Research*, 77(2-3), pp.155-171. <https://doi.org/10.1071/PP01201>
- Reich, K.J., Bjorndal, K.A. and Martínez del Rio, C. 2008. Effects of growth and tissue type on the kinetics of <sup>13</sup>C and <sup>15</sup>N incorporation in a rapidly growing ectotherm. *Oecologia*, 155, pp.651-663. <https://doi.org/10.1007/s00442-007-0949-y>
- Reinfelder, J.R., Kraepiel, A.M. and Morel, F.M. 2000. Unicellular C<sub>4</sub> photosynthesis in a marine diatom. *Nature*, 407(6807), pp.996-999. <https://doi.org/10.1038/35039612>
- Reinfelder, J.R. 2011. Carbon concentrating mechanisms in eukaryotic marine phytoplankton. *Annual review of marine science*, 3(1), pp.291-315. <https://doi.org/10.1146/annurev-marine-120709-142720>
- Revelles, M., Carreras, C., Cardona, L., Marco, A., Bentivegna, F., Castillo, J.J., De Martino, G., Mons, J.L., Smith, M.B., Rico, C. and Pascual, M. 2007a. Evidence for an asymmetrical size exchange of loggerhead sea turtles between the Mediterranean and the Atlantic through the Straits of Gibraltar. *Journal of Experimental Marine Biology and Ecology*, 349(2), pp.261-271. <https://doi.org/10.1016/j.jembe.2007.05.018>
- Revelles, M., Isern-Fontanet, J., Cardona, L., San Félix, M., Carreras, C. and Aguilar, A., 2007b. Mesoscale eddies, surface circulation and the scale of habitat selection by immature loggerhead sea turtles. *Journal of Experimental Marine Biology and Ecology*, 347(1-2), pp.41-57. <https://doi.org/10.1016/j.jembe.2007.03.013>
- Robineau, D. and Vely, M. 1998. Les cétacés des côtes de Mauritanie (Afrique du Nord-ouest). Particularités et variations spatio-temporelles de répartition: Rôle des facteurs océanographiques. *Revue d'Ecologie, Terre et Vie, Société nationale de protection de la nature*, 53 (2), pp.123-152. hal-03529162.
- Rossman, S., Ostrom, P.H., Gordon, F. and Zipkin, E.F. 2016. Beyond carbon and nitrogen: Guidelines for estimating three-dimensional isotopic niche space. *Ecology and Evolution*, 6(8), pp.2405-2413. <https://doi.org/10.1002/ece3.2013>
- Schlacher, T.A. and Connolly, R.M. 2014. Effects of acid treatment on carbon and nitrogen stable isotope ratios in ecological samples: a review and synthesis. *Methods in Ecology and Evolution*, 5(6), pp.541-550. <https://doi.org/10.1111/2041-210X.12183>
- Schlichting, H. and Gersten, K. 2016. *Boundary-layer theory*, 9<sup>th</sup> edition, Springer, pp.805.
- Schmitz Jr., W.J. and McCartney, M.S. 1993. On the north Atlantic circulation. *Reviews of Geophysics*, 31(1), pp.29-49. <https://doi.org/10.1029/92RG02583>
- Schoeninger, M.J. 2010. Chapter 15: Toward a  $\delta^{13}\text{C}$  Isoscape for Primates. In *Isoscapes: Understanding movement, pattern, and process on Earth through isotope mapping*, eds. West, J.B., Bowen, G.J., Dawson, T.E. and Tu, K.P., 319-333. Dordrecht: Springer Science & Business Media. doi:10.1007/978-90-481-3354-315.
- Schofield, G., Scott, R., Dimadi, A., Fossette, S., Katselidis, K.A., Koutsoubas, D., Lilley, M.K., Pantis, J.D., Karagouni, A.D. and Hays, G.C. 2013a. Evidence-based marine protected area planning for a highly mobile endangered marine vertebrate. *Biological Conservation*, 161, pp.101-109. <https://doi.org/10.1016/j.biocon.2013.03.004>

- Schofield, G., Dimadi, A., Fossette, S., Katselidis, K.A., Koutsoubas, D., Lilley, M.K., Luckman, A., Pantis, J.D., Karagouni, A.D. and Hays, G.C. 2013b. Satellite tracking large numbers of individuals to infer population level dispersal and core areas for the protection of an endangered species. *Diversity and Distributions*, 19(7), pp.834-844. <https://doi.org/10.1111/ddi.12077>
- Sharp, Z. 2017. Principles of Stable Isotope Geochemistry, 2nd Edition. University of New Mexico. <https://doi.org/10.25844/h9q1-0p82>
- Soukissian, T.H., Denaxa, D., Karathanasi, F., Prospathopoulos, A., Sarantakos, K., Iona, A., Georgantas, K. and Mavrakos, S. 2017. Marine renewable energy in the Mediterranean Sea: status and perspectives. *Energies*, 10(10), p.1512. <https://doi.org/10.3390/en10101512>
- Sevrin-Reyssac, J. 1993. Hydrology and underwater climate of the Banc d'Arguin, Mauritania: a review. In *Ecological Studies in the Coastal Waters of Mauritania: Proceedings of a Symposium held at Leiden, The Netherlands*, Springer Netherlands, pp.1-8. [https://doi.org/10.1007/978-94-011-1986-3\\_1](https://doi.org/10.1007/978-94-011-1986-3_1)
- Syväranta, J., Lensu, A., Marjomäki, T.J., Oksanen, S. and Jones, R.I. 2013. An empirical evaluation of the utility of convex hull and standard ellipse areas for assessing population niche widths from stable isotope data. *PloS one*, 8(2), p.e56094. <https://doi.org/10.1371/journal.pone.0056094>
- Tieszen, L.L., Boutton, T.W., Tesdahl, K.G. and Slade, N.A. 1983. Fractionation and turnover of stable carbon isotopes in animal tissues: implications for  $\delta^{13}\text{C}$  analysis of diet. *Oecologia*, 57, pp.32-37. <https://doi.org/10.1007/BF00379558>
- Tobias, C.R., Böhlke, J.K. and Harvey, J.W. 2007. The oxygen-18 isotope approach for measuring aquatic metabolism in high productivity waters. *Limnology and Oceanography*, 52(4), pp.1439-1453. <https://doi.org/10.4319/lo.2007.52.4.1439>
- Trueman, C.N., MacKenzie, K.M. and Palmer, M.R. 2012. Identifying migrations in marine fishes through stable-isotope analysis. *Journal of Fish Biology*, 81(2), pp.826-847. <https://doi.org/10.1111/j.1095-8649.2012.03361.x>
- Turner Tomaszewicz, C.N., Seminoff, J.A., Ramirez, M.D. and Kurle, C.M. 2015. Effects of demineralization on the stable isotope analysis of bone samples. *Rapid Communications in Mass Spectrometry*, 29(20), pp.1879-1888. <https://doi.org/10.1002/rcm.7295>
- Turner Tomaszewicz, C.N., Seminoff, J.A., Price, M. and Kurle, C.M. 2017a. Stable isotope discrimination factors and between-tissue isotope comparisons for bone and skin from captive and wild green sea turtles (*Chelonia mydas*). *Rapid Communications in Mass Spectrometry*, 31(22), pp.1903-1914. <https://doi.org/10.1002/rcm.7974>
- Turner Tomaszewicz, C. N., Seminoff, J. A., Peckham, S. H., Avens, L., y Kurle, C. M. 2017b. Intrapopulation variability in the timing of ontogenetic habitat shifts in sea turtles revealed using  $\delta^{15}\text{N}$  values from bone growth rings. *Journal of Animal Ecology*, 86(3), pp.694–704. <https://doi.org/10.1111/1365-2656.12618>
- Valdivia, M., Valenzuela, L.O., Berriel, V., Rodríguez, D., Laporta, P., Drago, M., Cani, A. and Bergamino, L. 2024. Resource partitioning in a cetacean community from Uruguayan waters. *Marine Mammal Science*, 40(2), p.e13077. <https://doi.org/10.1111/mms.13077>
- Vander Zanden, H.B., Bjorndal, K.A., Mustin, W., Ponciano, J.M. and Bolten, A.B. 2012. Inherent variation in stable isotope values and discrimination factors in two life stages of green turtles. *Physiological and Biochemical Zoology*, 85(5), pp.431-441. DOI:10.1086/666902

- Vander Zanden, M.J., Clayton, M.K., Moody, E.K., Solomon, C.T. and Weidel, B.C. 2015. Stable isotope turnover and half-life in animal tissues: a literature synthesis. *PloS one*, 10(1), p.e0116182. <https://doi.org/10.1371/journal.pone.0116182>
- Vander Zanden, H.B., Soto, D.X., Bowen, G.J. and Hobson, K.A. 2016. Expanding the isotopic toolbox: applications of hydrogen and oxygen stable isotope ratios to food web studies. *Frontiers in Ecology and Evolution*, 4, pp.20. <https://doi.org/10.3389/fevo.2016.00020>
- Van Waerebeek, K., Ofori-Danson, P.K., Debrah, J., Collins, T., Djiba, A. and Samba Ould Bilal, A. 2016. On the status of the common bottlenose dolphin *Tursiops truncatus* in western Africa, with emphasis on fisheries interactions, 1947-2015. *Document SC/66b/SM19 presented to the Scientific Committee of the International Whaling Commission, Bled, Slovenia*, 20.
- Wassenaar, L.I. 2019. Chapter 2 - Introduction to Conducting Stable Isotope Measurements for Animal Migration Studies. In: *Tracking Animal Migration with Stable Isotopes (Second Edition)*, eds. Keith A. Hobson, Leonard I. Wassenaar, Academic Press, pp.25-51. <https://doi.org/10.1016/B978-0-12-814723-8.00002-7>
- West, J.B., Bowen, G.J., Dawson, T.E. and Tu, K.P. (eds). 2010. *Isoscapes: understanding movement, pattern, and process on Earth through isotope mapping*. Springer Science & Business Media, pp.487.
- Wolff, W.J. and Smit, C.J. 1990. The Banc d'Arguin, Mauritania, as an environment for coastal birds. *Ardea*, 78(1), pp.17-38.
- Yokoyama, H., Tamaki, A., Harada, K., Shimoda, K., Koyama, K. and Ishihi, Y. 2005. Variability of diet-to-tissue isotopic fractionation in estuarine macrobenthos. *Marine Ecology Progress Series*, 296, pp.115-128. DOI:10.3354/meps296115
- Zabala, S., Bigatti, G., Botto, F., Iribarne, O.O. and Galván, D.E. 2013. Trophic relationships between a Patagonian gastropod and its epibiotic anemone revealed by using stable isotopes and direct observations. *Marine Biology*, 160, pp.909-919. <https://doi.org/10.1007/s00227-012-2143-y>
- Zbinden, J.A., Bearhop, S., Bradshaw, P., Gill, B., Margaritoulis, D., Newton, J. and Godley, B.J. 2011. Migratory dichotomy and associated phenotypic variation in marine turtles revealed by satellite tracking and stable isotope analysis. *Marine Ecology Progress Series*, 421, pp.291-302. <https://doi.org/10.3354/meps08871>
- Zeebe, R.E. and Wolf-Gladrow, D. 2001. CO<sub>2</sub> in seawater: equilibrium, kinetics, isotopes. Ed. David Halpern, Elsevier Oceanography Series, 65, pp.346.
- Zeebe, R.E. 2014. Kinetic fractionation of carbon and oxygen isotopes during hydration of carbon dioxide. *Geochimica et cosmochimica acta*, 139, pp.540-552. <https://doi.org/10.1016/j.gca.2014.05.005>
- Zenk, W., Klein, B. and Schroder, M. 1991. Cape Verde frontal zone. *Deep Sea Research Part A. Oceanographic Research Papers*, 38, p.S505-S530. [https://doi.org/10.1016/S0198-0149\(12\)80022-7](https://doi.org/10.1016/S0198-0149(12)80022-7)
- Zopfi, J., Böttcher, M.E. and Jørgensen, B.B. 2008. Biogeochemistry of sulfur and iron in Thioploca-colonized surface sediments in the upwelling area off central Chile. *Geochimica et Cosmochimica Acta*, 72(3), pp.827-843. <https://doi.org/10.1016/j.gca.2007.11.031>
- Zug, G.R., Wynn, A.H. and Ruckdeschel, C. 1986. Age determination of loggerhead sea turtles, *Caretta caretta*, by incremental growth marks in the skeleton.





## **Annex: Original articles**





## Original Article 1

**“Niche partitioning among marine mammals inhabiting a large estuary as revealed by stable isotopes of C, N, S and O”**

**Caní, A.**, Cardona, L., Valdivia, M., González, E.M. and Drago, M. 2023. Niche Partitioning Among Marine Mammals Inhabiting a Large Estuary as Revealed by Stable Isotopes of C, N, S, and O. *Estuaries and Coasts*, 46(4), pp.1083-1097, <https://doi.org/10.1007/s12237-023-01193-y>

